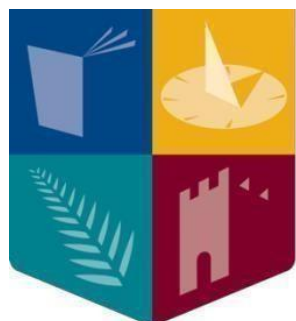


Characterisation of host adaptation processes in the fungal pathogen *Aspergillus fumigatus*



**Maynooth
University**
National University
of Ireland Maynooth

A thesis submitted to Maynooth University for the degree of
Doctor of Philosophy

Aaron Joseph Reddington Curtis, B.Sc.

August 2025

Supervisor
Prof. Kevin Kavanagh

Medical Mycology Unit
Department of Biology
Maynooth University
Co. Kildare

Head of Department
Prof. Paul Moynagh

Department of Biology
Maynooth University
Co. Kildare

Declaration

This thesis has not been submitted whole or in part to this or any university for any other degree and is the original work of the author except where otherwise stated.

Signed 

Aaron Curtis, B.Sc.

Date 19/08/2025

Acknowledgements

Research doesn't happen in a vacuum; it influences and is influenced by the world around it. This can also be said of the researcher, who is influenced by the environment in which they work and the people around them. The work presented here is the product of eight amazing years spent at Maynooth University, a place that was my home away from home, a place where I made many friends and experienced some of my highest highs and lowest lows. Over those eight years there were many bus trips, many early mornings and late evenings, countless conversations and cups of coffee and too many amazing people to count who were there for part or the entirety of my time there. As I prepare to leave Maynooth I do so with a heavy heart as I have so many cherished memories that will stay with me for a lifetime. I entered Maynooth as an unsure undergraduate student with so much to learn and I leave it transformed into a slightly less unsure researcher who still has so much to learn! In Maynooth and in this PhD I have been challenged, inspired and have become even more enamoured with the world around us and the ability of researchers to understand a tiny piece of it and shed light on it for everyone else to see. I move forward, not forgetting my time here but remembering that every new beginning starts with some other beginnings end, and what a beginning I've been fortunate to have. I look forward to the continuation of my research journey, wherever it may take me knowing that I have a strong foundation shaped by an amazing team, working diligently in an amazing department to inspire, innovate and spark a lifelong passion for science in so many students lives.

None of this work would have been possible without the guidance of Professor Kevin Kavanagh, a man who once compared applying for a PhD scholarship with me to betting on the right horse, one who would finish strong, I hope I have done you proud. You saw potential in me when I didn't see it in myself and pushed me to be who I am today. You taught me that every experiment is a question and even if it doesn't work as expected you still learn something, even if its as simple as "well let's not do it that way again". You always fostered a friendly and collaborative atmosphere in the lab and hearing your keys shake before you walked through the door was always a reassuring sound. You were patient and kind to me every step of the way and I truly couldn't have gotten through all the failed experiments and the frustration of peer review without your words of wisdom and constant encouragement. You are the finest example of a scientist and a man whose passion for science, wisdom and investment in future researchers is second to none. Your constant optimism and my pessimism clashed on occasion, and my love of saga length paper drafts drove you mad, but we have balanced each other nicely. I am proud to have worked under you and to join the long line of researchers who can say the same. You are a true inspiration, and I can only hope to have picked up a fraction of your commitment to excellence, your enthusiasm for your work and your respect and willingness to push people to be the best they can be.

I want to thank my fellow members of the Medical Mycology unit past and present who were in the trenches with me and were always willing to help when needed. I want to particularly thank Magda, my first in lab supervisor. You taught me the ropes through my undergraduate project and were always patient despite my many questions. Thank you for encouraging me to stay on in research and being so kind to me while you were here. Seeing you graduate was bittersweet, but I am delighted to see you and Joy along with many other previous students succeed. Thank you, Pranay

for your friendship. You are one of my closest friends and I cherish our friendship and conversations over the years. I was delighted when you joined the lab and started with the good omics, proteomics before shifting to the dark side of transcriptomics of which we have debated the merits of both on many occasions with great intensity. I wish you every success in the future, you are an incredibly talented researcher, believe in yourself you've got this. To Daryl my student turned lab mate, it has been amazing to see you grow as a researcher. You are going to achieve great things, and I wish you every success in the future. I would also like to thank other students and research assistants within the department who have become my friends many of which have gradated ahead of me Katie, Maria, Sarah, Melissa, Enya, Jacob, Meabh, Julia, Cathal and Shauna, among many others who made my days exponentially easier with their friendship and encouragement. Jamie, I enjoyed our coffee times and discussions we made it through, despite the challenges. I would like to say a special thank you to the original biomedics who also pursued PhDs and have been there with me since day one, Conall, my undergrad lab partner, Courteney my bus buddy, Sarah, Ardena and Cathal I wish you every success wherever you go, the future is bright with you in research.

I would also like to acknowledge the work of the wonderful technical staff in the biology department who kept everything running smoothly during my project. Michelle you're some woman for one woman and always on the ball. You were also so helpful and available for a quick chat between your endless phone calls. Fidelma, Tina, Alison and Aine thank you for being so helpful despite the number of times I asked questions about booking meeting rooms or setting up package collections and for getting us the best deals on the marketplace. Thank you, Patricia, for keeping an eye on me and keeping everyone accountable for getting their grading done on time and for being great for the chats. Thank you, Gillian and Deirdre, for going above and beyond your work to help neurodivergent children engage in science, your work is amazing and deserves more credit. Thank you, Noel, for fixing our dodgy autoclave as many times as you did and for teaching me the basics or repairing and troubleshooting equipment. Thank you to the prep lab for always bailing me out when I was low on a particular supply and letting me into stores out of opening hours, you saved more experiments than you know, particular thanks to Sam for saving my package from DHLs mistakes, you saved me some serious hassle. Thank you also to Frances who was always great for a chat and always brightened my day. I want to express my heartfelt gratitude to Caroline, the mass spec wizard. You are amazing and despite many setbacks and frustrations you always had time for a chat or a discussion about details for an upcoming run. Half of my work can be credited to how well you have managed and maintained the QE and the Ascend. Thank you for your encouragement and your willingness to trust me and experiment with different things on some very expensive bits of kit. I have learnt so much from you and I look forward to applying them in future projects.

Thank you to my many collaborators who all helped to make the work presented here possible. I would like to thank the first Masters student I supervised Michelle who helped with the *Klebsiella pneumoniae* research, you were a natural in the lab and a delight to teach. I would like to thank Prof. David Fitzpatrick for all of his genomics expertise and advice over the years. I would also like to thank Prof. Pavel Hyrsł and Dr Pavel Dobeš and your team of talented students in Brno, Czech Republic. You taught me so many techniques in the month I was with you and took care of me like I was one of your own. I wish to offer a special thanks to Jacek you are a lifelong friend, and I will happily host you again for a “Vorty-Porty” even if you mislabel your tubes from time to time. I would also like to thank Dr Freya Harrison, who I met at a

Microbiology Society meeting who offered a free training course on the EVPL model system. Your openness to collaborations and supporting other researchers is commendable and I wish it was more common among researchers. Thank you for all of the advice in the troubleshooting of the model and your constant enthusiasm for the angle in which we took it. I would also like to give a special acknowledgement to Prof. Bill Watson from UCD who visited my school and inspired me as a 12-year-old boy to be curious about the World around me and gave his time freely to inspire future generations

Thank you to the scientific community, particularly the Microbiology Society as well as all of the conference organisers, societies, editors and peer-reviewers, even reviewer number 2. The organisation of conferences, meetings and seminars offered a crucial opportunity to learn from, contribute to and feel a part of something bigger than any individual. These events bring our community closer together and facilitate collaborations to advance science beyond lab walls or even borders. Science cannot progress without the thankless jobs you do and though your comments may sting at times they have improved my work to a standard fit for publication.

I would like to thank my family, the people who raised me and love me through every situation and circumstance. Your love and support has been invaluable, and I owe all of my successes to you. Mam and Dad thank you for everything for fostering my interest in the natural world from a young age watching countless David Attenborough documentaries and reruns of Crocodile hunter and for supporting me every step of the way. You always pushed me to go after the things I wanted, not the things that were easy and even when the odds were against me and you were always there in the highs and the lows of life. You supported and encouraged me to pursue this PhD even when I thought it was a crazy idea and way beyond my ability, thank you. Dad thank you for all the early morning drives to the airport for conferences and to the morning panic to get to the bus stop for college and for proof-reading my work even though you hadn't a notion what it meant. Dave and Leah, thank you for setting great examples for me growing up and being amazing older siblings and I love you both very much and I'm proud to be your little brother.

Cara you are the love of my life. You have gone from being my girlfriend in undergraduate despite my awkwardness to my fiancée and my wife during this PhD, even though everyone thought we were mad. We have survived long distance, a pandemic, wedding planning and a PhD together and are stronger than ever because of it, life wouldn't be as fun without a little bit of chaos. You have stuck by me and pushed me to be the man I am today and have believed in me despite all the times I threatened to quit (you wouldn't let me anyway!). You have shown remarkable patience with me despite my constant yapping about research, my inability to switch off and the overuse of my "lecturer voice" when discussing any and all topics. You were always the best test audience for presentations even when I would go through them repeatedly to shave 30 seconds off for a conference. You are my biggest source of strength and reassurance when I need it, and you believe in me even when I feel incapable. Every hardship was faced together, and I never had to struggle alone. You did vow on our wedding day, as Kevin can attest to that you would learn more about Aspergillus, I hope you enjoy this work as some light reading. I couldn't have gotten through this process without you, and I can't wait to have you by my side for the next and all future steps in our lives together, I love you with all my heart.

Table of Contents

Chapter 1: Introduction	1
1.1 The Global burden of Fungal disease	3
1.1.1 Host adaptation within fungi.....	5
1.2 <i>Aspergillus fumigatus</i>	6
1.2.1 Clinical manifestations of <i>Aspergillus fumigatus</i> infection.....	7
1.2.2 Host immune response to <i>Aspergillus fumigatus</i>	9
1.2.3 <i>Aspergillus fumigatus</i> virulence factors	13
1.2.4 <i>Aspergillus fumigatus</i> response to stress	19
1.2.5 <i>Aspergillus fumigatus</i> metabolism	20
1.2.6 Current approaches to <i>Aspergillus fumigatus</i> treatment.....	23
1.2.7 Antifungal resistance in <i>Aspergillus fumigatus</i>	25
1.3 Microbial interactions in the airways	28
1.4 <i>Klebsiella pneumoniae</i> infections, virulence and coinfection.....	29
1.5 <i>Pseudomonas aeruginosa</i> infections, virulence and coinfection	31
1.6 The need for model systems to study fungal pathogens	34
1.6.1 Mammalian models	35
1.6.2 <i>In vitro</i> cell models.....	37
1.6.3 Invertebrate model systems	40
1.6.4 <i>Galleria mellonella</i> as a model of the innate immune response.....	42
1.6.5 Mechanisms employed by Fungi to Infect <i>Galleria mellonella</i> Larvae	43
1.6.6 The <i>ex-vivo</i> pig lung model as an analogue of host tissue	44
1.6.7 A Combinational approach to disease modelling	46
1.7 Omics approaches in mycology	47
1.7.1 Label-free quantitative proteomics	51
1.7.2 Proteomics as a tool for uncovering host adaptation processes.....	52
1.8 Thesis objectives	52
Chapter 2: Prolonged subculturing of <i>Aspergillus fumigatus</i> on Galleria Extract Agar results in altered virulence and sensitivity to Antifungal agents	54
2.1 Introduction.....	57
2.2 Materials and Methods	59
2.2.1 <i>Aspergillus fumigatus</i> Culture Conditions.....	59
2.2.2 Generation of passaged strains of <i>Aspergillus fumigatus</i>	59

2.2.3 Virulence assessment of passaged strains <i>in vivo</i>	60
2.2.4 Haemocyte kill assay.....	60
2.2.5 Susceptibility testing	60
2.2.6 Gliotoxin extraction and quantification.....	61
2.2.7 Total secreted siderophore quantification.....	61
2.2.8 Protein extraction and purification from <i>A. fumigatus</i> hyphae.....	61
2.2.9 Mass spectrometry.....	62
2.2.10 Data analysis.....	63
2.2.11 Statistical analysis	63
2.3 Results	64
2.3.1 Characterisation of growth characteristics of serially subcultured <i>A. fumigatus</i> strains	64
2.3.2 Passaged <i>A. fumigatus</i> strains show reduced virulence in <i>G. mellonella</i> larvae.....	64
2.3.3 Passaged <i>A. fumigatus</i> strains show altered susceptibility to Antifungal agents	66
2.3.4 Proteomic characterisation of Passaged <i>A. fumigatus</i> strain E25	68
2.4 Discussion.....	71
2.5 Conclusion	73
2.6 References.....	74
Chapter 3: Characterisation of <i>Aspergillus fumigatus</i> secretome during sublethal infection of <i>Galleria mellonella</i> larvae.....	77
3.1 Introduction.....	80
3.2 Materials and methods	82
3.2.1 <i>A. fumigatus</i> culture conditions	82
3.2.2 Virulence assessment of <i>A. fumigatus</i> <i>in vivo</i>	82
3.2.3 Assessment of larval movement.....	82
3.2.4 Quantification of total protein and carbohydrate in larval haemolymph....	82
3.2.5 <i>In vivo</i> gliotoxin extraction and quantification	83
3.2.6 Total secreted siderophore quantification.....	83
3.2.7 Protein extraction	83
3.2.8 Proteomic analysis.....	84
3.2.9 Data analysis.....	85
3.3 Results	85
3.3.1 Virulence of <i>A. fumigatus</i> in <i>G. mellonella</i> larvae	85
3.3.2 Metabolite concentrations in larvae post <i>A. fumigatus</i> infection	87

3.3.3 Gliotoxin quantification in <i>G. mellonella</i> larvae post <i>A. fumigatus</i> infection	89
3.3.4 Siderophore quantification in <i>G. mellonella</i> larvae post <i>A. fumigatus</i> infection	89
3.3.5 Proteomic analysis of <i>A. fumigatus</i> during larval infection	90
3.3.6 Proteomics analysis of <i>G. mellonella</i> response to infection	91
3.4 Discussion.....	92
3.5 References.....	98
Chapter 4: Exposure of <i>Aspergillus fumigatus</i> to <i>Klebsiella pneumoniae</i> culture filtrate inhibits growth and stimulates gliotoxin production.....	103
4.1 Introduction.....	106
4.2 Materials and Methods.....	107
4.2.1 <i>A. fumigatus</i> growth conditions	107
4.2.2 Preparation of the bacterial culture filtrate	108
4.2.3 Assessment of fungal biomass	108
4.2.4 Gliotoxin extraction and quantification by RP-HPLC.....	108
4.2.5 Extraction of protein from <i>K. pneumoniae</i> culture filtrate	108
4.2.6 Protein extraction from <i>A. fumigatus</i> exposed to bacterial culture filtrate	109
4.2.7 Label-Free Mass Spectrometry (LF/MS).....	109
4.2.8 Mass Spectrometry and the parameters for <i>A. fumigatus</i> and <i>K. pneumoniae</i> culture filtrate proteomic data procurement	110
4.2.9 Data Analysis of <i>A. fumigatus</i> and <i>K. pneumoniae</i> culture filtrate Proteomes.....	110
4.3 Results	111
4.3.1 Analysis of the effects of <i>K. pneumoniae</i> culture filtrate on <i>A. fumigatus</i>	111
4.3.2 Characterisation of <i>K. pneumoniae</i> culture filtrate.....	112
4.3.3 Analysis of the effect of <i>K. pneumoniae</i> culture filtrate on the <i>A. fumigatus</i> proteome.....	114
4.4 Discussion.....	119
4.5 References.....	123
Chapter 5: Proteomic characterisation of <i>Aspergillus fumigatus</i>- host interactions using the <i>ex-vivo</i> pig lung (EVPL) model.....	126
5.1 Introduction.....	129
5.2 Materials and Methods	132
5.2.1 <i>Aspergillus fumigatus</i> culture conditions and conidial preparation	132

5.2.2 Preparation of <i>ex-vivo</i> pig lung sections.....	132
5.2.3 Quantification of fungal burden	133
5.2.4 Proteomic extraction from infected tissue sections	133
5.2.5 Mass spectrometry.....	134
5.2.6 Data analysis.....	135
5.3 Results	136
5.3.1 Confirmation of <i>Aspergillus fumigatus</i> growth on EVPL tissue	136
5.3.2 Proteomic analysis of alterations in <i>A. fumigatus</i> proteome during growth on EVPL tissue	137
5.3.3 Characterisation of proteomic alterations in EVPL tissue during <i>A. fumigatus</i> colonisation	141
5.4 Discussion.....	147
5.5 References.....	153
Chapter 6: More potent together: <i>Aspergillus fumigatus</i> the facilitates the dominance of <i>Pseudomonas aeruginosa</i> during coinfection of an <i>ex-vivo</i> pig lung model	162
6.1 Introduction.....	165
6.2 Results	167
6.2.1 Visual confirmation of tissue pathology	167
6.2.2 Initial amplicon analysis.....	167
6.2.3 <i>Sus scrofa</i> lung tissue microbiome	169
6.2.4 Characterisation of <i>A. fumigatus</i> Proteome from coinfected explants relative to that from mono-infected tissue	172
6.2.5 Analysis of changes in <i>P. aeruginosa</i> Proteome from coinfected explants relative to mono-infected samples	173
6.2.6 <i>Sus scrofa</i> proteome in various infection states relative to control	175
6.2.7 Proteomic response of <i>Sus scrofa</i> to <i>A. fumigatus</i> mono-infection relative to control	176
6.2.8 Proteomic response of <i>Sus scrofa</i> to <i>P. aeruginosa</i> mono- infection relative to control	179
6.2.9 Proteomic response of <i>Sus scrofa</i> to co-infection infection relative to control	181
6.2.10 Analysis of <i>Sus scrofa</i> proteome in coinfecting EVPL relative to mono-infected explants.....	184
6.3 Discussion.....	186
6.4 Conclusion	192
6.5 Materials and Methods	193

6.5.1 <i>Aspergillus fumigatus</i> culture conditions and conidial preparation	193
6.5.2 <i>Pseudomonas aeruginosa</i> culture conditions and liquid suspension preparation.....	193
6.5.3 Preparation of <i>ex-vivo</i> pig lung sections.....	193
6.5.4 Visualisation of tissue pathology	194
6.5.5 DNA Extraction, Library Preparation, and Sequencing	194
6.5.6 Sequence Data Processing and Quality Control	194
6.5.7 OTU Clustering and Chimera Removal	195
6.5.8 Taxonomic Annotation.....	195
6.5.9 Proteomic extraction	195
6.5.10 Mass spectrometry.....	195
6.5.11 Data analysis.....	196
6.6 References.....	198
Chapter 7: General discussion	207
7.1 General discussion	208
7.2 Concluding remarks and future work.....	223
Chapter 8: Bibliography.....	225
Chapter 9: Appendix	254

List of Figures

Chapter 1

Figure 1.1: Fungal pathogens designated as critical, high and medium priority by the World health organisation marking their route of exposure as either commensal or environmental in nature published by (Brown <i>et al.</i> , 2019)	5
Figure 1.2: Radiographical images of different forms of pulmonary aspergillosis adapted from (Singh <i>et al.</i> , 2023; Garg <i>et al.</i> , 2022 and Panse <i>et al.</i> , 2016).	9
Figure 1.3: Schematic of the Human complement cascade published by (Detsika <i>et al.</i> 2024)	11
Figure 1.4: Forms of stress and competition in both the soil niche and the human airways highlighting the similarities in these environments	13
Figure 1.5: The role of selected secondary metabolites produced by <i>A. fumigatus</i> in the environment and in the human lung adapted from figure published by (Raffa <i>et al.</i> , 2019).	18
Figure 1.6: Schematic of the shikimate pathway utilised by fungi to produce aromatic amino acids published by (Kuplińska <i>et al.</i> , 2021)	22
Figure 1.7: Targets of antifungal agents Echinocandins, Azoles and Polyenes and some resistance mechanisms observed in fungal pathogens published by (Lee <i>et al.</i> , 2023)	27
Figure 1.8: Examples of interaction studies between <i>A. fumigatus</i> and bacterial pathogens <i>K. pneumoniae</i> and <i>P. aeruginosa</i> .	29
Figure 1.9: Overview of <i>Galleria mellonella</i> infection and haemolymph collection methodologies	42
Figure 1.10: Comparison of toll-like receptor signalling in <i>G. mellonella</i> compared to the gold standard murine model demonstrating their similarities	43
Figure 1.11: Methodology for extraction, infection and assessment of <i>ex-vivo</i> pig lung explants	46
Figure 1.12: Generic Label -free proteomics methodology.	51

Chapter 2

Figure 2.1: Response of larvae to infection by the conidia of control and passaged <i>A. fumigatus</i> strains	65
Figure 2.2: Response of control and passaged <i>A. fumigatus</i> conidia to haemocyte-mediated killing	66
Figure 2.3: Analysis of the response of Control and passaged <i>A. fumigatus</i> conidia to hydrogen peroxide, amphotericin B and itraconazole	67
Figure 2.4: Heat map showing protein clustering between control and passaged <i>A. fumigatus</i> strain E25.	70
Figure 2.5: Volcano plots showing alterations in protein abundance in control and passaged <i>A. fumigatus</i> proteomes.	71

Chapter 3

Figure 3.1: Dose-dependent survival of <i>G. mellonella</i> larvae infected with <i>A. fumigatus</i> .	86
Figure 3.2: FIMTrack analysis of larval movement over time following infection with 1×10^5 conidia.	87
Figure 3.3: Assessment of haemolymph carbohydrate content post-infection	88
Figure 3.4: Assessment of haemolymph protein content post-infection	88
Figure 3.5: Quantification of gliotoxin in Galleria infected with 1×10^5 <i>A. fumigatus</i> conidia	89
Figure 3.6: Quantification of total siderophore concentration detected in Galleria haemolymph infected with 1×10^5 <i>A. fumigatus</i> conidia.	90
Figure 3.7: Pie chart summarizing high-confidence qualitative <i>A. fumigatus</i> protein detections.	91
Figure 3.8: Bar graph summarizing (a) high-confidence qualitative <i>G. mellonella</i> protein detections categorized into seven subcategories in control larvae and in larvae at 96 hours post-infection. (b) Immune proteins further subdivided into 11 subcategories	92

Chapter 4

Figure 4.1: Analysis of the effects of <i>K. pneumoniae</i> culture filtrate on <i>A. fumigatus</i> mycelial growth (A) and Gliotoxin production (B)	112
Figure 4.2: Principal component analysis of <i>A. fumigatus</i> after exposure to <i>K. pneumoniae</i> culture filtrate (25% v/v) (green) and control <i>A. fumigatus</i> (red). (B) Heatmap generated through Two-way unsupervised hierarchical clustering of the median protein expression values of all statistically significant differentially abundant proteins.	114
Figure 4.3: Volcano plot showing the distribution of statistically significant and differentially abundant (SSDA) proteins which have a $-\log$ (p-value) > 1.3 and difference $+/-0.58$. <i>A. fumigatus</i> exposed to <i>K. pneumoniae</i> culture filtrate compared to control <i>A. fumigatus</i> .	116

Chapter 5

Figure 5.1: Phenotypic analysis and confirmation of fungal growth on agar and <i>ex-vivo</i> pig lung explants. (A) Representative image of sections at each 24 hour interval imaged via dissection microscope. (B) Graph of fungal burden calculated from agar and EVPL explants showing a significant decrease in CFU at 72 hours ($P=0.002$) calculated by two-way ANOVA. (C) Microscopy image of hyphal growth on an EVPL section at 40x magnification.	136
Figure 5.2: (A) Principal component analysis of <i>A. fumigatus</i> proteins at 24, 48, 72 and 96 hours. (B) Heatmap generated through Two-way unsupervised hierarchical clustering of the median protein	

expression values of all statistically significant differentially abundant proteins.	138
Figure 5.3: (A) Principal component analysis of <i>Sus scrofa</i> proteins at 24, 48, 72 and 96 hours. (B) Heatmap generated through Two-way unsupervised hierarchical clustering of the median protein expression values of all statistically significant differentially abundant proteins.	142
Figure 5.4: Volcano plots showing the distribution of statistically significant and differentially abundant (SSDA) proteins which have a $-\log(p\text{-value}) > 1.3$ and difference $+/-0.58$. (A) <i>Sus scrofa</i> infected lung explants with <i>A. fumigatus</i> compared to uninfected lung explants at 24 hours and (B) <i>Sus scrofa</i> infected lung explants with <i>A. fumigatus</i> compared to uninfected lung explants at 48 hours.	143
Figure 5.5: Volcano plots showing the distribution of statistically significant and differentially abundant (SSDA) proteins which have a $-\log(p\text{-value}) > 1.3$ and difference $+/-0.58$. (A) <i>Sus scrofa</i> infected lung explants with <i>A. fumigatus</i> compared to uninfected lung explants at 72 hours and (B) <i>Sus scrofa</i> infected lung explants with <i>A. fumigatus</i> compared to uninfected lung explants at 96 hours.	145

Chapter 6

Figure 6.1: Representative image of various treatments at 96 hours post inoculation; uninfected control, <i>A. fumigatus</i> mono-infected, <i>P. aeruginosa</i> mono-infected and <i>A. fumigatus</i> and <i>P. aeruginosa</i> coinfecting explants at 20x magnification.	167
Figure 6.2: Metataxonomic analysis of infected explants (i) Phylum level relative abundance of Bacterial OTUs found in five lung tissue treatments A: unwashed tissue, B: washed tissue, C: <i>P. aeruginosa</i> infection, D: <i>A. fumigatus</i> infection, E: coinfection.	170
Figure 6.3: (A) Principal component analysis of <i>A. fumigatus</i> proteins grown on <i>ex-vivo</i> pig lung explants in mono-infection (Green) and coinfection (Red). (B) Volcano plots showing the distribution of statistically significant and differentially abundant proteins	173
Figure 6.4: (A) Principal component analysis of <i>P. aeruginosa</i> proteins grown on <i>ex-vivo</i> pig lung explants in mono-infection (Blue) and coinfection (Red). (B) Volcano plots showing the distribution of statistically significant and differentially abundant proteins.	175
Figure 6.5: (A) Principal component analysis of <i>S. scrofa</i> proteins in control (Black circle) or infected with <i>A. fumigatus</i> mono-infection (white square), <i>P. aeruginosa</i> mono-infection (White Square) and coinfection (Black Square) demonstrating good separation in the proteome between conditions. (B) Heatmap generated through Two-way unsupervised hierarchical clustering of the median protein expression values of all statistically significant differentially abundant proteins.	176

Figure 6.6: (A) Volcano plot of *S. scrofa* proteins in response to *A. fumigatus* mono-infection relative to uninfected explants showing the distribution of statistically significant and differentially abundant (SSDA) proteins which have a $-\log(p\text{-value}) > 1.3$ and difference $+/-0.58$. (B) Gene enrichment analysis highlight KEGG pathways increased and decreased in response to *A. fumigatus* infection relative to healthy control

178

Figure 6.7: (A) Volcano plot of *S. scrofa* proteins in response to *P. aeruginosa* mono-infection relative to uninfected explants showing the distribution of statistically significant and differentially abundant (SSDA) proteins which have a $-\log(p\text{-value}) > 1.3$ and difference $+/-0.58$. (B) Gene enrichment analysis highlight KEGG pathways increased and decreased in response to *P. aeruginosa* infection relative to healthy control

180

Figure 6.8: (A) Volcano plot of *S. scrofa* proteins in response to *A. fumigatus* and *P. aeruginosa* coinfection relative to uninfected explants showing the distribution of statistically significant and differentially abundant (SSDA) proteins which have a $-\log(p\text{-value}) > 1.3$ and difference $+/-0.58$. (B) Gene enrichment analysis highlight KEGG pathways increased and decreased in response to coinfection relative to healthy control

183

Figure 6.9: (A) Volcano plot of *S. scrofa* proteins in response to *A. fumigatus* relative to coinfection and (B) *P. aeruginosa* relative to coinfection showing the distribution of statistically significant and differentially abundant (SSDA) proteins which have a $-\log(p\text{-value}) > 1.3$ and difference $+/-0.58$.

185

List of Tables

Chapter 2

Table 2.1: All proteins detected to be statistically significant and differentially abundant in passaged strain E25 relative to the control <i>A. fumigatus</i> strain.	69
-------------------------------------------------------------------------------------------------------------------------------------------------------------------------	----

Chapter 4

Table 4.1: Proteins identified in <i>K. pneumoniae</i> culture filtrate with potential antifungal activity	113
Table 4.2: The Top 20 proteins most increased in abundance in <i>A. fumigatus</i> after exposure to <i>K. pneumoniae</i> culture filtrate for 24 h.	116
Table 4.3: The Top 20 proteins most decreased in abundance in <i>A. fumigatus</i> after exposure to <i>K. pneumoniae</i> culture filtrate for 24 h.	117

Chapter 5

Table 5.1: Statistically significantly and differentially abundant <i>Aspergillus fumigatus</i> proteins associated with virulence or involvement in eliciting an immunological response within the host detected at two or more timepoints relative to a 24-hour sample.	140
---------------------------------------------------------------------------------------------------------------------------------------------------------------------------------------------------------------------------------------------------------------------------	-----

Chapter 6

Table 6.1: OTU statistics	169
---------------------------	-----

Publications (first author)

Curtis, A., Binder, U. and Kavanagh, K., 2022. *Galleria mellonella* Larvae as a Model for Investigating Fungal-Host Interactions. *Frontiers in Fungal Biology*, 3, 893494.

Curtis, A., Ryan, M. and Kavanagh, K., 2023. Exposure of *Aspergillus fumigatus* to *Klebsiella pneumoniae* Culture Filtrate Inhibits Growth and Stimulates Gliotoxin Production. *Journal of Fungi*, 9 (2), 222.

Curtis, A., Walshe, K. and Kavanagh, K., 2023. Prolonged Subculturing of *Aspergillus fumigatus* on Galleria Extract Agar Results in Altered Virulence and Sensitivity to Antifungal Agents. *Cells*, 12 (7), 1065.

Curtis, A., Dobes, P., Marciniak, J., Hurychova, J., Hyrsil, P. and Kavanagh, K., 2024. Characterization of *Aspergillus fumigatus* secretome during sublethal infection of *Galleria mellonella* larvae. *Journal of Medical Microbiology*, 73 (6), 001844.

Curtis, A., Oladimeji, F., Kavanagh, K. (2025). Models for Studying Fungal Pathogenesis. *Current Clinical Microbiology Reports*, 12: 12.

Curtis, A., Harrison, F., Kavanagh, K. (2025). Proteomic characterization of *Aspergillus fumigatus* – host interactions using the *ex-vivo* pig lung (EVPL) model. *Virulence*, 16: 2530675.

Curtis, A., Kavanagh, K. and Murphy, F., 2025. Bridging Model for Nanotoxicology. *Nanosafety: A Comprehensive Approach to Assess Nanomaterial Exposure on the Environment and Health*, 313

Curtis, A., FitzPatrick, D., Harrison, F., Kavanagh, K. More potent together: *Aspergillus fumigatus* facilitates the dominance of *Pseudomonas aeruginosa* during coinfection of an *ex-vivo* pig lung model mBio mBio02571-25 (submitted)

Publications (Co-author)

Bianchi, M., Kaya, E., Logiudice, V., Maisetta, G., **Curtis, A.**, Kavanagh, K., Batoni, G., Esin, S. (2025). Biotherapeutic potential of different fractions of cell-free supernatants from *Lacticaseibacillus rhamnosus* against *Pseudomonas aeruginosa*. *Frontiers in Cellular and Infection Microbiology*, 15.

Rigotto-Caruso, G., **Curtis, A.**, Kavanagh, K. and von Zeska Kress, M. R., 2025. Label-Free Quantitative Proteomic Analysis Reveals the Effects of Biogenic Silver Nanoparticles on *Fusarium keratoplasticum* and Their Therapeutic Potential in *Galleria mellonella* Larvae. *ACS Omega* [online]. Available from: <https://doi.org/10.1021/acsomega.5c03275>

Phair, K., **Curtis, A.**, Kavanagh K, Periera, S., Kealey, C. and Brady, D., Alpha-linolenic acid reduces virulence of *Cronobacter sakazakii* as shown in larval model. *Journal of food safety* (submitted).

Phair, K., **Curtis, A.**, Kavanagh K, Kealey, C. and Brady, D Negative regulation of flagellar genes of *C. sakazakii* exposed to alpha-linolenic acid. *Journal of Applied Microbiology* (submitted).

Woods, D., Flynn, S., Moore-Machacek, A., **Curtis, A.**, Kavanagh, K., Mac Sharry, J., Sadofsky, L., Mahony, J., O'Gara, F., and Reen, FJ., Bile orchestrates a shift in signalling networks and metabolic flux in the respiratory pathogen *Pseudomonas aeruginosa*. *Plos Pathogens* (Submitted).

Invited presentations

Student Entomology Society seminar series online. September 12th, 2022 Title: *Galleria mellonella*: a mini-model for characterizing fungal pathogens

Oral presentations

Irish Fungal Society Online Conference Programme Wednesday June 22nd, 2022 Title: Use of *Galleria mellonella* larvae for characterising fungal pathogens

Biology summer school presentation July 26th 2022 (MU) Title: The study of Fungal pathogens in Insect mini-models

Irish Fungal society Dublin City University 22nd June 2023 Title: Host adaptation mechanisms and phenotype of *Aspergillus fumigatus* elicited by prolonged subculturing on a host agar system.

Microbiology society Annual Meeting in Ireland November 2024 title: Proteomic characterisation of *Aspergillus fumigatus*- host interaction within the *ex-vivo* Pig Lung model

Microbiology Society annual conference Monday 31th March–Thursday 3rd April 2025. Liverpool Title: Proteomic characterisation of *Aspergillus fumigatus*- host interaction within the *Ex-Vivo* Pig Lung model

Irish fungal society meeting Thursday 19th June 2025. Dublin Title: Proteomic analysis of *Aspergillus fumigatus* and *Pseudomonas aeruginosa* interactions within the *ex-vivo* pig lung model system

Poster presentations

Microbiology Society annual conference Monday April 17th, 2023. Birmingham Title: Exposure to *Klebsiella pneumoniae* culture filtrate inhibits *Aspergillus fumigatus* growth and stimulates gliotoxin production.

Irish fungal society June 2023 Title: Exposure to *Klebsiella pneumoniae* culture filtrate inhibits *Aspergillus fumigatus* growth and stimulates gliotoxin production.

11th Annual Advances Against Aspergillosis and Mucormycosis NH Milano Congress Centre 25-27th January 2024 Title: Prolonged Subculturing of *Aspergillus fumigatus* on *Galleria* Extract Agar Results in Altered Virulence and Sensitivity to Antifungal Agents

Microbiology Society ICC, Edinburgh 8-11th April 2024 Title: Prolonged Subculturing of *Aspergillus fumigatus* on *Galleria* Extract Agar Results in Altered Virulence and Sensitivity to Antifungal Agents.

Irish Fungal Society June 2024 Title: Prolonged Subculturing of *Aspergillus fumigatus* on *Galleria* Extract Agar Results in Altered Virulence and Sensitivity to Antifungal Agents

Abbreviations

°C: Degrees Celsius

ABPA: Allergic bronchopulmonary aspergillosis

CAN: Acetonitrile

AMBIc: Ammonium Bicarbonate

ANOVA: Analysis of variance

ATP: Adenosine triphosphate

CF: Cystic Fibrosis

CFU: Colony forming units

CGD: Chronic granulomatous disease

Cm: Centimetre

COPD: Chronic obstructive pulmonary disease

CPA: Chronic pulmonary aspergillosis

CXCR4+: C-X-C chemokine receptor type 4

CXCL1: C-X-C motif chemokine ligand 1

CXCL8: C-X-C motif chemokine ligand 8

ddH₂O: Deionised water

dH₂O: Distilled water

DMEM: Dulbecco's Modified Eagle Medium

DNA: Deoxyribonucleic acid

DTT: Dithiothreitol

EVLP: *Ex-vivo* lung perfusion

EVPL: *Ex-vivo* pig lung

FC: Fusarinine C

FDR: False discovery rate

FASP: filter associated sample preparation

g: Grams

g: g-force

GEA20: Galleria extract agar 20%

GO: Gene ontology

h: Hours

HIV/AIDS: Human immunodeficiency virus and acquired immune deficiency syndrome

HPLC: High-performance liquid chromatography

IAA: Iodoacetamide

IFN- γ : Interferon Gamma
IL: interleukin
IPA: Invasive pulmonary aspergillosis
iTRAQ: Isobaric tags for relative and absolute quantitation
ITS2: Internal transcribed spacer 2
kDa: Kilodaltons
L: Litre
LFQ: Label free quantification
LC: Liquid chromatography
M: Molar
MEA: Malt extract agar
MFS: major facilitator superfamily
mg: milligram
MIC: Minimum inhibitory concentration
Min: Minute
mL: Millilitre
mM: Millimolar
mm: Millimetre
mRNA: Messenger ribonucleic acid
MS: Mass spectrometry
MS/MS: Tandem mass spectrometry
NA: Nutrient agar
NADPH: Nicotinamide adenine dinucleotide phosphate
NF- κ B: nuclear factor-kappa B
nL: Nanolitre
OD: Optical density
OTU: Operational Taxonomic Unit
PAMP: Pathogen-associated molecular pattern
PBS: Phosphate buffered saline
PCA: Principal component analysis
PCN: Pyocyanin
PMSF: Phenylmethylsulphonyl fluoride
pH: Potential hydrogen
PRIDE: PRoteomics IDEntifications

ROS: Reactive oxygen species
rpm: Revolutions per minute
RPMI: Roswell Park Memorial Institute
RNA: Ribonucleic acid
rRNA: Ribosomal ribonucleic acid
SDB: Sabouraud dextrose liquid broth
SD: Standard deviation
SILAC: Stable Isotope Labeling by Amino Acids in Cell Culture
SLA class II: Swine Leukocyte Antigen class II
SSDA: Statistically significantly differentially abundant
STRING: Search Tool for the Retrieval of INteracting Genes/Proteins
TAFC: Triacetylfusarinine C
TB: Tuberculosis
TFA: Trifluoroacetic acid
TGF- β : Transforming Growth Factor beta
THP-1: Tohoku Hospital Pediatrics-1
TLCK: N-Tosyl-L-lysine chloromethyl ketone hydrochloride
TLR: Toll-like receptor
TMT: Tandem Mass Tag
TNF- α : Tumour necrosis factor alpha
tRNA: transfer ribonucleic acid
v: Volume
v/v: Volume per volume
w/v: Weight per volume
 μ g: Microgram
 μ L: Microliter
 μ M: Micromolar

Abstract

Aspergillus fumigatus represents an ever-present threat for vulnerable individuals as fungal conidia are ubiquitous and are inhaled daily. Infection occurs when optimal conditions are present resulting in a range of disease states, primarily in the context of preexisting lung damage and immunosuppression. Despite the threat this species imposes it appears to be an accidental pathogen as its primary niche is as a saprophyte in decaying plant matter. Survival in the soil has shaped *A. fumigatus* traits that facilitate survival in human host. This existence also equipped *A. fumigatus* with an array of effectors that have cross-reactivity through targeting of conserved mechanisms which can be repurposed to survive in the human body. The human lung is a terminal host for fungal development and dissemination and as such the fungus can only aim to survive but not disseminate. The lung represents a hostile environment consisting of challenges from the innate immune response, nutrient limitation and competition with microorganisms competing for the same limited resources. The rates of *A. fumigatus* infections are increasing globally, compounded by climate change and the rise in drug resistant strain. Despite the growing burden of disease, the mechanisms governing host adaptation and persistence remain poorly elucidated. To examine the host adaptation processes occurring in the lung, phenotypic and proteomic analysis of *A. fumigatus* growth in response to isolated aspects of this environment was performed.

Examination of *A. fumigatus* development using *Galleria mellonella* as an innate immune system analogue, patterns regarding fungal metabolic preferences and virulence factor production have been further characterised. Prolonged subculture of *A. fumigatus* within an agar system containing components of the immune response and the nutritional profile of *G. mellonella* identified reduced virulence and increased tolerance to oxidative stress and antifungal agents. These changes were governed by minor alteration to the fungal proteome, suggesting the requirements for survival as an environmental saprobe to persistence in a human host may not be a difficult transition. Examination of released fungal proteins *in vivo* in *G. mellonella* demonstrated an initial preference for carbon metabolism and an emphasis on amino acid metabolism in later stages of infection which may fuel the production of fungal secondary metabolites. Similar trends were observed in the *ex-vivo* pig lung (EVPL) model, an analogue of host lung tissue, where *A. fumigatus* induced immune activation and fibrosis within the tissue. Similar metabolic patterns and secondary metabolites were detected during colonisation in this model. Characterisation of fungal growth in response to bacterial lung pathogens identified secreted product of *Klebsiella pneumoniae* could induce secondary metabolite production including gliotoxin and inhibited fungal growth. Physical interaction with *P. aeruginosa* also demonstrated inhibited fungal development in the EVPL model. These studies provide key insight into the initial interaction of the fungus to its host and highlights key metabolic and fungal developmental factors integral to successful colonisation. These insights can be utilised in the development of next generation, more effective and specific antifungal agents to treat this deadly disease.

Chapter 1

Introduction

Partially adapted from:

Curtis, A., Binder, U. and Kavanagh, K., 2022. *Galleria mellonella* Larvae as a Model for Investigating Fungal-Host Interactions. *Frontiers in Fungal Biology*, 3, 893494.

Curtis, A., Oladimeji, F., Kavanagh, K. (2025). Models for Studying Fungal Pathogenesis. *Current Clinical Microbiology Reports*, **12**: 12.

Author Contributions

Curtis, A., Binder, U. and Kavanagh, K., 2022. *Galleria mellonella* Larvae as a Model for Investigating Fungal-Host Interactions. *Frontiers in Fungal Biology*, 3, 893494.

A.C, U.B and K.K wrote the manuscript. A.C and U.B generated the figures All authors have read and agreed to the published version of the manuscript. All material presented in the thesis was produced by A.C

Curtis, A., Oladimeji, F., Kavanagh, K. (2025). Models for Studying Fungal Pathogenesis. *Current Clinical Microbiology Reports*, 12: 12.

A.C, F.O and K.K wrote the manuscript. A.C generated the figures. All authors have read and agreed to the published version of the manuscript. All material presented in the thesis was produced by A.C

1.1 The Global burden of Fungal disease

Fungi comprise a eukaryotic kingdom of life that diverged from a common ancestor with animalia over 1 billion years ago (Wang *et al.*, 2023). Since this divergence this vast kingdom, ranging from single celled to complex multicellular organisms has impacted other organisms through complex relationships forged over evolutionary time (Bahram and Netherway, 2022). The vast reach of this kingdom can be partially attributed to the ability of its multicellular species to grow indefinitely as a cylindrical multinucleated cells known as hyphae. This morphology in addition to the extreme metabolic diversity observed in fungi enabled them to conquer numerous ecological niches (Naranjo-Ortiz and Gabaldón, 2019). Microorganisms, including bacteria and fungi compete in the soil and other niches, and as a result they have evolved diverse range of effector molecules and strategies dominate their competitors. These include antibiotics, toxic proteins and nutrient sequestering molecules (Granato *et al.*, 2019). These naturally occurring effectors have been harnessed and modified by humanity to combat life threatening diseases. Penicillin was first isolated from *Penicillium rubens* by Sir Alexander Fleming (Fleming, 1929). Other significant antibiotic classes isolated from fungi include cephalosporins, fusidans, fusafungin, and fumigacin (helvolic acid) (Sułkowska-Ziaja *et al.*, 2023).

Despite these benefits to humanity a small percentage of fungal species have the capacity to cause infections among vulnerable individuals. Among the estimated 2.2 to 3.8 million fungal species on Earth (Hawksworth and Lücking, 2017), only several hundred cause disease in immunocompromised patients, and fewer can affect immunocompetent individuals (Köhler *et al.*, 2015). This is often attributed to the coevolution of animals and fungi resulting in the development of a potent immune response as a result of constant exposure to microbes. This resistance to fungal pathogens observed in mammals is hypothesised to have created a “fungal filter” conveying evolutionary advantage to mammals enabling them to emerge as the dominant land species (Casadevall, 2012). Despite this, fungi have also adapted to overcome or persist in the presence of the immune response through growth in other host species including insects and amoebae before encountering and colonising humans hosts (Novohradská *et al.*, 2017). This co-evolutionary process has selected for fungi with adapted traits that facilitate persistence despite the hostile environment present in human hosts. Some of these pathogenic fungi are commensals, found in the gastrointestinal tract and mucosal surfaces such as members of the *Candida*

genus (Gow and Hube, 2012). These species can outcompete other commensals or overgrow following antibiotic therapy resulting in opportunistic infection (Kumamoto *et al.*, 2020). Others are environmental fungi that are inhaled or introduced to the body through wounds such as members of the *Mucorales* order and *Aspergillus* genus (Oliveira *et al.*, 2023).

The global burden of fungal disease is estimated to have an annual incidence of 6.5 million invasive fungal infections resulting in 3.8 million deaths, of which approximately 2.5 million were directly attributable to fungi (Denning, 2024). This would suggest that mortality associated with fungal disease is comparable to that of tuberculosis and 3 times higher than malaria (Bongomin *et al.*, 2017). The number of at-risk individuals for fungal disease is likely to increase as the numbers of susceptible patients with HIV/AIDS, tuberculosis (TB), chronic obstructive pulmonary disease (COPD), asthma and cancers have increased (Burke *et al.*, 2025; Goletti *et al.*, 2025; Boers *et al.*, 2023; Kim *et al.*, 2025; Siegel *et al.*, 2024). In addition, climate change has increased the geographical range of many fungal pathogens (George *et al.*, 2025). The evolution of thermotolerance, in response to rising environmental temperatures correlated with the rise in emerging fungal pathogens such as that observed in *Candida auris* (Nnadi and Carter, 2021). The growing prevalence of fungal disease highlights the pressing need to understand the factors governing pathogenesis and persistence in human hosts. This understanding can be employed to develop more effective and specific antifungal agents to bolster the dwindling supply of effective antifungal therapies in order to protect vulnerable cohorts and stave off the rising tide of fungal disease.

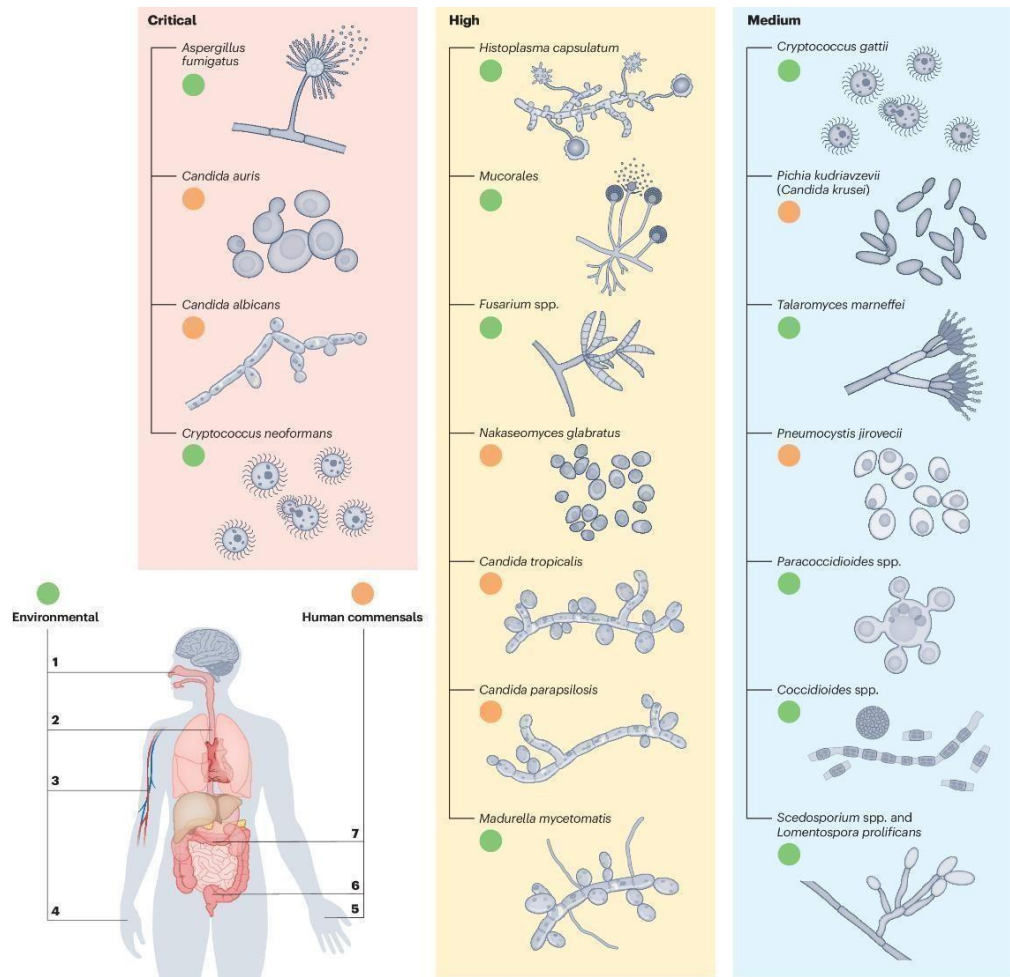


Figure 1.1: Fungal pathogens designated as critical, high and medium priority by the World Health Organisation marking their route of exposure as either commensal or environmental in nature published by (Brown *et al.*, 2019)

1.1.1 Host adaptation within fungi

Host adaptation can be defined as the ability of a pathogen to circulate and cause disease in a particular host population (Kingsley and Bäumler, 2000). This can include the assessment of factors such as colonisation, nutrient acquisition, and immune evasion (Barber and Fitzgerald, 2024). Host adaptation is typically shaped by the stressor and host antagonism that must be overcome in order for colonisation to be successful. Many fungal pathogens demonstrate traits indicating that host specific selection is occurring as exemplified by *Aspergillus flavus* whose genetic diversity significantly decreased following continued exposure to a host indicating host selection and genetic bottlenecking occurred (Scully and Bidochka, 2006). Other pathogens display specific immune evasion processes such as capsule shedding by *Cryptococcus neoformans* which was serial passaged in *Galleria mellonella* larvae resulting in downregulation of host haemocyte hydrogen peroxide production (Ali *et al.*, 2020).

Candida species, which are often commensals in the human body regulate specific sets of genes, associated with stress mitigation and metabolic pathways, in order to thrive in the human host. In addition to conferring metabolic flexibility and stress resistance, physiological reprogramming has been associated with enhanced virulence through impaired immune recognition, increased biofilm formation, and acquired antifungal tolerance (Alves *et al.*, 2020). Understanding how these factors change in response to a host can provide insights into microbial strategies for colonisation and provide targets for more effective therapeutics. Similar host- adaptation strategies may be utilised by *Aspergillus fumigatus* during development in humans hosts and understanding these is crucial to overcoming its impact.

1.2 *Aspergillus fumigatus*

Aspergillus fumigatus is a filamentous fungus belonging to the subphylum Pezizomycotina, a group characterized by septate hyphae, each with a specialized pore and the ability to produce woronin bodies that can seal the pore if hyphae are damaged (Beck *et al.*, 2013). The natural niche of *A. fumigatus* is composting plant-waste material in the soil, which is known to contribute to the species thermotolerance, up to 70°C (Zhang *et al.*, 2022). This fungus is highly evolved for success in colonising soil and withstanding competition, providing some strains with the ability to colonise and cause disease in a compromised human or animal hosts upon entering the lungs (Paulussen *et al.*, 2016). *A. fumigatus* produces small asexual conidia that are readily dispersed in the environment, producing dense clouds of conidia containing up to 1×10^8 conidia per cubic meter (Schiefermeier-Mach *et al.*, 2025). *A. fumigatus* conidia are ubiquitous in the air and are found in all environments (Rhijn *et al.*, 2025). Disturbance of soil such as construction work can increase the exposure risk and rate of aspergillosis since conidia are well adapted for airborne dissemination (Talento *et al.*, 2019). The average size of these conidia is between 2 to 3 μm and it is estimated that the average human inhales hundreds of *Aspergillus* conidia daily (Takazono and Sheppard, 2017). The small size of the conidia facilitates deep penetration into the alveoli, whereas larger conidia of other fungi are readily removed by mucociliary clearance (Dagenais and Keller, 2009). *A. fumigatus* is an opportunistic pathogen of the human airway in specific patient cohorts but the process from development in the soil to persistence in the human body remains poorly elucidated.

1.2.1 Clinical manifestations of *Aspergillus fumigatus* infection

A. fumigatus has been listed as a critical threat pathogen alongside *Candida albicans*, *Candida auris* and *Cryptococcus neoformans* (Figure 1.1) (WHO, 2022). *A. fumigatus* infection is primarily initiated following inhalation of fungal conidia followed by the host's failure to clear the fungal burden. *A. fumigatus* is one of a few pathogens that can cause a range of clinical manifestations at both ends of the immune spectrum (Moldoveanu *et al.*, 2021). There are three broad categories of pulmonary aspergillosis: allergic aspergillosis of which one form, Allergic bronchopulmonary aspergillosis (ABPA) is the most studied example, chronic pulmonary aspergillosis (CPA) and invasive pulmonary aspergillosis (IPA). The manifestation of disease is heavily influenced by the underlying host characteristics and the interaction between the fungus and the host and impacts on the lung can be distinguished through radiographical imaging (Figure 1.2) (Kanaujia *et al.*, 2023). The widespread use of chemotherapeutic and immunosuppressive agents has resulted in increased ambiguity between these categorisations, resulting in increased overlap in their characteristics in some cohorts (Kanj *et al.*, 2018).

Allergic bronchopulmonary aspergillosis has an estimated global burden of 4.8 million people (He *et al.*, 2025). ABPA is characterised by hypersensitivity to *A. fumigatus* and is prevalent in patients with cystic fibrosis or asthma. The prevalence of ABPA is increased in patients with cystic fibrosis that have *Pseudomonas aeruginosa* in their sputum (Tarizzo *et al.*, 2025). Such patients are susceptible due to compromised mucus clearance and airway obstruction which may favour germination of conidia and release of antigens resulting in airway inflammation and pathology (Lv *et al.*, 2021). The immune response in ABPA is driven by T-helper cell-2 responses which do not eliminate *A. fumigatus* but drives acute but persisting inflammation associated with CXCR4+ granulocytes (Chatterjee *et al.*, 2024). Failure to diagnose ABPA can result in preventable and irreversible lung damage, such as bronchiectasis and “honeycomb” pulmonary fibrosis (Greenberger, 2013).

Unlike acute forms of aspergillosis including allergic and invasive infections which typically impact individuals with altered immune states, chronic pulmonary aspergillosis is a saprophytic infection that can impact immunocompetent individuals. Infected individuals are typically asymptomatic but have developed fungal masses in preexisting lung cavities and in rare cases these infections can progress into invasive

fungal disease (Pathak *et al.*, 2011). It has been estimated that 1,837,272 cases of CPA arise annually from previous pulmonary tuberculosis cases. Moreover, approximately 340,000 patients with CPA die within the first year of disease onset (Tashiro *et al.*, 2024) and impacts many more with other conditions characterised by lung damage (Denning *et al.*, 2011). Lung cancer patients are also a vulnerable cohort with saprophytic fungal disease compounding lung pathology resulting in profound restrictive lung function and deterioration (Kim *et al.*, 2022).

Chronic pulmonary aspergillosis has several distinct clinical manifestations including aspergilloma, chronic cavitary pulmonary aspergillosis, chronic fibrosing pulmonary aspergillosis, Aspergillus nodules, and subacute invasive aspergillosis (Denning *et al.*, 2016). These forms vary from one another, but all have a poor prognosis with a 1-year mortality rate ranging from 7-32% and a 5-year mortality range of 38-52% (Tashiro *et al.*, 2024). Chronic infection and colonisation are initiated by conidial attachment and germination within damaged lung tissue. Conidia adhere to fibrinogen and laminin which are known to be deposited on wounded surfaces. Fungal attachment to these components is partially mediated by sialic acid residues and other proteins on the conidial surface (Santos *et al.*, 2023). Following attachment, the fungus germinates inducing an inflammatory response but does not typically invade surrounding healthy tissue. Fungal hyphae, mucus and cellular debris contained within a fibrotic and thickened wall form a mass known as an aspergilloma, which becomes mobile within the cavity which can result in haemoptysis in patients (Tunnicliffe *et al.*, 2013).

Invasive pulmonary aspergillosis is the most severe form of infection, resulting in rapid growth, invading healthy tissue and blood vessels and disseminates into numerous body sites (Challa, 2018). This form of disease primarily impacts severely immunocompromised patients, but also in critically ill patients and those with chronic obstructive pulmonary disease (Bao *et al.*, 2017). Annually, over 2.1 million people develop invasive aspergillosis associated with chronic obstructive pulmonary disease, intensive care admittance, lung cancer, or haematological malignancy, with a crude annual mortality of 85.2% (Denning, 2024). The incidence of invasive disease is growing as the numbers of at-risk patients with impaired immune status continues to increase. Vulnerable cohorts include individuals with neutropenia, haematopoietic Stem Cell and solid-organ transplantation, prolonged therapy with high-dose

corticosteroids, haematological malignancy, cytotoxic therapy, advanced HIV/AIDS and chronic granulomatous disease (CGD) (Kousha *et al.*, 2011).

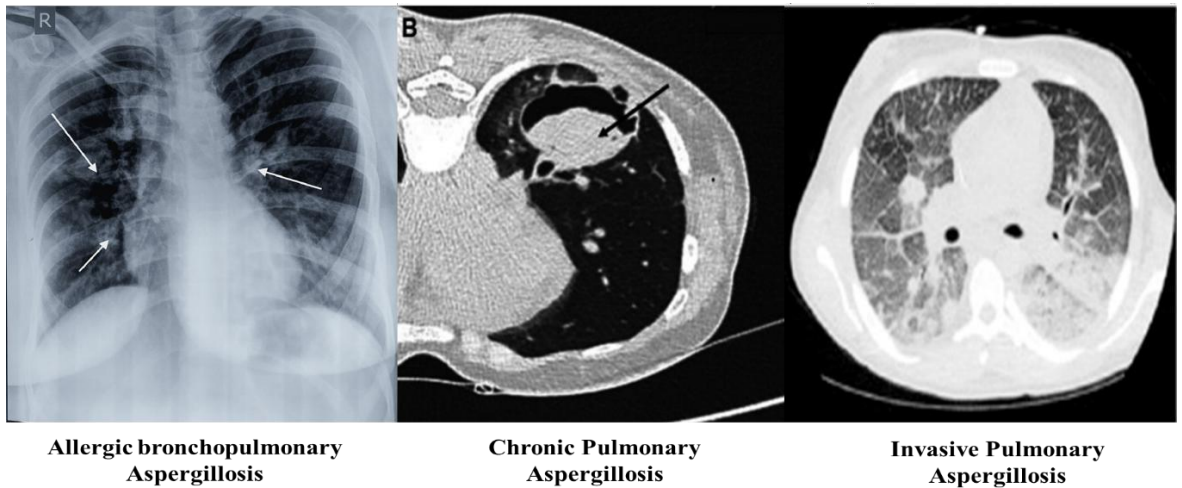


Figure 1.2: Radiographical images of different forms of pulmonary aspergillosis adapted from (Singh *et al.*, 2023; Garg *et al.*, 2022 and Panse *et al.*, 2016).

1.2.2 Host immune response to *Aspergillus fumigatus*

The host elicits a range of defence mechanisms to mitigate the risk of infection upon inhalation of *A. fumigatus* conidia. These defences include physical barriers such as ciliated epithelial and mucus secreting cells that line the upper airways (Hewitt and Lloyd, 2021). The majority of inhaled conidia are trapped in the mucus produced by goblet cells and then actively transported by the beating of cilia for clearance by swallowing or expelled by coughing (Kuek and Lee, 2020). In addition, conidia can be phagocytosed and killed by host cells including epithelial cells which vastly outnumber professional phagocytic cells such as macrophages (Ben-Ghazzi *et al.*, 2021). Epithelial cells can activate an immune response as demonstrated by human bronchial epithelial cells which induce a time-dependent synthesis of interleukin-8 in response to germinated *Aspergillus* elements but not resting conidia (Bigot *et al.*, 2020). Conidia that bypass this barrier interact with type I and II pneumocytes in the alveoli. Type II pneumocytes secrete pulmonary surfactants (Cerrada *et al.*, 2015). Surfactant protein D plays a crucial role in host immunity and has been demonstrated to enhance the clearance of inhaled conidia and specifically is protective against both allergic and invasive aspergillosis (Geunes-Boyer *et al.*, 2010). Surfactant D reduces fungal growth and weakens the surface of fungal hyphae by increasing its permeability (Wong *et al.*, 2022). In addition, alveolar epithelial cells can bind to and phagocytose fungal conidia and stimulate a pro-inflammatory response through generation of IL-6

and CXCL8 (Paplińska-Goryca *et al.*, 2013).

Innate immune cells resident in the respiratory tract include alveolar macrophages and recruited neutrophils which can clear fungal conidia. Alveolar macrophages can phagocytose and degrade swollen conidia in the phagolysosomal compartment, preventing germination (Margalit and Kavanagh, 2015). Polymorphonuclear neutrophils constitute the largest population of intravascular phagocytes, the vascular network of the lung, particularly the capillaries are a reservoir of neutrophils, containing 40% of the body's total neutrophils (Anderson *et al.*, 2014). Neutrophils are recruited to the lung following stimulation by fungal cell wall components but also the release of chemokines from alveolar macrophages such as CXCR2 and CXCL1 (Toya *et al.*, 2024). Recruited neutrophils can phagocytose fungal conidia but can also eliminate *A. fumigatus* hyphae, by releasing the contents of their granules into the extracellular space. The primary granules released by neutrophils contain high concentrations of enzymes such as myeloperoxidase, elastase and cathepsin G (Sheshachalam *et al.*, 2014). Secondary granules contain lactoferrin, neutrophil gelatinase-associated lipocalin, cathelicidin, and lysozyme (Heinekamp *et al.*, 2015). These extracellular molecules have potent effects resulting in *A. fumigatus* clearance (Prüfer *et al.*, 2014). These mechanisms along with the release of extracellular nets during NETosis enable inhibition of *A. fumigatus* following germination when the fungus is too large to phagocytose (McCormick *et al.*, 2010).

Importantly, opsonization, phagocytosis and killing by neutrophils is complement cascade dependent. The complement cascade is a series of tightly regulated reactions that occur in the blood resulting in pathogen clearance (Vandendriessche *et al.*, 2021). The complement cascade can be activated through three major routes: classical, alternative and lectin pathways (Figure 1.3). Dormant conidia trigger the alternative pathway while exposure of cell wall polysaccharides as the conidia germinate triggers the classical/lectin pathway (Delliére and Aimanianda, 2023). The classical complement pathway is the main initiator of complement activation on *A. fumigatus* swollen conidia and germ tubes (Braem *et al.*, 2015). C1q is the target recognition protein of the classical complement pathway which indirectly recognizes pathogens through bound antibodies. The C1 complex is necessary to activate C4 and C2 leading to C3 convertase (van de Bovenkamp *et al.*, 2021). C3

Convertase is a central step in the complement cascade as it activates C3 into C3b and C3a. C3b opsonizes *A. fumigatus* dormant conidia through RodA-rodlets and mycelia by binding to cell wall β -glucan and galactomannan (Wong *et al.*, 2020). C5a and C5b are generated through cleavage of C5 by C5 convertase at a common checkpoint to all complement pathways. C5 cleavage could also result from a non-canonical pathway triggered by *A. fumigatus* swollen conidia or hyphae (Shende *et al.*, 2022).

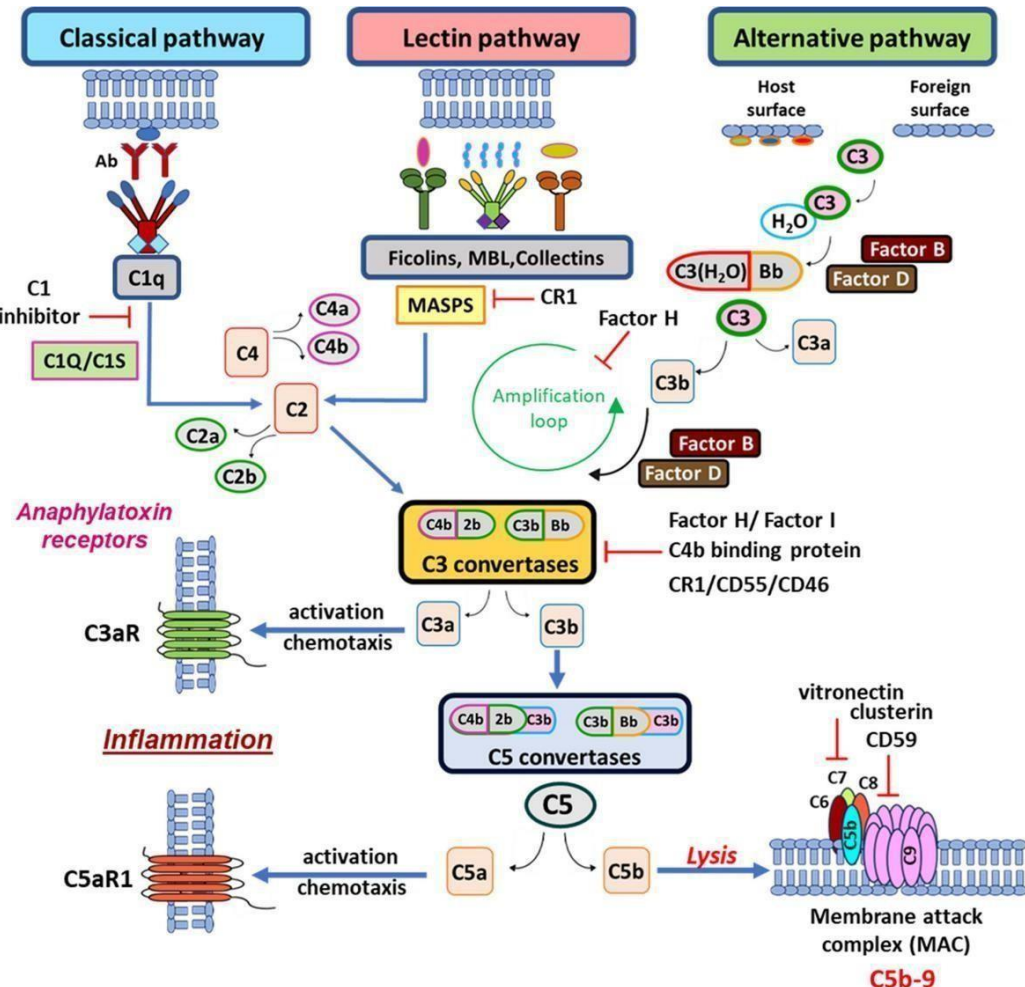


Figure 1.3: Schematic of the Human complement cascade published by (Detsika *et al.* 2024)

Dendritic cells and other professional antigen presenting cells bridge the innate and adaptive immune response against *A. fumigatus* by activating naïve CD4⁺ T-cells and triggering their differentiation into different lineages of effector cells following MHC class II activation and activity of secreted molecules (Ramirez-Ortiz and Means, 2012). Following stimulation with *A. fumigatus* conidia, dendritic cells trigger the production of IL-12, which is the main cytokine inducing IFN γ -producing T-cells (Gilmour *et al.*, 2024). Different subsets of dendritic cells have distinct responses to

the fungus producing pro-inflammatory cytokines IL-1 β , TNF α , chemokines IL-8, CXCL1, as well as anti-inflammatory cytokines IL-4 and IL-10 specifically upon stimulation with hyphae (Shankar *et al.*, 2024). TNF α released by dendritic cells can determine whether Th17 or Th2 responses are induced leading to either neutrophil or eosinophil-mediated inflammation (Dewi *et al.*, 2017). A small number of conidia bypass the innate immune response to establish infection; the adaptive immune response provides further protection against these remaining conidia. Though less thoroughly examined, the role of the adaptive immune response to *A. fumigatus* appears to primarily bolster the innate response including the role of T-helper 1 cells in macrophage polarisation to a proinflammatory M1 phenotype (Mills, 2015). This feeds back to activate T cells through IL-12 production and antigen presentation (Muraille *et al.*, 2014). T-helper 1 cells protect the host primarily through production of IFN γ which drives the activity of the innate immune cells (Ivashkiv, 2018).

Invasive *Aspergillus* infection alters the population dynamics of T cells leading to a reduction in the percentage of cytotoxic CD8 $^{+}$ and CD28 $^{+}$ CD8 $^{+}$ T-cells associated with higher risk and early mortality (Cui *et al.*, 2013). Th17 T helper cells, known for their role in pro-inflammatory cytokine production also plays an important role in host defence against microorganisms, which is associated with neutrophil migration and increased inflammation (Fan *et al.*, 2023). There is a fine balance between proinflammatory T-helper 1 and anti-inflammatory T-helper 2 populations in response to *A. fumigatus* that still is not fully elucidated in response to disease. The T- helper 2 response is characterized by production of IL-4, IL-5, IL-13 and IL-10, which mediate anti-inflammatory responses, allergy, and fungal persistence in the lungs (León, 2023). B-cells are thought to play a less prominent role in the response to *A. fumigatus* as evidenced by the lack of literature examining their interactions. Studies in B cell-deficient mice which were infected with *A. fumigatus* demonstrated an element of passive immunity through transfer of antibodies but a compensatory increase in both innate and Th1-mediated resistance to infection was seen in B cell deficient mice (Singh *et al.*, 2021). Despite this some studies have described B cell activation and antibody production following *A. fumigatus* exposure (Boita *et al.*, 2015). The host immune response can also indirectly produce a hostile environment for *A. fumigatus* through increased temperature, production of antimicrobial peptides and production of reactive oxygen species (Duarte-Mata and Salinas-Carmona, 2023). The products are generated through the activity of enzymes. Enzymes involved in the production

of reactive oxygen species during phagocytosis include myeloperoxidase (MPO) and nicotinamide adenine dinucleotide phosphate (NADPH) oxidase resulting in production of hypochloric acid and superoxide anions, respectively. These molecules are cytotoxic and result in clearance of *A. fumigatus* (Ulfig and Leichert, 2021).

1.2.3 *Aspergillus fumigatus* virulence factors

Despite the robust immune defences present in the host *A. fumigatus* remains capable of colonisation and growth within human hosts. *A. fumigatus* has been classified as an “accidental pathogen” as its evolution in its soil niche have equipped it with a vast arsenal of effectors that also impact colonisation within human hosts (Figure 1.4) (Price *et al.*, 2024). This understanding arises from the fact that *Aspergillus* species are not dependent on their hosts for survival and that humans are a terminal host as the fungi cannot complete their life cycle inside this host (Lee *et al.*, 2016). This indicates that their pathogenic effects are potentially accidental or opportunistic. To understand the evolution of pathogenicity in the *Aspergillus* genus, examination of traits that facilitate survival in the soil can provide insight into how some of them have rendered a few species capable of establishing infections in human hosts (Rokas *et al.*, 2020). There is still debate regarding if these mechanisms represent human host adaptation or if the fungus can employ these adaptations from the soil to persist in a new hostile environment.

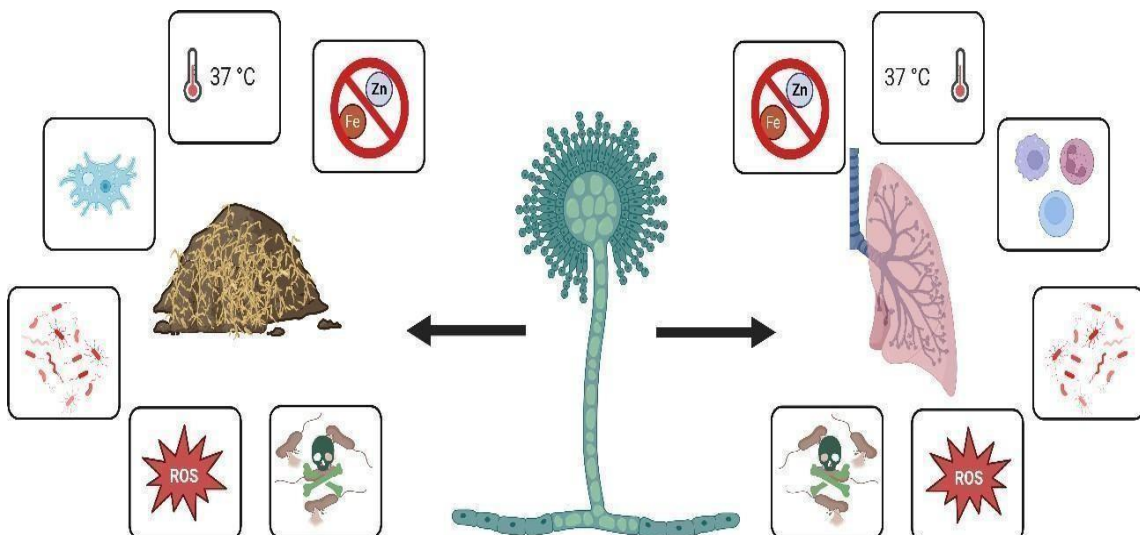


Figure 1.4: Forms of stress and competition in both the soil niche and the human airways highlighting the similarities in these environments (generated in Biorender)

A. fumigatus displays remarkable intrinsic thermotolerance and unlike other *Aspergillus* species, *A. fumigatus* can germinate under temperatures above 40°C, and its conidia remain viable up to 70°C (Fabri *et al.*, 2021). This ability allows *A. fumigatus* to persist in the environment and is an essential determinant for its pathogenicity since it allows the fungus to develop at temperatures found before and during the infection of mammalian host and favours the persistence within the human lungs even at febrile temperature (Haas *et al.*, 2016). Thermotolerance has been attributed to the transcription factor HsfA which is increased in expression at 37°C and contributes to cell wall maintenance reinforcing the role the cell wall plays in thermotolerance. This transcription factor also displays cross talk with heat shock proteins and the cell wall integrity pathway during the cell wall and heat stresses while also modulating lipid metabolism and iron homeostasis (Fabri *et al.*, 2021).

Adhesion to host tissue is an integral aspect of fungal virulence and is the first step of host colonisation. This interaction is primarily driven by sugar moieties on the surface of fungal conidia including the hydrophobic Rodlet layer which mediates adherence to host collagen (Croft *et al.*, 2016), which is deposited during fibrosis (Jessen *et al.*, 2021). Conidial adhesion has also been attributed to laminin binding facilitated by the extracellular thaumatin domain protein AfCalAp (Upadhyay *et al.*, 2009). There are many identified fungal adhesins including Asp f2 and a repeat-rich glycophosphatidylinositol-anchored cell wall protein, encoded by the CspA gene (Levdansky *et al.*, 2010). In addition to adhesins secreted galactosaminogalactan and exopolysaccharide from hyphae can drive adherence to the host. Galactosaminogalactan requires deacetylation mediated by Agd3 for fungal adhesion and full virulence. Galactosaminogalactan mediated adhesion is regulated through the action of fungal epimerase uge3 and mediates adhesion to plastic, fibronectin and epithelial cells (Gravelat *et al.*, 2013), it is also an essential component of the extracellular matrix making it important for biofilm formation (Earle *et al.*, 2023).

Tolerance to stresses experienced within the host including the immune response and oxidative stress are essential to fungal development in the host, these responses are often specific, multilayered and in many cases are evolutionarily conserved (Yaakoub *et al.*, 2022). Macrophages serve as the first line of defence against *A. fumigatus* and phagocytose fungal spores and inhibiting spore germination to prevent the development of tissue-invasive hyphae through production of reactive oxygen species (Tanner and Rosowski, 2024; Hatinguais *et al.*, 2021). Several factors

influence this interaction and *A. fumigatus* has been demonstrated to manipulate the host response to promote its own development. When *A. fumigatus* conidia are phagocytosed it induces mechanisms to protect itself including hyphal germination and production of dihydroxynaphthalene (DHN)-melanin to mitigate oxidative stress (Heinekamp *et al.*, 2013). In alveolar macrophages germination and growth of conidia are significantly impaired, however about 60% of conidia and germlings can persist when surrounded by the host phagolysosome membrane and are not acidified, enabling hyphal development. The hyphae then escape in a non-lytic manner by fusing to the host plasma membrane (Seidel *et al.*, 2020). The production of DHN-melanin has also been attributed to the survival in this harsh environment. This pigment is found in the outer layer of the conidial cell wall and interferes with endocytosis and acidification by impacting Rab5- and Vamp8-mediated endocytic trafficking, and cathepsin recruitment (Amin *et al.*, 2014). Melanin's mechanism of action has been attributed to remodelling the intracellular calcium machinery and preventing signalling through calmodulin. This process stimulates glycolysis and hypoxia inducible factor 1 resulting in fungal survival by blocking phagosome biogenesis and acidification of phagolysosomes (Gonçalves *et al.*, 2020).

Iron sequestering is essential for microbial growth and survival and to accomplish this *A. fumigatus* produces four siderophores, fusarinine C and its derivative triacetyl fusarinine C are secreted for iron scavenging and acquisition and intracellular ferrichrome-type siderophores ferricrocin and hydroxyferricrocin for iron storage and handling (Misslinger *et al.*, 2021). Siderophores may also play an important role in microbial warfare as chelation of environmental iron by siderophore-types that are not recognized by competitors might be used to starve competitors of iron (Haas, 2012). Iron sequestering can serve as a form of immunometabolism and can protect fungal conidia from host macrophages. *A. fumigatus* affects the regulation of macrophage iron homeostasis and innate immune effector pathways through production of iron chelating molecules called siderophores, resulting in increased survival following phagocytosis (Seifert *et al.*, 2008). In addition, siderophore-mediated iron acquisition has been shown to be essential for virulence and is involved in fungal survival in peroxisomes and endosome-like vesicles (Moore, 2013).

A. fumigatus also produces a suite of mycotoxin effectors that evolved as a result of microbial competition in the soil (Figure 1.5) (Pflieger *et al.*, 2020). The

targets of these toxins are highly conserved and as a result it is postulated that this conservation results in toxic effects on human cells, thus impacting fungal virulence. Several conidial and hyphal mycotoxins have been well characterised including gliotoxin, fumagillin, helvolic acid and Asp-hemolysin (Paulussen *et al.*, 2016). *A. fumigatus* can also produce a range of alkaloids, terpenes, sterols, quinones and benzophenones including less studied toxins such as fumitremorgin and fumigaclavine (Ibrahim *et al.*, 2025). These toxins have various effects in the soil and in the host and can aid in fungal persistence in the host.

Gliotoxin is the most studied mycotoxin produced by *A. fumigatus* and is a hydrophobic metabolite belonging to the Epidithiodioxopiperazine class of compounds. The mechanism of action is not fully understood but is thought to be associated with a disulfide bridge across the piperazine ring, which is essential for its toxicity (Scharf *et al.*, 2016). Gliotoxin is recognised as a virulence factor and has been demonstrated to inhibit the activity of phagocytes and decrease the cytotoxic effects of T cells (Günther *et al.*, 2024; Ye *et al.*, 2021), however the specificity of this response is not well characterized. The connection to virulence and persistence in the host is compounded by the fact that 90% of clinical isolates from cancer and invasive aspergillosis patients produce gliotoxin, and rapid gliotoxin production is observed at 37°C under conditions similar to the host lung environment (Gayathri *et al.*, 2020).

The production of gliotoxin is heavily influenced by zinc availability and is produced under zinc-limiting conditions. Dithiol gliotoxin has been demonstrated to have zinc-chelating properties (Traynor *et al.*, 2021). This ability has been attributed to its cytotoxic effects of gliotoxin as it can sequester zinc from the environment resulting in starvation by neighbouring cells or directly strip zinc, iron and copper from bacterial species and potentially host cells (Downes *et al.*, 2023).

Fumagillin is a meroterpenoid toxin produced by hyphae that is known for its anti-angiogenic activity by binding to human methionine aminopeptidase (Lin *et al.*, 2013). Fumagillin contributes to tissue damage during invasive aspergillosis and thus it is probable that *A. fumigatus* progression through the lungs is supported through its production, combined with the secretion of lytic enzymes that allow fungal growth, angioinvasion and the disruption of the lung parenchymal structure (Guruceaga *et al.*, 2018). Fumagillin is produced in the early stages of colonisation and aids in evasion of the host immune response. Fumagillin inhibition of the NADPH oxidase complex

formation in neutrophils resulting in reduced superoxide production and degranulation (Fallon *et al.*, 2010). Some studies also suggest that gliotoxin and fumagillin work synergistically as glutathione, the hall mark of cellular redox homeostasis, is affected by both mycotoxins resulting in the generation of intracellular reactive oxygen species inducing apoptosis (Gayathri *et al.*, 2020).

Pseurotin A is a unique spiro-heterocyclic γ -lactam alkaloid isolated from *A. fumigatus* (Abdelwahed *et al.*, 2020), which has been demonstrated to induce immunomodulatory effects in the host by inhibiting immunoglobulin E function in response to hypoxic conditions (Ghazaei, 2017). *A. fumigatus* also produces ergot alkaloid compounds including festuclavine and fumigaclavine A, B and C present on fungal conidia (Robinson and Panaccione, 2015). Fumigaclavine C has been demonstrated to have potent anti-inflammatory properties including inhibiting the expression of s IL-1 β , IL-2, IL-12 α , IFN- γ , TNF- α in lymph node cells. In addition, it can attenuate TNF α production *via* the TLR4-NF κ B signalling transduction pathway by decreasing expression of the p65 subunit of NF- κ B (Bailly and Vergoten, 2020). Fumitremorgens are less studied ergot alkaloids derived from tryptophan, proline and mevalonic acid (Li, 2011). It has been reported that fumitremorgin A, B and C are neurotropic toxins that cause tremors, seizures, and abnormal behaviour in mice (Abad *et al.*, 2010). Helvolic acid, produced by *A. fumigatus* is a potent antibacterial compound (Kong *et al.*, 2018) which conveys advantage in the soil niche but has a dual function in slowing cilia beat frequency in the host reducing fungal clearance in a similar manner to gliotoxin and fumagillin (Kuek and Lee, 2020). The factors influence fungal persistence and virulence and protect the fungus from the effectors of the host immune response.

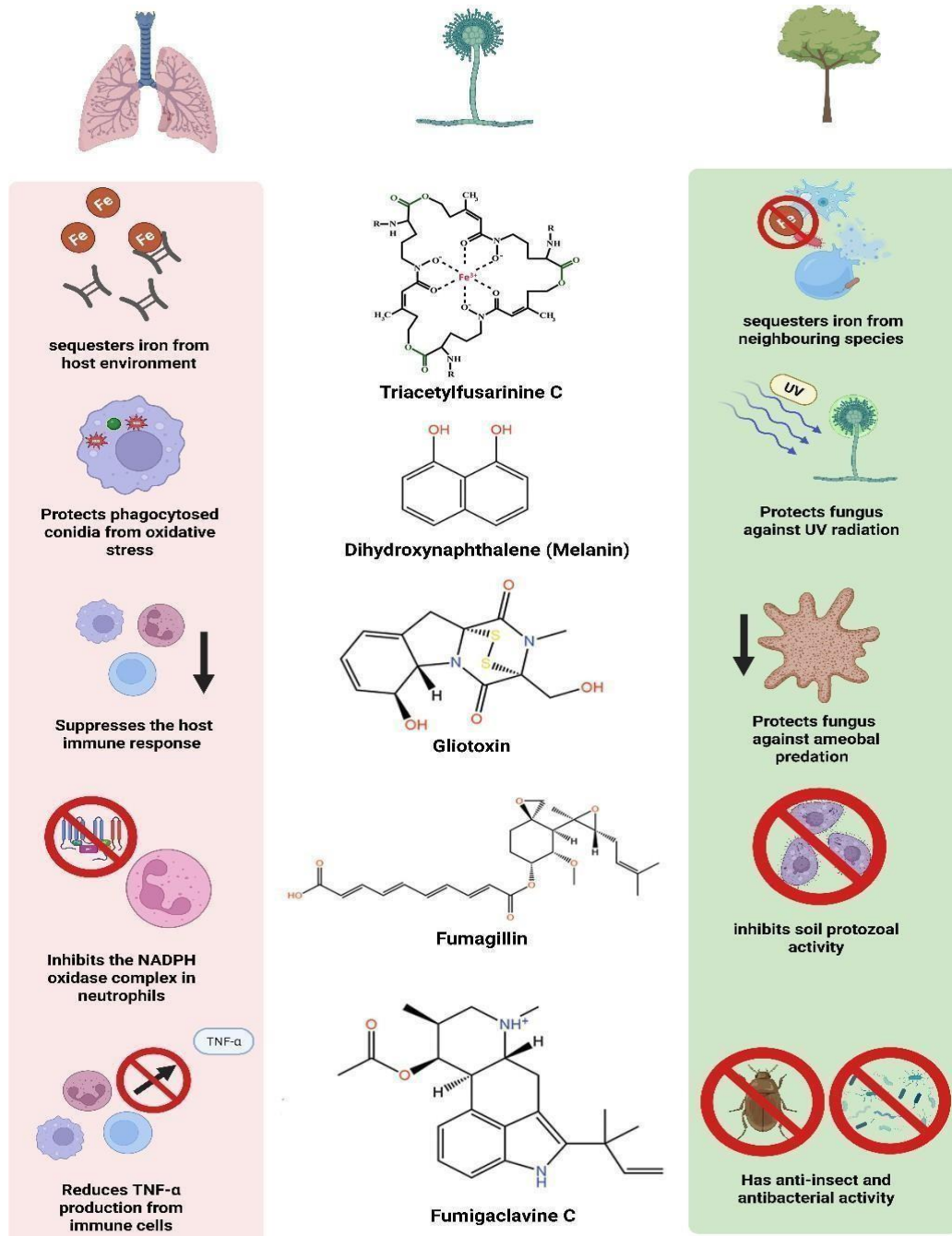


Figure 1.5: The role of selected secondary metabolites produced by *A. fumigatus* in the environment and in the human lung adapted from figure published by (Raffa *et al.*, 2019).

1.2.4 *Aspergillus fumigatus* response to stress

The development of *A. fumigatus* in hostile environments, both in the soil and in a human host requires adaptation and mechanisms to mitigate against various forms of stress including hypoxic, osmotic and oxidative stresses (Ross *et al.*, 2021). Many of these stressors are likely to be encountered in the host including hypoxia in damaged tissue following inflammation and necrosis (Gresnigt *et al.*, 2016). To persist in this hypoxic environment the sterol regulatory element binding protein pathway which is regulated by the transcription factor SrbA is activated. This transcription factor is crucial for antifungal drug resistance and virulence as loss of SrbA results in complete loss of virulence in murine models of invasive pulmonary aspergillosis (Chung *et al.*, 2014). In low oxygen environments *A. fumigatus* has also been observed to increase expression of ergosterol biosynthetic genes and genes involved in cell wall maintenance (Puerner *et al.*, 2023).

To mitigate oxidative stress, typically induced by innate immune cells during infection, several effectors and enzymes are produced by the fungus including catalases, superoxide dismutases, elements of the thioredoxin and glutathione-glutaredoxin system, as well as the conidial pigment melanin. Importantly, oxidative stress response and iron metabolism are tightly linked (Emri *et al.*, 2024). Iron overload can induce the formation of reactive oxygen species, but detoxification of these species through production of heme peroxidases, requires heme as a cofactor (Kurucz *et al.*, 2018). Oxidative stress mitigation can also fuel virulence as evidenced by *oxrA* which regulates catalase production in *A. fumigatus*. Deficiency of *oxrA* decreased the virulence of *A. fumigatus* and altered the host immune response resulting in reduced tissue damage (Zhai *et al.*, 2021). Alterations to the mitochondrial electron transport chain can also influence susceptibility to oxidative stress and virulence. Loss of cytochrome C demonstrates increased resistance to external reactive oxygen species and macrophage killing while loss of alternative oxidase increased susceptibility to external reactive oxygen species and *in vitro* macrophage killing at the expense of virulence capacity (Grahl *et al.*, 2012).

Many substances target the fungal cell membrane or cell wall to damage the fungus. This type of stress is mitigated in fungi by the action of several conserved components: the cell integrity pathway, the HOG-MAPK cascade, which has evolved to compensate for osmotic stress, and the TOR and calcineurin phosphatase signalling

pathways (Hartmann *et al.*, 2011). *A. fumigatus* MpkC and SakA, the homologs of the *Saccharomyces cerevisiae* Hog1 are important to adaptations to oxidative and osmotic stresses, heat shock, cell wall damage, macrophage recognition, and full virulence. They also play a role in the regulation of the response to cell wall damage, oxidative stress, drug resistance, and establishment of infection (Manfiolli *et al.*, 2019). These factors and systems enable fungal persistence in host microenvironments and make it successful in various niches.

1.2.5 *Aspergillus fumigatus* metabolism

A. fumigatus is a successful species in a variety of niches which can be in part attributed to its metabolic flexibility, being able to thrive in diverse conditions and recycling organic carbon and nitrogen sources in its soil and persisting in the nutrient limited human body (Cramer, 2015). Nutritional versatility along with the evolution of means to acquire and utilise a wide array of nutrient sources during infection represent fundamental aspects of *A. fumigatus* pathogenicity (Feng *et al.*, 2011). During invasive growth, the nutritional microenvironment can rapidly change depending on the stage of the infection (Obar *et al.*, 2016). There is strong evidence that *A. fumigatus* can sustain itself and thrive in infected tissue, exploiting the lung as sole source of nutrients (Amich and Krappmann, 2012). This metabolism is partially driven by the release of enzymes and effectors such as siderophores to scavenge iron and the use of various transporter systems to enable the effective uptake and breakdown of products (Yoon *et al.*, 2009).

Host carbon sources used by *A. fumigatus* include glucose, lactate and acetate, whose availability largely depends on the host niche. In addition, potential nitrogen sources can also be broken down to be used as carbon sources and are available throughout the human host mainly in the form of proteins (Ries *et al.*, 2018). Acetate is present in the body fluids and peripheral tissues and is metabolised under the regulation of the FacB transcription factor which is subject to carbon catabolite repression (Ries *et al.*, 2021). Acquisition and subsequent metabolism of different carbon and nitrogen sources plays a crucial role in virulence of *A. fumigatus*, including the secretion of host tissue-damaging proteases and fungal cell wall integrity (Ries *et al.*, 2019). Gliotoxin production has also been identified to be stimulated through access to simple, fermentable sugars such as glucose. An additional potential source of carbon is *via* the glyoxylate cycle. This pathway allows organisms to

use lipids for the synthesis of carbohydrates to fuel development (Willger *et al.*, 2009).

Another source of nutrients utilised by *A. fumigatus* during infection is amino acids. Fungal amino acid biosynthesis mediated by the Cross-Pathway Control system, a conserved regulatory circuit evolved to counteract conditions of nutritional stress (Bultman *et al.*, 2017). This pathway can compensate for nutrient starvation by degradation of host proteins to acquire amino acids for protein biosynthesis (Krappmann and Braus, 2005). Fungi acquire amino acids from their environment either by transport processes, from precursors, which are derivatives of carbon and nitrogen primary metabolism, or from degradation of proteins which are no longer required under specific conditions or from destruction of host tissue (Braus *et al.*, 2004). Amino acid degradation through the methylcitrate cycle, essential for the degradation of propionyl-CoA, which is a degradation product of valine, methionine and isoleucine (Brock and Buckel, 2004) significantly influences fungal survival and virulence (Maerker *et al.*, 2005). Methionine, a source of sulphur ions metabolism has been demonstrated to alter fungal growth and virulence (Scott *et al.*, 2020). Degradation of tryptophan to kynurenes by Indoleamine 2,3-dioxygenases can drive the *de novo* synthesis of nicotinamide adenine dinucleotide under hypoxia or tryptophan abundance (Zelante *et al.*, 2021).

A. fumigatus produces all three aromatic amino acids through the shikimate–chorismate pathway (Figure 1.6), this pathway is not found in higher eukaryotes and has been considered a viable target for antifungal therapy (Choera *et al.*, 2018). This pathway converts phosphoenolpyruvate and erythrose 4-phosphate to chorismate which is a precursor to the synthesis of a variety of aromatic compounds, such as p-aminobenzoic, 2,3-dihydroxybenzoic, prephenic and anthranilic acids (Khedr *et al.*, 2018). These amino acids are not only essential for growth and development but also the production of virulent secondary metabolites of the fungus. Pentafunctional AROM polypeptide interconverts metabolites of quinic acid in the shikimate pathway, to produce aromatic amino acids. Corruption of this pathway results in attenuated virulence in murine studies (Sasse *et al.*, 2016). This confirms the importance of this pathway in *A. fumigatus* virulence and the drive in production of secondary metabolites harmful to the host. The downstream metabolites of tryptophan in *A. fumigatus* include the immunomodulatory kynureneine derived from indoleamine 2,3-

dioxygenase and toxins such as fumiquinazolines, gliotoxin, and fumitremorgins (Choera *et al.*, 2018).

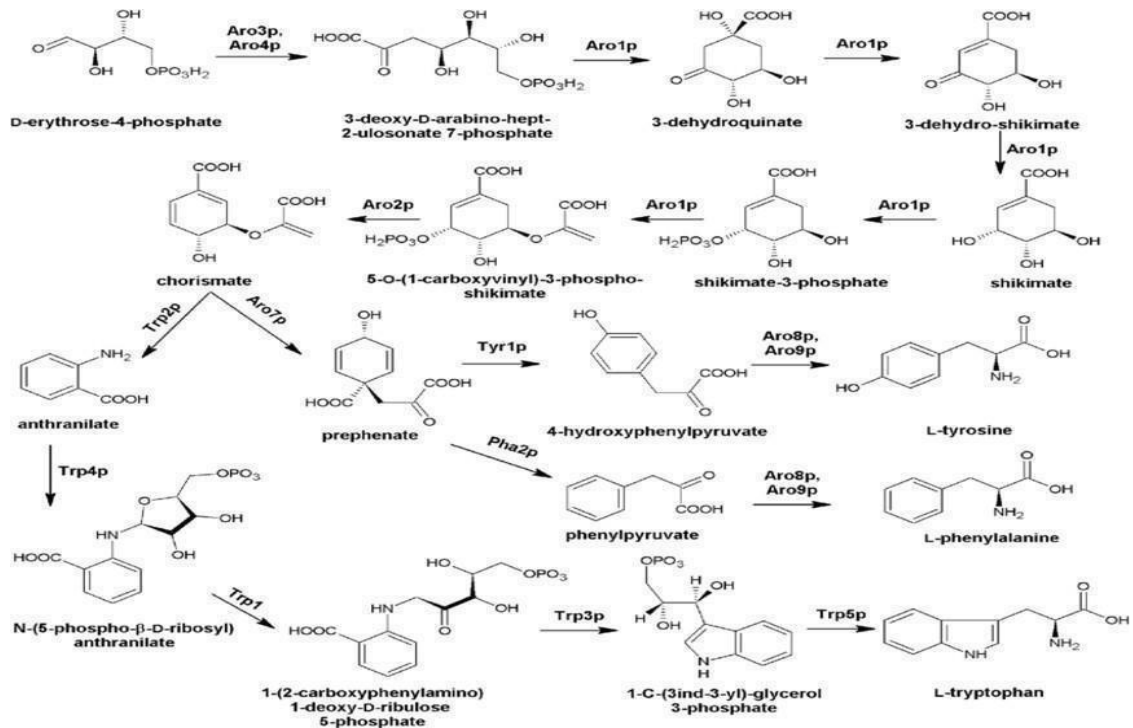


Figure 1.6: Schematic of the shikimate pathway utilised by fungi to produce aromatic amino acids published by (Kuplińska and Rząd, 2021).

Sulphur is another essential nutrient that *A. fumigatus* needs to acquire from the surrounding tissue during intrapulmonary growth. Sulphur is essential to the production of cysteine and methionine and the production of molecules including coenzyme-A, glutathione and iron-sulphur clusters (Amich *et al.*, 2013). The proper regulation of sulphur metabolism is crucial for *A. fumigatus* virulence and persistence in host tissue and sulphur containing amino acids are required for virulence. Methionine synthase, an enzyme in the trans-sulfuration pathway, has been identified as a promising antifungal target (Scott *et al.*, 2020). The assimilation of sulphur is regulated by the MetR transcription factor but dispensable for utilization of methionine and orchestrates the fungal response to sulphur starvation (Amich *et al.*, 2013).

The use of trace elements is also essential to fungal growth and virulence. These resources are often contested between microbe and the host and include iron, zinc, manganese, and copper. Iron metabolism is fuelled through high-affinity iron uptake mechanisms including reductive iron assimilation and siderophore-mediated iron acquisition (Schrettl and Haas, 2011). Iron serves as a cofactor for essential metabolic processes including the electron transport chain, amino acid metabolism,

DNA biosynthesis, sterol formation, and oxidative stress detoxification (Perez-Cuesta *et al.*, 2021). Zinc is the second most prevalent transition metal in cells, after iron, and the second most abundant metal-cofactor of enzymes after magnesium. Zinc has been recognized for its structural and regulatory roles within cells, playing an essential role in immunomodulatory responses during host-pathogen interactions (Silva-Gomes *et al.*, 2024). The metabolic plasticity and adaptability displayed by *A. fumigatus* and its ability to acquire resources from its environment facilitates its survival in the ever shifting and metabolite limited host microenvironment and is integral to understand its development and pathogenicity in a hostile environment.

1.2.6 Current approaches to *Aspergillus fumigatus* treatment

The current suite of antifungal compounds is limited and often accompanied by high toxicity to patients, elevated treatment costs, increased frequency of resistance rates, and the emergence of intrinsically resistant species (Souza *et al.*, 2025). These compounds mainly target the fungal cell membrane or the cell wall. The three major classes of antifungal agents, utilised for *A. fumigatus* infection are triazoles, polyenes and echinocandins. These target ergosterol biosynthesis, fungal membrane formation and synthesis of the (1-3) β -D-glucan respectively (Cortés *et al.*, 2019).

Triazoles are a class of antifungal agent that are characterised by a triazole ring. These agents inhibit sterol 14- α -demethylase, an enzyme essential for ergosterol synthesis. These compounds disrupt the integrity of fungal cell membranes, leading to the accumulation of sterol intermediates that are toxic to the cell and have broad activity against fungal pathogens (Lal *et al.*, 2025). *A. fumigatus* has an intrinsic tolerance to fluconazole, however voriconazole, itraconazole, posaconazole and isavuconazole are common drugs of choice for prevention and treatment of aspergillosis (Esquivel *et al.*, 2015; Donnelley *et al.*, 2016).

Polyenes including Amphotericin B, nystatin and natamycin are used to treat various forms of *A. fumigatus* infection (Carolus *et al.*, 2020). Amphotericin B is a cyclic heptaene produced by the Gram-positive bacterium *Streptomyces nodosus* (Zhang *et al.*, 2020). Amphotericin B incorporates into the fungal lipid bilayer and binds to ergosterol. Ergosterol sequestration results in pore formation and leakage of monovalent ion and glucose. The rapid depletion of intracellular ions results in fungal

cell death. Amphotericin B exposure can also result in the accumulation of reactive oxygen species, resulting in DNA, protein, mitochondrial, and membrane damage resulting in fungal death (Xiaochun Wang *et al.*, 2021). Amphotericin B is poorly tolerated by patients and alternative formulations including amphotericin B lipid complex and liposomal amphotericin B are more commonly used as they display reduced toxicity, facilitating the administration of higher doses, and improve treatment outcomes (Botero Aguirre and Restrepo Hamid, 2015).

Echinocandins constitute an important class of antifungal agents, with three drugs currently approved for clinical use: caspofungin, micafungin and anidulafungin (Mroczyńska and Brzózka-Dąbrowska, 2020). These compounds are the modified products of non-ribosomal lipopeptides derived from filamentous fungi (Hüttel, 2021). Echinocandins target the fungal cell wall, specifically β -(1,3)-glucan synthase, a key enzyme involved in the development of fungal cell walls. Disruption of this enzyme leads to the destabilization of cell wall, causing fungal death (Szymański *et al.*, 2022). A newly developed echinocandin, rezafungin which has a longer half-life and better safety profile compared to compounds in this class (Andes *et al.*, 2025). Rezafungin also has activity against both azole-sensitive and azole-resistant strains of *Aspergillus* (Wiederhold *et al.*, 2018). Rezafungin has exhibited *in vivo* activity in a murine model of azole-resistant disseminated invasive aspergillosis (Wiederhold *et al.*, 2019). Despite these advantages echinocandins are fungicidal against most pathogenic yeasts but they are fungistatic against *Aspergillus* species and some other pathogenic filamentous fungi and thus clearance of filamentous fungi is dependent on host immune effectors (Aruanno *et al.*, 2019).

In addition to these well-established drug families other emerging classes with novel mechanisms have been developed. Manogepix is a first-in-class antifungal that inhibits the fungal Gwt1 protein, a conserved enzyme that catalyzes inositol acylation, an early step in the GPI-anchor biosynthesis pathway (Dai *et al.*, 2024). Gwt1 is essential for trafficking and anchoring mannoproteins to the cell membrane and outer cell wall and since these mannoproteins are required for cell wall integrity, adhesion, pathogenicity, and evading the host immune system. As a result, inhibition of Gwt1 by manogepix has many physiological effects. Importantly, the closest mammalian ortholog, PIGW, is not sensitive to inhibition by manogepix (Shaw and Ibrahim, 2020). Manogepix has been proven to be effective against both itraconazole-sensitive and

resistant *A. fumigatus* (Jørgensen *et al.*, 2020). Another emerging class is the orotomide class of which the first member is olorofim which is a reversible inhibitor of dihydroorotate dehydrogenase, a key enzyme in the biosynthesis of pyrimidines (Oliver *et al.*, 2016). Olorofim has activity against Mold species and thermally dimorphic fungi, including species that are resistant to azoles and amphotericin B, but lacks activity against yeasts and the Mucorales (Georgacopoulos *et al.*, 2023). Olorofim has demonstrated strong inhibition during disseminated *A. fumigatus* and *A. flavus* infection in murine models (Seyedmousavi *et al.*, 2019).

1.2.7 Antifungal resistance in *Aspergillus fumigatus*

Despite the wide array of antifungal agents available in the clinic *A. fumigatus* has developed mechanisms to circumvent their activity (Figure 1.7), and many of these mechanisms are conserved among pathogenic fungi (Nywening *et al.*, 2020). There are two accepted origins for azole antifungal resistance: prolonged use of antifungals to treat patients with chronic *A. fumigatus* infection and increased use of agricultural fungicides against plant-pathogenic moulds with cross-activity against *A. fumigatus* (Guegan *et al.*, 2021). Environmental fungicides containing active ingredients such as triazoles and their widespread distribution in the environment are the link between clinical and environmental antifungal resistant strains of *A. fumigatus* (Williams *et al.*, 2024). Resistance emerges following mutation of the *cyp51A* gene and the TR₃₄/L98H and TR₄₆/Y121F/T289A alleles in the *cyp51A* gene are the most common ones conferring pan-azole resistance with evidence that these mutations may have arisen in agricultural settings (Burks *et al.*, 2021). In addition, once multidrug-resistant genotypes emerge in fungal pathogens, such genotypes can spread very quickly to other geographical regions and ecological niches through vegetative cells and airborne spores (Achilonu *et al.*, 2024). The primary mechanism governing azole resistance is mutation or overexpression of the *cyp51A* gene reducing the affinity between the azole drug and its target or increasing the azole concentration required to inhibit fungal growth (De Francesco, 2023). Another mechanism to evade azoles is the overexpression of efflux pump systems which decrease the intracellular drug concentration, in *A. fumigatus*. The ABC transporter Cdr1B and MdrA were the only MFS transporters found to be related to azole resistance (Paul *et al.*, 2017; Meneau *et al.*, 2016).

Despite its long history of use resistance in *A. fumigatus* to amphotericin B remains uncommon but has been observed among *Aspergillus terrei* species, associated with the modulation of molecular chaperones, targeting reactive oxygen species by mitochondria and influencing cellular redox homeostasis (Blum *et al.*, 2008). The rates of amphotericin B resistance in *A. fumigatus* is rising with as much as 27% of isolate in a Brazilian hospital demonstrating elevated MIC (Reichert-Lima *et al.*, 2018). The mechanisms governing this resistance are poorly elucidated in *A. fumigatus* but RTaA was found to be increased specifically in response to polyenes amphotericin B and nystatin. Its overexpression results in modest resistance, indicating it could be a novel resistance mechanism (Abou-Kandil *et al.*, 2025). Echinocandins only display fungistatic activity against *Aspergillus* species and is often used only in combination with a polyene or an azole to obtain synergistic effects (De Francesco, 2023). To date, echinocandin resistance is rarely found in *Aspergillus* species, although tolerance is observed through epigenetic alteration which, unlike resistance, is not the result of acquired mutations but driven by activation of stress responses. This is known as the paradox effect which describes decreased activity of the drug and recovery of fungal growth at increasing concentrations above a certain threshold. This paradoxical effect can be observed in ~60% to 80% of *A. fumigatus* clinical isolates, occurring mainly in response to caspofungin, whereas this phenotype is usually absent with micafungin and anidulafungin or occurs only at higher concentrations (Aruanno *et al.*, 2019). The paradoxical effect results in cell wall remodelling to compensate for the loss of β -1,3- glucan including inducing the increased expression of Ichitin, chitosan, and highly polymorphic α -1,3-glucans, whose physical association with chitin maintains cell wall integrity and modulates water permeability while avoiding the activity of the drug. (Dickwella Widanage *et al.*, 2024). Alteration to the β -(1,3)-glucan synthase enzymes encoded by the *fks1* gene induce echinocandin resistance in *Candida* species and point mutation can give rise to this resistance in *A. fumigatus*. A strain harbouring such a mutation was isolated in the clinic from a patient who initially failed azole and polyene therapy and subsequently failed echinocandin therapy (Jiménez-Ortigosa *et al.*, 2017).

Despite relatively recent advances in antifungal therapy resistance is likely to follow closely behind as *A. fumigatus* strains with acquired increased tolerance to olorofim has already been identified, associated with amino acid substitution in the

PyrE gene (Buil *et al.*, 2022). This highlights the importance in the continued development of novel therapeutics and the requirement to understand mechanisms facilitating fungal disease in patients. The rise of fungal resistance is a growing concern as the effective defences continue to dwindle with only a few emerging options to take their place. This further emphasises the need to understand fungal development *in vivo* to develop effective strategies against these pathogens.

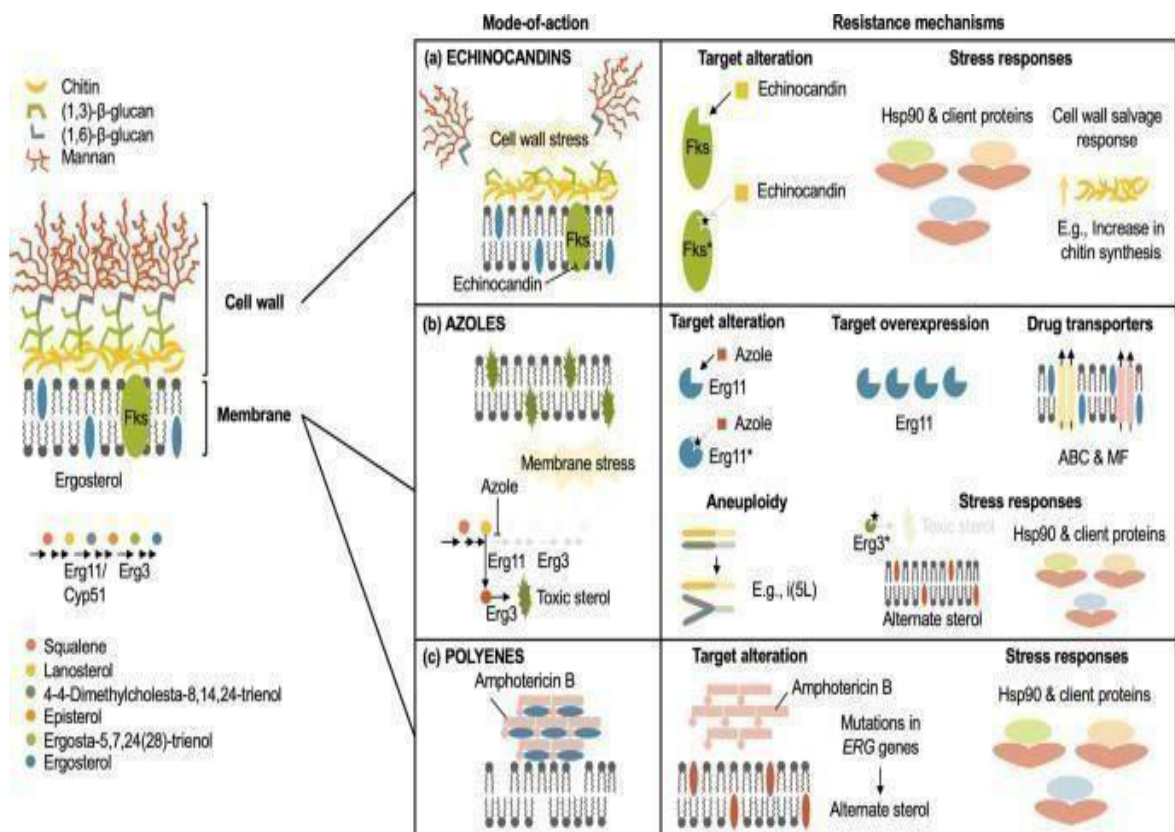


Figure 1.7: Targets of antifungal agents Echinocandins, Azoles and Polyenes and some resistance mechanisms observed in fungal pathogens published by (Lee *et al.*, 2023)

1.3 Microbial interactions in the airways

The human lung is constantly exposed to microbes through inhalation of various viruses, bacteria and fungi (Invernizzi *et al.*, 2020). In susceptible individuals the airways can be colonised by a range of microbial pathogens which are in dynamic competition with the host and each other for dominance in the niche (Figure 1.8) (Gannon and Darch, 2021). The growing utilisation of immunomodulatory drugs and antibiotics result in increased fluctuation of the human airway microenvironment and as a result pulmonary bacterial-fungal coinfections have become more prevalent (Katsoulis *et al.*, 2024). A recent study identified that bacterial coinfections was present in more than 40% of patients with fungal pneumonia, specifically in patients with underlying immune deficiency and the presence of pulmonary cavities (Zhao *et al.*, 2021). *A. fumigatus* infections typically occur in the context of preexisting conditions including in individuals who are more susceptible to bacterial infection such as cystic fibrosis patients or individuals with latent tuberculosis infection (Petrocheilou *et al.*, 2022; Magwalivha *et al.*, 2025). As a result, *A. fumigatus* development and virulence can be shaped by interactions with other microorganisms within the human airways.

In the context of coinfection these species must compete for nutrients and dominance in the niche, and many are equipped with virulence factors from co-evolution in the soil to inhibit their competitors (Rezzoagli *et al.*, 2020). These species can interact directly through physical cell-cell interaction or indirectly through secretion of various effectors. These can include toxins, siderophores and small molecules that are involved in quorum sensing, environmental modifications and alterations in host responses (Peleg *et al.*, 2010; Kramer *et al.*, 2020). Pulmonary pathogens can also influence each other through production of volatile organic compounds (Margalit *et al.*, 2022). These interactions are bidirectional and occur across kingdoms with bacteria heavily influencing fungal survival and *vice versa* and these interactions can be beneficial or antagonistic (Pawlowska, 2024). The microbiome can also influence patient susceptibility to fungal infection (Chow *et al.*, 2023). Some commensal bacterial taxa such as *Prevotella* and *Veillonella* species can protect against pathogenic fungi including *Candida palmoleophila* and *Aspergillus* species (Liu *et al.*, 2021).

The competition for resources and nutrients is not only between competing pathogens but also between host cells and indigenous microbiota. Both host and microbial cells may potentially compete for growth-limiting resources. Metabolic alteration and strategies are crucial to survival and the microbiota may play a role in host metabolism (Costantini *et al.*, 2024). *A. fumigatus* can influence this environment by inducing dysbiosis, shaping it towards a beneficial environment with increased availability of aromatic amino acids (Mirhakkak *et al.*, 2023). Tryptophan is central to host and microbial interactions in the airway as it is utilised by the host and microbial competitors (Nunzi *et al.*, 2025). Tryptophan can be produced by various bacteria through the indole pathway (Dong and Perdew, 2020) which can then be degraded by fungal enzymes when adapting to the host niche (Zelante *et al.*, 2021). These interactions are an often overlooked but highly influential factors in *A. fumigatus* growth and virulence and should be factored in when examining these traits.

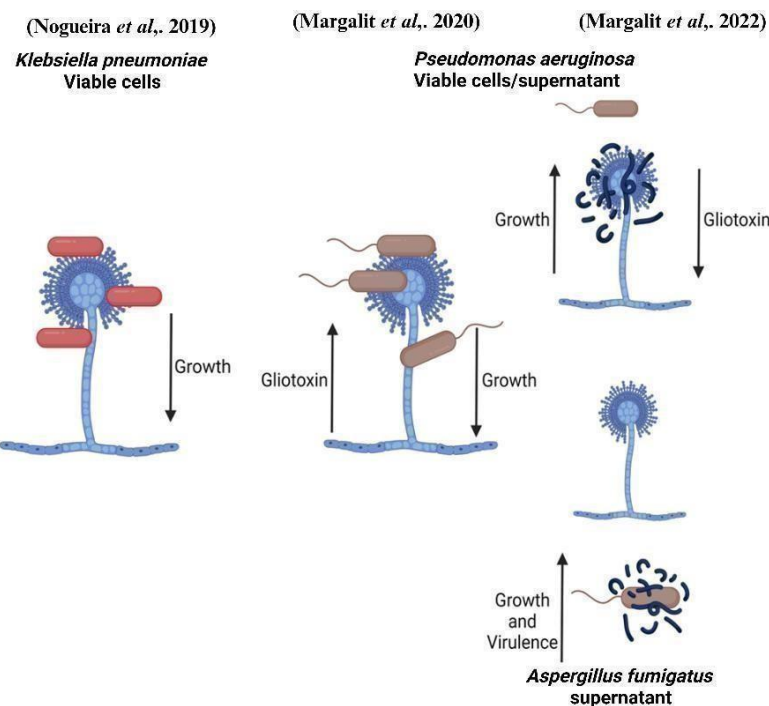


Figure 1.8: Examples of interaction studies between *A. fumigatus* and bacterial pathogens *K. pneumoniae* and *P. aeruginosa* (generated in biorender).

1.4 *Klebsiella pneumoniae* infections, virulence and coinfection

Klebsiella pneumoniae is a Gram negative, rod shaped non-motile member of the Enterobacteriaceae family (Abbas *et al.*, 2024). *K. pneumoniae* is an opportunistic pathogen and is a considerable cause of nosocomial infections, particularly in low and middle-income countries (Alcántar-Curiel *et al.*, 2018). *K. pneumoniae* can cause a

range of infections at many distinct body sites such as urinary tract infections, meningitis, respiratory tract infections, pneumonia, bloodstream infections, and surgical site infections and predominantly affects neonates, the elderly, and immunocompromised individuals (Chang *et al.*, 2021). *K. pneumoniae* is also responsible for community-acquired infections and a defining feature of these infections is their morbidity and mortality, and the *Klebsiella* strains associated with these infections are considered hypervirulent (Bengoechea and Sa Pessoa, 2018). Immunocompromised patients who are hospitalized and suffer from underlying chronic illnesses as well as elderly individuals are prone to be infected with *K. pneumoniae* as their immune system's defences are low (Mohd Asri *et al.*, 2021). *Klebsiella* infections are rare at any individual time point in cystic fibrosis patients. However, they are observed in almost 10% of a patient cohort followed longitudinally. *K. pneumoniae* is not a chronic coloniser of the cystic fibrosis airway like *Pseudomonas aeruginosa* but can influence infection outcome through production of carbapenemases which degrade type beta lactamases complicating therapy (Leão *et al.*, 2011).

Rates of *K. pneumoniae* antibiotic resistance has steadily increased, rendering infection by these strains challenging to treat (Santella *et al.*, 2024). Virulent *K. pneumoniae* strains are significantly heterogenous making identification of virulence factors difficult although the bacterial capsule, lipopolysaccharide, fimbriae, and siderophores have been widely accepted to contribute to virulence (Paczosa and Mecsas, 2016). The bacterial capsule is significant in pathogenicity as it protects the bacteria from phagocytosis and can directly inhibit aspects of the host immune response. Several capsule types are associated with community-acquired invasive pyogenic liver abscess, septicemia, and pneumonia and others are predominantly detrimental to experimental infections in mice and are frequently associated with severe infections in humans (Riwu *et al.*, 2022). Some *K. pneumoniae* lipopolysaccharide serotypes can modulate the host immune response leading to activation or immune evasion contributing to virulence (Bulati *et al.*, 2021). *K. pneumoniae* adherence and biofilm formation are associated with fimbriae. The bacteria express at least three different fimbrial types: mannose-sensitive type 1 fimbriae, mannose-resistant type 3 fimbriae, and the *Escherichia coli* (*E. coli*) common pilus (Alcántar-Curiel *et al.*, 2018). Other structural components of the bacteria have been found to contribute to virulence including several outer membrane proteins.

The outer membrane protein OmpA modulates the immune response, providing resistance against macrophage-dependent phagocytosis and the absence of OmpA, enhances susceptibility to antimicrobial peptides (Singh *et al.*, 2025). Another important virulence factor is the production of siderophores for iron acquisition, enterobactin, yersiniabactin, salmochelin, and aerobactin are the main forms of siderophores expressed by *K. pneumoniae*. Enterobactin is highly conserved and distributed in all *K. pneumoniae* strains while the other siderophores are mainly expressed in hypervirulent isolates (Lan *et al.*, 2021).

K. pneumoniae is among the most common coinfection agents in chronic pulmonary aspergillosis patients (Akyil *et al.*, 2025) and was shown to be detrimental to patient outcomes (Bhatia *et al.*, 2024). Interactions between these species have indicated inhibition of spore germination following physical interaction. This is thought to be driven by a stress response in the fungus as there is an increased expression of cell wall-related genes and decrease of hyphae-related genes resulting in suppression of filamentous growth (Nogueira *et al.*, 2019). The interaction between these species remains poorly elucidated in the literature but could provide important insight into fungal development in the lung microenvironment.

1.5 *Pseudomonas aeruginosa* infections, virulence and coinfection

Pseudomonas aeruginosa is a Gram-negative, rod shaped, motile bacterial species belonging to the order Pseudomonadaceae. It is widely dispersed in the environment including in soil and water but is readily found in human and animal impacted environments (Diggle and Whiteley, 2020). *P. aeruginosa* has been identified as an opportunistic pathogen and is a major cause of hospital-acquired infections. *P. aeruginosa* infections primarily impact immunocompromised hosts, and chronic infections in patients with structural lung disease such as cystic fibrosis (Reynolds and Kollef, 2021). *P. aeruginosa* often displays multi-drug resistance due to its ability to rapidly mutate to gain resistance to antibiotics (Blomquist and Nix, 2021). *P. aeruginosa* is a leading cause of bacteraemia and sepsis in neutropenic cancer patients and hospital-acquired pneumonia and respiratory failure (Albasanz- Puig *et al.*, 2019; Nickerson *et al.*, 2024). Chronic *P. aeruginosa* infections are a characteristic of individuals with cystic fibrosis and accounts for pulmonary failure that leads to death in these individuals (Wood *et al.*, 2023).

P. aeruginosa possesses a large genome enabling great genetic diversity which facilitates the growth of the bacterium in diverse environments and production of a range of virulence factors and resistance mechanisms to persist in the human host (Sathe *et al.*, 2023). Structural components of the bacteria associated with virulence include pili and membrane components. Attachment to the host is facilitated by type IV pilus which are associated with bacterial twitching and swarming motility and adhesion on various surfaces. These structures are involved in biofilm formation, regulation of virulence factors, and facilitate bacterial exchange of antibiotic resistance genes and confers resistance to host surfactant A (Lighthart *et al.*, 2020; Tan *et al.*, 2013). Lipopolysaccharide can be found in all *P. aeruginosa* strains and represents an important immunomodulatory molecule that can stimulate the host immune response and neutrophils to release neutrophil extracellular traps to capture invading pathogens. Lipopolysaccharide can also protect bacteria from killing and pattern recognition following phagocytosis (Huszczyński *et al.*, 2020).

Secreted factors also heavily influence *P. aeruginosa* virulence and are distributed by a range of specialised secretion systems. Exopolysaccharides secreted by *P. aeruginosa* are crucial to biofilm formation and convey bacterial tolerance to harsh environments such as desiccation, oxidative stress, and host defences (Kaur and Dey, 2023) and has a secondary role as an adhesin contributing to bacterial persistence in the host (Myszka and Czacyk, 2009). Siderophores released by *P. aeruginosa* are another virulence factor fuelling iron metabolism and microbial growth. Two siderophores are produced by *P. aeruginosa* pyoverdine and pyochelin are capable of stripping iron from host transferrin and lactoferrin to promote bacterial growth and are both required for full virulence of *P. aeruginosa* (Sass *et al.*, 2020).

P. aeruginosa is also equipped with a range of enzymes and toxins that facilitate tissue invasion and protect against the host immune response. Alkaline protease, secreted by the type I secretion system can degrade aspects of the immune response including IFN- γ and TNF- α , and aspects of the complement cascade resulting in immune evasion (Peignier and Parker, 2020). Protease IV, a serine protease can also degrade complement proteins C1q and C3, as well as fibrinogen, plasminogen, immunoglobulin G, and pulmonary surfactant proteins A, B, and D (Hastings *et al.*, 2023). *P. aeruginosa* elastase A and B also facilitate bacterial invasion through destruction of host elastin resulting in impaired lung function and haemorrhage

(Chadha *et al.*, 2022). Elastase B is a potent modulator of the immune response including manipulation of neutrophils, macrophages, natural killer cells and T cells recruitment and activation (Cigana *et al.*, 2021). Elastase B is more prevalent in early-stage colonisation in cystic fibrosis patients and once a chronic infection is established the elastase activity is significantly diminished (Llanos *et al.*, 2023). Lipase A and phospholipase C can result in host tissue degradation by targeting the cell membrane and induce vascular permeability, organ damage and cell death (Qin *et al.*, 2022; Singh *et al.*, 2023).

Toxins produced by *P. aeruginosa* exert a range of effects on the host including ExoS and ExoT which can disrupt the host actin cytoskeleton to interfere with cell-to-cell adhesion and induce apoptosis of host cells. ExoU is a potent phospholipase that causes rapid necrotic cell death (Hauser, 2009). In addition, exolysin can produce pores in host cells resulting in membrane permeabilization (Basso *et al.*, 2017). Lipoxygenase can inhibit the expression of major chemokines and the subsequent recruitment of immune cells (Aldrovandi *et al.*, 2018) and leukocidin demonstrates specific inhibition of leukocytes (Bouillot *et al.*, 2020). Pyocyanin is a blue-green, redox-active pigment derived from chorismic acid produced by *P. aeruginosa*. The low molecular weight and zwitterionic properties of PCN are believed to permit the toxin to easily permeate cell membranes (Hall *et al.*, 2016). It is crucial to virulence, serving as a redox-active secondary metabolite and a quorum sensing (QS) signalling molecule. Pyocyanin inhibits the growth of bacterial, fungal, and mammalian cells by inducing oxidative stress (Mudaliar and Bharath Prasad, 2024).

P. aeruginosa and *A. fumigatus* represent the dominant bacterial and fungal pathogen in the airways of adults with cystic fibrosis. Coinfection occurs in an estimated 15.8% of Irish cystic fibrosis patients although a definitive number is difficult to determine (Keown *et al.*, 2020). Coinfection is not associated with reduced lung function but typically requires additional IV antibiotics (Hughes *et al.*, 2022). *P. aeruginosa* and *A. fumigatus* are ubiquitous microorganisms found in soil, water and plants and as such their interactions are ancient (Nazik *et al.*, 2020). These interactions have been the focus for many studies including examination in culture which identified secreted products from *A. fumigatus* that can promote *P. aeruginosa* development and result in metabolic shifts including denitrification and amino acid metabolism but

also induces a bacterial stress response (Margalit *et al.*, 2020). In contrast exposure of *A. fumigatus* to *P. aeruginosa* cells results in increased secondary metabolite production including gliotoxin at the expense of fungal growth while exposure to secreted products has the opposite effect (Margalit *et al.*, 2022). Interactions studies in *Galleria mellonella* larvae demonstrated increased mortality when the species coinfect and human bronchial epithelial cells produce more proinflammatory IL-6 and IL-8 when coinfection occurs relative to mono-infections (Reece *et al.*, 2018). Coinfection in an immunocompetent murine model with both pathogens isolated in agar beads demonstrated a proximity dependent microbial inhibition (Sass and Stevens, 2023). These studies have provided insights into specific aspects of the interaction between these two pathogens but often fail to demonstrate the host impact which plays a crucial role in shaping this interaction.

1.6 The need for model systems to study fungal pathogens

To fully understand the processes fungi utilize to infect susceptible individuals and to develop antifungal resistance it is essential to be able to study host-fungal interactions with both *in vivo* or *in vitro* model systems before applying findings to clinical use (Last *et al.*, 2021). The scope and complexity of infection modalities and virulence capabilities of fungal pathogens and the range of susceptible hosts has resulted in a steady rise in the requirement for complex and diverse model systems (Torres *et al.*, 2020). These systems enable the dissection of the fungal pathogenic processes in isolation, or in combination, providing key insights into adaptation processes occurring within the host.

Model systems are crucial as they provide platforms through which the development and response of a pathogen to a given environment can be studied within a defined window of infection. Various model systems have been utilized to effectively isolate, predict, and understand aspects of host-pathogen interactions instead of studying them in uncontrolled conditions through observation of patients directly (Mukherjee *et al.*, 2022). Models for understanding fungal pathogenesis have advanced dramatically, from simple *in vitro* studies to a wide range of *in vivo* techniques. The original *in vitro* models provided necessary insights into fungal-host interactions, but their inability to recreate the physiological complexity of entire organisms meant that these models had limitations (Luming Wang *et al.*, 2024). These limitations highlighted the need to produce complex *in vitro* models, such as organoids and organ-on-chip

systems, that provide a more accurate representation of human tissue structure and function. These new models have proven useful for understanding fungal mechanisms such as tissue invasion and immune evasion (Baran *et al.*, 2022). In addition, *in vivo* models including mammalian and invertebrates such as insects or nematodes have facilitated better understanding of fungal pathogenicity and host responses. These developments represent a shift towards combining modelling approaches, to provide high-throughput and biologically accurate platforms from which to study fungal development in the host as well as the development and testing of effective antifungal therapies (Junqueira and Mylonakis, 2019)

1.6.1 Mammalian models

Rodents, particularly mice and rats, are the most frequently utilized vertebrate models due to their accessibility and anatomical, physiological and genetic similarity to humans (Bryda, 2013). Domesticated rats, *Rattus norvegicus* emerged as a pioneering animal model in the early twentieth century and were the first rodent species to be used for scientific purposes (Modlinska and Pisula, 2020). This system is still utilised but was eclipsed following the publication of the whole genome of the mouse (*Mus musculus*) in 2002 which opened up new avenues of genetic research and established its key place in modern biomedical research (Franco and Olsson, 2014). It has been estimated that 85% of publications regarding experimental aspergillosis utilized murine models (Desoubeaux and Cray, 2018). This is likely due to the accessibility of the model, and their body size, allowing for the use of a relatively large number of animals simultaneously under identical conditions, which can enhance the power of statistical analysis. In addition, the widespread use of genetically defined inbred murine strains, humanized mice, and gene knockout mice has enabled researchers to understand how pathogens cause disease, define the role of specific host genes in either controlling or promoting disease, and identify potential targets for the prevention or treatment of a wide range of infectious agents (Sarkar and Heise, 2019).

Murine models were fundamental to early studies of the genetic and molecular origins of host resistance and the sensitivity of immunocompromised individuals to fungal infections. These insights included identifying the interaction of various immune effectors. Examination of the complement system in mice identified that C3 knockout mice were highly susceptible to systemic infection by *A. fumigatus*, although C4 and complement factor B mutants show comparable susceptibility to the wild-type

mice. This suggested that specific factors are crucial to this response and that either the complement pathways display functional redundancy during infection or complement is activated non-canonically by *A. fumigatus* infection (Shende *et al.*, 2022). Gene knockout experiments in mice have also highlighted that IL-6, IL-12, and IFN- γ were protective factors against *A. fumigatus* and that IL-17, TLR4, and TLR2 are crucial in the innate response. *Aspergillus*-infected TLR2 knockout mice have low TNF α and IL-12 levels as well as lower survival and higher tissue fungal burden when compared to immunocompetent mice (Desoubeaux and Cray, 2018). Murine models can also enable the study of *Aspergillus* infection in specific disease contexts including bacterial coinfection (Sass and Stevens, 2023), solid organ transplant (Herbst *et al.*, 2013), chronic granulomatous disease (King *et al.*, 2023) and cystic fibrosis (Bercusson *et al.*, 2025). Murine models are especially favoured when compared to many alternative and *in vitro* models for their ability to imitate human disease pathways and systemic or multi-organ infection pathologies allowing researchers to study the complicated dynamic of fungal infections and the host's immune system, in a controlled setting (MacCallum, 2013). Murine models also aid in the development of specific antifungal therapies that are more effective and less hazardous to humans (Lange and Inal, 2024). For example, the antifungal drug fosmanogepix, which has been shown to be effective *in vivo* in mouse and rabbit models against *Candida* species, *Coccidioides immitis* and *Fusarium solani* (Alkhazraji *et al.*, 2020).

Murine models do have limitations, including physiologic differences that limit how well mice reproduce key aspects of host-pathogen interactions and pathology. In addition, genetic differences between mice and humans can also interfere with a pathogen's ability to replicate or cause human-like disease outcomes in mice (Sarkar and Heise, 2019). Murine models demonstrate important physiological and biochemical variations from humans including the localisation of basal cells in the trachea and the abundance of bronchioalveolar stem cells rather than multi-ciliated cells in mice (Miller and Spence, 2017). In addition, Goblet cells are prevalent in the proximal human airway, but they primarily appear in mice following injury (Pardo- Saganta *et al.*, 2013). The metabolome of mice also differs from humans containing significantly more fatty acids and lower acetate, asparagine, glutamate, lactate, lysine, myo-inositol, syllo-inositol, and valine concentrations (Benahmed *et al.*, 2014). These alterations could influence fungal metabolism and colonisation. Murine models can also fail

to replicate pivotal aspects of human diseases and infections such as aberrant abscess formation which occurs in murine lungs during *Staphylococcus aureus* infection (Cigana *et al.*, 2018), but is rarely observed in human Cystic fibrosis patients (Patradoon-Ho and Fitzgerald, 2007). In addition, mammalian model systems are expensive to maintain, require high levels of expertise and are subject to strict ethical and legal regulations limiting the volume of output from these sources (Kiani *et al.*, 2022). These factors have emphasised the need to develop numerous alternative models to dissect aspects of host-fungal interaction in isolation or holistically. They are often used prior to studying them in more complex systems and have revolutionized novel antifungal screening practices (Hunter, 2022).

1.6.2 *In vitro* cell models

In vitro cell models enable researchers to have complete control of the conditions present in the experiment, such as oxygen and carbon dioxide concentration, temperature, pH, and nutrition availability (Klein *et al.*, 2022). This level of control facilitates reproducible results and highlights the importance these factors play in the development of infection (Rafiq *et al.*, 2022). The use of cultured cell lines or tissue is standard laboratory practice and facilitates the evaluation of aspects of host biology enabling researchers to study a complex interaction by dissecting it to its component parts. Additionally, *in vitro* models can include components of the host microbiota, including the addition of synthetic microbial consortium to mimic host microbiome in intestinal model systems (Calatayud *et al.*, 2019) replicating the *in vivo* situation on skin and mucosal surfaces. A549 adenocarcinomic human alveolar basal epithelial cells, which have been utilized to examine *Aspergillus* colonization in the alveoli. This includes examination of how conidial surface proteins reprogram endosome pathways in mammalian cells, preventing conidial destruction following initiation of infection (Jia *et al.*, 2023).

Endothelial cell models aid in understanding how fungi such as *Candida spp.* and *A. fumigatus* penetrate vascular barriers, resulting in systemic infections. Interactions between fungi and endothelial cells can cause tissue damage and inflammation, both of which are common hallmarks of invasive fungal infections (Netea *et al.*, 2015). Endothelial cell models are important for understanding how fungi enter the bloodstream and infect endothelial cells, leading to serious infections. They demonstrate how fungi disperse through blood vessels and the endothelial

damage that accompanies severe fungal infections. *A. fumigatus* demonstrates different mechanisms of invasion, magnitude of endothelial cell stimulation, and time course of endothelial cell damage when interacting with abluminal and luminal surfaces. These differences in the endothelial cell response suggest that there may be significant differences in the pathogenesis of invasive versus hematogenously disseminated aspergillosis (Kamai *et al.*, 2009).

Cells of the innate immune response such as macrophages, dendritic cells, and neutrophils play a pivotal role in the initial host's responses against fungal infections. Phagocytosis, cytokine production, recruitment and activation of other immune responses to fungal infections can be studied using *in vitro* models by examining each of these cell types in isolation (Lionakis *et al.*, 2023). Cell lines including J774A.1, RAW 264.7, and THP-1 are often used to study macrophage - fungal interactions. Additionally, bone marrow-derived macrophages (BMDMs) from genetically engineered mice provide insight into specific immunological mechanisms involved in antifungal defence (Frank *et al.*, 2018). The role of specific immunological effectors such as progranulin in attenuating the inflammatory response of *A. fumigatus* keratitis was characterized using RAW 264.7 cells where it was demonstrated to enhance the phagocytic activity against conidia (Qi *et al.*, 2024).

Despite these applications and advances, *in vitro* cell models have a major limitation as they are not able to replicate cell-cell interactions and they fail to demonstrate the conditions of cells in an organism, limiting the value of *in vitro* data to predict *in vivo* behaviour (Habanjar *et al.*, 2021). Another limitation of cell culture is the expense and effort involved to obtain a relatively low number of cells. Cell culture approaches also lack complex connections found in whole organisms, such as those involving various cell types, tissues, and systemic immune responses (Kim *et al.*, 2023). More complex *in vitro* models include transwell systems, complex organ- on-chip models and 3D organoid systems. These offer varying levels of complexity and specificity to mimic human conditions and physiology (Mosig, 2016). Transwell plate systems have been utilized to study dendritic cell maturation (Lothe *et al.*, 2014) and the effects of mycotoxins including gliotoxin in disruption of the blood brain barrier integrity (Patel *et al.*, 2018). The air-liquid interface model utilizes human

bronchial epithelial cells at the air-liquid interface to simulate the bronchial epithelial barrier in the conductive zone of the respiratory tract. This provides novel insights into the molecular response of bronchial epithelial cells upon exposure to *A. fumigatus* conidia (Braakhuis *et al.*, 2020). This model demonstrates some physiologically relevant responses to *A. fumigatus* infection including upregulation of apoptosis/autophagy, translation, unfolded protein response and cell cycle while the complement and coagulation pathways and iron homeostasis were downregulated (Toor *et al.*, 2018). Despite the many uses and outputs from transwell model systems, they demonstrate low physiological relevance, are only beneficial when studying single cell types. In addition, migration and invasion assays can produce conflicting data making it difficult to relate data to clinically observed phenotypes and cellular behaviours (Katt *et al.*, 2016).

Organ on chip models represent the smallest functional entity of an organ as well as a versatile and promising resource to study host-pathogen interactions (Ahadian *et al.*, 2018). The microfluidic devices are three-dimensional cell culture devices constructed of elastomers, glass or plastics. In such microfluidic devices, multiple cell types can be arranged in a 3D manner to mimic internal organ structures, allowing for the evaluation of cellular responses, cell-cell interactions, and organ structure disruptions. By perfusing air or culture medium through microfluidic devices with a micropump, cells can be exposed to shear stress mimicking air or blood flow (Yokoi *et al.*, 2023). These microfluidic systems create conditions that are more physiologically relevant and can be considered humanized *in vitro* models. These systems offer controls over biologically relevant dynamics such as microenvironments, vascularization, near-physiological tissue constitutions and partial integration of functional immune cells (Alonso-Roman *et al.*, 2024). The limitation of these systems is the inability to emulate multi-system interactions and pathogen dissemination. This has been by-passed by the combination of chip systems to simulate multi-organ cross communication in an enclosed microfluidic network (Luni *et al.*, 2014). An invasive aspergillosis on chip system has been developed including epithelial, endothelial and immune cells demonstrating human cells inhibited the growth of the fungus, contributed to the release of proinflammatory cytokines and chemokines

and demonstrated the *in vitro* activity of the antifungal drug caspofungin (Hoang *et al.*, 2022).

Another advance in *in vitro* model utilisation was the development of 3D organoid systems which use stem cells to more accurately recreate the architecture and physiology of human organs with or without a 3D matrix support. These systems are self-organizing and can in some cases be histologically indistinguishable from the organs they mimic (Turco *et al.*, 2017). These advances allow for more diverse cell types being studied simultaneously enabling the simulation of complex tissue structures (Huch and Koo, 2015). Organoids utilize human induced pluripotent stem cells which are differentiated through exposure to a variety of stimuli to produce complex tissues found in the organ of interest. Organoids offer a number of potential benefits over animal models including the ability to be derived from patient biopsies (Qu *et al.*, 2024). They provide rapid and more robust outcomes compared to mammalian models and are a more accurate representation of human tissue and generate a larger quantity of material to work with when compared to animal models. These models have been utilized to study Toll-like receptor activation following *A. fumigatus* exposure in 3D lung models (Bosáková *et al.*, 2023) and have been utilized to examine the response of *A. fumigatus* to *P. aeruginosa* within a realistic lung environment (Barkal *et al.*, 2017). Organoids, like other *in vitro* models, have limitations including the lack of inter-organ communication and can only show certain aspects of the host response (Jensen and Little, 2023; Kim *et al.*, 2020). Organoids and other *in vitro* systems also cannot mimic the host microbiome which is found at prominent sites of infection including the lungs and gastrointestinal tracts. This is because organoids are static and are prone to bacterial overgrowth and due to their nature require an aerobic environment, preventing the introduction of strictly anaerobic bacteria, thus failing to represent bacterial species that play a major role in relevant body sites (Poletti *et al.*, 2020).

1.6.3 Invertebrate model systems

Many insect species can be utilized as *in vivo* models including *Drosophila melanogaster* (fruit fly) and *Galleria mellonella* (greater wax moth larvae) which have become valuable assets for the research community. Compared to conventional mammalian models, insects have advantages such as easier handling requirements, fewer expenses, and the absence of the need for ethical or legal approval (Drinkwater

et al., 2019). These models characterize the dynamic host responses including immune activation, migration and complete metabolic and nutritional composition which may not be fully captured in 2D model systems (Stewart Merrill *et al.*, 2021). Insect models facilitate the study of systemic infection more readily than *in vitro* approaches (Ménard *et al.*, 2021). These models are in accordance with the 3Rs principles of replacement, reduction, and refinement applied in animal research facilitating large- scale investigations (Franco and Olsson, 2014). The immune systems of *D. melanogaster* and *G. mellonella* are especially useful because they act in a similar manner to the innate immune system of mammals (Browne *et al.*, 2013). This specificity enables an examination of the responses typically observed in the initial host-pathogen interaction, which is crucial in determining the establishment of infection and the downstream immune responses.

D. melanogaster is the most widely employed insect model for genetic manipulation (Atoki *et al.*, 2025). In many ways is the invertebrate counterpart to the murine model as both genomes were among the first to be fully sequenced and an array of mutants are readily available (Baenas and Wagner, 2019). Despite the availability of mutants and the compatibility with genetic manipulation *D. melanogaster* larvae are typically incubated at 25°C rather than 37°C, this is important as volatile organic compounds produced by *A. fumigatus* are significantly reduced at this temperature (Almaliki *et al.*, 2021). Despite this limitation, the combination of *Drosophila* studies with other model organisms can generate valuable data regarding the immune response to human fungal pathogens.

Galleria mellonella, the greater wax moth, is one of the most widely employed insect model for mycological research (Giamberardino *et al.*, 2022). *G. mellonella* larvae can persist at 37°C making them more suitable than *D. melanogaster* for studying human pathogens. *G. mellonella* methodology is well established (Figure 1.9) and the model has been employed for molecular analysis including proteomics and transcriptomic analysis. *G. mellonella* immune cells share many features with vertebrate innate immune cells such as macrophages and neutrophils being capable of phagocytosis, encapsulation, and the generation of antimicrobial peptides (Smith and Casadevall, 2021). These processes have also been shown to be inhibited by the action of mycotoxins in a similar manner to that observed in human neutrophils (Fallon

et al., 2011). The reduced cost of larvae also enables the use of larger test populations resulting in more robust and statistically significant data.

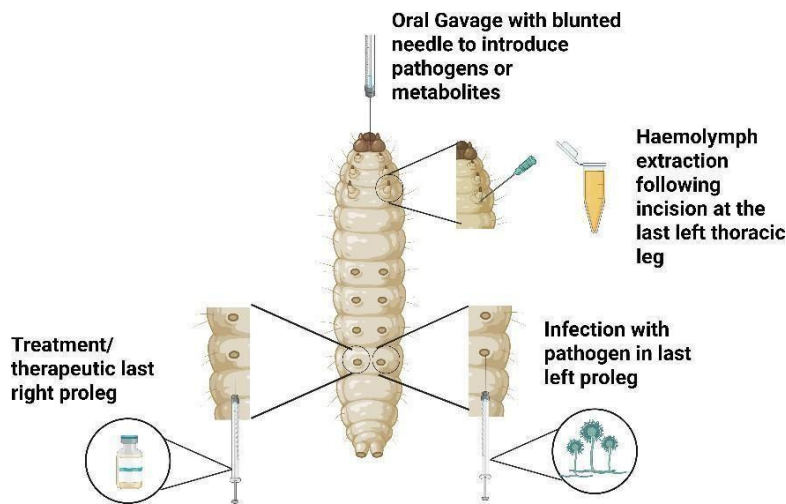


Figure 1.9: Overview of *Galleria mellonella* infection and haemolymph collection methodologies (generated in biorender).

1.6.4 *Galleria mellonella* as a model of the innate immune response

The utilisation of *G. mellonella* larvae as a model system is due to the structural and functional similarities between the insect immune response and the innate immune system of mammals (Browne *et al.*, 2013). Insect haemocytes demonstrate specificity and capability to distinguish between classes of microorganisms inducing an appropriate response (Trevijano-Contador and Zaragoza, 2018). This recognition of infection is mediated through germ-line encoded pattern recognition receptors which recognise pathogen-associated molecular patterns (PAMPs) (Lin *et al.*, 2020). These are homologous to those expressed on mammalian innate immune cells (Figure 1.10) resulting in signalling cascades initiating cellular and humoral immune responses including phagocytosis, nodulation, agglutination, encapsulation, and production of antimicrobial peptides (Lin *et al.*, 2020). Fungal α - 1,3-glucan can be recognised by specific recognition proteins which induce antifungal humoral responses when *G. mellonella* larvae were exposed to *Aspergillus niger* resulting in increased expression of antifungal antimicrobial peptides galiomycin and gallerimycin (Stączek *et al.*, 2021). Haemocytes can produce superoxide when activated and have a comparable mechanism to the NADPH oxidase complex of human neutrophils (Bergin *et al.*, 2005). The action of insect haemocytes could also be inhibited in a similar manner to neutrophils following exposure to the mycotoxins gliotoxin and fumagillin produced

by *A. fumigatus* (Fallon *et al.*, 2011). This similarity enables comparable results to be obtained to murine models with larval studies yielding data within two days compared to two months in murine studies (Firacative *et al.*, 2020).

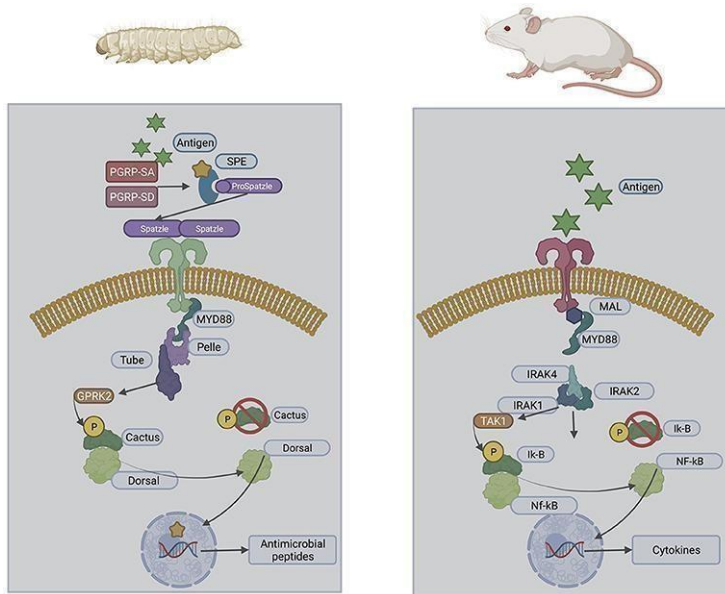


Figure 1.10: Comparison of toll-like receptor signalling in *G. mellonella* compared to the gold standard murine model demonstrating their similarities (generated in biorender).

1.6.5 Mechanisms employed by Fungi to Infect *Galleria mellonella* Larvae

Virulence factors utilised in the colonisation of mammalian hosts are also important when colonising invertebrates. Siderophores are crucial for survival of *A. fumigatus* in *G. mellonella* as deletion of genes involved in siderophore biosynthesis rendered the fungus avirulent or reduced fungal virulence and the results were comparable with data obtained in murine studies (Slater *et al.*, 2011). Adherence of *A. fumigatus* to host tissue is driven by the conserved C-terminal domain encoded by MedA which regulates conidiogenesis, adherence to host cells, and pathogenicity. Mutants lacking this region demonstrated impaired biofilm formation and reduced adherence capacity in pulmonary epithelial cells *in vitro* and reduced virulence in murine models of invasive aspergillosis and in *G. mellonella* larvae (Abdallah *et al.*, 2012). In addition, conidial pigmentation, which protects against reactive oxygen species through melanin production can influence *G. mellonella* infection. Deletion of genes associated with melanin production results in highly virulent strains in *G. mellonella* larvae. It has been speculated that these mutants induce an exaggerated immune response of *G. mellonella*, possibly triggered by the altered surface properties of the colour mutant conidia, inducing an over-reactive immune response preventing conidial clearance

(Jackson *et al.*, 2009).

Secreted aspartic proteases have been implicated as a virulence factor facilitating tissue invasion by fungal pathogens. CtsD, an aspartic protease distinct to *A. fumigatus* was examined as a virulence factor in *G. mellonella* larvae (Vickers *et al.*, 2007). Larvae infected with conidia had a higher mortality rate than larvae infected following treatment with an anti-CtsD antibody indicating the enzyme is produced and secreted during infection and has a potential role in facilitating virulence of the fungus *in vivo* (Vickers *et al.*, 2007). Both fumagillin and gliotoxin affect the immune response of *G. mellonella* larvae and have been detected in larvae post infection. Fumagillin induces similar effects in insect haemocytes thus demonstrating further similarities mammalian and insect cells (Fallon *et al.*, 2011). Gliotoxin can be quantified using HPLC *in vivo* and *ex-vivo* in *Galleria* larvae and the level of gliotoxin secretion was found to correlate with virulence in larvae whereas elastase, catalase and growth rate did not (Reeves *et al.*, 2004). The similarity in both the fungal and the host response supports the suitability of *G. mellonella* larvae as an ethical model to examine fungal virulence factors. Despite being a suitable analogue of the human innate immune response, differences in the metabolite profile, the lack of an adaptive immune response and lack specific organ sites limit the translatability of findings from *G. mellonella* experimentation in isolation (Gallorini *et al.*, 2024) but can be used in combination with other approaches to provide robust and meaningful data.

1.6.6 The *ex-vivo* pig lung model as an analogue of host tissue

The initial attachment and colonisation of host cells by *A. fumigatus* is facilitated by binding to extracellular matrix, and basal lamina components, which may not be exposed in the healthy host (Bertuzzi *et al.*, 2018). In some patients with an altered lung structure such as asthmatics or cystic fibrosis patients fungal spores can adhere to collagen and fibronectin fibres in the basal lamina facilitating its persistence and the development of fungal disease (Gago *et al.*, 2019). The microbiome of the lung also plays an important role in the prevention of pulmonary aspergillosis as the components and metabolites of the microbiome can influence immune responses (Kolwijck and van de Veerdonk, 2014). Dysbiosis of the lung microbiome is related to the exacerbations of several respiratory diseases such as bronchiectasis, cystic fibrosis and chronic obstructive pulmonary disease (Cai *et al.*, 2022). These factors are difficult to simulate in many models of fungal disease such as cell culture, organoids and murine models.

Pig lung models offer an alternative to murine studies and better demonstrate host responses due to their immunological and physiological similarities with humans (Meurens *et al.*, 2012). The microbiome of healthy pig lungs also shows a similar phylum distribution to that found in human lungs (Beck *et al.*, 2012; Huang *et al.*, 2018). In addition, the metabolome of pig lungs demonstrated a similar composition to that of humans, with the main difference being the concentration of some metabolites (Benahmed *et al.*, 2014). The *ex-vivo* pig lung model (EVPL) offers a high- throughput, low-cost, and ethical model that closely mimics the lung environment (Figure 1.11) (Harrison *et al.*, 2014). Lungs can be obtained from pigs slaughtered for commercial meat production and since little or no lung tissue is used in food production, lungs are classified as a waste product whose use does not raise ethical questions (Harrison *et al.*, 2014). This model has been optimized to mimic factors observed in the cystic fibrosis airways and has been widely used to study bacterial pathogenicity (Harrison and Diggle, 2016) and antibiotic tolerance (Sweeney *et al.*, 2021; Harrington *et al.*, 2020). This model has demonstrated strain-specific virulence differences, including quorum sensing-deficient mutants of *P. aeruginosa* demonstrating reduced damage to alveolar tissue (Harrison *et al.*, 2014). It has also been demonstrated that the EVPL model shows *in vivo*-like aspects of *P. aeruginosa* gene expression and that the pathogen forms a biofilm using known *in vivo* pathways required during infection, resulting in the formation of clinically realistic structures not seen in other *in vitro* studies (Harrington *et al.*, 2020; Harrington *et al.*, 2022). The structural, biochemical and microbial similarities make the EVPL model attractive for adaptation and implementation for mycological infection studies.

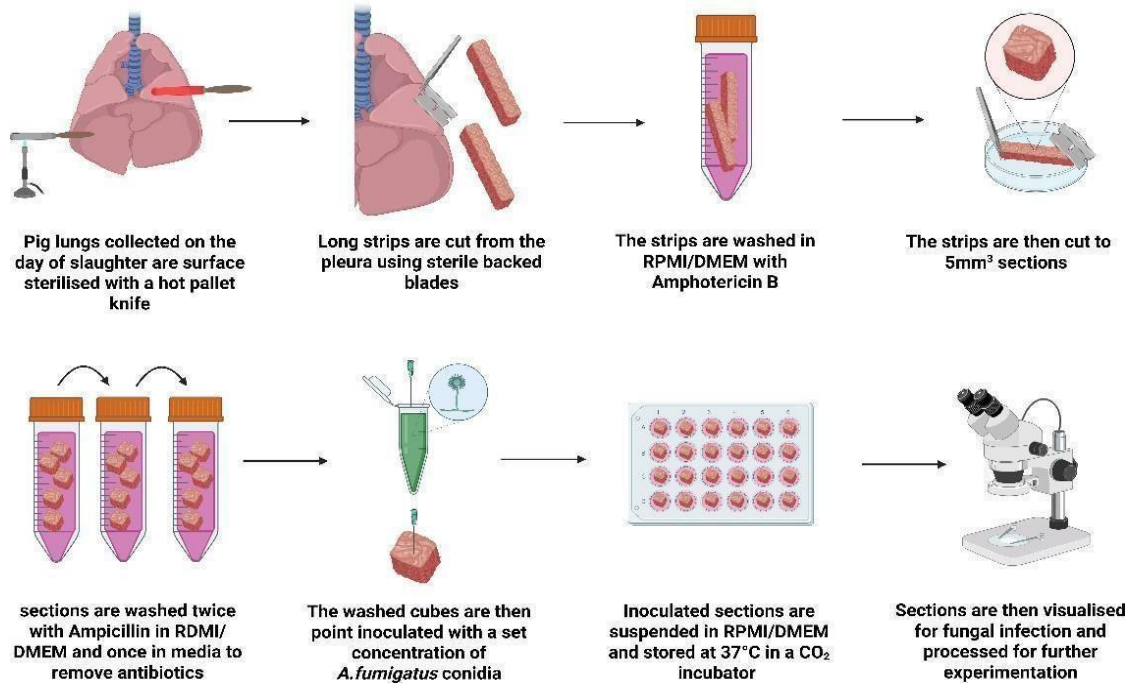


Figure 1.11: Methodology for extraction, infection and assessment of *ex-vivo* pig lung explants (generated in biorender).

1.6.7 A Combinational approach to disease modelling

Infection pathology and microbial virulence in patients is complex and multifactorial (Kumari *et al.*, 2021). As many model systems provide insight into specific aspects of a disease state or microbial virulence a combination of models is required to provide holistic insight into factors governing disease (Kaplan *et al.*, 2024). The in-depth examination of specific factors in isolation and combining these results offers novel insight into processes occurring during human infection. The selection of models is influenced by the question posed and the strengths and weaknesses of each model must be carefully considered (Swearengen, 2018). *Ex-vivo* systems offer greater control over variables and higher throughputs when compared to *in vivo* animal models (Hao Wang *et al.*, 2021). *In vivo* systems often offer more dynamic interplay with the pathogen of interest as the pathogen interacts with a diverse network of cells, tissues and organs and an active immune system (Bertorello *et al.*, 2024).

In this study the *G. mellonella* larvae model offers insight into the *in vivo* innate immune response which is the main source of antagonism against *A. fumigatus* during the early stages of colonisation. The larval model also enables simulation of systemic infection and behavioural outputs. This model cannot mimic host tissue or physiology which is why it has been combined with the *ex-vivo* pig lung model of infection.

The EVPL model offers insight into saprophytic infections in a realistic host tissue context through accurate emulation of tissue architecture, microbiome and immune antagonism. In combination these models provide insight into the response and adaptation of *A. fumigatus* to host immune antagonism and colonisation of host tissue. The isolation of these crucial aspects provides insights into the growth of *A. fumigatus* *in vivo* in a more focused and controllable, but dynamic environment.

1.7 Omics approaches in mycology

High throughput analysis has fundamentally altered biological research and facilitated in depth molecular analysis of the response of species to specific factors or environments (Khan *et al.*, 2019). These high-throughput methodologies have been broadly coined as “omics” approaches and each focus on the extraction and analysis of various biological molecules including DNA, RNA, proteins, and metabolites (Subramanian *et al.*, 2020). The widespread adoption of omics approaches by researchers has been facilitated by the development of more sensitive equipment, refined approaches and the ever-evolving suite of bioinformatics tools (Dai and Shen, 2022). The expansion of this field in microbiology through application of proteomics, transcriptomics and metabolomics to study host-pathogen interaction has provided previously unobtainable insight into the mechanisms involved in these interactions (Al-Maleki *et al.*, 2023)

The first omics technology to appear in the literature was Genomics in 1987. This approach examines an organisms entire genome and goes beyond genetics by examining the interactions between genes within the genome and the environment rather than examination of a gene in isolation (Cordell, 2009; McColl *et al.*, 2019). Genomic analysis can now be conducted on a vast scale due to the development of next-generation sequencing technologies with projects including sequencing of thousands of genomes (Alser *et al.*, 2025). Advanced technology also enables functional genomic analysis to examine other aspects of the genome, such as how genes are differentially expressed, which transcription factors are bound, or how chromatin is formed and organized (Gürsoy *et al.*, 2022). Pan-genomic analysis of 260 genome sequences of *A. fumigatus* using a combination of population genomics, phylogenomics, and pan-genomics determined that there are high levels of recombination within the species. This study also identified that there are three primary clades defined by genes encoding diverse metabolic functions, hinting that population

structure may be shaped by environmental niche occupation or substrate specificity, which may have implications for disease progression (Lofgren *et al.*, 2022).

Transcriptomics is one of the most developed fields in the post-genomic era. The transcriptome is defined as the complete set of RNA transcripts including mRNA, tRNA, rRNA and non-coding RNA in a specific cell type or tissue at a certain developmental stage and under a specific physiological condition (Dong and Chen, 2013). While genomics provides insight into genes that are hypothetically involved in a response, transcriptomic analysis enables a deeper understanding of how a cell is functioning (Postel *et al.*, 2022). Transcriptomics provides in-depth insight into the expression of genes in the cell, as each gene transcribed to produced multiple transcripts leading to a diverse set of functional molecules including splice variants providing insight beyond what a simple gene count could provide (Lowe *et al.*, 2017). *In vivo* transcriptomics of *A. fumigatus* has also been used frequently to understand pathogenicity. The transcriptome obtained from conidia germinating in murine lungs with germlings obtained under *in vitro* conditions expected to match the *in vivo* environment confirmed that *A. fumigatus* encounters nutrient limitations as well as alkaline and oxidative stress during the early stages of infection (McDonagh *et al.*, 2008). Epigenomics is a step beyond transcriptomics and investigates DNA methylation variations and the functional consequences of the spatial behaviour of the DNA (Serafini *et al.*, 2020). This approach has been utilised to demonstrate the role of EGR2 as a key proximal transcriptional activator and epigenomic marker in alveolar macrophage interactions (Kolostyak *et al.*, 2024).

Metabolomics investigates global metabolic alterations associated with chemical, biological, physiological, or pathological processes. These metabolic changes are measured with various analytical platforms including liquid chromatography-mass spectrometry, gas chromatography-mass spectrometry and nuclear magnetic resonance spectroscopy (Wishart *et al.*, 2022). This approach can identify metabolites elevated in response to specific conditions including the role of glutathione, histidine, proline and tryptophan metabolism in reducing *A. fumigatus* damage resulting from exposure to cadmium (Tian *et al.*, 2024).

Proteomics offers insights beyond the static frameworks of genomics and transcriptomics facilitating the unravelling of the dynamic behaviour

of proteins within the cell. Proteomics enables insight into protein–protein interactions and post- translational modifications representing critical layers of biological regulation which are often altered in disease states (Palabiyik and Palabiyik, 2025). Proteomics characterises the interactions, function and structure of the entire set of expressed proteins in a cell, tissue or organism. Proteomics provides a better understanding of the structure and function of the organism than genomics as it captures alteration in protein expression according to time and environmental conditions (Al-Amrani *et al.*, 2021). Many proteomics approaches rely on mass spectrometry which measures the mass to charge ratio of ions and offers a comprehensive method for separation, identification and quantification of peptides from complex mixtures (Sinha and Mann, 2020). Proteomics is broadly divided into two approaches; discovery proteomics, which aims to identify and quantify as many proteins as possible in a sample, often using shotgun proteomics workflows and targeted proteomics in which predefined targets are quantified (Mendes and Dittmar., 2022).

Discovery proteomics is generally divided into three categories; Top-down proteomic in which a whole proteoform can be assessed, middle-down, in which large peptides produced by specific enzymatic digestion such as Glu-C to generate large peptides (>3 kDa) that are analyzed by mass spectrometry (MS). This method is useful for characterizing high-molecular-weight proteins and post-translational modifications that are difficult to detect by top-down proteomics (Takemori *et al.*, 2024) and Bottom-up proteomics which utilises the advantages that peptides have over proteins, being more easily separated by reversed-phase liquid chromatography, ionize well, and fragment in a more predictable manner. This translates into a robust methodology that enables high-throughput analysis, allowing for identification and quantification of thousands of proteins from complex lysates (Dupree *et al.*, 2020). Discovery proteomics can further be divided into two main approaches, gel based and gel free methods. Gel based methods facilitates the analysis of a small number of pre-fractionated targets, separated by size from complex mixtures of proteins enabling intact protein analysis. Efficiency of recovery of proteins from gels have complicated this approach (Takemori *et al.*, 2020) but significant progress has recently been made with the development of PEPPi-MS (Passively Eluting Proteins from Polyacrylamide gels as Intact species for MS), an efficient passive extraction method for intact proteins

in gels (Takemori *et al.*, 2022) breathing new life into this technique by overcoming the recovery challenges. Gel-free discovery proteomics, also called shotgun proteomics is characterised by the identification of digested peptides in a high-throughput bottom-up approach. This facilitates immediate protein identification, automation and ongoing advancement of data processing capacity (Ercan *et al.*, 2023). This approach is further divided into data-dependent acquisition and data-independent acquisition. Data-dependent acquisition is particularly effective for capturing intense peptide ions, whereas data-independent acquisition excels in capturing low-intensity peptides (Liang *et al.*, 2025). GeLC-MS, a multidimensional separation workflow, combines gel-based prefractionation with LC-MS, for deep Middle-down proteomics where only proteins in the desired molecular weight range are gel-fractionated and their Glu-C digestion products are analyzed giving great depth of read when compared to other approaches (Takemori *et al.*, 2024)

Targeted proteomics is a more specific approach to verify expected findings and is typically coupled with stable isotope labelling techniques involving the incorporation of stable isotopes into different samples, combining them for sample preparation and analysis, then distinguishing them in the mass spectrometer based on their *m/z* difference. Isotopic labelling allows for the direct comparison of different samples within the same run, thereby reducing variability and improving quantitative accuracy. The most commonly employed labels are isobaric tags for relative and absolute quantitation (iTRAQ), Stable Isotope Labeling by Amino Acids in Cell Culture (SILAC) or Tandem Mass Tag (TMT) (Zicong Wang *et al.*, 2024). These approaches offer insight into specific aspects of microbial life and have varying levels of depth and outputs which are suited to answering different questions.

It is widely accepted that multi-omics approaches offer a more accurate and comprehensive understanding of a system being studied as it profiles multiple levels of cellular response and the flow from one level of function to the next (Hasin *et al.*, 2017). This combinational approach provides a holistic view of the response of an organism or a system to various stimuli (Gutierrez Reyes *et al.*, 2024). A multi-omics approach can be utilised to confirm results obtained in one approach or another providing a robust understanding of the response elicited in response to stimulation or interactions (Perakakis *et al.*, 2018). However multi-omics is costly, time consuming and is beyond the access of many researchers (Chen *et al.*, 2023) due to this constraint label-free quantitative proteomics was the main approach utilised in this study.

1.7.1 Label-free quantitative proteomics

Label-free quantitative proteomics offers a reliable, versatile, and cost-effective alternative to labelled quantitation (Neilson *et al.*, 2011). This method determines quantitation by comparing the Mass spectrometer signal intensities of peptides across a set of samples. Specifically, it involves extracting MS¹ chromatographic peak areas and employing parallel reaction monitoring for MS²-based quantitation (Yu *et al.*, 2022; Wippel *et al.*, 2022). Quantification is based on the chromatographic peak intensities and spectral counting of identified proteins after MS² analysis (Geis-Asteggiante *et al.*, 2016). Due to the lack of labelling and the fact that each sample is individually processed, the robustness and reproducibility of sample preparation are two of the most important aspects for a successful quantitative proteome analysis. As a result every step within the experimental pipeline is a potential source of error and can introduce several biases that might produce misleading results (Megger *et al.*, 2013). Typical sample preparation involves cell lysis, protein reduction, alkylation and digestion, typically with trypsin and then rigorous clean up to remove impurities such as salts and remaining solid particles (Figure 1.12). Samples are then subjected to fractionation and separation of the tryptic digest *via* high performance liquid chromatography (Duong and Lee, 2023).

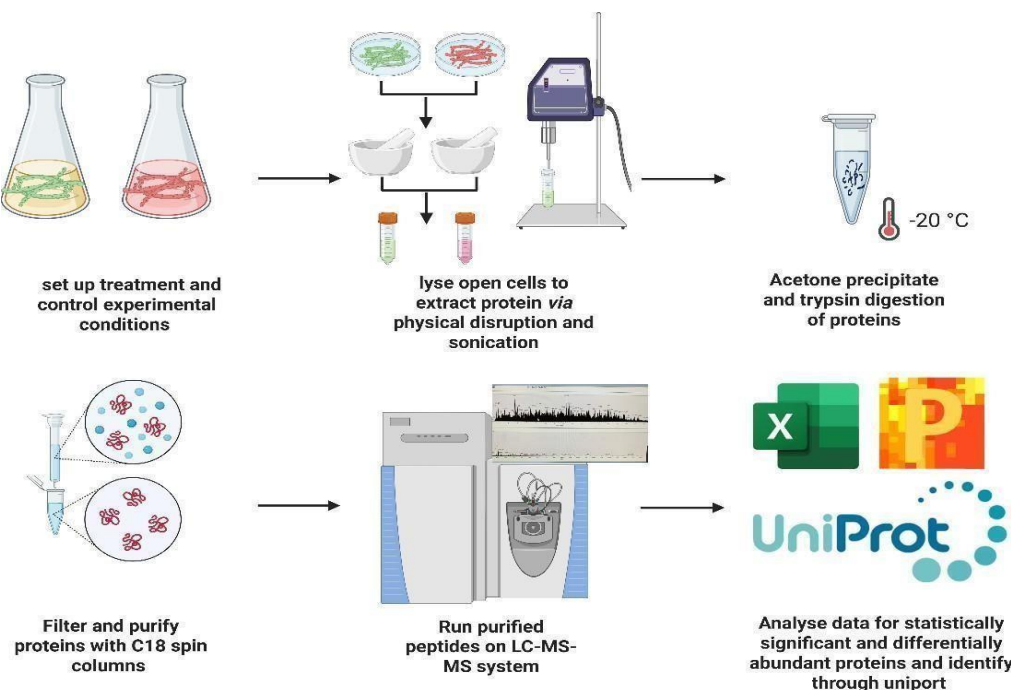


Figure 1.12: Generic Label-free proteomics methodology (generated in biorender).

1.7.2 Proteomics as a tool for uncovering host adaptation processes

Proteomics offers in-depth insights into the constant interactions between hosts and pathogens and can provide insight into the temporal and spatial expression of proteins during these interactions (Jean Beltran *et al.*, 2017). The ability of a pathogen to survive in a hostile environment can be understood by examining changes at the protein level (Poirier and Av-Gay, 2015). Proteomics provides a rapid and effective platform to identify these changes, enabling the detection of alterations in protein abundance, quantifies protein secretion and release, measures an array of post-translational modifications that influence signalling cascades, and profiles protein–protein interactions (Sukumaran *et al.*, 2021). Total extraction of protein from a system can enable identification and quantification of multiple species simultaneously in a single sample (Grassl *et al.*, 2016). This can provide new insight into how the pathogen promotes invasion, and evasion of the host immune system, and simultaneously, profiles how the host responds to the attack and provides protection from the intruder (Jo, 2019; Sukumaran *et al.*, 2019). Proteomics provides insight into changes in total protein profiles when an organism encounters environmental stress, elucidating changes to biological functions and metabolic networks (Guo *et al.*, 2021). These are factors which are associated with host adaptation. This approach has been applied extensively to study bacterial, viral and fungal pathogens proving insight into various interactions between these species and their hosts and reveal insight into immune evasion processes elicited by these pathogens (Greco and Cristea, 2017; Torres-Sangiao *et al.*, 2022). Understanding both sides of these interactions enables a basis for which to dissect and disrupt host evasion and pathogenesis resulting in the development of more effective and specific antimicrobial agents or drug target to better combat or prevent disease.

1.8 Thesis objectives

The primary objective of this research was to further our understanding of host adaptation processes exhibited by *A. fumigatus* through proteomic characterisation in response to various host environments and stressors. This study also aimed to understand the role of microbial interactions, which often occur in vulnerable patients and to understand how these interactions shape the outcome for the host.

The aims for this study were:

1. To contribute to our understanding of host adaptation processes through generation and characterisation of an adapted *A. fumigatus* strain through subculturing on media containing host specific nutrients and stressors. The strain was also examined through proteomics to gain insight into protein changes governing any observed alterations
2. To characterise the metabolic profile and secretome of *A. fumigatus* in a sublethal infection within the *G. mellonella* model. To conduct proteomic analysis on the haemolymph of infected larvae to understand what products are released by the fungus over the first 96 hours of infection while simultaneously characterising the response of the host at the peak of this infection.
3. To characterise the response of *A. fumigatus* to secreted products of a common co-pathogen in the lung *K. pneumoniae*. The phenotype of *A. fumigatus* and the production of mycotoxins was assessed in addition to the proteomic response to the secreted products. The secretome of *K. pneumoniae* was also characterised through proteomic analysis to identify the causative agents of the fungal alterations.
4. To characterise processes associated with tissue colonisation by *A. fumigatus* during saprophytic infection. This was conducted through adaptation of the *ex-vivo* pig lung (EVPL) model of infection. This provided novel insight into host metabolism and fungal virulence in the presence of a realistic analogue of decaying host tissue with a host microbiome, immune response and 3D architecture.
5. The characterisation of the interactions between *A. fumigatus* and *P. aeruginosa* in a realistic host tissue context. To establish mono-infected and coinfecte *ex-vivo* pig lung explants and conduct proteomic analysis to characterise how the three species interact. This provided novel insight into how the pathogens impact each other's development and the response of the host to the pathogens in isolation and in combination.

Chapter 2

Prolonged Subculturing of *Aspergillus* *fumigatus* on Galleria Extract Agar Results in Altered Virulence and Sensitivity to Antifungal Agents

Aaron Curtis, Kieran Walshe and Kevin Kavanagh

Department of Biology, Maynooth University, W23 F2H6 Maynooth, Co.
Kildare, Ireland

Published as:

Curtis, A., Walshe, K. and Kavanagh, K., 2023. Prolonged Subculturing of *Aspergillus fumigatus* on Galleria Extract Agar Results in Altered Virulence and Sensitivity to Antifungal Agents. *Cells*, 12 (7), 1065.

Author Contributions

A.C. and K.K. designed the experiments. A.C. and K.W. performed the experiments and analysed the results. A.C. and K.K. wrote the manuscript. All authors have read and agreed to the published version of the manuscript.

Abstract

Aspergillus fumigatus is an environmental saprophyte and opportunistic fungal pathogen of humans. The aim of the work presented here was to examine the effect of serially subculturing *A. fumigatus* on agar generated from *Galleria mellonella* larvae in order to characterize the alterations in the phenotypes that might occur. The passaged strains showed alterations in virulence, antifungal susceptibility, and in protein abundances that may indicate adaptation after 25 passages over 231 days on *Galleria* extract agar. Passaged strains demonstrated reduced virulence in *G. mellonella* larvae and increased tolerance to haemocyte-mediated killing, hydrogen peroxide, itraconazole, and amphotericin B. A label-free proteomic analysis of control and passaged *A. fumigatus* strains revealed a total of 3329 proteins, of which 1902 remained following filtration, and 32 proteins were statistically significant as well as differentially abundant. Proteins involved in the response to oxidative stress were altered in abundance in the passaged strain and included (S)-S-oxide reductase (+2.63-fold), developmental regulator FlbA (+2.27-fold), and histone H2A.Z (-1.82-fold). These results indicate that the prolonged subculturing of *A. fumigatus* on *Galleria* extract agar results in alterations in the susceptibility to antifungal agents and in the abundance of proteins associated with the oxidative stress response. The phenomenon may be a result of selection for survival in adverse conditions and highlight how *A. fumigatus* may adapt to tolerate the pulmonary immune response in cases of human infection.

2.1 Introduction

Aspergillus fumigatus is a ubiquitous soil-dwelling saprophyte and opportunistic fungal pathogen of humans (Mousavi *et al.*, 2016). *A. fumigatus* has been labelled as an ‘accidental’ pathogen primarily due to its independence of a host for survival, and its pathogenic potential may have evolved to facilitate survival in the environment (Rokas *et al.*, 2020). Virulence factors that facilitate infection in mammals include siderophore secretion, the ability to grow at 37 °C, and the production of immunosuppressive toxins such as gliotoxin (Raksha *et al.*, 2017). *A. fumigatus* can initiate growth within the host phagolysosome partially aided through the production of siderophores, and this process also occurs when *A. fumigatus* is engulfed by soil-dwelling amoebae (Van Waeyenberghe *et al.*, 2013). Gliotoxin biosynthesis is thought to have evolved to combat free-living predatory amoebae during its saprophytic existence, posing a selection pressure on *A. fumigatus* (Hillmann *et al.*, 2015). These adaptations may contribute to the ability of the fungus to colonize and disseminate in human hosts.

In humans, aspergillosis can develop in neutropenic individuals, hematopoietic stem cell or solid organ transplant recipients, and patients on immunosuppressive therapy, and can manifest as a number of clinical conditions, ranging from allergic bronchopulmonary aspergillosis (ABPA) to acute invasive aspergillosis (Ben-Ami *et al.*, 2010; El-Baba *et al.*, 2020). ABPA occurs as a result of hypersensitivity to *A. fumigatus* and affects 2–3.5% of patients with asthma (Denning *et al.*, 2013) in addition to approximately 10.5% of cystic fibrosis (CF) patients, of which about 10% are chronically colonized (Maleki *et al.*, 2020; LiPuma, 2010). Patients can be simultaneously colonized with different *A. fumigatus* strains, not all of which have the ability to persist in the pulmonary microenvironment (LiPuma, 2010). A genotypic analysis demonstrated the persistence of *A. fumigatus* for at least 4.5 years within a CF patient, that persistent strains adapted to growth in hypoxic conditions, and that conidia were more sensitive to oxidative stress (Ross, 2022). Repeat isolation from a single host with chronic granulomatous disease with persistent and recurrent invasive aspergillosis over two years revealed that the strains were isogenic and demonstrated resistance to itraconazole (Ballard *et al.*, 2018).

Chronic pulmonary aspergillosis requires prolonged antifungal therapy, with a recommended minimum course of 4–6 months (Denning *et al.*, 2016); therapy for up

to 12 months may be required to improve long-term survival (Im *et al.*, 2021). The long-term persistence of *A. fumigatus* in the lungs raises the possibility that the phenotype of the infecting strain may alter or adapt to the host microenvironment. The characterization of aspergillomas revealed resistance following antifungal therapy emerging from genetic alterations occurring within a fungal mass from a single parent strain (Howard *et al.*, 2013). An aspergilloma demonstrated an initial itraconazole MIC of 0.25 mg/L; after six months of antifungal therapy an MIC > 16 mg/L was evident, but after the cessation of therapy for four months the isolate MIC returned to 0.5 mg/L (Chen *et al.*, 2005). An analysis of *A. fumigatus* Af293 and CEA17, which share a 99.8% identical genome, demonstrated altered growth rates, virulence, and susceptibility to drug treatment and immune killing. The observed similarity in genomes and difference in phenotypes indicated that epigenetic alterations could be responsible for these physiological differences (Colabardini *et al.*, 2022). Another possible cause of these variations could be the presence of single-nucleotide polymorphisms, insertions, and deletions, which have been demonstrated to greatly impact heterogeneity (Keller, 2017).

The serial passaging of *A. fumigatus* on a murine lung homogenate medium revealed the selection of a rapidly germinating strain, after 13 passages, that produced an enhanced inflammatory response in mice. Genome sequencing revealed conserved mutations of the ssKA gene, which is part of the SakA mitogen-activated protein kinase (MAPK) stress pathway (Kirkland *et al.*, 2021). Serial passaging can also be conducted *in vivo*, and insects serve as an excellent model in which to passage as they are simple to maintain and inoculate, have short life cycles, and are easily manipulated (Scully and Bidochka, 2006). *Galleria mellonella* larvae are a well-characterized model for studying bacterial and fungal pathogenesis due to the strong similarities between the insect immune response and the innate immune response of mammals in addition to the ability to grow at 37 °C (Curtis *et al.*, 2022; Trevijano-Contador and Zaragoza, 2018). Due to the similarities in the immune response, the preparation of agar from these larvae would contain products found in the human innate immune response, allowing for insights into how these products may shape fungal responses to the lung microenvironment. The serial passaging of *Cryptococcus neoformans* in *G. mellonella* larvae for 15 passages resulted in the generation of a distinct phenotype, which grew faster in hemolymph but was more susceptible to hydrogen peroxide in

vitro, killed fewer murine macrophages, and produced a smaller fungal burden in human macrophages *ex vivo* compared to the parental strain (Ali *et al.*, 2020). Haemocytes exposed to the passaged strains produced less hydrogen peroxide, and a histopathological analysis also indicated that the passaged strain increased larval nodulation (Ali *et al.*, 2020). The serial passaging of *Aspergillus flavus* in *G. mellonella* larvae demonstrated that the genetic diversity of the passaged strain decreased significantly, which emphasizes the impact that the host exerts on shaping the evolution of a pathogen population *in vivo* (Scully and Bidochka, 2006).

G. mellonella larvae are susceptible to infection with *A. fumigatus*, and previously published results show a strong correlation with those obtained in mammals (Slater *et al.*, 2011). Larvae infected with *A. fumigatus* show many of the symptoms evident in infected mammals, including the development of granulomas and the *in vivo* production of toxins (Sheehan *et al.*, 2018). The aim of the work presented here was to characterize the effect of prolonged subculturing on Galleria extract agar on the virulence and antifungal response of *A. fumigatus*.

2.2 Materials and Methods

2.2.1 Aspergillus fumigatus Culture Conditions

Aspergillus fumigatus ATCC 26933 was cultured for 72 h at 37 °C on malt extract agar (MEA) (Oxoid, Basingstoke, UK) plates following point inoculation. Czapek–Dox broth (Duchefa Biochemie, Haarlem, The Netherlands) (50 mL) was inoculated with *A. fumigatus* conidia at an initial density of 1×10^5 conidia/mL and grown at 37 °C for 72 h at 200 rpm in an orbital incubator. The wet biomass of mycelia was weighed at 72 h following filtration through Miracloth (Millipore, Millipore, MA, USA).

2.2.2 Generation of passaged strains of Aspergillus fumigatus

Galleria extract agar (termed GEA20) was produced by grinding 20 *G. mellonella* larvae in 20 µL of sterile phosphate-buffered saline (PBS) *via* the use of a sterile mortar and pestle. The extract was centrifuged at 538x g for 5 min to remove particulate matter, and 20 mL of the supernatant was added to 80 mL of autoclaved agar (2 g w/v) supplemented with 0.1 g (w/v) of glucose, allowed to cool prior to addition, and 100 µL of penicillin–streptomycin (pen–strep) (Merck, Branchburg, NJ, USA) (10,000 U/10 mg/mL). *A. fumigatus* conidia were point inoculated onto GEA20

plates and incubated at 37 °C until growth reached the edge of the agar plate, which took an average of 9.24 days before subculturing onto fresh GEA20 plates. Three strains were selected after being serially passaged for a total of 25 passages over 231 days, and referred to as A25, C25, and E25. Control strains were serially sub-cultured on MEA plates for the same period of time.

2.2.3 Virulence assessment of passaged strains *in vivo*

Six instar larvae of *G. mellonella* (Livefoods Direct Ltd., Sheffield, UK) were stored at 15 °C prior to use. Twelve larvae weighing 0.2–0.3 g, without signs of melanization, were inoculated with 20 mL of PBS containing 5 $\times 10^5$ control or passaged *A. fumigatus* conidia *via* intra-hemocoel injection using a 26 G 1 mL syringe (Terumo, Tokyo, Japan). The larvae were placed in 9 cm Petri dishes and incubated at 37 °C. Larval viability was assessed over 72 h. Experiments were performed on four independent occasions.

2.2.4 Haemocyte kill assay

Hemolymph (500 μ L) was extracted from *G. mellonella* larvae and haemocytes were harvested by centrifugation at 8609 x g for 8 min. Cell-free haemolymph was retained on ice. Haemocytes were resuspended in 500 mL of sterile PBS and enumerated using a haemocytometer. The conidia of control and passaged *A. fumigatus* strains were harvested and resuspended in cell-free haemolymph for 30 min at 37 °C. The opsonized conidia were harvested and resuspended in 500 μ L of sterile PBS. Conidial and haemocyte suspensions were mixed in a ratio of 1:1 (approximately 5 $\times 10^6$ haemocyte and conidia) in a final volume of 1 mL in a 50 mL Falcon tube (Sarstedt, Numbrecht, Germany) and incubated at 37 °C and 200 rpm. A 20 μ L aliquot was taken at 20-minute intervals and serially diluted for plating on MEA plates in triplicate. Fungal colonies were enumerated to assess viability after incubation at 37 °C for 24 h.

2.2.5 Susceptibility testing

Hydrogen peroxide (Sigma, St. Louis, MO, USA) was serially diluted in Sabouraud dextrose broth (SDB) (Oxoid, Hampshire, UK) on a 96-well plate (Corning, Corning, NY, USA) to produce a concentration range between 30.62 and 245 mM. Amphotericin B (Sigma, St. Louis, MO, USA) and itraconazole (Sigma, St. Louis, MO, USA) were serially diluted in SDB, producing ranges of 0.78 to 6.25 mg/mL and 7.81 to 62.5 μ g/mL, respectively. Conidia from the control and passaged strains were

harvested and enumerated. Aliquots (100 µL) of conidia were added to each well of a 96-well plate (Corning, Corning, NY, USA) to provide a concentration of 1×10^5 conidia per well. Plates were incubated at 37 °C and growth was assessed at 24 h at 600 nm using a plate reader (Bio-Tek Synergy HT, Somerset, NJ, USA).

2.2.6 Gliotoxin extraction and quantification

A. fumigatus cultures ($n = 3$) were grown in 50 mL of Czapek–Dox broth for 72 h. The supernatant was filtered through Miracloth, and 20 mL of supernatant was mixed 1:1 with chloroform for 2 h at room temperature. The chloroform fraction was stored at -20 °C overnight and samples were dried through rotary evaporation in a Büchi rotor evaporator (Brinkmann Instruments, Brea, CA, USA). Samples were dissolved in 500 µL of methanol and stored at -20 °C. Gliotoxin was detected by reverse phase HPLC (RP-HPLC; Shimadzu, Columbia, MD, USA). The mobile phase was 34.9% (v/v) acetonitrile (Fisher Scientific, Waltham, MA, USA), 0.1% (v/v) trifluoroacetic acid (TFA), (Sigma Aldrich, St Louis, MO, USA) and 65% (v/v) HPLC-grade water (ddH₂O). Samples (20 µL) were loaded onto an Agilent ZORBAX SB-Aq 5 µm polar LC column and quantified based on the standard curve generated using gliotoxin standards dissolved in methanol ranging from 6.25 to 100 mg/mL.

2.2.7 Total secreted siderophore quantification

A. fumigatus cultures ($n = 3$) were grown in 50 mL of Czapek–Dox broth for 72 h. Siderophore activity in supernatants was determined *via* the use of a SideroTec HiSens assay (Accuplex, Maynooth, Ireland). Briefly, 100 µL of sample was added to a 96-well microplate followed by the addition of 100 µL of a ready-to-use detector. After 10 min of incubation at 37 °C, the plate was read on a fluorescent reader (360 excitation/460 emission). The siderophore concentration was determined by using desferoxamine as a reference standard

2.2.8 Protein extraction and purification from *A. fumigatus* hyphae

Protein extractions were performed as outlined previously (Margalit *et al.*, 2022). *A. fumigatus* mycelia of control and passaged strain E25 ($n = 3$ per group) were grown for 72 h at 37 °C in Czapek–Dox media. Mycelium was harvested by filtration, snap-frozen in liquid nitrogen, and ground to a fine dust in a mortar *via* the use of a pestle. A lysis buffer (8 M urea, 2 M thiourea, and 0.1 M Tris-HCl (pH 8.0) dissolved in HPLC-grade ddH₂O), supplemented with protease inhibitors (aprotinin, leupeptin, pepstatin A, tosyllysine chloromethyl ketone hydrochloride (TLCK) (10 µg/mL), and

phenylmethylsulfonyl fluoride (PMSF) (1 mM/mL), was added (4 mL/g of hyphae). The lysates were sonicated (Bandelin Senopuls), three times for 10 s at 50% power. The cell lysate was subjected to centrifugation (Eppendorf Centrifuge 5418) for 8 min at 14,500 \times g to pellet cellular debris. The protein concentration was quantified by the Bradford method and samples (100 μ g) were subjected to overnight acetone precipitation. Samples were subjected to centrifugation at 14,500 \times g for 10 min to pellet proteins, acetone was removed, and the pellet was resuspended in a 25 μ L sample resuspension buffer (8 M urea, 2 M thiourea, and 0.1 M Tris-HCl (pH 8.0) dissolved in HPLC-grade ddH₂O). A 2 μ L aliquot was removed from each sample for quantification *via* the Qubit quantification system (Invitrogen, Waltham, MA, USA). Ammonium bicarbonate (Ambic) (125 μ L, 50 mM) was added to the remaining samples, which were subjected to reduction *via* the addition of 1 μ L of 0.5 M dithiothreitol and incubated at 56 °C for 20 min, followed by alkylation with 0.55 M iodoacetamide (IAA) at room temperature in the dark for 15 min. Proteins were digested *via* the addition of 1 μ L of sequence-grade trypsin (Promega) (0.5 μ g/ μ L), supplemented with 1 μ L of Protease Max Surfactant Trypsin Enhancer (Promega 1% w/v), and incubated at 37 °C for 18 h. Digestion was quenched *via* the addition of 1 μ L of TFA incubated at room temperature for 5 min. Samples were subjected to centrifugation at 14,500 \times g for 10 min prior to clean-up using C18 spin columns (Pierce). The eluted peptides were dried *via* the use of a SpeedyVac concentrator (Thermo Scientific (Waltham, MA, USA) Savant DNA120) and resuspended in 2% (v/v) acetonitrile and 0.05% (v/v) TFA aided by sonication for 5 min. The samples were centrifuged to pellet any debris at 14,500 \times g for 5 min, and 2 μ L from each sample was loaded onto the mass spectrometer.

2.2.9 Mass spectrometry

Purified peptide extracts (2 μ L containing 750 ng protein) were loaded onto a Q Exactive mass spectrometer (Thermo Fisher Scientific, Waltham, MA, USA) using a 133 min reverse-phase gradient, as per previous methods (Margalit *et al.*, 2020). Raw MS/MS data files were processed through the Andromeda search engine in MaxQuant software v.1.6.3.4 110 using a *Neosartorya fumigata* reference proteome obtained from a UniProt-SWISS-PROT database to identify proteins (9647 entries, downloaded July 2022). The search parameters followed those described in (Margalit *et al.*, 2020).

2.2.10 Data analysis

Perseus v.1.6.15.0 was used for the analysis, processing, and visualization of data. Normalized LFQ intensity values were used as the quantitative measurement of protein abundance. The data matrix generated was filtered to remove contaminants, and peptides were identified by site. LFQ intensity values were log2-transformed, and each sample was assigned to its corresponding group (control and E25). Proteins not found in all replicates in at least one group were omitted from further analysis. A data-imputation step was conducted to replace missing values with values that simulate signals of low-abundance proteins chosen randomly from a distribution specified by a downshift of 1.8 times the mean standard deviation of all measured values and a width of 0.3 times this standard deviation. Principal component analysis (PCA) was plotted using normalized intensity values. The proteins identified were then defined using a Perseus annotation file (downloaded in July 2022) to assign extract terms for biological process, molecular function, and Kyoto Encyclopedia of Genes and Genomes (KEGG) names.

To visualize the differences between two samples, pairwise Student's *t*-tests were performed using a cut-off of $p < 0.05$ on the post-imputation dataset. Volcano plots were generated by plotting the log2 fold change on the x-axis against the log *p*-values on the y-axis for each pairwise comparison. Statistically significant and differentially abundant (SSDA) proteins (ANOVA, $p < 0.05$) with a relative fold change greater than ± 1.5 were retained for analysis. SSDA proteins were z-score normalized and then used for hierarchical clustering to produce a heat map. Identified SSDAs could then be assessed using Uniprot codes generated by Perseus to gain insights into their roles within the cells. The mass spectrometry proteomics data have been deposited to the ProteomeXchange Consortium *via* the PRIDE (Perez-Riverol *et al.*, 2021) partner repository with the dataset identifier PXD036787.

2.2.11 Statistical analysis

Results from the phenotypic testing were assessed in Graphpad Prism Version 8.0.1. A 2-way ANOVA analysis or multiple paired *t*-tests were performed for the binary comparison of passaged and control *A. fumigatus* strains. Significance was set at $p < 0.05$. Proteomic analysis was conducted in Perseus V.1.6.15.0, as described above.

2.3 Results

2.3.1 Characterisation of growth characteristics of serially subcultured *A. fumigatus* strains

At the end of 25 passages, *A. fumigatus* conidia were isolated from GEA20 plates by washing with PBS/tween, and an aliquot of a diluted culture ($5 \times 10^6/\text{mL}$) was used to point inoculate MEA plates so that radial growth could be measured over 48 h at 37 °C. The results indicated no significant difference in the growth of the three passaged strains compared to the control (Figure S2.1). Conidia were also used to inoculate a flask of Czapex–Dox broth at a density of $1 \times 10^5/\text{mL}$ as well as incubated at 200 rpm and 37 °C for 72 h. At the end of the incubation period the mycelial wet biomass of the serially sub-cultured strains was not significantly different to that of the control (Figure S2.2). The gliotoxin concentration of culture filtrates at the end of 72 h was higher in the passaged strains than in the control, but only passaged strain A25 showed a significant result ($p = 0.01$) (Figure S2.3). There was no difference in the secreted siderophore concentrations between the control and passaged *A. fumigatus* strains (Figure S4). Pen–strep (0.1% v/v) was used in the GEA20 plates to prevent the overgrowth of bacteria from the *G. mellonella* digestive tract. The exposure of *A. fumigatus* to pen–strep did not affect the radial growth rate (Figure S2.5), and strains that were serially passaged on MEA agar plates containing 0.1% (v/v) pen–strep showed no significant alteration in their tolerance of hydrogen peroxide (Figure S2.6) or amphotericin B (Figure S2.7), but did demonstrate increased susceptibility to itraconazole (Figure S2.8), which was not observed in the GEA- passaged strains.

2.3.2 Passaged *A. fumigatus* strains show reduced virulence in *G. mellonella* larvae

G. mellonella larvae were inoculated via an intra-hemocoel injection with the conidia ($1 \times 10^5/20 \mu\text{L}$) of control or passaged *A. fumigatus* strains, and viability was assessed over 72 h (Figure 2.1). Infection with the control strain resulted in 30% mortality at 48 h compared to 5–8% mortality due to the passaged strains. By 72 h, the larvae infected with the control *A. fumigatus* conidia showed 44% mortality, compared to a mortality rate of 21–25% in the larvae infected with the conidia from the passaged strains (** $p = 0.004$ for A25 and C25; * $p = 0.0106$ for E25 relative to the control).

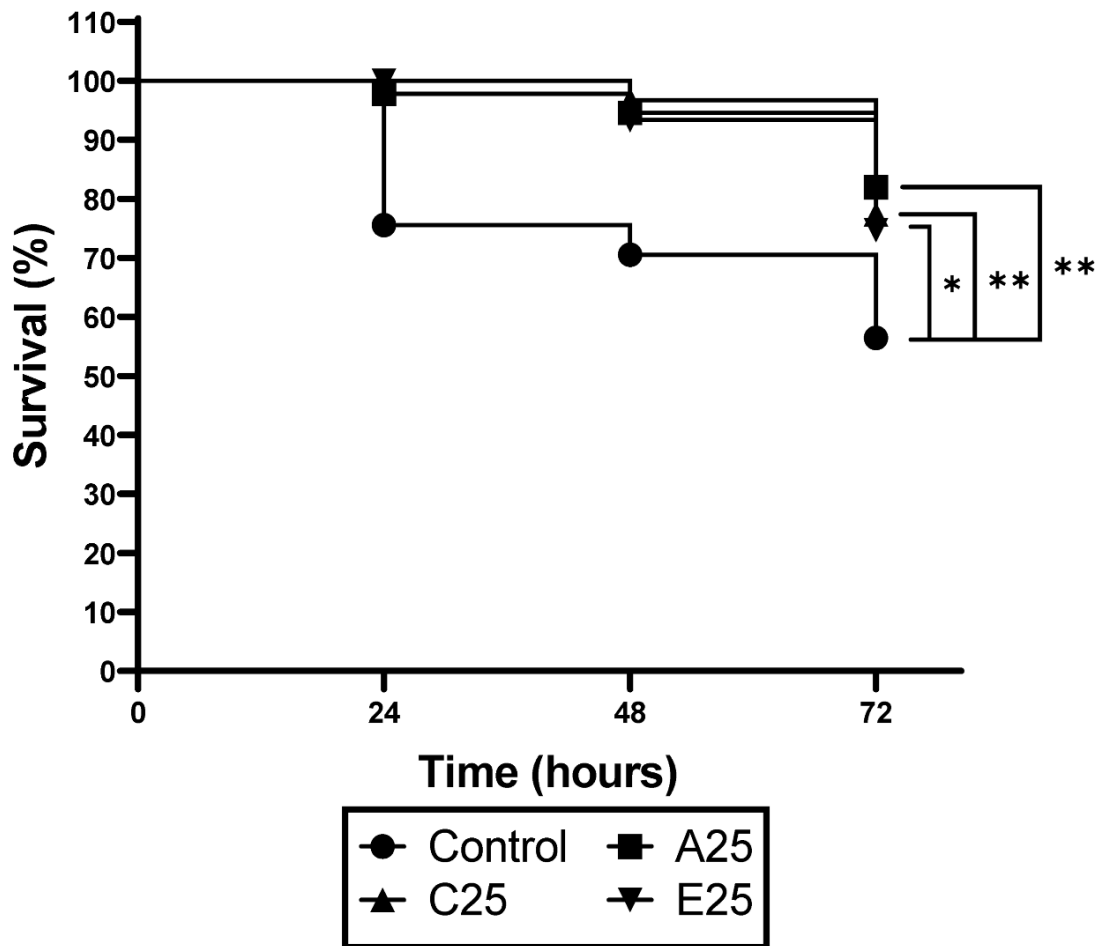


Figure 2.1: Response of larvae to infection by the conidia of control and passaged *A. fumigatus* strains. Larvae were infected with the conidia as described, and their survival was monitored over 72 h. Passaged strains showed significantly reduced virulence at 72 h ((A25, * $p = 0.0458$; C25 and E25, ** $p = 0.042$. Logrank (Mantel–Cox) test).

The response of the conidia from the control and passaged strains to *G. mellonella* haemocytes was assessed. Haemocytes were extracted from the larvae as described and mixed with haemolymph-opsonized conidia in a ratio of 1:1 at 37 °C. The viability in the conidia was assessed by serially diluting and plating them onto MEA plates. The results indicate that the haemocytes killed 92.8% of the control *A. fumigatus* conidia by 40 min and 98.04% by 100 min (Figure 2.2). In contrast, the conidia of the passaged strains were significantly less susceptible to haemocyte-mediated killing, demonstrating a 9.19–41.37% kill rate at 40 min and a 36.78–52.84% kill rate at 100 min (**** $p < 0.0001$ at both time points).

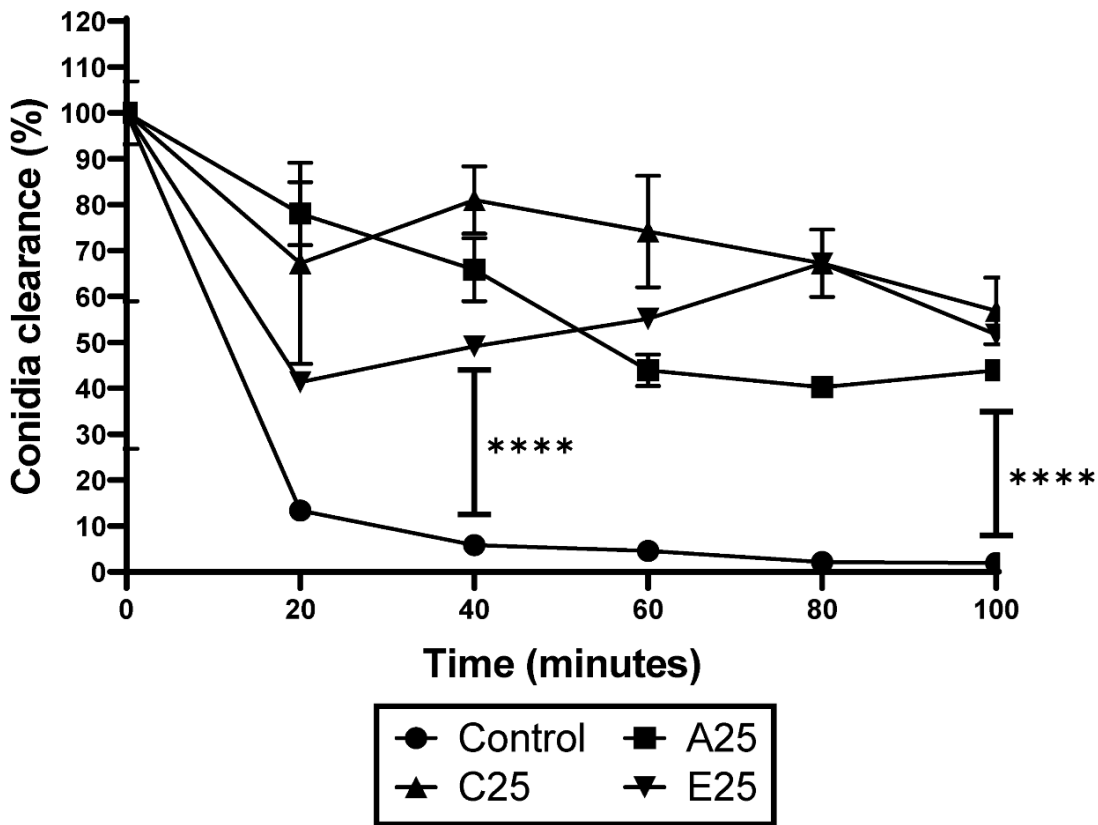


Figure 2.2: Response of *A. fumigatus* conidia to haemocyte-mediated killing. The conidia of *A. fumigatus* passaged and control strains were exposed to *G. mellonella* haemocytes ex vivo. The passaged strains demonstrated significantly increased tolerance to immune cell killing at 40 min (**** $p < 0.0001$) and 100 min (**** $p < 0.0001$), determined by a one-way ANOVA followed by pair-wise multiple comparisons using the Tukey test.

2.3.3 Passaged *A. fumigatus* strains show altered susceptibility to Antifungal agents

In order to confirm the tolerance to oxidative stress indicated in Figure 2.2, the susceptibility of the conidia of control and passaged *A. fumigatus* strains to hydrogen peroxide, as well as the antifungal agents amphotericin B and itraconazole, was assessed as described. The passaged strains showed increased growth in the presence of hydrogen peroxide compared to the control *A. fumigatus* strain at concentrations from 30.62 to 245 mM, with a significant increase in the growth of the E25 strain at concentrations of 30.62, 61.25, and 245 mM (*** $p < 0.0001$) (Figure 2.3A). All passaged strains demonstrated significantly increased growth at amphotericin B concentrations of 0.78–3.125 mg/mL compared to the control (**** $p < 0.0001$) (Figure 2.3B). The passaged strains showed significantly increased growth at all of the itraconazole concentrations tested (Figure 2.3C).

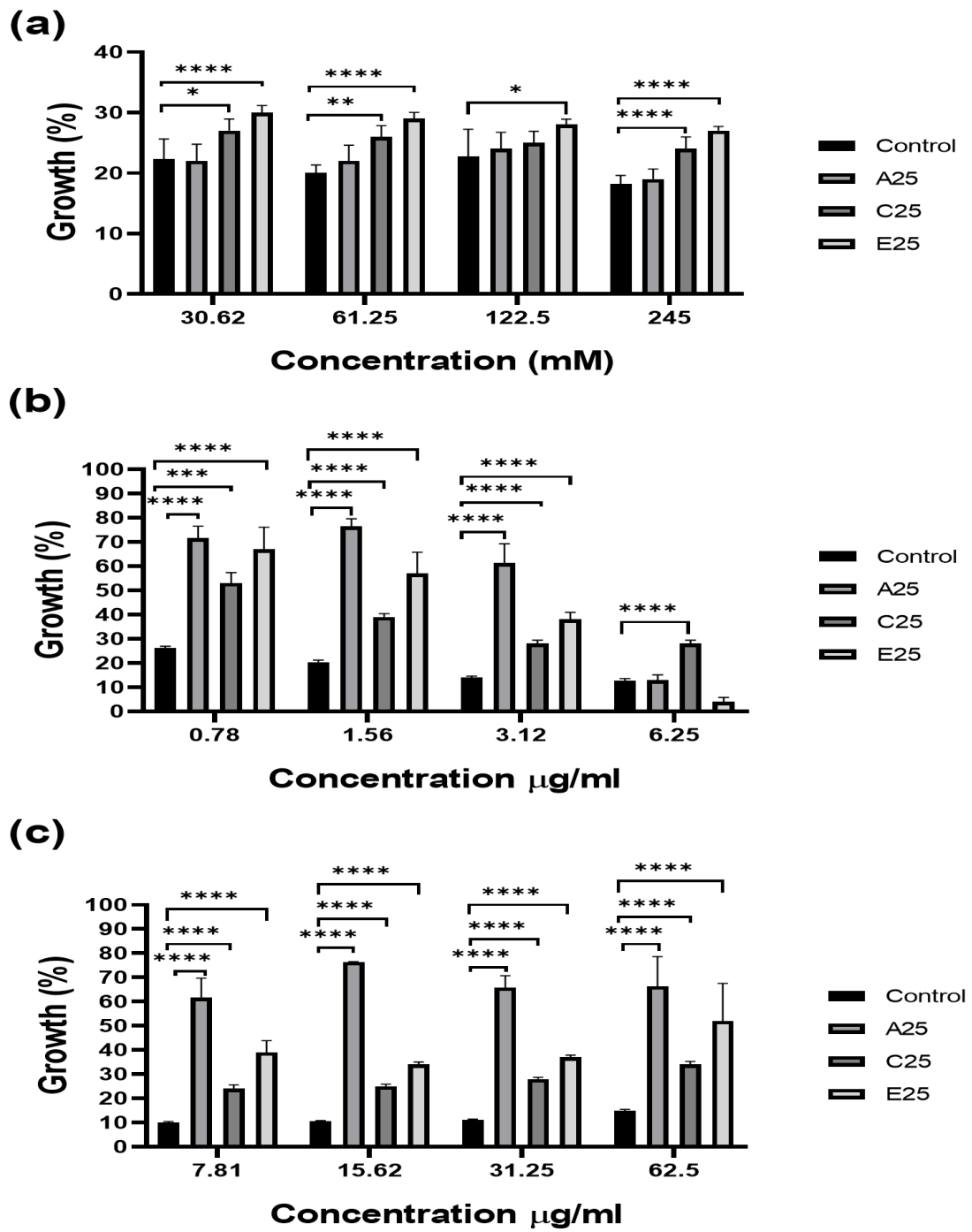


Figure 2.3: Analysis of the response of control and passaged *A. fumigatus* conidia to hydrogen peroxide, amphotericin B, and itraconazole. Passaged *A. fumigatus* conidia demonstrated significantly increased tolerance to (a) hydrogen peroxide (strain E25 at concentrations of 122.5, 62.5 and 30.62 mM Amphotericin B (**** p < 0.0001)); (b) amphotericin B at concentrations of 3.12–0.78 mg/mL in all of the passaged strains compared to the control (**** p < 0.0001); and (c) itraconazole in all of the passaged strains compared to the control with C25 at 62.5 μg/mL (*** p = 0.0017) and all other strains as well as concentrations (**** p < 0.0001) determined by a one-way ANOVA followed by pair-wise multiple comparisons using the Tukey test for each treatment dose (* p = 0.01, ** p = 0.001).

2.3.4 Proteomic characterisation of Passaged *A. fumigatus* strain E25

A quantitative proteomic analysis was employed to identify alterations in the proteome of passaged strain E25 that might explain the altered susceptibilities to haemocyte-mediated killing and the antifungal agents described above. In total, 3329 proteins were detected, of which 1902 remained following filtering. Thirty-two proteins were statistically significant and differentially abundant (SSDA) (Table 2.1). The heat map of proteins altered in abundance indicates a clear difference between the control and passaged strains (Figure 2.4). Proteins such as polyadenylation factor subunit CstF64 (+3.58-fold) and nuclear cap-binding protein subunit 2 (+2.47-fold), involved in mRNA stability, were increased in abundance in the passaged strain. Peptide-methionine (S)-S-oxide reductase (+2.63-fold) and developmental regulator FlbA (+2.27-fold), involved in the response to oxidative stress, were also increased in abundance in the passaged strains. Proteins decreased in abundance in the passaged strain included zinc/cadmium resistance protein (-5.17-fold), translation initiation regulator (Gcn20) (-1.96-fold), and glucose repressible protein Grg1 (-1.87-fold). In addition, nucleoporin NUP49/NSP49 (-2.24-fold), guanyl-nucleotide exchange factor (Sec7) (-1.76-fold), and histone H2A.Z (-1.82-fold) were also decreased in abundance (Figure 2.5). The results indicate that passaged strain E25 showed some alterations in the proteome, and those that are present may contribute to the increased tolerance to oxidative stress.

Table 2.1: All proteins detected to be statistically significant and differentially abundant in passaged strain E25 relative to the control *A. fumigatus* strain.

Protein Name	Gene Name	Peptides	Sequence Coverage (%)	Score	Fold Change
Polyadenylation factor subunit CstF64, putative	AFUA_2G09100	3	18.9	17.95	3.58
Complex I intermediate associated protein (Cia30), putative	AFUA_3G06220	4	15.2	14.82	3.44
KH domain protein	AFUA_4G07220	6	19.1	22.51	3.04
Uncharacterized protein	AFUA_3G08440	3	22.6	9.074	2.77
50S ribosomal protein L3	AFUA_4G06000	4	20.5	19.30	2.77
Peptide-methionine (S)-S-oxide reductase	AFUA_2G03140	3	49.1	26.35	2.63
Nuclear cap-binding protein subunit 2	AFUA_2G08570	5	25	7.55	2.46
Post-SET domain-containing protein	AFUA_6G10080	2	23.3	8.33	2.28
Developmental regulator FlbA	AFUA_2G11180	4	7.4	10.65	2.27
Thiamine biosynthetic bifunctional enz, putative	AFUA_2G08970	8	27.2	19.26	2.11
RING-type E3 ubiquitin transferase	AFUA_2G11040	4	29.2	6.07	1.88
Small nuclear ribonucleoprotein E	AFUA_7G05980	4	32.6	9.08	1.81
Phosphatidylglycerol/phosphatidylinositol transfer protein	npc2	10	35.4	29.44	1.74
DlpA domain protein	AFUA_4G10940	5	23.4	15.65	1.64
RSC complex subunit (RSC1), putative	AFUA_3G05560	4	7.8	9.43	1.63
Probable mannosyl-oligosaccharide alpha-1,2-mannosidase 1B	mns1B	14	47.5	64.36	1.60
ATP-dependent RNA helicase dbp2	dbp2	17	43	109.23	-1.53
Rhomboid protein 2	rbd2	2	15.4	19.36	-1.69
Integral ER membrane protein Scs2, putative	AFUA_4G06950	9	40.2	53.75	-1.75
Translation elongation factor eEF-3, putative	AFUA_7G03660	68	77.1	323.31	-1.76
Guanyl-nucleotide exchange factor (Sec7), putative	AFUA_7G05700	8	5.8	27.80	-1.76
Histone H2A.Z	htz1	6	51.4	65.54	-1.82
Glucose repressible protein Grg1, Putative	AFUA_5G14210	2	34.8	68.31	-1.87
Translation initiation regulator (Gcn20), putative	AFUA_4G06070	9	20.2	37.21	-1.96
ANK REP REGION domain-containing protein	AFUA_5G14930	20	48	190.54	-1.98
Nucleoporin NUP49/NSP49, putative	AFUA_6G10730	4	10.8	10.05	-2.24
Aminotransferase, putative	AFUA_6G02030	6	23	16.58	-2.26
GABA permease (Uga4), putative	AFUA_4G03370	4	8.9	12.47	-2.72
U5 snRNP complex subunit, putative	AFUA_7G02280	7	32.6	19.75	-3.14
Zinc/cadmium resistance protein	AFUA_2G14570	1	3	9.01	-5.17
Uncharacterized protein	AFUA_1G16030	16	38.2	62.94	-6.54

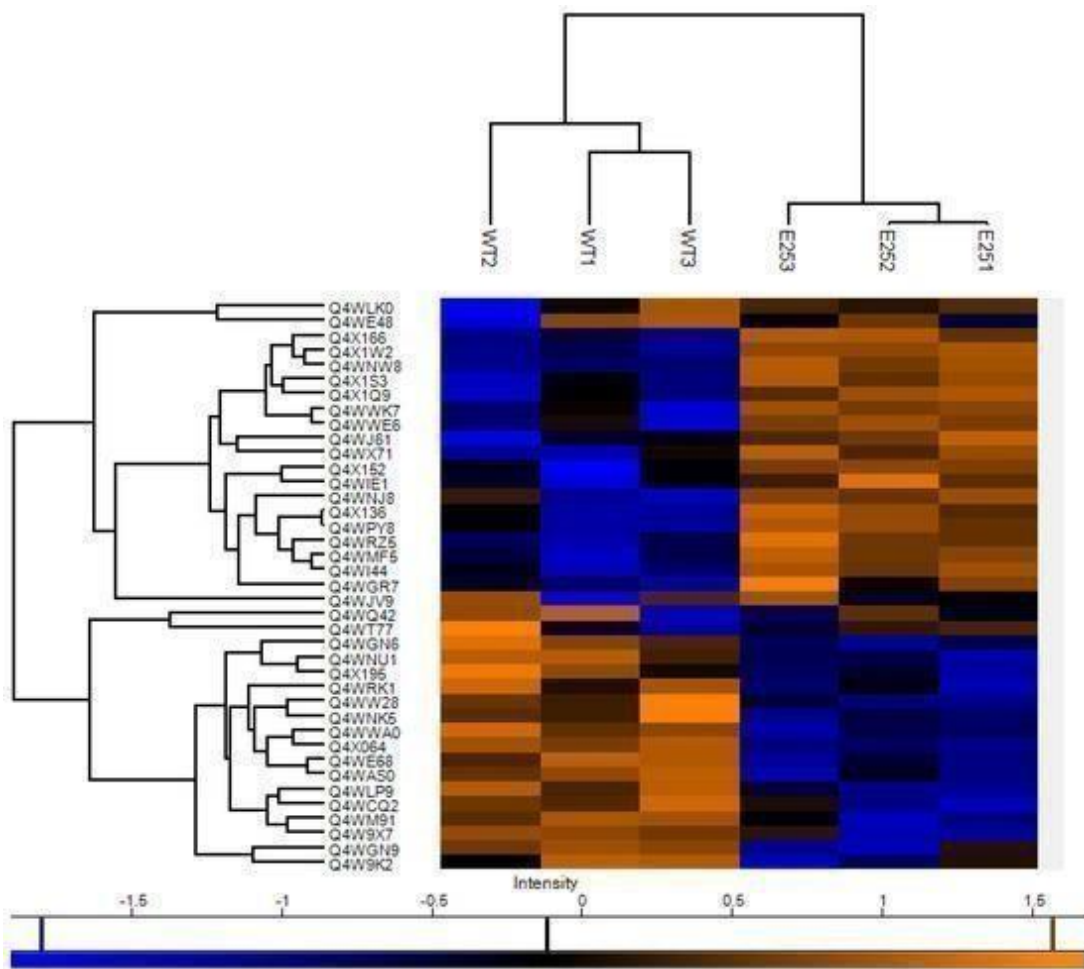


Figure 2.4: Heat map showing protein clustering between control and passaged *A. fumigatus* strain E25. Shotgun quantitative proteomic analysis of passaged strain and control mycelia grown in Czapex–Dox broth for 72 h. Two-way unsupervised hierarchical clustering of the median protein expression values of all statistically significant differentially abundant proteins. Hierarchical clustering (columns) identified two distinct clusters comprising the three replicates from their original sample groups.

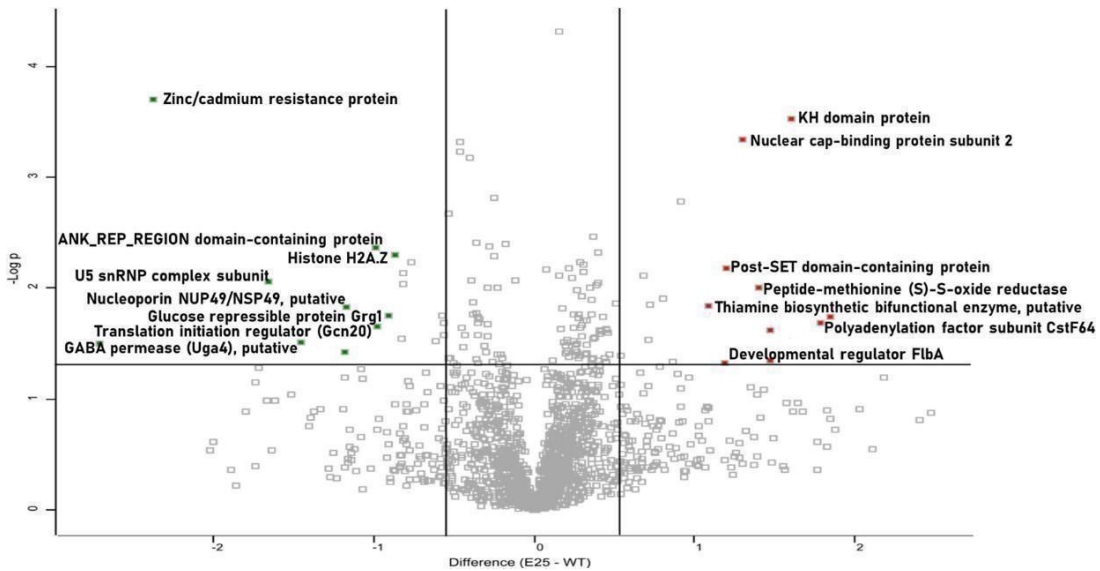


Figure 2.5: Volcano plots showing alterations in protein abundance in control and passaged *A. fumigatus* proteomes. Volcano plot of all identified proteins based on relative abundance differences between passaged strains and control mycelia. Volcano plots showing the distribution of quantified proteins. Proteins above the line are considered statistically significant (p value < 0.05), and those to the right and left of the vertical lines indicate relative fold changes greater than 1.5-fold.

2.4 Discussion

To examine the factors facilitating the selection and persistence of *A. fumigatus* in a host, *in vivo* or *in vitro* serially passaging can be employed to impose specific conditions for prolonged periods of time. The selective serial culturing of an organism can result in genetic modifications as the organism responds to a given environmental pressure (Scully and Bidochka, 2006). To facilitate prolonged passaging and overcome the relatively short lifespan of *G. mellonella* larvae, an agar system was formulated. The results presented show that the prolonged subculturing of *A. fumigatus* on GEA20 plates selected strains showing reduced virulence in *G. mellonella* larvae but with greater tolerance of haemocyte-mediated killing as well as hydrogen peroxide, amphotericin B, and itraconazole. Reduced virulence was not a result of altered growth, as control and passaged strains grew at the same rate (Figures S2.1 and S2.2). In addition, only one passaged strain demonstrated significant alterations in gliotoxin production (Figure S2.3), and there was no significant alteration in siderophore secretion (Figure S2.4). A small number of changes in the proteome was detected in passaged strain E25 (Table 2.1), and those proteins increased in abundance, such as peptide-methionine (S)-S-oxide reductase (+2.63-fold) and developmental regulator FlbA (+2.27-fold), coupled with the reduced abundance of histone H2A.Z (-1.82-fold) could have contributed to the observed tolerance of oxidative stress.

FlbA negatively affects the responses of detoxification to reactive oxygen species (ROS) as well as gliotoxin and negatively regulates GliT expression. The absence of FlbA increased ROS accumulation in hyphae, which elevates the expression of ROS scavengers such as catalase and superoxide dismutase (Shin *et al.*, 2013). H2A.Z has been found to be involved in genome stability, DNA repair, and transcriptional regulation across eukaryotes. In *Neurospora crassa*, H2A.Z regulates the oxidative stress response (Chen and Ponts, 2020). H2A.Z antagonizes CPC1 binding to restrict cat-3 expression in a normal setting, whereas under oxidative stress H2A.Z is removed from chromatin, leading to a rapid and full activation of cat-3 transcription, enhancing the capacity of resistance to physiological stimuli (Dong *et al.*, 2018). Proteomic evidence also indicates that these alterations have not arisen as a result of starvation or nutrient deprivation, as proteins involved in the starvation response, such as zinc/cadmium resistance protein (-5.17-fold), expressed in low-iron environments (Vicentefranqueira *et al.*, 2018), and glucose repressible protein grg1 (-1.81-fold), which is expressed in low-nutrient environments (Xie *et al.*, 2004), were reduced in abundance.

The data presented here indicate that the prolonged subculturing of *A. fumigatus* on GEA20 plates resulted in the selection of phenotypically fit variants that could persist in the culture conditions and withstand oxidative stress. The proteomic analysis of the passaged and control strains indicated alterations primarily involved in mRNA stability and oxidative stress tolerance. The results suggest that culture conditions may serve as a selective bottleneck, as previously demonstrated in work conducted with *A. flavus* (Scully and Bidochka, 2006). In addition, *C. neoformans* strains passaged in *G. mellonella* larvae demonstrated increased oxidative stress tolerance by downregulating hydrogen peroxide production *via* the shedding of the immunomodulatory capsule (Ali *et al.*, 2020). In the work presented here, the passaged *A. fumigatus* strains also demonstrated increased tolerance to oxidative stress, further emphasizing the importance of these mechanisms. Itraconazole and amphotericin B, which target the fungal cell membrane, affect fungal redox homeostasis by increasing intracellular ROS production. These responses were abolished *via* the inhibition of mitochondrial respiratory complex I, which suggests that mitochondrial complex I is the main source of deleterious ROS production in *A. fumigatus* challenged with

antifungal compounds (Shekhova *et al.*, 2017). Interestingly, the proteomic analysis indicated an increased expression of complex I intermediate associated protein (+3.44-fold) independent of exposure to any antifungal agent. Previous work has shown that the exposure of *Candida albicans* to hydrogen peroxide for 60 min increased tolerance to caspofungin through the simultaneous activation of the Cap and Hog pathways (Kelly *et al.*, 2009), indicating that prior exposure to elevated internal ROS could be attributed to reduced susceptibility to amphotericin B and itraconazole. The production of ROS by the innate immune response is crucial to protection against colonization. The ability of *A. fumigatus* to adapt and persist in the presence of these stressors and innate immune products could play a role in influencing antifungal susceptibility and response to the immune cells *in vivo*.

2.5 Conclusion

The data presented here suggest that prolonged subculturing on GEA20 plates can alter the phenotype and proteome of *A. fumigatus*. The passaged strains demonstrated reduced virulence *in vivo* and increased tolerance to haemocyte-mediated killing, hydrogen peroxide, itraconazole, and amphotericin B. This tolerance may be due to the proteomic alterations evident in the passaged strains conferring tolerance to oxidative stress. Prolonged *A. fumigatus* colonization *in vivo* may also lead to strains better adapted to the pulmonary environment as well as those that display enhanced tolerance to antifungal agents. Such a process may have implications for human health, as inadvertent selection for drug-tolerant and persistent strains could complicate therapy.

2.6 References

Ali, M. F., Tansie, S. M., Shahan, J. R., Seipelt-Thiemann, R. L. and McClelland, E. E., 2020. Serial Passage of *Cryptococcus neoformans* in *Galleria mellonella* Results in Increased Capsule and Intracellular Replication in Hemocytes, but Not Increased Resistance to Hydrogen Peroxide. *Pathogens*, 9 (9), 732.

Ballard, E., Melchers, W. J. G., Zoll, J., Brown, A. J. P., Verweij, P. E. and Warris, A., 2018. In-host microevolution of *Aspergillus fumigatus*: A phenotypic and genotypic analysis. *Fungal Genetics and Biology*, 113, 1–13.

Ben-Ami, R., Lewis, R. E. and Kontoyiannis, D. P., 2010. Enemy of the (immunosuppressed) state: an update on the pathogenesis of *Aspergillus fumigatus* infection. *British Journal of Haematology*, 150 (4), 406–417.

Chen, J., Li, H., Li, R., Bu, D. and Wan, Z., 2005. Mutations in the cyp51A gene and susceptibility to itraconazole in *Aspergillus fumigatus* serially isolated from a patient with lung aspergilloma. *The Journal of Antimicrobial Chemotherapy*, 55 (1), 31–37.

Chen, Z. and Ponts, N., 2020. H2A.Z and chromatin remodelling complexes: a focus on fungi. *Critical Reviews in Microbiology*, 46 (3), 321–337.

Colabardini, A. C., Wang, F., Miao, Z., Pardeshi, L., Valero, C., de Castro, P. A., Akiyama, D. Y., Tan, K., Nora, L. C., Silva-Rocha, R., Marcat-Houben, M., Gabaldón, T., Fill, T., Wong, K. H. and Goldman, G. H., 2022. Chromatin profiling reveals heterogeneity in clinical isolates of the human pathogen *Aspergillus fumigatus*. *PLoS Genetics*, 18 (1), e1010001.

Curtis, A., Binder, U. and Kavanagh, K., 2022. *Galleria mellonella* Larvae as a Model for Investigating Fungal—Host Interactions. *Frontiers in Fungal Biology* [online], 3. Available from: <https://www.frontiersin.org/articles/10.3389/ffunb.2022.893494> [Accessed 31 Jan 2023].

Denning, D. W., Cadrel, J., Beigelman-Aubry, C., Ader, F., Chakrabarti, A., Blot, S., Ullmann, A. J., Dimopoulos, G. and Lange, C., 2016. Chronic pulmonary aspergillosis: rationale and clinical guidelines for diagnosis and management. *European Respiratory Journal*, 47 (1), 45–68.

Denning, D. W., Pleuvry, A. and Cole, D. C., 2013. Global burden of allergic bronchopulmonary aspergillosis with asthma and its complication chronic pulmonary aspergillosis in adults. *Medical Mycology*, 51 (4), 361–370.

Dong, Q., Wang, Y., Qi, S., Gai, K., He, Q. and Wang, Y., 2018. Histone variant H2A.Z antagonizes the positive effect of the transcriptional activator CPC1 to regulate catalase-3 expression under normal and oxidative stress conditions. *Free Radical Biology & Medicine*, 121, 136–148.

El-Baba, F., Gao, Y. and Soubani, A. O., 2020. Pulmonary Aspergillosis: What the Generalist Needs to Know. *The American Journal of Medicine*, 133 (6), 668–674.

Hillmann, F., Novohradská, S., Mattern, D. J., Forberger, T., Heinekamp, T., Westermann, M., Winckler, T. and Brakhage, A. A., 2015. Virulence determinants of the human pathogenic fungus *Aspergillus fumigatus* protect against soil amoeba predation. *Environmental Microbiology*, 17 (8), 2858–2869.

Howard, S. J., Pasqualotto, A. C., Anderson, M. J., Leatherbarrow, H., Albarraq, A. M., Harrison, E., Gregson, L., Bowyer, P. and Denning, D. W., 2013. Major variations in *Aspergillus fumigatus* arising within aspergillomas in chronic pulmonary aspergillosis. *Mycoses*, 56 (4), 434–441.

Im, Y., Jhun, B. W., Kang, E.-S., Koh, W.-J. and Jeon, K., 2021. Impact of treatment duration on recurrence of chronic pulmonary aspergillosis. *Journal of Infection*, 83 (4), 490–495.

Keller, N. P., 2017. Heterogeneity Confounds Establishment of ‘a’ Model Microbial Strain. *mBio*, 8 (1), e00135-17.

Kelly, J., Rowan, R., McCann, M. and Kavanagh, K., 2009. Exposure to caspofungin activates Cap and Hog pathways in *Candida albicans*. *Medical Mycology*, 47 (7), 697–706.

Kirkland, M. E., Stannard, M., Kowalski, C. H., Mould, D., Caffrey-Carr, A., Temple, R. M., Ross, B. S., Lofgren, L. A., Stajich, J. E., Cramer, R. A. and Obar, J. J., 2021. Host Lung Environment Limits *Aspergillus fumigatus* Germination through an SskA-Dependent Signaling Response. *mSphere*, 6 (6), e00922-21.

LiPuma, J. J., 2010. The Changing Microbial Epidemiology in Cystic Fibrosis. *Clinical Microbiology Reviews*, 23 (2), 299–323.

Maleki, M., Mortezaee, V., Hassanzad, M., Mahdaviani, S. A., Poorabdollah, M., Mehrian, P., Behnampour, N., Mirenayat, M. S., Abastabar, M., Tavakoli, M. and Hedayati, M. T., 2020. Prevalence of allergic bronchopulmonary aspergillosis in cystic fibrosis patients using two different diagnostic criteria. *European Annals of Allergy and Clinical Immunology*, 52 (3), 104–111.

Margalit, A., Carolan, J. C., Sheehan, D. and Kavanagh, K., 2020. The *Aspergillus fumigatus* Secretome Alters the Proteome of *Pseudomonas aeruginosa* to Stimulate Bacterial Growth: Implications for Co-infection. *Molecular & cellular proteomics: MCP*, 19 (8), 1346–1359.

Margalit, A., Sheehan, D., Carolan, J. C. and Kavanagh, K., 2022. Exposure to the *Pseudomonas aeruginosa* secretome alters the proteome and secondary metabolite production of *Aspergillus fumigatus*. *Microbiology (Reading, England)*, 168 (3), 001164.

Mousavi, B., Hedayati, M., Hedayati, N., Ilkit, M. and Syedmousavi, S., 2016. *Aspergillus* species in indoor environments and their possible occupational and public health hazards. *Current Medical Mycology*, 2 (1), 36–42.

Perez-Riverol, Y., Bai, J., Bandla, C., García-Seisdedos, D., Hewapathirana, S., Kamatchinathan, S., Kundu, D. J., Prakash, A., Frericks-Zipper, A., Eisenacher, M., Walzer, M., Wang, S., Brazma, A. and Vizcaíno, J. A., 2021. The PRIDE database resources in 2022: a hub for mass spectrometry-based proteomics evidences. *Nucleic Acids Research*, 50 (D1), D543–D552.

Raksha, Singh, G. and Urhekar, A. D., 2017. Virulence Factors Detection in *Aspergillus* Isolates from Clinical and Environmental Samples. *Journal of Clinical and Diagnostic Research : JCDR*, 11 (7), DC13–DC18.

Rokas, A., Mead, M. E., Steenwyk, J. L., Oberlies, N. H. and Goldman, G. H., 2020. Evolving moldy murderers: *Aspergillus* section Fumigati as a model for studying the repeated evolution of fungal pathogenicity. *PLOS Pathogens*, 16 (2), e1008315.

Ross, B. S., 2022. *Aspergillus fumigatus* in Cystic Fibrosis: Persistence and Adaptation to CF Conditions Through Unique Stress Response Mutation and Convergent Hypoxia Fitness. Ph.D. [online]. Dartmouth College, United States -- New Hampshire. Available from: <https://www.proquest.com/docview/2668421722/abstract/16B0D855553B45D0PQ/1> [Accessed 31 Jan 2023].

Scully, L. R. and Bidochnka, M. J., 2006. The host acts as a genetic bottleneck during serial infections: an insect-fungal model system. *Current Genetics*, 50 (5), 335–345.

Sheehan, G., Clarke, G. and Kavanagh, K., 2018. Characterisation of the cellular and proteomic response of *Galleria mellonella* larvae to the development of invasive aspergillosis. *BMC Microbiology*, 18 (1), 63.

Shekhova, E., Kniemeyer, O. and Brakhage, A. A., 2017. Induction of Mitochondrial Reactive Oxygen Species Production by Itraconazole, Terbinafine, and Amphotericin B as a Mode of Action against *Aspergillus fumigatus*. *Antimicrobial Agents and Chemotherapy*, 61 (11), e00978-17.

Shin, K.-S., Park, H.-S., Kim, Y.-H. and Yu, J.-H., 2013. Comparative proteomic analyses reveal that FlbA down-regulates gliT expression and SOD activity in *Aspergillus fumigatus*. *Journal of Proteomics*, 87, 40–52.

Slater, J. L., Gregson, L., Denning, D. W. and Warn, P. A., 2011. Pathogenicity of *Aspergillus fumigatus* mutants assessed in *Galleria mellonella* matches that in mice. *Medical Mycology*, 49 Suppl 1, S107-113.

Trevijano-Contador, N. and Zaragoza, O., 2018. Immune Response of *Galleria mellonella* against Human Fungal Pathogens. *Journal of Fungi (Basel, Switzerland)*, 5 (1), 3.

Van Waeyenbergh, L., Baré, J., Pasman, F., Claeys, M., Bert, W., Haesebrouck, F., Houf, K. and Martel, A., 2013. Interaction of *Aspergillus fumigatus* conidia with *Acanthamoeba castellanii* parallels macrophage-fungus interactions. *Environmental Microbiology Reports*, 5 (6), 819–824.

Vicentefranqueira, R., Amich, J., Marín, L., Sánchez, C. I., Leal, F. and Calera, J. A., 2018. The Transcription Factor ZafA Regulates the Homeostatic and Adaptive Response to Zinc Starvation in *Aspergillus fumigatus*. *Genes*, 9 (7), 318.

Xie, X., Wilkinson, H. H., Correa, A., Lewis, Z. A., Bell-Pedersen, D. and Ebbol, D. J., 2004. Transcriptional response to glucose starvation and functional analysis of a glucose transporter of *Neurospora crassa*. *Fungal Genetics and Biology*, 41 (12), 1104.

Acknowledgments

Aaron Curtis is the recipient of an Irish Research Council postgraduate studentship GOIPG/2021/860.

The Q Exactive mass spectrometer was funded under the SFI Research Infrastructure Call 2012, grant number 12/RI/2346 (3).

Kieran Walshe is supported by H2020-fnr-11-2020: SECRETed, grant number 101000794.

Chapter 3

Characterisation of *Aspergillus fumigatus* secretome during sublethal infection of *Galleria mellonella* larvae

Aaron Curtis¹, Pavel Dobes², Jacek Marciniak², Jana Hurychova²,
Pavel Hyrsl² and Kevin Kavanagh¹

¹Department of Biology, Maynooth University, Maynooth, Co. Kildare,
Ireland

²Department of Experimental Biology, Faculty of Science, Masaryk
University, Kamenice 5, 625 00 Brno, Czech Republic

Published as:

Curtis, A., Dobes, P., Marciniak, J., Hurychova, J., Hyrsl, P. and Kavanagh, K., 2024.
Characterization of *Aspergillus fumigatus* secretome during sublethal infection
of *Galleria mellonella* larvae. *Journal of Medical Microbiology*, 73 (6),
001844.

Author contributions

A.C. and K.K. designed the experiments. A.C, J.M and P.D. performed the experiments and analysed the results. J.H conducted FIMTrack experiments and analysed the results. A.C. and K.K. wrote the manuscript. All authors have read and agreed to the published version of the manuscript.

Abstract

Introduction: The fungal pathogen *Aspergillus fumigatus* can induce prolonged colonization of the lungs of susceptible patients, resulting in conditions such as allergic bronchopulmonary aspergillosis and chronic pulmonary aspergillosis.

Hypothesis: Analysis of the *A. fumigatus* secretome released during sub-lethal infection of *G. mellonella* larvae may give an insight into products released during prolonged human colonisation.

Methodology: *Galleria mellonella* larvae were infected with *A. fumigatus*, and the metabolism of host carbohydrate and proteins and production of fungal virulence factors were analysed. Label-free qualitative proteomic analysis was performed to identify fungal proteins in larvae at 96 hours post-infection and also to identify changes in the *Galleria* proteome as a result of infection.

Results: Infected larvae demonstrated increasing concentrations of gliotoxin and siderophore and displayed reduced amounts of haemolymph carbohydrate and protein. Fungal proteins (399) were detected by qualitative proteomic analysis in cell-free haemolymph at 96 hours and could be categorized into seven groups, including virulence ($n = 25$), stress response ($n = 34$), DNA repair and replication ($n = 39$), translation ($n = 22$), metabolism ($n = 42$), released intracellular ($n = 28$) and cellular development and cell cycle ($n = 53$). Analysis of the Galleria proteome at 96 hours post-infection revealed changes in the abundance of proteins associated with immune function, metabolism, cellular structure, insect development, transcription/translation and detoxification.

Conclusion: Characterizing the impact of the fungal secretome on the host may provide an insight into how *A. fumigatus* damages tissue and suppresses the immune response during long-term pulmonary colonization.

3.1 Introduction

Aspergillus fumigatus is a ubiquitous environmental fungus and a significant pathogen capable of producing a variety of pulmonary infections in susceptible patients (Seif *et al.*, 2022). The most serious form of infection is invasive aspergillosis, and this can induce a mortality rate of 50 % in neutropenic patients and 90 % in stem cell therapy recipients (Naaraayan *et al.*, 2015). Prolonged fungal colonization is a common characteristic of allergic bronchopulmonary aspergillosis (ABPA), which typically affects those with hyperactive immune responses, such as asthma or cystic fibrosis (Eraso *et al.*, 2020). ABPA is characterized by repeated exacerbations arising from *Aspergillus* sensitization resulting in severe immune response and inflammation leading to haemoptysis or, in severe cases, lung collapse (Agarwal *et al.*, 2023). The development of ABPA depends upon fungal persistence and non- lethal colonization despite intense inflammatory cell infiltration driven by a number of fungal virulence factors including secreted proteases capable of detaching cells from the basement membrane leading to altered epithelial integrity (Wark, 2004). In the case of pre-existing lung damage or modest immunosuppression, chronic pulmonary aspergillosis (CPA) can occur. CPA is characterized by slow progressive destruction of lung parenchyma and recurrence upon discontinuation of antifungal therapy. The condition often results in cavity formation or expansion of pre-existing cavities from previous insults (Bongomin *et al.*, 2020). Damage caused to the lung tissue, commonly following tuberculosis infection, facilitates saprophytic colonization (Bongomin, 2020). *A. fumigatus* produces a range of enzymes, toxins and small molecules that facilitate the growth and survival of the fungus in the environment, and these may facilitate persistence in the host. The thermotolerance of *A. fumigatus* may have evolved to allow survival in its environmental niche, and this is facilitated by the thick conidia walls coupled with transcriptional regulation of heat shock response proteins in response to the loss of cell wall integrity (Fabri *et al.*, 2021). *A. fumigatus* produces low- molecular- mass ferric- iron- specific chelators known as siderophores, which are upregulated during iron starvation and are integral to fungal virulence (Aguiar *et al.*, 2022). Siderophores such as fusarine C, and its acetylated form triacetyl fusarine C, capture extracellular iron, while ferricrocin may be intracellular and involved in iron distribution and storage (Schrettl *et al.*, 2010). The conidial siderophore hydroxyferricrocin plays a crucial role in iron storage, germination and oxidative stress resistance (Schrettl *et al.*, 2008). Gliotoxin, an immunosuppressive

epipolythiodioxopiperazine toxin, can induce apoptosis in neutrophils, which are an important part of the immune response to fungal infection (König *et al.*, 2019). Gliotoxin and fumagillin may damage lung epithelial cells by producing reactive oxygen species (Gayathri *et al.*, 2020).

Galleria mellonella larvae are widely used for assessing the virulence of bacterial (Asai *et al.*, 2023) and fungal (Curtis *et al.*, 2022) pathogens and for assessing the *in vivo* efficacy and toxicity of antimicrobial agents (Tsai *et al.*, 2016). The use of *G. mellonella* larvae provides results comparable to those obtained using mammals (Brennan *et al.*, 2023; Slater *et al.*, 2011) due to the many structural and functional similarities between the insect immune response and the innate immune response of mammals (Browne *et al.*, 2013). Such similarities include the presence of pattern recognition receptors, which can induce signalling cascades initiating cellular and humoral immune responses such as phagocytosis, nodulation, agglutination, encapsulation, coagulation and the production of antimicrobial peptides and enzymes (Lin *et al.*, 2020). Larvae can be maintained at 37 °C, enabling analysis of temperature-dependent virulence factors (Firacative *et al.*, 2020). *G. mellonella* larvae are susceptible to infection with a variety of fungal pathogens, including *Candida albicans* (Vertyporokh and Wojda, 2020), *Madurella mycetomatis* (Sheehan *et al.*, 2020) and *A. fumigatus* (Durieux *et al.*, 2021), and symptoms demonstrate strong similarities to those evident during mammalian infection. While *G. mellonella* larvae have many advantages as a convenient, easy- to- use *in vivo* model, previous work has often used lethal doses of pathogens (Figueiredo-Godoi *et al.*, 2019; Jemel *et al.*, 2023).

In the present work, the secretome produced by *A. fumigatus* during sublethal colonization of *G. mellonella* larvae was monitored as this might provide an insight into the processes that occur during long- term colonization of human tissue by *A. fumigatus*.

3.2 Materials and methods

3.2.1 *A. fumigatus* culture conditions

A. fumigatus ATCC 26933 was cultured for 72 hours at 37 °C on Malt extract agar (Oxoid) plates following point inoculation. Conidia were harvested by washing plates with sterile PBS supplemented with 0.1 % (v/v) Tween 20 (Sigma Aldrich, USA) and enumerated using a haemocytometer.

3.2.2 Virulence assessment of *A. fumigatus* *in vivo*

Sixth instar larvae of *G. mellonella* (Livefoods Direct Ltd, Sheffield, England) were stored at 15 °C prior to use. Larvae ($n = 20$) weighing 0.2–0.3 g without signs of melanization were inoculated with 20 µl PBS containing 1×10^5 , 1×10^6 or 1×10^7 *A. fumigatus* conidia *via* intra-haemocoel injection using a 26G 1 ml syringe (Terumo). Larvae were placed in 9 cm petri dishes and incubated at 37 °C. Larval viability was monitored over 96 hours. In all subsequent experiments, 1×10^5 conidia/larva was used as the inoculation dose.

3.2.3 Assessment of larval movement

The movement of larvae infected with 1×10^5 *A. fumigatus* conidia at 24, 48, 72 and 96 hours post-infection was assessed *via* the FIMTrack method (Maguire *et al.*, 2017; Risse *et al.*, 2013) using frustrated total internal reflection of infrared light in acrylic glass. Images were captured *via* Basler acA2040-90uc camera in a dark room and with a frequency of one frame per second for 600 s. The scale factor was 80 pixels/cm. Images were processed by FIMTrack v2 Windows ($\times 86$) software (downloaded from <http://fim.uni-muenster.de/>). Data gathered from the software were processed and visualized in Prism 8.0.1 (USA GraphPad).

3.2.4 Quantification of total protein and carbohydrate in larval haemolymph

Haemolymph was extracted from larvae infected with 1×10^5 *A. fumigatus* conidia at 24-hour intervals over 96 hours and diluted 50× in Milli-Q water. The total protein concentration was measured according to the Lowry method using a commercial kit (DC Protein Assay, Bio-Rad, Hercules, CA, USA). Bovine serum albumin (Sigma-Aldrich, St. Louis, MO, USA) was used as a standard, and the absorbance was measured with Multiscan GO (ThermoFisher Scientific, Waltham, MA, USA) spectrophotometer at 700 nm. The concentration of total carbohydrates was determined by the anthrone method (Carroll *et al.*, 1956). Specifically, 50 µl of 40× diluted haemolymph was used per reaction, and absorbance was measured at

620 nm with a spectrophotometer Sense (Hidex, Turku, Finland). The concentration of total carbohydrates was calculated according to a calibration curve prepared with glucose (Sigma-Aldrich, St. Louis, MO, USA) as a standard

3.2.5 *In vivo* gliotoxin extraction and quantification

G. mellonella larvae were infected with 1×10^5 *A. fumigatus* conidia. Larvae ($n = 25$) were flash frozen in liquid nitrogen at 24, 48, 72 and 96 hours post-infection and ground using a mortar and pestle. The material was transferred with 5 ml of 6 M hydrochloric acid (HCl) to a centrifuge tube, and the mortar was washed twice with 5 ml volumes of HCl. Chloroform (25 ml) was added to the tube, which was mixed constantly for 30 min. Chloroform fraction was extracted and mixed with another 25 ml of chloroform; the process was repeated, and the chloroform fractions were pooled. The chloroform fraction was stored at -20 °C overnight, and the lipid fraction was removed. The samples were dried in a Büchi rotor evaporator (Brinkmann Instruments). Samples were dissolved in 500 μ l methanol and stored at -20 °C for further use. Gliotoxin was detected by reverse-phase HPLC (Shimadzu) and quantified through the generation of a standard curve using gliotoxin standards (100, 50, 25, 12.5 and 6.25 μ g ml^{-1}) dissolved in methanol. The mobile phase consisted of 34.9 % (v/v) acetonitrile (Fisher Scientific), 0.1 % (v/v) trifluoroacetic acid (Sigma Aldrich) and 65 % (v/v) HPLC-grade water (ddH₂O). Sample (20 μ l) was loaded onto an Agilent ZORBAX SB-Aq 5 μ m polar LC column.

3.2.6 Total secreted siderophore quantification

Siderophore activity in haemolymph was determined using SideroTec HiSens assay (Accuplex, www.accuplexdiagnostics.com). Briefly, 100 μ l of haemolymph from infected larvae ($n = 3$) diluted 1/10 in PBS was added to a 96-well microplate followed by the addition of 100 μ l of the ready-to-use detector. After 10 min incubation at 37 °C, fluorescence was measured on a fluorescence reader (Bio-Tek Synergy HT) using the emission/excitation filter 360/460 nm. Siderophore concentration was quantified using deferoxamine as a reference standard

3.2.7 Protein extraction

G. mellonella larvae ($n = 3$) infected with 1×10^5 *A. fumigatus* conidia and a PBS control were bled *via* the third left thoracic leg at 96 hours post-infection yielding 40 μ l haemolymph per larva. The pooled haemolymph was centrifuged at 10 000 **g**, and the cell-free haemolymph was diluted 1/5 in sterile PBS. Protein concentration

was determined using the Qubit quantification system (Invitrogen, Waltham, MA, USA). An aliquot containing 55 µg of protein was purified and digested using filter-aided sample preparation (Wiśniewski, 2019). Briefly, samples were mixed with 200 µl 8 M urea in the filter unit and spun at 14 000 g for 30 min. An additional 200 µl was added and spun again, and the flowthrough was discarded. Iodoacetamide (100 µl, 0.05 M) was added, and samples were mixed at 600 rpm in a thermomixer for 1 min and incubated for 20 min at room temperature without mixing. Urea (100 µl) was added, and samples were centrifuged at 14 000 g for 15 min; this step was repeated. Ammonium bicarbonate (100 µl, 0.05 M) was added, and samples were centrifuged at 14,000 g for 15 min; this step was repeated. A digestion buffer containing 0.4 µg ml⁻¹ trypsin, 0.05 % protease max and 0.05 M ammonium bicarbonate was added to give a final trypsin to protein ratio of 1 : 40. Samples were incubated for 18 hours in a humidified chamber at 37 °C. Samples were transferred to fresh collection tubes; 40 µl ammonium bicarbonate was added, and the samples were centrifuged for 10 min at 14,000 g and acidified with acidification buffer (1 : 10 ratio; 78 % LC-MS-grade water, 20 % acetonitrile and 2 % trifluoracetic acid).

3.2.8 Proteomic analysis

Of the digested protein, 600 ng was loaded onto a Q Exactive (ThermoFisher Scientific) high-resolution mass spectrometer, which was connected to a Dionex Ultimate 3000 (RSICnano) chromatography system. An increasing acetonitrile gradient was used to separate the peptides in the samples. This gradient was created on a 50-cm EASY-Spray PepMap C18 column with a 75 mm diameter using a 133- min reverse-phase gradient at a flow rate of 300 nL min⁻¹. The data were obtained, while the mass spectrometer was functioning in an automatic-dependent switching mode.

Qualitative analysis of the fungal and larval protein content of the cell-free haemolymph was investigated using Proteome Discoverer 2.5 and Sequest HT (SEQUEST HT algorithm; Thermo Scientific). Identified proteins were searched against the UniProtKB database *A. fumigatus*, 9647 entries, (UP000002530) and *G. mellonella*, 18,342 entries, (UP000504614). Search parameters applied for protein identification were as follows: (i) enzyme name – trypsin, (ii) an allowance of up to two missed cleavages, (iii) peptide mass tolerance set to 10 ppm, (iv) MS/MS mass tolerance set to 0.02 Da, (v) carbamidomethylation set as a fixed modification and (vi)

methionine oxidation set as a variable modification. Peptide probability was set to high confidence (with an FDR $\leq 0.01\%$ as determined by Percolator validation in Proteome Discoverer). Peptides identified by two or more unique peptides were retained for analysis.

3.2.9 Data analysis

Data gathered from the analyses were processed and visualized in Prism 8.0.1 (USA GraphPad). Survival curves of *Aspergillus*-infected larvae were compared to the survival of the PBS-injected group using the Mantel–Cox test. All other data were assessed for normality and homogeneity of variance, followed by one-way ANOVA with post hoc Dunnett's test comparing data from all treated groups to the control group. The changes in proteins and carbohydrates between PBS-injected and *Aspergillus*-injected groups were compared by unpaired t-tests at each time of sample collection. Results with *P*-values less than 0.05 were considered statistically significant.

3.3 Results

3.3.1 Virulence of *A. fumigatus* in *G. mellonella* larvae

G. mellonella larvae were infected with *A. fumigatus* conidia at an initial dose of 1×10^5 , 1×10^6 or 1×10^7 per larva and incubated at 37 °C for 96 hours. Larvae infected with 1×10^7 *A. fumigatus* conidia showed 0 % survival at 48 hours, while those infected with 1×10^6 conidia/larva showed 85 % (17/20) survival at 48 hours and 35 % (7/20) survival at 96 hours. Larvae infected with 1×10^5 conidia/larva showed 100 % (20/20) survival at 48 hours and 90 % (18/20) survival at 96 hours (Figure 3.1).

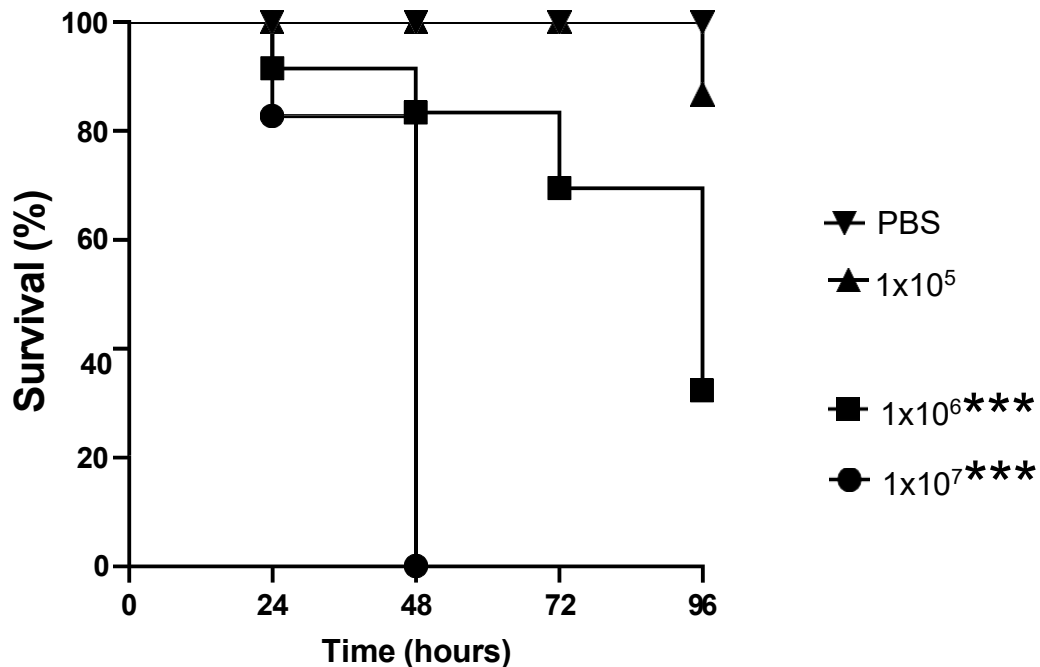


Figure 3.1: Dose-dependent survival of *G. mellonella* larvae infected with *A. fumigatus*, demonstrating a significant reduction in survival at 96 hours at concentrations of 1×10^6 and 1×10^7 (*** $P < 0.001$) determined by log-rank (Mantel–Cox) test.

FIMTrack analysis was performed to monitor the activity of larvae infected with a dose of 1×10^5 conidia/larva. The results showed that after infection, the larvae continued to move; however, the rate of movement was significantly reduced at 48 ($P = 0.0046$), 72 ($P = 0.0038$) and 96 hours ($P = 0.0018$) when compared to control larvae (Figure 3.2). For all subsequent experiments, only larvae that had been infected with 1×10^5 conidia/larva and showing signs of viability at 96 hours were used.

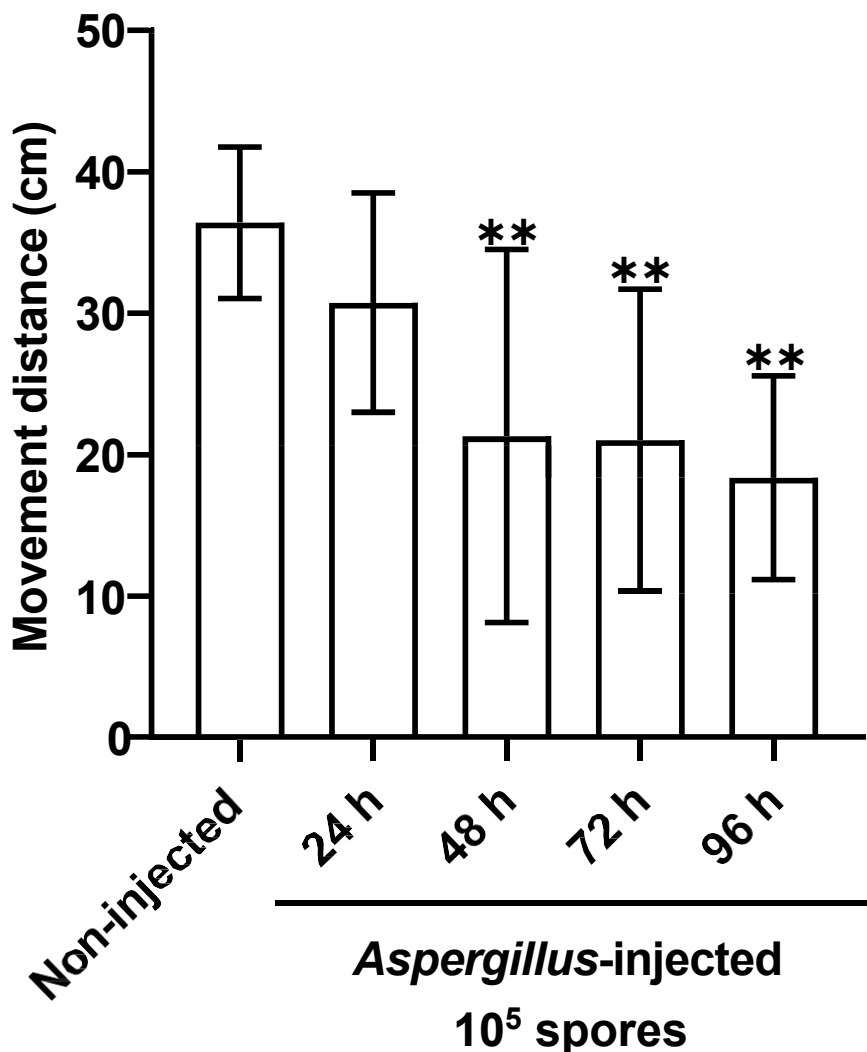


Figure 3.2: FIMTrack analysis of larval movement over time following infection with 1×10^5 conidia, demonstrating a significant reduction in larval movement at all timepoints post 48 hours ($P < 0.05$) determined by Dunnett's multiple comparisons test

3.3.2 Metabolite concentrations in larvae post *A. fumigatus* infection

The carbohydrate concentration of haemolymph collected from larvae infected with 1×10^5 conidia/larva was lower than that of control larvae at 48 ($P = 0.000373$), 72 and 96 hours (Figure 3.3). However, the protein content remained relatively constant until showing a statistically significant decrease at 96 hours ($P = 0.000124$) (Figure 3.4).

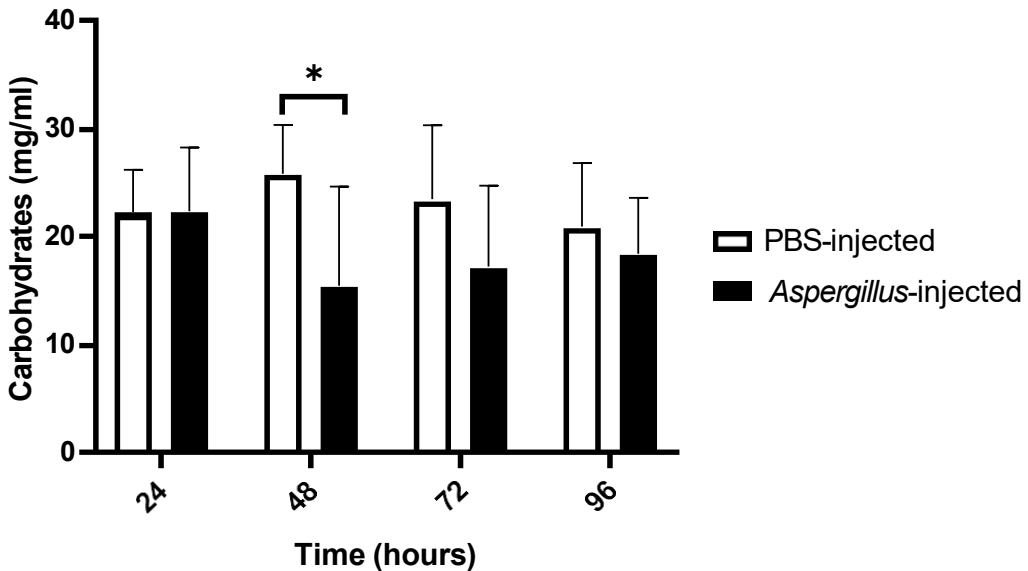


Figure 3.3: Assessment of haemolymph carbohydrate content post-infection with 1×10^5 *A. fumigatus* conidia. Significant reduction in host carbohydrate content 48 hours post-infection ($P = 0.0003$) determined by unpaired t-test ($n = 7$ –15 individual larvae per group). The experiment was conducted in three independent replicates.

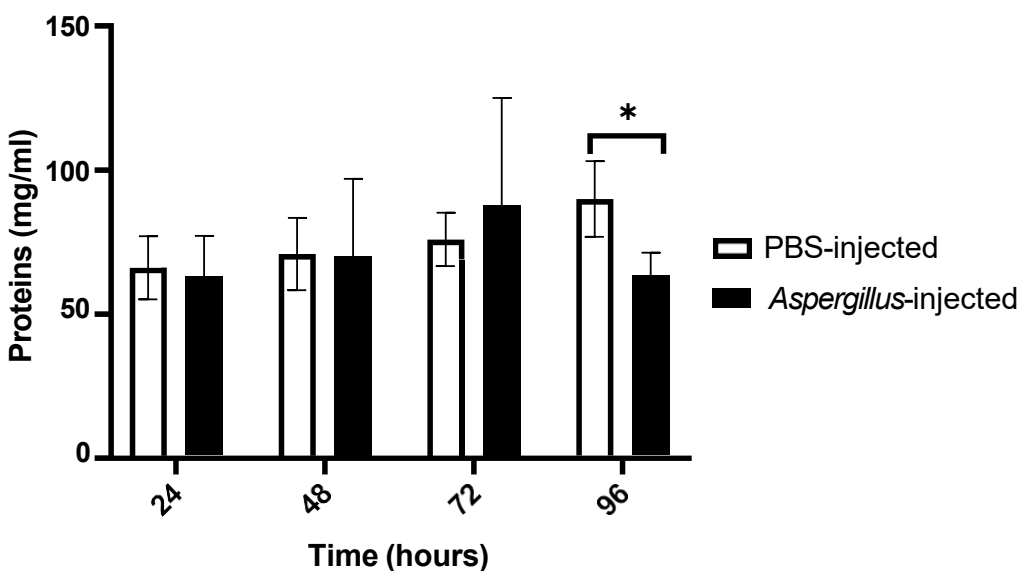


Figure 3.4: Assessment of haemolymph protein content post-infection with 1×10^5 *A. fumigatus* conidia. Significant reduction in host protein content 96 hours post-infection ($P = 0.0001$) determined by unpaired t-test ($n = 7$ –15 individual larvae per group). The experiment was conducted in three independent replicates.

3.3.3 Gliotoxin quantification in *G. mellonella* larvae post *A. fumigatus* infection

The gliotoxin in larvae infected with 1×10^5 conidia/larva was determined and indicated a steady increase over the course of the experiment with a concentration of $5.41 \pm 1.57 \mu\text{g/larva}$ being recorded at 48 hours and $16.96 \pm 1.66 \mu\text{g/larva}$ 96 hours ($P = 0.0003$) (Figure 3.5).

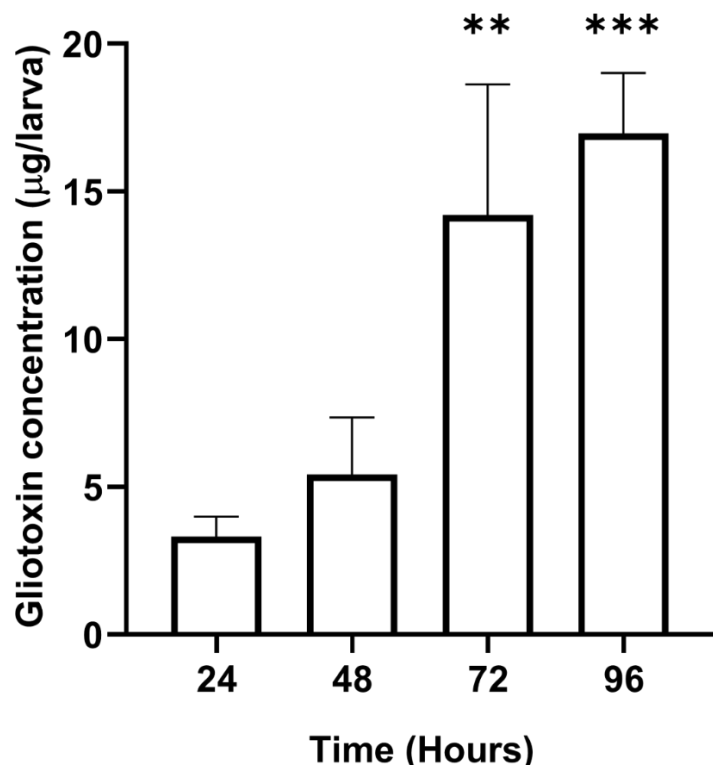


Figure 3.5: Quantification of gliotoxin in *Galleria* infected with 1×10^5 *A. fumigatus* conidia, demonstrating significant increase production at 72 (** $P = 0.02$) and 96 (*** $P = 0.0006$) hours post-infection when compared to the initial detection of 24 hours post-infection determined by Dunnett's multiple comparisons test.

3.3.4 Siderophore quantification in *G. mellonella* larvae post *A. fumigatus* infection

The fungal siderophore concentration was also assessed and revealed a concentration of $5.54 \pm 0.33 \mu\text{g/larva}$ at 48 hours and $12.59 \pm 0.70 \mu\text{g/larva}$ at 96 hours ($P < 0.0001$) (Figure 3.6).

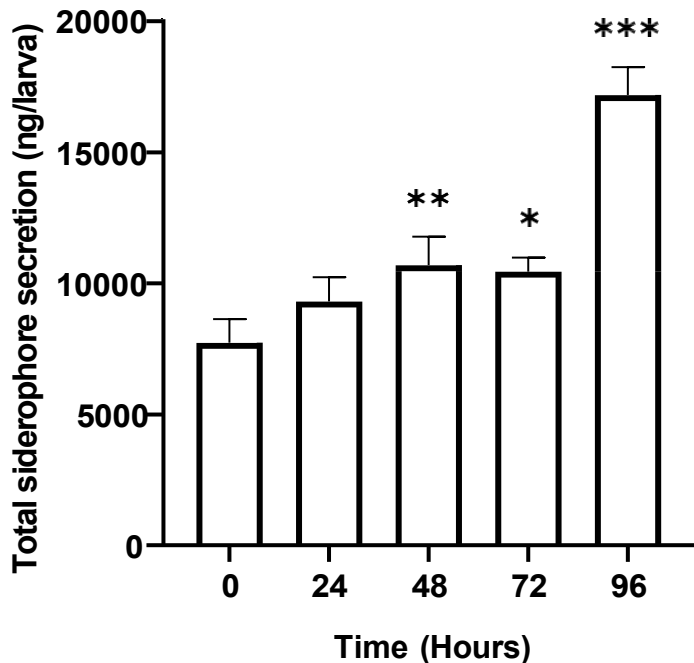


Figure 3.6: Quantification of total siderophore concentration detected in *Galleria haemolymph* infected with 1×10^5 *A. fumigatus* conidia, demonstrating significantly increased production at 48 hours ($P = 0.009$) and all subsequent timepoints post-infection as determined by Dunnett's multiple comparisons test.

3.3.5 Proteomic analysis of *A. fumigatus* during larval infection

Qualitative proteomic analysis of cell-free haemolymph from control larvae revealed 22 *Aspergillus* proteins, which were removed from subsequent analysis (Table S3.1, available in the online Supplementary Material), whereas larvae infected with 1×10^5 conidia/larva for 96 hours revealed 339 *A. fumigatus* proteins (>2 unique peptide hits). Of these, 243 were well characterized and could be divided into 7 categories with assigned functions (Figure 3.7). Virulence-associated proteins ($n = 25$) (Table S3.2.1) included non-ribosomal peptide synthase 13, O-methyltransferase af390-400 and dual-functional monooxygenase/methyltransferase psoF. Stress response proteins ($n = 34$) (Table S3.2.2) included proteins associated with environmental and drug-mediated stress, including glutathione S-transferase, HSP 70, PAB1-binding protein and ABC multidrug transporter A-2, atrI and H. Proteins associated with DNA repair/replication ($n = 39$) (Table S3.2.3) included fungal-specific transcription factor, kinetochore protein fta7, DNA polymerase and RAD52 DNA repair protein RDAC. Proteins associated with translation ($n = 22$) (Table S3.2.4) included elongation factor G, RNA-binding protein and RNA-dependent RNA polymerase. Proteins associated with metabolism ($n = 42$) (Table S3.2.5) included

pyruvate carboxylase, trehalase, UTP-glucose-1-phosphate uridylyltransferase and tryptophan synthase. Released intracellular proteins ($n = 28$) (Table S3.2.6) include mitochondrial carrier protein, nuclear pore complex subunit NUP 192 and vacuolar ABC heavy metal transporter. Proteins associated with the cell cycle/cell development ($n = 53$) (Table S3.2.7) included cell cycle checkpoint protein Rad 17, meiosis protein ME12 and chitin synthase. Many of the proteins identified at this timepoint were associated with fungal secondary metabolism: non-ribosomal peptide synthetase 13, O-methyltransferase af390-400, pentafunctional AROM polypeptide, toxin biosynthesis protein (Tri7), putative and cytochrome P450 monooxygenase helB2.

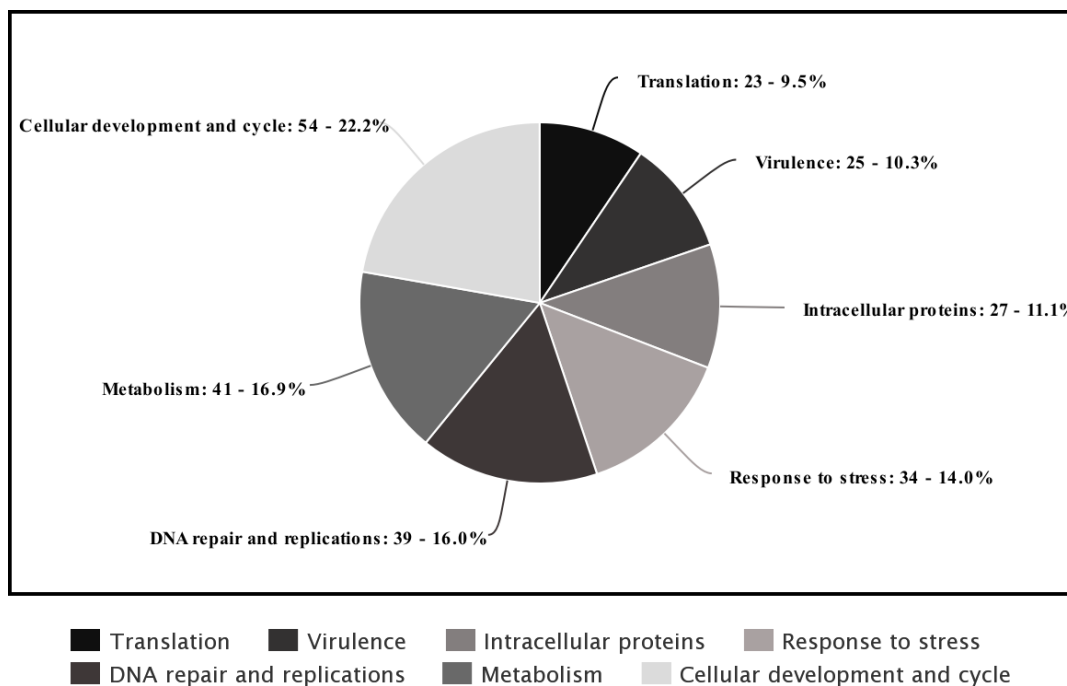


Figure 3.7: Pie chart summarizing high-confidence qualitative *A. fumigatus* protein detections categorized into seven subcategories: virulence ($n = 25$), stress response ($n = 34$), DNA repair and replication ($n = 39$), translation ($n = 22$), metabolism ($n = 42$), released intracellular ($n = 28$) and cellular cycle and development ($n = 53$) proteins.

3.3.6 Proteomics analysis of *G. mellonella* response to infection

Qualitative proteomic analysis of cell-free haemolymph from control larvae revealed 215 *G. mellonella* proteins (>2 unique peptide hits), and of these, 171 were well characterized (Table S3.3.1a). In contrast, larvae infected with 1×10^5 conidia/larva for 96 hours revealed 671 proteins, of which 532 were well characterized (Table S3.3.2a). Identified proteins could be divided into seven categories with assigned functions: immune function (38 in control, 52 in infected), metabolism

(36 in control, 118 in infected), cellular structure (22 in control, 97 in infected), insect development (42 in control, 90 in infected), movement (6 in control, 39 in infected), transcription/translation (13 in control, 90 in infected) and detoxification (14 in control, 46 in infected) (Figure 3.8a). Due to the importance of these proteins in the context of infection, the immune function proteins were further subdivided into 11 subcategories, and the greatest differences in protein abundance between the control and infected larvae were AMP(antimicrobial peptides) (4 control, 9 infected larva), inflammation (3 control, 6 infected), nutrient reservoir (7 control, 5 infected) and pathogen binding (2 control, 7 infected) (Figure 3.8b, Tables S3.3.1b and S3.3.2b).

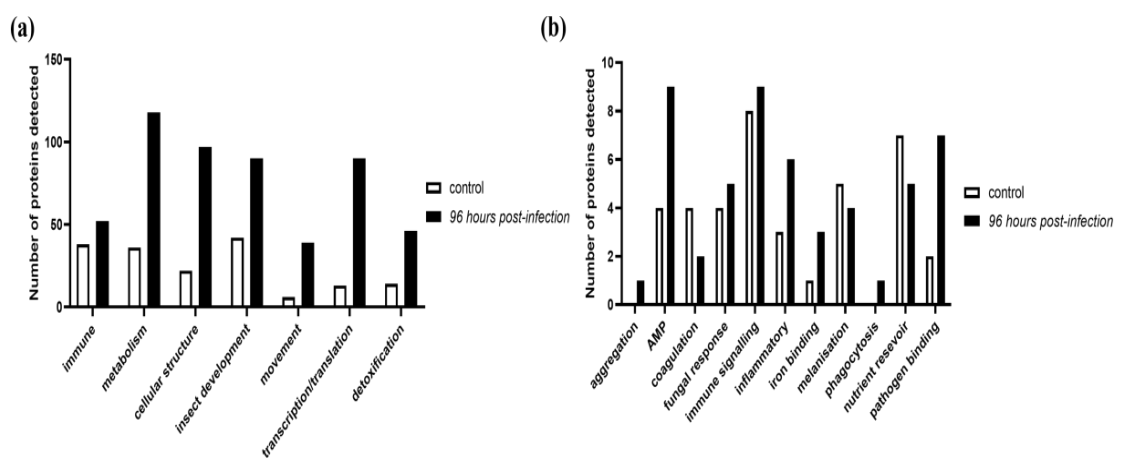


Figure 3.8: Bar graph summarizing (a) high-confidence qualitative *G. mellonella* protein detections categorized into seven subcategories in control larvae and in larvae at 96 hours post-infection. (b) Immune proteins further subdivided into 11 subcategories, and the greatest differences in protein abundance between the control and infected larvae were AMP (antimicrobial peptides), inflammation, nutrient reservoir and pathogen binding.

3.4 Discussion

Prolonged colonization of pulmonary tissue is a feature of ABPA and CPA, and results in exaggerated immune responses and tissue damage (Davda *et al.*, 2018; Earle *et al.*, 2023). In the work presented here, *G. mellonella* larvae were infected with a sublethal dose of *A. fumigatus* conidia, and the development of the fungus within the host was monitored as it might give an insight into the fungal–host interactions during prolonged colonization of human tissue. Infection of larvae with a dose of 1×10^5 conidia/larva resulted in only 10 % mortality at 96 hours (Figure 3.1). The remaining live larvae continued to move, although at a slower rate, when compared to the control cohort (Figure 3.2). Fungal colonization of larvae resulted in the production of

gliotoxin and siderophore, and the metabolism of host carbohydrates and proteins in the haemolymph. Qualitative proteomic analysis revealed a wide range of fungal proteins in the cell-free haemolymph at 96 hours, and these may have been released from the cell wall/conidia surface (e.g. beta-N-acetylglucosaminidase putative and chitin synthase) produced as a result of hyphal lysis (e.g. nuclear pore complex subunit Nup192 and sorting nexin-4) or secreted (e.g. pectin methylesterase), in addition to those released as a result of innate immune killing by the host. Understanding the impact of these and other proteins on the host may provide new insight into fungal–host interaction.

Hyphal development by *A. fumigatus* has been associated with the induction of inflammation, increased CD4/CD8 ratio and Th2 cell differentiation, promoting a proinflammatory environment (Luo *et al.*, 2022). ABPA is characterized by an exaggerated Th2-mediated response, triggering the release of inflammatory cytokines and growth factors leading to airway hyperresponsiveness, goblet cell hyperplasia and subepithelial fibrosis (Chotirmall *et al.*, 2013). The detection of class V myosin (Myo4), putative (Table S3.2.7) at 96 hours indicates that hyphal development was actively occurring within infected larvae (Figure. S3.1). Class V myosin is required for hyphal extension, septation, conidiation and conidial germination (Renshaw *et al.*, 2016). In addition, chitin synthase and chitin synthase ChsE (Table S3.2.7) are essential for hyphal development and were also detected in the proteomic screen. Chitin synthase has been attributed to hyphal development and virulence in murine corneal infection (de Jesus Carrion *et al.*, 2019). Analysis of the *G. mellonella* proteomics results identified increased abundance of proteins associated with inflammation at 96 hours, including inter-alpha-trypsin inhibitor heavy chain H4- like isoform X6 and leukotriene A-4 hydrolase-like protein. ITIH4 is linked to cell proliferation, as well as migration during the acute-phase inflammatory response, and serves a role in inflammatory and infectious responses, particularly in bacterial bloodstream infection (Ma *et al.*, 2021). Leukotriene A-4 hydrolase-like protein is an important inflammatory modulator, both promoting production of the pro-inflammatory mediator leukotriene B₄ but also degrading the neutrophil chemoattractant Pro-Gly-Pro (PGP) which could reduce inflammation (Lee *et al.*, 2022; Low *et al.*, 2017). The production of antimicrobial peptides such as cecropin-d-like peptide and gloverin-like protein- and fungal-specific recognition such as beta-

1,3-glucan-binding protein-like isoform X2 was increased, indicating activation of an immune response of *A. fumigatus* proliferation.

Several *A. fumigatus* proteins involved in enzymatic degradation of tissue which may facilitate host colonization and tissue damage were detected. Proteins such as d-lactate dehydrogenase, aldehyde dehydrogenase, beta-glucosidase and trehalase may be involved in metabolizing tissue (Tables S3.2.5 and S3.2.7). The major sugar in insect haemolymph is trehalose; therefore, the detection of trehalase indicates the active metabolism of the larval haemolymph carbohydrate (Figure 3.3) (Shukla *et al.*, 2015). Several identified proteins displayed protease activity (ATP-dependent Clp protease, putative, intermembrane space AAA protease IAP-1, calpain-like protease PalBory and intermembrane space AAA protease IAP-1) (Tables S3.2.1 and S2.6) and could have a role in metabolizing the protein content of insect haemolymph (Figure 3.4). Detection of transcriptional activator of proteases prtT (Table S3.2.1) in the cell-free haemolymph could indicate that proteases are actively involved in the early steps of sublethal fungal colonization. PrtT is integral to the infection processes as it mediates the expression of extracellular proteases that are involved in the penetration of the pulmonary epithelium (Hagag *et al.*, 2012). Protease-dependent changes to the host cellular actin cytoskeleton can lead to cell peeling and death (Sharon *et al.*, 2009). The combination of enzymatic and physical disruption to host membranes during tissue invasion has been identified as the causal agent of haemoptysis in aspergillosis patients, typically arising from bronchial blood vessel damage (Kousha *et al.*, 2011).

Analysis of the *G. mellonella* proteome at 96 hours indicated the release of tissue-specific proteins into cell-free haemolymph, indicating tissue damage, which can be a hallmark of *A. fumigatus* infections (Okaa *et al.*, 2023). These proteins include tropomyosin-1 isoform X1, troponin T, skeletal muscle isoform X1 and myosin heavy chain muscle isoform X10. Troponin T is used as a biomarker in human diseases involving tissue degradation (Tanindi and Cemri, 2011). It has recently been identified that tissue damage may be mediated by immune response dysregulation driven by secondary metabolites produced during hyphal development through mediation of the PacC regulator, which mediates expression of over 250 secreted proteins, including proteases prtT and nonribosomal peptide synthetase GliP, essential for gliotoxin production, of which evidence of expression was evident in our study and that these molecules work synergistically to drive host epithelial damage (Okaa *et al.*, 2023).

In addition, allergens can promote a proinflammatory state, driving tissue remodelling. These include Hsp70 family protein, which was detected in our analysis (Table S3.2.2), and Hsp70 is a known fungal allergen classified as an IgE reactive cytosolic protein from germinating conidia (Singh *et al.*, 2010). Many other allergens may aggravate asthma symptoms and, in combination with the ability of *A. fumigatus* to colonize the airways, could drive the sustained release of allergens (Namvar *et al.*, 2022).

Several pathogenic *Aspergillus* species produce secondary metabolites from aromatic amino acids, including fumiquinazoline and fumitremorgin, which can be derived from tryptophan (Choera *et al.*, 2018). Nonribosomal peptide synthetase 13 and tryprostatin B 6-hydroxylase were detected (Table S3.2.1), and both are involved in fumitremorgin production. This mycotoxin elicits tremorgenic effects resulting in tremors, seizures and abnormal behaviour in mice (Maiya *et al.*, 2006), and fumitremorgin could be responsible for reduced movement of *G. mellonella* larvae (Figure 3.2). Non-ribosomal peptide synthetase *fmqA* was also detected and is involved in fumiquinazoline C production, a conidia-associated metabolite with anti-phagocytic properties (Rocha *et al.*, 2021). *fmqA* is required to produce fumiquinazoline metabolites because it condenses antranilic acid, l-tryptophan and l-alanine in the presence of ATP to form fumiquinazoline C (Rocha *et al.*, 2021).

Many of the above products are derived from aromatic amino acids, which can be synthesized through the Shikimate pathway (Sasse *et al.*, 2016). The detection of pentafunctional AROM polypeptide (Table S3.2.1) along with other aromatic amino acid biosynthesis proteins as shown in the STRING analysis (Figure S3.2) indicates that this pathway may be involved in the virulence of *A. fumigatus* *in vivo*. Another detected protein involved in virulence was indoleamine 2,3-dioxygenase subfamily (IDO) (Table S3.2.1). It is a key enzyme important in immune homeostasis and converts tryptophan to kynurenone and related metabolites. This enzyme is an essential component of host responses to *Aspergillus* and can be exploited by this pathogen as a method of immune evasion (Romani *et al.*, 2009). IDO inhibits macrophage recruitment and phagocytosis in *A. fumigatus* keratitis and is involved in M1 macrophage polarization (Jiang *et al.*, 2020).

Gliotoxin is a secondary metabolite implicated in fungal virulence, and the toxicity is attributed to the presence of a disulfide bridge across a piperazine ring. The toxin serves many functions, including oxidative stress homeostasis (Traynor *et al.*, 2021) and suppressing the activity of the NADPH oxidase complex in neutrophils (Abad *et al.*, 2010) and in insect haemocytes (Renwick *et al.*, 2006). The secretion of this toxin may suppress the local immune response, enabling the continued persistence of *A. fumigatus*. The detection of gliotoxin is clinically relevant as indicated by numerous studies characterizing its role in immunomodulation (Ries *et al.*, 2020). The concentration detected in this study (Figure 3.5) at 72 hours ($14.2 \pm 3.6 \mu\text{g} / \text{larva}$) was higher than that detected at 72 hours in *A. fumigatus*-infected murine lung tissue ($6-8 \mu\text{g g}^{-1}$) (Ali and Abdallah, 2022; Abdallah and Ali, 2022).

Siderophore concentration also increased over time and reached a level of $12.59 \pm 0.70 \mu\text{g} / \text{larva}$ at 96 hours (Figure 3.6). Siderophores are small iron-chelating molecules that play an essential role in acquiring iron which is essential for fungal growth. The release of iron from the host through haemolysis can bolster fungal growth and development through acquisition by siderophores (Michels *et al.*, 2022). Proteomic analysis detected proteins associated with siderophore production and activity, such as non-ribosomal peptide synthetase sidC involved in ferricrocin synthesis (Hissen *et al.*, 2005), and fusarinine C esterase SidJ (Table S3.2.1), which hydrolyses internalized siderophores (Gründlinger *et al.*, 2013). SidC is involved in conidial iron storage required for germ tube formation, asexual sporulation, catalase A activity and virulence (Schrettl *et al.*, 2007).

Cell wall-associated proteins in the cell-free haemolymph included chitin synthase, chitin synthase ChsE, alpha 1, 2 mannosidase and conidial pigment polyketide synthase alb 1 (Table S3.2.1). Conidial pigment polyketide synthase alb1 is associated with the production of DHN-melanin. DHN-melanin disruption results in the formation of smooth conidia and subsequently increases phagocytosis by neutrophils. Deleting alb1 deletion results in a significant loss of virulence in murine models (Tsai *et al.*, 1998).

The wide range of secondary metabolites produced by *A. fumigatus* and biological processes occurring in infected larvae could physically and enzymatically damage tissue, sequester nutrients, alter larval behaviour and suppress the immune

response of the host. The results presented here demonstrate that even in the absence of larval death, *A. fumigatus* produces a wide range of potent metabolites and proteins, which have the capacity to damage host tissue or alter the immune response. Prolonged colonization of pulmonary tissue by *A. fumigatus* may lead to the release of similar metabolites that may have adverse effects on the host and may facilitate long-term fungal persistence.

3.5 References

Abad, A., Victoria Fernández-Molina, J., Bikandi, J., Ramírez, A., Margareto, J., Sendino, J., Luis Hernando, F., Pontón, J., Garaizar, J., Rementeria, A. (2010). What makes *Aspergillus fumigatus* a successful pathogen? Genes and molecules involved in invasive aspergillosis. *Revista Iberoamericana de Micología*, **27**: 155–182.

Abdallah, B.M., Ali, E.M. (2022). Therapeutic Potential of Green Synthesized Gold Nanoparticles Using Extract of *Leptadenia hastata* against Invasive Pulmonary Aspergillosis. *Journal of Fungi*, **8**: 442.

Agarwal, R., Muthu, V., Sehgal, I.S., Dhooria, S., Prasad, K.T., Soundappan, K., Rudramurthy, S.M., Aggarwal, A.N., Chakrabarti, A. (2023). Prevalence of *Aspergillus* Sensitization and Allergic Bronchopulmonary Aspergillosis in Adults With Bronchial Asthma: A Systematic Review of Global Data. *The Journal of Allergy and Clinical Immunology: In Practice*, **11**: 1734-1751.e3.

Aguiar, M., Orasch, T., Shadkhan, Y., Caballero, P., Pfister, J., Sastré-Velásquez, L.E., Gsaller, F., Decristoforo, C., Osherov, N., Haas, H. (2022). Uptake of the Siderophore Triacetyl fusarinine C, but Not Fusarinine C, Is Crucial for Virulence of *Aspergillus fumigatus*. Goldman, G.H. (ed). *mBio*, **13**: e02192-22.

Ali, E.M., Abdallah, B.M. (2022). Effective Inhibition of Invasive Pulmonary Aspergillosis by Silver Nanoparticles Biosynthesized with *Artemisia sieberi* Leaf Extract. *Nanomaterials*, **12**: 51.

Asai, M., Li, Y., Newton, S.M., Robertson, B.D., Langford, P.R. (2023). *Galleria mellonella* –intracellular bacteria pathogen infection models: the ins and outs. *FEMS Microbiology Reviews*, **47**: fuad011.

Bongomin, F. (2020). Post-tuberculosis chronic pulmonary aspergillosis: An emerging public health concern. *PLOS Pathogens*, **16**: e1008742.

Bongomin, F., Otu, A., Harris, C., Foden, P., Kosmidis, C., Denning, D.W. (2020). Risk factors for relapse of chronic pulmonary aspergillosis after discontinuation of antifungal therapy. *Clinical Infection in Practice*, **5**: 100015.

Brennan, L.E., Kumawat, L.K., Piatek, M.E., Kinross, A.J., McNaughton, D.A., Marchetti, L., Geraghty, C., Wynne, C., Tong, H., Kavanagh, O.N., O'Sullivan, F., Hawes, C.S., Gale, P.A., Kavanagh, K., Elmes, R.B.P. (2023). Potent antimicrobial effect induced by disruption of chloride homeostasis. *Chem*, **9**: 3138–3158.

Browne, N., Heelan, M., Kavanagh, K. (2013). An analysis of the structural and functional similarities of insect hemocytes and mammalian phagocytes. *Virulence*, **4**: 597–603.

Carroll, N.V., Longley, R.W., Roe, J.H. (1956). The determination of glycogen in liver and muscle by use of anthrone reagent. *The Journal of Biological Chemistry*, **220**: 583–593.

Choera, T., Zelante, T., Romani, L., Keller, N.P. (2018). A Multifaceted Role of Tryptophan Metabolism and Indoleamine 2,3-Dioxygenase Activity in *Aspergillus fumigatus*–Host Interactions. *Frontiers in Immunology*, **8**.

Chotirmall, S.H., Al-Alawi, M., Mirkovic, B., Lavelle, G., Logan, P.M., Greene, C.M., McElvaney, N.G. (2013). *Aspergillus*-Associated Airway Disease, Inflammation, and the Innate Immune Response. *BioMed Research International*, **2013**: 723129.

Curtis, A., Binder, U., Kavanagh, K. (2022). *Galleria mellonella* Larvae as a Model for Investigating Fungal-Host Interactions. *Frontiers in Fungal Biology*, **3**: 893494.

Davda, S., Kowa, X.-Y., Aziz, Z., Ellis, S., Cheasty, E., Cappocci, S., Balan, A. (2018). The development of pulmonary aspergillosis and its histologic, clinical, and radiologic manifestations. *Clinical Radiology*, **73**: 913–921.

Durieux, M.-F., Melloul, É., Jemel, S., Roisin, L., Dardé, M.-L., Guillot, J., Dannaoui, É., Botterel, F. (2021). *Galleria mellonella* as a screening tool to study virulence factors of *Aspergillus fumigatus*. *Virulence*, **12**: 818–834.

Earle, K., Valero, C., Conn, D.P., Vere, G., Cook, P.C., Bromley, M.J., Bowyer, P., Gago, S. (2023). Pathogenicity and virulence of *Aspergillus fumigatus*. *Virulence*, **14**: 2172264.

Eraso, I.C., Sangiovanni, S., Morales, E.I., Fernández-Trujillo, L. (2020). Use of monoclonal antibodies for allergic bronchopulmonary aspergillosis in patients with asthma and cystic fibrosis: literature review. *Therapeutic Advances in Respiratory Disease*, **14**: 1753466620961648.

Fabri, J.H.T.M., Rocha, M.C., Fernandes, C.M., Persinoti, G.F., Ries, L.N.A., Cunha, A.F. da, Goldman, G.H., Del Poeta, M., Malavazi, I. (2021). The Heat Shock Transcription Factor HsfA Is Essential for Thermotolerance and Regulates Cell Wall Integrity in *Aspergillus fumigatus*. *Frontiers in Microbiology*, **12**.

Figueiredo-Godoi, L.M.A., Menezes, R.T., Carvalho, J.S., Garcia, M.T., Segundo, A.G., Jorge, A.O.C., Junqueira, J.C. (2019). Exploring the Galleria mellonella model to study antifungal photodynamic therapy. *Photodiagnosis and Photodynamic Therapy*, **27**: 66–73.

Firacative, C., Khan, A., Duan, S., Ferreira-Paim, K., Leemon, D., Meyer, W. (2020). Rearing and Maintenance of Galleria mellonella and Its Application to Study Fungal Virulence. *Journal of Fungi*, **6**: 130.

Gayathri, L., Akbarsha, M.A., Ruckmani, K. (2020). In vitro study on aspects of molecular mechanisms underlying invasive aspergillosis caused by gliotoxin and fumagillin, alone and in combination. *Scientific Reports*, **10**: 14473.

Gründlinger, M., Gsaller, F., Schrettl, M., Lindner, H., Haas, H. (2013). *Aspergillus fumigatus* SidJ Mediates Intracellular Siderophore Hydrolysis. *Applied and Environmental Microbiology*, **79**: 7534–7536.

Hagag, S., Kubitschek-Barreira, P., Neves, G.W.P., Amar, D., Nierman, W., Shalit, I., Shamir, R., Lopes-Bezerra, L., Osherov, N. (2012). Transcriptional and Proteomic Analysis of the *Aspergillus fumigatus* ΔprtT Protease-Deficient Mutant. *PLOS ONE*, **7**: e33604.

Hissen, A.H.T., Wan, A.N.C., Warwas, M.L., Pinto, L.J., Moore, M.M. (2005). The *Aspergillus fumigatus* Siderophore Biosynthetic Gene sidA, Encoding l-Ornithine N5-Oxygenase, Is Required for Virulence. *Infection and Immunity*, **73**: 5493–5503.

Jemel, S., Raveloarisaona, Y., Bidaud, A.-L., Djenontin, E., Kallel, A., Guillot, J., Kallel, K., Botterel, F., Dannaoui, E. (2023). In vitro and in vivo evaluation of antifungal combinations against azole-resistant *Aspergillus fumigatus* isolates. *Frontiers in Cellular and Infection Microbiology*, **12**: 1038342.

de Jesus Carrion, S., Abbondante, S., Clark, H.L., Marshall, M.E., Mouyna, I., Beauvais, A., Sun, Y., Taylor, P.R., Leal Jr., S.M., Armstrong, B., Carrera, W., Latge, J.-P., Pearlman, E. (2019). *Aspergillus fumigatus* corneal infection is regulated by chitin synthases and by neutrophil-derived acidic mammalian chitinase. *European Journal of Immunology*, **49**: 918–927.

Jiang, N., Zhang, L., Zhao, G., Lin, J., Wang, Q., Xu, Q., Li, C., Hu, L., Peng, X., Yu, F., Xu, M. (2020). Indoleamine 2,3-Dioxygenase Regulates Macrophage Recruitment, Polarization and Phagocytosis in *Aspergillus fumigatus* Keratitis. *Investigative Ophthalmology & Visual Science*, **61**: 28.

König, S., Pace, S., Pein, H., Heinekamp, T., Kramer, J., Romp, E., Straßburger, M., Troisi, F., Proschak, A., Dworschak, J., Scherlach, K., Rossi, A., Sautebin, L., Haeggström, J.Z., Hertweck, C., Brakhage, A.A., Gerstmeier, J., Proschak, E., Werz, O. (2019). Gliotoxin from *Aspergillus fumigatus* Abrogates Leukotriene B4 Formation through Inhibition of Leukotriene A4 Hydrolase. *Cell Chemical Biology*, **26**: 524–534.e5.

Kousha, M., Tadi, R., Soubani, A.O. (2011). Pulmonary aspergillosis: a clinical review. *European Respiratory Review*, **20**: 156–174.

Lee, K.H., Ali, N.F., Lee, S.H., Zhang, Z., Burdick, M., Beaulac, Z.J., Petruncio, G., Li, L., Xiang, J., Chung, E.M., Foreman, K.W., Noble, S.M., Shim, Y.M., Paige, M. (2022). Substrate-dependent modulation of the leukotriene A4 hydrolase aminopeptidase activity and effect in a murine model of acute lung inflammation. *Scientific Reports*, **12**: 9443.

Lin, Z., Wang, J.-L., Cheng, Y., Wang, J.-X., Zou, Z. (2020). Pattern recognition receptors from lepidopteran insects and their biological functions. *Developmental and Comparative Immunology*, **108**: 103688.

Low, C.M., Akthar, S., Patel, D.F., Löser, S., Wong, C.-T., Jackson, P.L., Blalock, J.E., Hare, S.A., Lloyd, C.M., Snelgrove, R.J. (2017). The development of novel LTA4H modulators to selectively target LTB4 generation. *Scientific Reports*, **7**: 44449.

Luo, Y., Liu, F., Deng, L., Xu, J., Kong, Q., Shi, Y., Sang, H. (2022). Innate and Adaptive Immune Responses Induced by *Aspergillus fumigatus* Conidia and Hyphae. *Current Microbiology*, **80**: 28.

Ma, Y., Li, R., Wang, J., Jiang, W., Yuan, X., Cui, J., Wang, C. (2021). ITIH4, as an inflammation biomarker, mainly increases in bacterial bloodstream infection. *Cytokine*, **138**: 155377.

Maguire, R., Kunc, M., Hyrsl, P., Kavanagh, K. (2017). Caffeine administration alters the behaviour and development of *Galleria mellonella* larvae. *Neurotoxicology and Teratology*, **64**: 37–44.

Maiya, S., Grundmann, A., Li, S.-M., Turner, G. (2006). The Fumitremorgin Gene Cluster of *Aspergillus fumigatus*: Identification of a Gene Encoding Brevianamide F Synthetase. *ChemBioChem*, **7**: 1062–1069.

Michels, K., Solomon, A.L., Scindia, Y., Sordo Vieira, L., Goddard, Y., Whitten, S., Vaulont, S., Burdick, M.D., Atkinson, C., Laubenbacher, R., Mehrad, B. (2022). *Aspergillus* Utilizes Extracellular Heme as an Iron Source During Invasive Pneumonia, Driving Infection Severity. *The Journal of Infectious Diseases*, **225**: 1811–1821.

Naaraayan, A., Kavian, R., Lederman, J., Basak, P., Jesmajian, S. (2015). Invasive pulmonary aspergillosis – case report and review of literature. *Journal of Community Hospital Internal Medicine Perspectives*, **5**: 26322.

Namvar, S., Labram, B., Rowley, J., Herrick, S. (2022). *Aspergillus fumigatus*—Host Interactions Mediating Airway Wall Remodelling in Asthma. *Journal of Fungi*, **8**: 159.

Okaa, U.J., Bertuzzi, M., Fortune-Grant, R., Thomson, D.D., Moyes, D.L., Naglik, J.R., Bignell, E. (2023). *Aspergillus fumigatus* Drives Tissue Damage via Iterative Assaults upon Mucosal Integrity and Immune Homeostasis. Noverr, M.C. (ed). *Infection and Immunity*, **91**: e00333-22.

Renshaw, H., Vargas-Muñiz, J.M., Richards, A.D., Asfaw, Y.G., Juvvadi, P.R., Steinbach, W.J. (2016). Distinct Roles of Myosins in *Aspergillus fumigatus* Hyphal Growth and Pathogenesis. *Infection and Immunity*, **84**: 1556–1564.

Renwick, J., Daly, P., Reeves, E.P., Kavanagh, K. (2006). Susceptibility of larvae of *Galleria mellonella* to infection by *Aspergillus fumigatus* is dependent upon stage of conidial germination. *Mycopathologia*, **161**: 377–384.

Ries, L.N.A., Pardeshi, L., Dong, Z., Tan, K., Steenwyk, J.L., Colabardini, A.C., Filho, J.A.F., Castro, P.A. de, Silva, L.P., Preite, N.W., Almeida, F., Assis, L.J. de, Santos, R.A.C. dos, Bowyer, P., Bromley, M., Owens, R.A., Doyle, S., Demasi, M., Hernández, D.C.R., Netto, L.E.S., Pupo, M.T., Rokas, A., Loures, F.V., Wong, K.H., Goldman, G.H. (2020). The *Aspergillus fumigatus* transcription factor RglT is important for gliotoxin biosynthesis and self-protection, and virulence. *PLOS Pathogens*, **16**: e1008645.

Risse, B., Thomas, S., Otto, N., Llopmeier, T., Valkov, D., Jiang, X., Klämbt, C. (2013). FIM, a Novel FTIR-Based Imaging Method for High Throughput Locomotion Analysis. *PLOS ONE*, **8**: e53963.

Rocha, M.C., Fabri, J.H.T.M., Silva, L.P., Angolini, C.F.F., Bertolini, M.C., da Cunha, A.F., Valiante, V., Goldman, G.H., Fill, T.P., Malavazi, I. (2021). Transcriptional Control of the Production of *Aspergillus fumigatus* Conidia-Borne Secondary Metabolite Fumiquinazoline C Important for Phagocytosis Protection. *Genetics*, **218**: iyab036.

Romani, L., Zelante, T., De Luca, A., Bozza, S., Bonifazi, P., Moretti, S., D'Angelo, C., Giovannini, G., Bistoni, F., Fallarino, F., Puccetti, P. (2009). Indoleamine 2,3-

dioxygenase (IDO) in inflammation and allergy to *Aspergillus*. *Medical Mycology*, **47**: S154–S161.

Sasse, A., Hamer, S.N., Amich, J., Binder, J., Krappmann, S. (2016). Mutant characterization and *in vivo* conditional repression identify aromatic amino acid biosynthesis to be essential for *Aspergillus fumigatus* virulence. *Virulence*, **7**: 56–62.

Schrettl, M., Bignell, E., Kragl, C., Sabiha, Y., Loss, O., Eisendle, M., Wallner, A., Jr, H.N.A., Haynes, K., Haas, H. (2007). Distinct Roles for Intra- and Extracellular Siderophores during *Aspergillus fumigatus* Infection. *PLOS Pathogens*, **3**: e128.

Schrettl, M., Ibrahim-Granet, O., Droin, S., Huerre, M., Latgé, J.-P., Haas, H. (2010). The crucial role of the *Aspergillus fumigatus* siderophore system in interaction with alveolar macrophages. *Microbes and Infection*, **12**: 1035–1041.

Schrettl, M., Kim, H.S., Eisendle, M., Kragl, C., Nierman, W.C., Heinekamp, T., Werner, E.R., Jacobsen, I., Illmer, P., Yi, H., Brakhage, A.A., Haas, H. (2008). SreA-mediated iron regulation in *Aspergillus fumigatus*. *Molecular Microbiology*, **70**: 27–43.

Seif, M., Kakoschke, T.K., Ebel, F., Bellet, M.M., Trinks, N., Renga, G., Pariano, M., Romani, L., Tappe, B., Espie, D., Donnadieu, E., Hünniger, K., Häder, A., Sauer, M., Damotte, D., Alifano, M., White, P.L., Backx, M., Nerreter, T., Machwirth, M., Kurzai, O., Prommersberger, S., Einsele, H., Hudecek, M., Löffler, J. (2022). CAR T cells targeting *Aspergillus fumigatus* are effective at treating invasive pulmonary aspergillosis in preclinical models. *Science Translational Medicine*, **14**: eabh1209.

Sharon, H., Hagag, S., Osherov, N. (2009). Transcription Factor PrtT Controls Expression of Multiple Secreted Proteases in the Human Pathogenic Mold *Aspergillus fumigatus*. *Infection and Immunity*, **77**: 4051–4060.

Sheehan, G., Konings, M., Lim, W., Fahal, A., Kavanagh, K., Van De Sande, W.W.J. (2020). Proteomic analysis of the processes leading to *Madurella mycetomatis* grain formation in *Galleria mellonella* larvae. Xue, C. (ed). *PLOS Neglected Tropical Diseases*, **14**: e0008190.

Shukla, E., Thorat, L.J., Nath, B.B., Gaikwad, S.M. (2015). Insect trehalase: physiological significance and potential applications. *Glycobiology*, **25**: 357–367.

Singh, B., Sharma, G.L., Oellerich, M., Kumar, R., Singh, S., Bhadaria, D.P., Katyal, A., Reichard, U., Asif, A.R. (2010). Novel Cytosolic Allergens of *Aspergillus fumigatus* Identified from Germinating Conidia. *Journal of Proteome Research*, **9**: 5530–5541.

Slater, J.L., Gregson, L., Denning, D.W., Warn, P.A. (2011). Pathogenicity of *Aspergillus fumigatus* mutants assessed in *Galleria mellonella* matches that in mice. *Medical Mycology*, **49 Suppl 1**: S107-113.

Tanindi, A., Cemri, M. (2011). Troponin elevation in conditions other than acute coronary syndromes. *Vascular Health and Risk Management*, **7**: 597–603.

Traynor, A.M., Owens, R.A., Coughlin, C.M., Holton, M.C., Jones, G.W., Calera, J.A., Doyle, S. (2021). At the metal-metabolite interface in *Aspergillus fumigatus*: towards untangling the intersecting roles of zinc and gliotoxin. *Microbiology (Reading, England)*, **167**: 001106.

Tsai, C.J.-Y., Loh, J.M.S., Proft, T. (2016). *Galleria mellonella* infection models for the study of bacterial diseases and for antimicrobial drug testing. *Virulence*, **7**: 214–229.

Tsai, H.-F., Chang, Y.C., Washburn, R.G., Wheeler, M.H., Kwon-Chung, K.J. (1998). The Developmentally Regulated *alb1* Gene of *Aspergillus fumigatus*: Its Role in Modulation of Conidial Morphology and Virulence. *Journal of Bacteriology*, **180**: 3031–3038.

Vertyporokh, L., Wojda, I. (2020). Immune response of *Galleria mellonella* after injection with non-lethal and lethal dosages of *Candida albicans*. *Journal of Invertebrate Pathology*, **170**: 107327.

Wark, P. (2004). Pathogenesis of allergic bronchopulmonary aspergillosis and an evidence-based review of azoles in treatment. *Respiratory Medicine*, **98**: 915–923.

Wiśniewski, J.R. (2019). Filter Aided Sample Preparation – A tutorial. *Analytica Chimica Acta*, **1090**: 23–30

Acknowledgments

Aaron Curtis is the recipient of an Irish Research Council postgraduate studentship.

Q Exactive mass spectrometer was funded under the SFI Research Infrastructure Call 2012; Grant Number: 12/RI/2346 (3).

Erasmus+ is acknowledged for funding to allow AC travel to Masaryk University for training.

Chapter 4

Exposure of *Aspergillus fumigatus* to *Klebsiella pneumoniae* Culture

Filtrate Inhibits Growth and Stimulates Gliotoxin Production

Aaron Curtis, Michelle Ryan and Kevin Kavanagh

¹Department of Biology, Maynooth University, Maynooth, Co. Kildare, Ireland

Published as:

Curtis, A., Ryan, M. and Kavanagh, K., 2023. Exposure of *Aspergillus fumigatus* to *Klebsiella pneumoniae* Culture Filtrate Inhibits Growth and Stimulates Gliotoxin Production. *Journal of Fungi*, 9 (2), 222.

Author Contributions

Conceptualisation, K.K. and A.C.; methodology, K.K. and A.C.; formal analysis, A.C. and M.R. data curation, A.C. and M.R.; writing—original draft preparation, A.C. and M.R.; writing—review and editing K.K. and A.C. All authors have read and agreed to the published version of the manuscript.

Abstract

Aspergillus fumigatus is an opportunistic fungal pathogen capable of inducing chronic and acute infection in susceptible patients. *A. fumigatus* interacts with numerous bacteria that compose the microbiota of the lung, including *Pseudomonas aeruginosa* and *Klebsiella pneumoniae*, both of which are common isolates from cystic fibrosis sputum. Exposure of *A. fumigatus* to *K. pneumoniae* culture filtrate reduced fungal growth and increased gliotoxin production. Qualitative proteomic analysis of the *K. pneumoniae* culture filtrate identified proteins associated with metal sequestering, enzymatic degradation and redox activity, which may impact fungal growth and development. Quantitative proteomic analysis of *A. fumigatus* following exposure to *K. pneumoniae* culture filtrate (25% v/v) for 24 h revealed a reduced abundance of 1,3-beta-glucanosyltransferase (-3.97 fold), methyl sterol monooxygenase erg25B (-2.9 fold) and calcium/calmodulin-dependent protein kinase (-4.2 fold) involved in fungal development, and increased abundance of glutathione S-transferase GliG (+6.17 fold), non-ribosomal peptide synthase GliP (+3.67 fold), O-methyltransferase GliM (+3.5 fold), gamma-glutamyl acyltransferase GliK (+2.89 fold) and thioredoxin reductase GliT (+2.33 fold) involved in gliotoxin production. These results reveal that exposure of *A. fumigatus* to *K. pneumoniae* *in vivo* could exacerbate infection and negatively impact patient prognosis

4.1 Introduction

A wide range of microbes can be present in the lung as commensals or pathogens, and there is significant microbial diversity present (O'Dwyer *et al.*, 2016). There is reduced microbial diversity in the sputum of patients with acute exacerbations of chronic obstructive pulmonary disease, indicating a poor prognosis, and the presence of *Staphylococcus* and absence of *Veillonella* in sputum is associated with a high one-year mortality risk in patients (Leitao Filho *et al.*, 2019). In addition, coinfection with *Pseudomonas aeruginosa* and *Aspergillus fumigatus* has been implicated in a worsened disease state in Cystic Fibrosis (CF) patients, with each species stimulating the growth and colonisation of the other (Keown *et al.*, 2020). The bacterium *Klebsiella pneumoniae* and the fungus *A. fumigatus* are commonly isolated from the lungs of CF patients (LiPuma, 2010), indicating a similar interaction could occur, impacting disease development in patients.

K. pneumoniae is a Gram-negative rod-shaped bacterium that is responsible for approximately one-third of all Gram-negative infections worldwide (Navon- Venezia *et al.*, 2017). Pneumonia caused by *K. pneumoniae* is characterised by a strong inflammatory response which is due to the production of pro-inflammatory cytokines in addition to high neutrophil and macrophage counts (Vieira *et al.*, 2016). Within the host, *K. pneumoniae* is found in the gastrointestinal tract and the upper respiratory tract, where it is most frequently acquired through nosocomial acquisition (Fodah *et al.*, 2014). The first report of a CF patient becoming infected with a colistin-resistant strain of *K. pneumoniae* was in 2014 (Delfino *et al.*, 2015), and since then, the number of reports of critically ill patients becoming infected with such strains has increased.

The filamentous fungus *A. fumigatus* is widespread in the environment and can cause three types of infection in susceptible individuals. Allergic bronchopulmonary aspergillosis (ABPA) arises due to an allergic immune response to *A. fumigatus* stimulating T-helper cells to recruit immune cells, particularly eosinophils, resulting in inflammation of pulmonary tissue. Patients with asthma or CF are among the most susceptible to this form of aspergillosis, and early diagnosis of the disease is important for avoiding complications such as pulmonary fibrosis (Lattanzi *et al.*, 2020). Chronic pulmonary aspergillosis (CPA) occurs when pre-damaged pulmonary tissue becomes colonised by *A. fumigatus* (Schweer *et al.*, 2014). The colonisation results in the formation of an aspergilloma, or fungal ball, which can result in severe haemoptysis

(Kradin and Mark, 2008). Invasive aspergillosis is the most serious form of aspergillosis, with a one-year survival rate for solid organ transplant patients of 59%, while the rate for stem cell transplant recipients can be as low as 25% (Webb *et al.*, 2018). Patients suffering from neutropenia were once considered to be the main target group for this type of aspergillosis; however, non-neutropenic patients such as transplant patients, AIDS patients and ICU patients are also susceptible to infection (Bassetti *et al.*, 2018).

The interaction between *A. fumigatus* and *P. aeruginosa* has been characterised previously, indicating decreased fungal growth and increased gliotoxin production in the presence of bacterial cells. In contrast, exposure of *A. fumigatus* hyphae to *P. aeruginosa* culture filtrate led to increased growth and decreased gliotoxin production (Margalit *et al.*, 2022), and secreted products of *A. fumigatus* can promote *P. aeruginosa* growth in nutrient-poor conditions (Margalit *et al.*, 2020). *K. pneumoniae* is often found in polymicrobial interactions with *A. fumigatus* within the lung, and these interactions may be antagonistic or synergistic (Dees *et al.*, 2014). For example, *K. pneumoniae* is capable of inhibiting spore germination and hyphal development in different *Aspergillus* spp., and this effect was dependent upon the direct physical interaction between the bacteria and the fungus (Nogueira *et al.*, 2019). *A. fumigatus* and *K. pneumoniae* can co-exist in the lungs of immunocompromised patients, but the interaction between these two pathogens is poorly characterised.

The aim of the work presented was to characterise the effect of *K. pneumoniae* culture filtrate on the growth and proteomic response of *A. fumigatus*, as this might give an insight into an important bacterial-fungal interaction in the lungs of infected patients.

4.2 Materials and Methods

4.2.1 *A. fumigatus* Growth Conditions

Aspergillus fumigatus ATCC 26933 was grown on malt extract agar plates at 37 °C for a minimum of 96 h, and conidia were harvested by washing with 0.1% (v/v) Tween-20 and phosphate buffered saline (PBS-T). Czapek–Dox liquid medium (Duchefa Biochemie) (50 mls) was inoculated with conidia at a density of 1.2 × 10⁶/mL.

4.2.2 Preparation of the Bacterial Culture Filtrate

K. pneumoniae ATCC 13439 was grown on nutrient agar plates for 96 h. Czapek–Dox broth was inoculated with bacteria and incubated at 37 °C and 200 rpm for 96 h. Cells were harvested by centrifugation for 15 min at 1258×*g* at room temperature, and the culture filtrate was filter sterilised using 0.45 µm filtropur S filters. Culture filtrates were stored at –20 °C until required.

4.2.3 Assessment of Fungal Biomass

A. fumigatus was grown for 48 h in Czapek–Dox broth prior to the addition of *K. pneumoniae* culture filtrate or PBS (n = 3) at a concentration of 25% *v/v*. The cultures were incubated at 37 °C and 200 rpm. The mycelia were harvested after 24 h using Miracloth (Millipore). The wet weight of the mycelia was then measured using a weighing scale and expressed as weight in grams.

4.2.4 Gliotoxin Extraction and Quantification by RP-HPLC

K. pneumoniae culture filtrate was added to the 48 h old *A. fumigatus* cultures at a final concentration of 25% *v/v* and incubated at 37 °C and 200 rpm for a further 24 h. Culture filtrate (20 mL) was mixed continuously with an equal volume of chloroform for 2 h. The chloroform layer was removed and evaporated to dryness, and the extract was dissolved in 500 µL HPLC grade methanol. Gliotoxin was quantified using Reverse-Phase HPLC. The mobile phase was 34.9% (*v/v*) acetonitrile, 0.1% (*v/v*) trifluoroacetic acid (TFA) and 65% (*v/v*) HPLC-grade deionised water. Gliotoxin extract (20 µL) was injected into an Agilent ZORBAX SB-Aq 5 µm polar LC column. A standard curve of peak area vs. gliotoxin concentration was generated using gliotoxin standards (Merck) dissolved in HPLC-grade methanol.

4.2.5 Extraction of Protein from *K. pneumoniae* Culture Filtrate

K. pneumoniae was grown for 96 h in Czapex Dox broth. Cells were harvested by centrifugation for 15 min at 1258×*g* at room temperature. The culture filtrate was passed through a 0.45 mm filtropur S filter. The culture filtrate was centrifuged at 14,500×*g* for 10 min to remove any remaining debris, and protein was acetone precipitated overnight at a ratio of 1:5 culture filtrate to acetone. Samples were processed in the same manner as the fungal mycelial samples for proteomic analysis.

4.2.6 Protein Extraction from *A. fumigatus* Exposed to Bacterial Culture Filtrate

A. fumigatus cultures (48 h growth) were supplemented with *K. pneumoniae* culture filtrate (25% v/v) for 24 h at 37 °C in Czapek–Dox media (n = 3 per group). Hyphae were harvested by filtration, snap-frozen in liquid nitrogen and ground to a fine dust in a mortar using a pestle. Lysis buffer [8 M urea, 2 M thiourea, and 0.1 M Tris-HCl (pH 8.0) dissolved in HPLC-grade dH₂O], supplemented with protease inhibitors [aprotinin, leupeptin, pepstatin A, Tosyllysine Chloromethyl Ketone hydrochloride (TLCK) (10 µg/mL) and phenylmethylsulfonyl fluoride (PMSF) (1 mM/mL)] was added (4 mL/g of hyphae). The lysates were sonicated (Bandelin Senopuls) three times for 10 s at 50% power. The cell lysate was subjected to centrifugation (Eppendorf Centrifuge 5418) for 8 min at 14,500× g to pellet cellular debris. The protein concentration was quantified by the Bradford method, and samples (100 µg) were subjected to overnight acetone precipitation.

4.2.7 Label-Free Mass Spectrometry (LF/MS)

Following centrifugation for 10 min at 14,500× g, acetone was removed, and the protein pellet was resuspended in 25 µL sample resuspension buffer (8 M urea, 2 M thiourea, 0.1 M tris-HCL (pH 8.0) dissolved in HPLC grade dH₂O). An aliquot of 5 µL was removed from each of the samples and quantified by the Qubit quantification system (Invitrogen). Ammonium bicarbonate (125 µL, 50 mM) was added to the remainder of the samples. Reduction of the sample was initiated by adding 1 µL 0.5 M dithiothreitol (DTT). The protein samples were then incubated for 20 min at 56 °C before alkylation with 2.7 µL 0.55 M iodoacetamide; this occurred at room temperature in the dark for 15 min. Protease max surfactant trypsin enhancer (Promega) (1 µL, 1% w/v) and sequence grade trypsin (ThermoFisher Scientific, Cork, Ireland) (0.5 µg/µL), were added to the proteins, respectively, and incubated for 18 h at 37 °C. TFA (1 µL, 100%) was added to each sample to end digestion. The samples were incubated for 5 min at room temperature and centrifuged for 10 min at 14,500× g. Samples were purified for mass spectrometry using C18 spin columns as per the manufacturer's instructions. A speedy vac concentrator was used to dry the peptides, and samples were resuspended in 2% v/v acetonitrile and 0.05% v/v TFA and sonicated for 5 min to help with this resuspension. The resulting final peptide concentration was (750 ng/2 µL).

4.2.8 Mass Spectrometry and the Parameters for *A. fumigatus* and *K. pneumoniae* Culture Filtrate Proteomic Data Procurement

The digested *K. pneumoniae* culture filtrate sample (500 ng) or *A. fumigatus* protein samples (750 ng) were each loaded onto a QExactive (ThermoFisher Scientific) high-resolution mass spectrometer which was connected to a Dionex Ultimate 3000 (RSICnano) chromatography system. An increasing acetonitrile gradient was used to separate the peptides in the samples. This gradient was created on a 50 cm EASY-Spray PepMap C18 column with a 75 mm diameter using a 133 min reverse phase gradient at a flow rate of 300 nL/min. All of the data were obtained while the mass spectrometer was functioning in an automatic dependent switching mode. A quantitative analysis of the *A. fumigatus* proteome after exposure to bacterial culture filtrate was conducted using MaxQuant version 1.5.3.3 (<http://www.maxquant.org>) (accessed on 14 September 2022) using the settings outlined previously (Margalit *et al.*, 2022). The search algorithm Andromeda included in the MaxQuant software was incorporated in the correspondence between MS/MS data and the Uniprot-SWISS-PROT database *Neosartorya fumigata* reference proteome obtained from a UniProt-SWISS-PROT database to identify proteins (9647 entries, downloaded July 2022). *K. pneumoniae* culture filtrate was analysed through proteome discoverer v 2.5, and proteins were searched against the UniProtKB database (*Klebsiella Pneumoniae* strain 342, 5738 entries, downloaded September 2022).

4.2.9 Data Analysis of *A. fumigatus* and *K. pneumoniae* Culture Filtrate Proteomes

Qualitative analysis of the proteome of the *K. pneumoniae* culture filtrate was investigated using Proteome Discoverer 2.5 and Sequest HT (SEQUEST HT algorithm; Thermo Scientific). Identified proteins were searched against the UniProtKB database (*Klebsiella Pneumoniae* strain 342, 5738 entries, accessed 16 September 2022). Search parameters applied for protein identification were as follows: (i) enzyme name—trypsin, (ii) an allowance of up to two missed cleavages, (iii) peptide mass tolerance set to 10 ppm, (iv) MS/MS mass tolerance set to 0.02 Da, (v) carbamidomethylation set as a fixed modification and (vi) methionine oxidation set as a variable modification. Peptide probability was set to high confidence (with an FDR $\leq 0.01\%$ as determined by Percolator validation in Proteome Discoverer). Peptides identified by 2 or more unique peptides were retained for analysis.

Perseus v.1.6.15.0 was employed to analyse *A. fumigatus* proteomic data, as well as to process and visualise the data. Measurement of protein abundance was based on normalised LFQ intensity values. The data was initially filtered for the removal of contaminants before LFQ intensity values were Log2 transformed, and each sample was placed in its relative group. Proteins which were not found in three out of three replicates in at least one group were excluded from further analysis. Normal intensity values were also used for principal component analysis (PCA). Proteins which were distinctively expressed in one group compared to another or those which were completely absent in one group were noted and included for all further analysis. Gene Ontology (GO) mapping was also conducted using the UniProt gene ID to gain more knowledge about the biological processes and molecular processes of the identified proteins. To gain a better visualisation of the variances between the samples, pairwise student T-tests were conducted for all data using a cut-off of $p < 0.05$. The generation of a volcano plot was done by plotting the log2 fold change values on the x-axis and the log p -values on the y-axis, which allowed for pairwise comparison. The top 20 most increased and decreased in abundance proteins identified in the groups were included in these volcano plots. The mass spectrometry proteomics data have been deposited to the ProteomeXchange Consortium *via* the PRIDE (Perez-Riverol *et al.*, 2021) partner repository with the dataset identifier PXD037833.

4.3 Results

4.3.1 Analysis of the Effects of *K. pneumoniae* Culture Filtrate on *A. fumigatus*

Exposure of 48 h old *A. fumigatus* to *K. pneumoniae* culture filtrate (25% v/v) for 24 h led to a decrease in fungal biomass (1.23 ± 0.20 g vs. 0.81 ± 0.12 g $p = 0.03$) (Figure 4.1A) and a large increase in gliotoxin secretion with a 371.55% increase ($p = 0.01$) (Figure 4.1B).

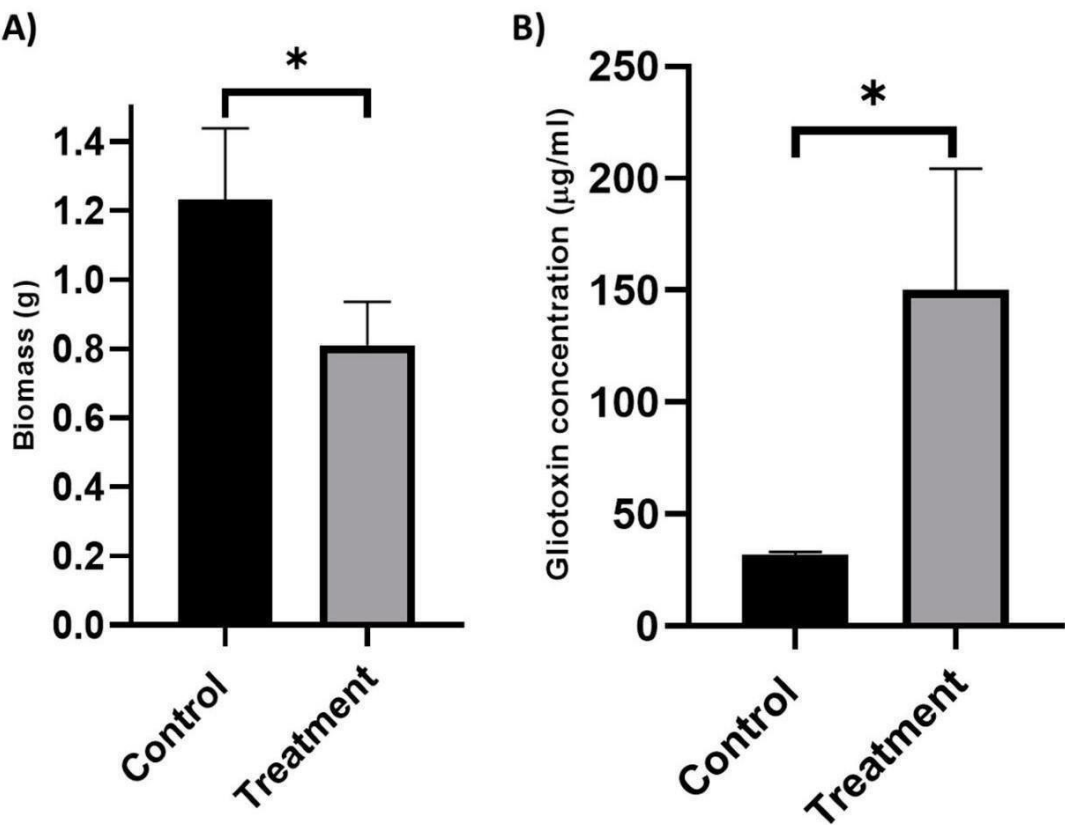


Figure 4.1: Analysis of the effects of *K. pneumoniae* culture filtrate on *A. fumigatus* mycelial growth (A) and Gliotoxin production (B). *K. pneumoniae* culture filtrate (25% v/v) or PBS (control) was added to 48 h old *A. fumigatus* and wet weight were recorded after 24 h growth (n = 3). Error bars represent SD. * p = 0.03 (B) Gliotoxin concentration was assessed by Reverse-Phase HPLC (n = 3), and error bars represent SD. * p = 0.01.

4.3.2 Characterisation of *K. pneumoniae* Culture Filtrate

Qualitative proteomic analysis of *K. pneumoniae* culture filtrate revealed the presence of 160 high-confidence proteins (Table S4.1), of which 35 were identified as having possible antifungal effects (Table 4.1). These could be subdivided into six categories; structurally bound (3 proteins), membrane-associated proteins (10 proteins), virulence-associated proteins (3 proteins), proteins with enzymatic activity (8 proteins), metal binding proteins (5 proteins) and proteins with detoxification activity (6 proteins).

Table 4.1: Proteins identified in *K. pneumoniae* culture filtrate with potential antifungal activity

Protein Name	Uniprot Code	Unique Peptides	% Coverage	Function
Outer membrane protein A	B5XY48	8	22.28	Membrane proteins
Outer membrane protein X	B5XYT0	7	39.76	
Outer membrane protein C	B5XNZ9	7	21.48	
Penicillin-binding protein activator LpoA	B5XSZ6	5	9.54	
OmpA family protein	B5XN00	3	24.54	
Penicillin-binding protein activator LpoB	B5XXG6	2	16.74	
OmpA family protein	B5XVK9	3	28.75	
LPS-assembly protein LptD	B5Y1Z1	3	5.37	
MrkF protein	B5XUK5	2	16.33	
LPS-assembly lipoprotein LptE	B5XZR3	2	13.26	
Elongation factor Tu	B5XN88	10	40.35	virulence
Elongation factor Ts	B5Y1K1	2	12.01	
Tol-Pal system protein TolB	B5XZC1	6	24.18	
Pectinesterase	B5XZ84	7	22.01	
Autonomous glycyl radical cofactor	B5XNF9	6	51.18	Enzymatic activity
Protease VII	B5RKF2	6	25.72	
Periplasmic serine endoprotease DegP-like	B5Y1K8	6	15.93	
Enolase	B5XV19	6	21.06	
Endolytic peptidoglycan transglycosylase RlpA	B5XZS1	5	15.06	
Beta-lactamase	B5XQY6	4	11.88	
Prephenate dehydratase/aro-ogenate dehydratase	B5XVG4	3	16.60	
Metal-binding protein	B5XZ21	6	39.35	
High-affinity zinc uptake system protein ZnuA	B5XQ08	5	25.47	Metal binding
Copper homeostasis protein CutF	B5Y1H9	3	16.81	
Iron uptake system component EfeO	B5XXM1	3	10.4	
Thiol:disulfide interchange protein	B5XZJ6	4	31.40	
Alkyl hydroperoxide reductase C	B5XZT7	4	35.82	
Thioredoxin	B5XYY8	5	51.37	Detoxification
Acriflavine resistance protein A	B5Y0P5	3	9.57	
Thiol peroxidase	B5XRV9	3	32.14	
Alkyl hydroperoxide reductase C	B5Y0Z0	3	35.82	
Glutathione ABC transporter, periplasmic glutathione-binding protein	B5XYQ7	2	2.92	
Inhibitor of vertebrate lysozyme	B5Y004	2	15.54	
Putative lipoprotein	B5XUP5	1	36.1	Structurally bound
Outer membrane protein A	B5XY48	6	19.1	
Chaperone protein DnaK	B5Y242	2	2.7	

4.3.3 Analysis of the Effect of *K. pneumoniae* Culture Filtrate on the *A. fumigatus* Proteome

Label-free mass spectrometry was employed to characterise the proteomic response of *A. fumigatus* following exposure to *K. pneumoniae* culture filtrate for 24 h. In total, 1960 proteins were identified, and 111 proteins were identified as being statistically significant ($p < 0.05$) differentially abundant (SSDA), having a fold change greater than ± 1.5 (Table S4.2). A principal component analysis (PCA) was conducted on all significant proteins to identify distinct proteomic differences between each of the groups. The PCA indicates that the *A. fumigatus* exposed to the *K. pneumoniae* culture filtrate displays a distinct proteomic pattern when compared to control samples (Figure 4.2A). Hierarchical clustering carried out in Perseus highlights the clear differences in protein abundance between the control and the *A. fumigatus* culture that was exposed to the *K. pneumoniae* culture filtrate. These differences in protein abundance are highlighted in a heat map (Figure 4.2B), with blue indicating proteins with increased abundance and orange indicating proteins with decreased abundance, respectively.

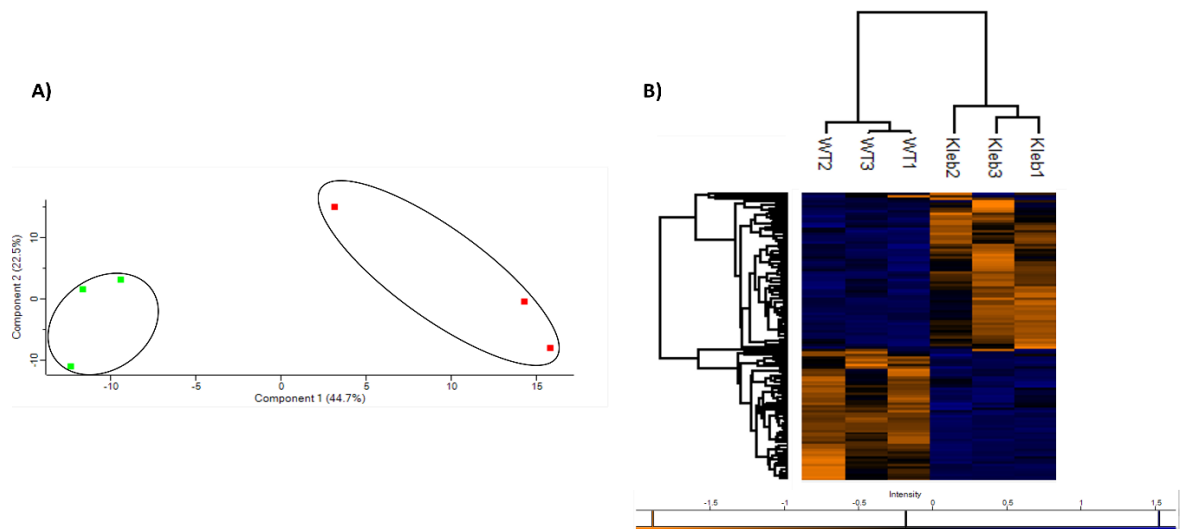


Figure 4.2: Principal component analysis of *A. fumigatus* after exposure to *K. pneumoniae* culture filtrate (25% v/v) (green) and control *A. fumigatus* (red). (B) Heatmap generated through Two-way unsupervised hierarchical clustering of the median protein expression values of all statistically significant differentially abundant proteins.

A volcano plot was generated by way of pairwise t-tests ($p < 0.05$) to determine the proteins which increased and decreased in abundance between control *A. fumigatus* samples and *A. fumigatus* exposed to *K. pneumoniae* culture filtrate (Figure 4.3). When analysing samples of *A. fumigatus* exposed to the *K. pneumoniae* culture filtrate, a significant increase in the relative abundance of proteins associated with secondary metabolism, in particular, proteins associated with gliotoxin biosynthesis was observed (Table 4.2), i.e., glutathione S-transferase GliG (+6.17 fold increase), non-ribosomal peptide synthase GliP (+3.67 fold), O-methyltransferase GliM (+3.5 fold), gamma-glutamyl acyltransferase GliK (+2.89 fold) and thioredoxin reductase GliT (+2.33 fold). In addition, ribonuclease mitogillin was increased in abundance by +4.9 fold. Fibrinogen C-terminal domain-containing protein and polysaccharide deacetylase family protein were increased by +63.3 fold and +6.9 fold, respectively, and both have been implicated in adherence to the lung epithelium. Decreased abundance of methyl sterol monooxygenase erg25B (-2.9 fold) and calcium/calmodulin-dependent protein kinase (-4.2 fold) indicates a decrease in fungal cell division (Table 4.3). Deoxyribose-phosphate aldolase was decreased in abundance by -2.3 fold and played a role in gluconeogenesis and lipid biogenesis. Protein synthesis was also affected by a decrease in the abundance of the 60 S ribosomal protein L22 and aspartyl aminopeptidase (-2.9 fold).

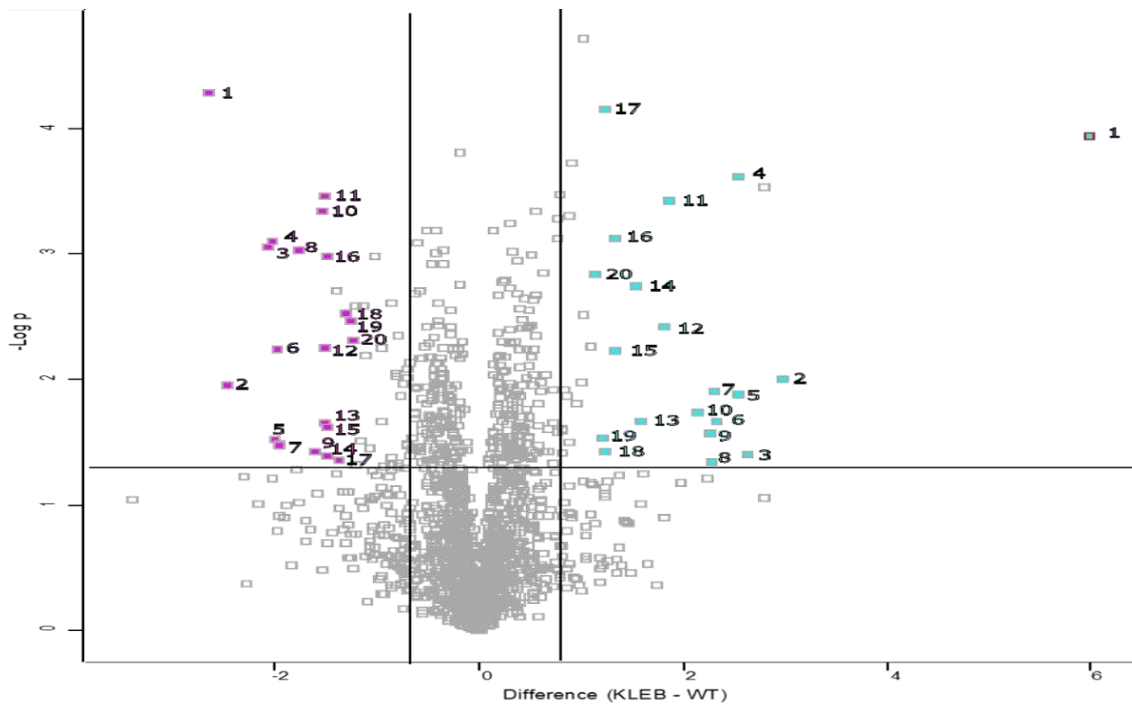


Figure 4.3: Volcano plot showing the distribution of statistically significant and differentially abundant (SSDA) proteins which have a $-\log(p\text{-value}) > 1.3$ and difference ± 0.58 . *A. fumigatus* exposed to *K. pneumoniae* culture filtrate compared to control *A. fumigatus*.

Table 4.2: The Top 20 proteins most increased in abundance in *A. fumigatus* after exposure to *K. pneumoniae* culture filtrate for 24 h.

Number	Fold Change	Protein Name	Protein IDs	Unique Peptides	Sequence Coverage [%]
1	63.39	Fibrinogen C-terminal domain-containing protein	Q4W8X0	3	38.5
2	7.88	SGL domain-containing protein	Q4WP91	4	15
3	6.93	Polysaccharide deacetylase family protein	Q4WUN9	9	48.7
4	6.17	Glutathione S-transferase gliG	A4GYZ0	18	73.3
5	5.81	ABM domain-containing protein	Q4WG08	2	24.3
6	5.80	Endonuclease/exonuclease/phosphatase family	Q4WKR6	8	31.9

7	5.04	D-xylose reductase (NAD(P)H)	Q4WI64	10	38.6
8	4.96	Ribonuclease mitogillin	P67875	6	44.9
9	4.86	Amine oxidase	Q4WFX6	16	46
10	4.79	DUF4468 domain-containing protein	Q4WMI8	9	49.7
11	4.42	DUF907 domain protein	Q4WHA4	1	3
12	3.67	Nonribosomal peptide synthetase gliP	Q4WMJ7	14	14.2
13	3.51	O-methyltransferase gliM	Q4WMJ5	12	32.9
14	2.98	Oxidoreductase, short-chain	Q4WUP1	5	40.5
15	2.89	Gamma-glutamyl cyclotransferase gliK	E9R9Y3	2	16.8
16	2.50	GPI anchored serine-threonine rich protein	Q4WTF2	2	34.5
17	2.50	Phosphatidylglycerol/phosphatidylinositol transfer	Q4X136	11	46.9
18	2.35	Cache_2 domain-containing protein	Q4WYY2	4	50.8
19	2.34	Thioredoxin reductase gliT	E9RAH5	20	85.9
20	2.33	Cell wall protein PhiA	Q4WF87	6	73

Table 4.3: The Top 20 proteins most decreased in abundance in *A. fumigatus* after exposure to *K. pneumoniae* culture filtrate for 24 h.

Number	Fold Change	Protein Name	Protein IDs	Unique Peptides	Sequence Coverage [%]
1	-6.30	HYPK_UBA domain-containing protein	Q4WPC3	2	17.7
2	-5.49	Methyltransferase	Q4X081	4	30.3
3	-4.20	Calcium/calmodulin dependent protein kinase	Q4WXH7	7	25.1
4	-4.05	Elongation of fatty acids protein	Q4WEE9	4	16
5	-3.97	1,3-beta-glucanosyltransferase	Q4WBF7	4	8.9
6	-3.96	Protein DOM34 homolog	Q4WI62	7	26.6

7	-3.86	Short chain dehydrogenase helC	Q4WR19	7	37.7
8	-3.84	Polyketide transferase af380	Q4WAY4	8	47.9
9	-3.42	BTB/POZ domain protein	Q4WFH8	6	32
10	-3.02	Methyltransferase psoC	Q4WB00	21	71.2
11	-2.86	Methylsterol monooxygenase erg25B	Q4W9I3	3	13.9
12	-2.86	DUF948 domain-containing protein	Q4WXM0	4	42.3
13	-2.85	Cytochrome P450 monooxygenase helB1	Q4WR17	9	20.5
14	-2.83	Aspartyl aminopeptidase	Q4WX56	5	23.4
15	-2.80	Protostadienol synthase helA	Q4WR16	14	28.2
16	-2.80	Signal recognition particle 54 kDa protein	Q4WEQ8	3	11.5
17	-2.79	Tripeptidyl-peptidase sed4	Q4WQU0	3	8.1
18	-2.64	60S ribosomal protein L22, putative	Q4WYA0	7	52.1
19	-2.58	Amino acid permease (Gap1), putative	Q4WG99	12	19
20	-2.46	3-ketosteroid 1-dehydrogenase helE	Q4WR24	6	18.3

4.4 Discussion

The aim of the work presented here was to characterise the response of *A. fumigatus* to *K. pneumoniae* culture filtrate, as this might give an indication of the *in vivo* interaction between the fungus and bacteria. The culture conditions were designed to represent conditions within the immunocompromised lung by exposing *A. fumigatus* to the *K. pneumoniae* culture filtrate as opposed to bacterial cells. Czapek–Dox was chosen for this investigation as this medium provides both a low-nutrient and high-nitrogen environment, which are characteristics of immunocompromised lungs (Line *et al.*, 2014; Lu *et al.*, 2018).

The results demonstrated that exposure to the *K. pneumoniae* culture filtrate inhibited the growth of *A. fumigatus* and induced increased secretion of gliotoxin. Previously, an examination of the interaction between *K. pneumoniae* cells and *A. fumigatus* demonstrated a reduction in spore germination and hyphal development which was dependent upon direct physical interaction between bacterial and fungal cells (Nogueira *et al.*, 2019). Exposure of *Penicillium verrucosum* to actinobacter-species cell-free supernatant also resulted in stimulation of ochratoxin A production and inhibition of fungal growth (Campos-Avelar *et al.*, 2020). *Aspergillus flavus* exposed to culture filtrate of *Streptomyces* spp. also showed reduced growth and elevated secretion of aflatoxin B1 (Campos-Avelar *et al.*, 2021).

Analysis of the *K. pneumoniae* culture filtrate identified 160 high-confidence proteins (Table S4.1), of which 35 were identified to have possible effects on fungal development (Table 4.1) and three of which (putative lipoprotein, outer membrane protein A and chaperone protein DnaK) were also bound to the fungal mycelia. Outer membrane protein A is essential for *A. baumannii* cell attachment to *Candida albicans* filaments and A549 human alveolar epithelial cells (Gaddy *et al.*, 2009) and has been demonstrated to induce leaky barriers in murine lungs and human A549 cells without affecting cell viability (Zhang *et al.*, 2022). Elongation factor Tu was identified in the *K. pneumoniae* culture filtrate is involved in bacterial virulence and is associated with adhesion to host extracellular matrix components. Secretion of EF-Tu increased after *Helicobacter pylori* infection, suggesting that *H. pylori* secrete EF-Tu to facilitate attachment to host cells (Chiu *et al.*, 2017).

The ability of the *K. pneumoniae* culture filtrate to inhibit fungal growth could have also arisen as a result of enzymatic activity. DegP-like periplasmic serine

endoprotease is a highly conserved periplasmic protease found in most Gram-negative bacteria. This protease is involved in the degradation of denatured or aggregated protein within the cell envelope in *Escherichia coli* (Jones *et al.*, 2001; Zhang *et al.*, 2019). Protease VII (OmpT), an aspartic protease, was identified in the culture filtrate and is associated with the inhibition of coagulation and antimicrobial peptide production (Sabotič and Kos, 2012).

Redox-active components and enzymes in the *K. pneumoniae* culture filtrate could also affect fungal growth and mycotoxin production. Thiol:disulfide interchange protein DsbA plays a role in oxidising the formation of disulfide bonds (Denoncin and Collet, 2013). Thiol:disulfide interchange protein DsbA may be implemented in the oxidation of gliotoxin's disulfide bond, increasing its biological accumulation and activity (Bernardo *et al.*, 2003). Alkyl hydroperoxide reductase C was identified in the *K. pneumoniae* culture filtrate and catalyses the reduction of hydrogen peroxide, organic hydroperoxides and thioredoxin in HeLa cells (Choi *et al.*, 2007).

The non-siderophore iron uptake component EfeO was identified in the *K. pneumoniae* culture filtrate, and this is a component in the main ferrous iron transport system that is present in both pathogenic and non-pathogenic microbes (Lau *et al.*, 2016). In addition, the high-affinity zinc uptake system protein ZnuA in *K. pneumoniae* culture filtrate is essential in acquiring zinc at the interface between bacteria and mammalian cells and counteracting host depletion mechanisms (Neupane *et al.*, 2019). It has been previously demonstrated that zinc limitation results in increased gliotoxin production and the growth-limiting effects of exogenous gliotoxin are relieved by the presence of zinc in media (Traynor *et al.*, 2021). In addition, certain genes of the gliotoxin biosynthetic cluster, including *gliZ*, are regulated by ZafA, which is the zinc-responsive transcription factor that controls the adaptive response to zinc starvation in *A. fumigatus* (Vicentefranqueira *et al.*, 2018). Analysis of *P. aeruginosa* culture filtrate, which also affected fungal growth and secondary metabolism, identified a similar protein profile to that found in this work (Margalit *et al.*, 2022). *P. aeruginosa* culture filtrate contained chaperone protein DnaK and components involved in the uptake of nutrients, including ferric iron-binding periplasmic protein HitA. Detoxification proteins such as thiol:disulphide interchange protein DsbA and thioredoxin reductase were found in both culture filtrates. Despite these similarities, *K. pneumoniae* culture filtrate promoted gliotoxin biosynthesis, while *P. aeruginosa* inhibited it.

A. fumigatus exposed to the *K. pneumoniae* culture filtrate demonstrated a reduction in growth and a shift towards secondary metabolism, particularly through the increased secretion of gliotoxin. Gliotoxin biosynthesis is mediated by a gene cluster consisting of 13 genes. Proteomic analysis revealed that five proteins involved in the biosynthesis of gliotoxin were increased in abundance; glutathione S-transferase (+6.17 fold), non-ribosomal peptide synthase (+3.67 fold), O-methyltransferase (+3.5 fold), gamma-glutamyl acyltransferase (+2.89 fold) and thioredoxin reductase (+2.33 fold). The increase in gliotoxin production may be attributed to the physical binding of outer membrane protein A, due to its ability to induce leakage in epithelial cells (Zhang *et al.*, 2022) in a similar manner to fungistatic concentrations of amphotericin B which increases *A. fumigatus* permeability and stimulates *de novo* gliotoxin biosynthesis (Reeves *et al.*, 2004).

There was also an increase (+63.3 fold) in the abundance of fibrinogen C-terminal domain-containing protein, and this could indicate increased virulence and adhesion to lung epithelium. Asthmatic lungs have damaged bronchioloalveolar epithelium, and fibrinogen deposits form at the surface of wounded epithelia, which facilitate microbial attachment (Upadhyay *et al.*, 2012). *A. fumigatus* also demonstrated increased binding affinity to fibrinogen compared with less pathogenic *Aspergillus spp.*, suggesting that adhesion to the extracellular matrix may be important in disease pathogenesis (Wasylka and Moore, 2000). Polysaccharide deacetylase family protein was increased in abundance (+6.9 fold) and is associated with adherence as proteins with similar domains, such as Agd3, are part of a group of metal- dependent polysaccharide deacetylases, which have been shown to remove *N*- or *O*- linked acetate groups from chitin, peptidoglycan, acetylxytan, and poly- β -1,6-*N*- acetylglucosamine, deletion of *agd3* was associated with a reduced adherence and virulence in murine models of invasive aspergillosis, indicating reduced fungal burden (Lee *et al.*, 2016).

The proteome of *A. fumigatus* exposed to *K. pneumoniae* culture filtrate also showed a reduced abundance of several proteins; 1,3 beta glucanosyltransferase was reduced in abundance by -3.9 fold and plays a role in cell wall biogenesis (Gastebois *et al.*, 2010). The membrane protein methyl sterol monooxygenase erg25B, essential for ergosterol biosynthesis (Alcazar-Fuoli *et al.*, 2008), was reduced by -2.9 fold,

calcium/calmodulin-dependent protein kinase was reduced by -4.2 fold and is essential for fungal nuclear cell division and hyphal development in *Aspergillus nidulans* (Alcazar-Fuoli and Mellado, 2013). Deoxyribose-phosphate aldolase was reduced in abundance by -2.3 fold and had a role in gluconeogenesis and the glyoxylate cycle (Dayton and Means, 1996). Decreased abundance of methyltransferase LaeA-like putative protein -2.16 fold could explain the downregulation of proteins associated with specific secondary metabolites (Vorapreeda *et al.*, 2021), including helvolic acid and fumagillin. Proteins associated with helvolic acid biosynthesis, including cytochrome P450 monooxygenase helB1 (-2.8 fold), short chain dehydrogenase helC (-3.8 fold), protostadienol synthase helA (-2.8 fold) and 3-ketosteroid 1-dehydrogenase helE (-2.4 fold) were decreased in abundance and the fumagillin associated protein polyketide transferase af380 (-3.8 fold) was also decreased in abundance (Keller *et al.*, 2006; Lin *et al.*, 2013).

This study provides evidence that exposure of *A. fumigatus* to *K. pneumoniae* culture filtrate results in a reduction in growth but an increase in gliotoxin production and in the abundance of associated proteins. The clinical implications of these alterations could inhibit the ability of the patient to mount an effective immune response to *A. fumigatus* infection resulting in more severe symptoms and an increase in mortality. This work provides novel insights into an important bacterial-fungal interaction that occurs in the lungs of immunocompromised patients. Understanding the extent and importance of such microbial interactions can help to identify better therapeutic strategies for the control of pulmonary infections in susceptible patients.

4.5 References

Alcazar-Fuoli, L., Mellado, E. (2013). Ergosterol biosynthesis in *Aspergillus fumigatus*: its relevance as an antifungal target and role in antifungal drug resistance. *Frontiers in Microbiology*, **3**.

Alcazar-Fuoli, L., Mellado, E., Garcia-Effron, G., Lopez, J.F., Grimalt, J.O., Cuenca-Estrella, J.M., Rodriguez-Tudela, J.L. (2008). Ergosterol biosynthesis pathway in *Aspergillus fumigatus*. *Steroids*, **73**: 339–347.

Bassetti, M., Peghin, M., Vena, A. (2018). Challenges and Solution of Invasive Aspergillosis in Non-neutropenic Patients: A Review. *Infectious Diseases and Therapy*, **7**: 17–27.

Bernardo, P.H., Brasch, N., Chai, C.L.L., Waring, P. (2003). A novel redox mechanism for the glutathione-dependent reversible uptake of a fungal toxin in cells. *The Journal of Biological Chemistry*, **278**: 46549–46555.

Campos-Avelar, I., Colas de la Noue, A., Durand, N., Cazals, G., Martinez, V., Strub, C., Fontana, A., Schorr-Galindo, S. (2021). *Aspergillus flavus* Growth Inhibition and Aflatoxin B1 Decontamination by *Streptomyces* Isolates and Their Metabolites. *Toxins*, **13**: 340.

Campos-Avelar, I., Colas de la Noue, A., Durand, N., Fay, B., Martinez, V., Fontana, A., Strub, C., Schorr-Galindo, S. (2020). Minimizing Ochratoxin A Contamination through the Use of Actinobacteria and Their Active Molecules. *Toxins*, **12**: 296.

Chiu, K.-H., Wang, L.-H., Tsai, T.-T., Lei, H.-Y., Liao, P.-C. (2017). Secretomic Analysis of Host–Pathogen Interactions Reveals That Elongation Factor-Tu Is a Potential Adherence Factor of *Helicobacter pylori* during Pathogenesis. *Journal of Proteome Research*, **16**: 264–273.

Choi, H.S., Shim, J.S., Kim, J.-A., Kang, S.W., Kwon, H.J. (2007). Discovery of gliotoxin as a new small molecule targeting thioredoxin redox system. *Biochemical and Biophysical Research Communications*, **359**: 523–528.

Dayton, J.S., Means, A.R. (1996). Ca(2+)/calmodulin-dependent kinase is essential for both growth and nuclear division in *Aspergillus nidulans*. *Molecular Biology of the Cell*, **7**: 1511–1519.

Dees, J., Connell, J., Stacy, A., Turner, K., Whiteley, M. (2014). Mechanisms of Synergy in Polymicrobial Infections. *Journal of microbiology (Seoul, Korea)*, **52**: 188–99.

Delfino, E., Giacobbe, D.R., Del Bono, V., Coppo, E., Marchese, A., Manno, G., Morelli, P., Minicucci, L., Viscoli, C. (2015). First Report of Chronic Pulmonary Infection by KPC-3-Producing and Colistin-Resistant *Klebsiella pneumoniae* Sequence Type 258 (ST258) in an Adult Patient with Cystic Fibrosis. *Journal of Clinical Microbiology*, **53**: 1442–1444.

Denoncin, K., Collet, J.-F. (2013). Disulfide Bond Formation in the Bacterial Periplasm: Major Achievements and Challenges Ahead. *Antioxidants & Redox Signaling*, **19**: 63–71.

Fodah, R.A., Scott, J.B., Tam, H.-H., Yan, P., Pfeffer, T.L., Bundschuh, R., Warawa, J.M. (2014). Correlation of *Klebsiella pneumoniae* Comparative Genetic Analyses with Virulence Profiles in a Murine Respiratory Disease Model. *PLOS ONE*, **9**: e107394.

Gaddy, J.A., Tomaras, A.P., Actis, L.A. (2009). The *Acinetobacter baumannii* 19606 OmpA protein plays a role in biofilm formation on abiotic surfaces and in the interaction of this pathogen with eukaryotic cells. *Infection and Immunity*, **77**: 3150–3160.

Gastebois, A., Fontaine, T., Latgé, J.-P., Mouyna, I. (2010). β (1-3)Glucanosyltransferase Gel4p Is Essential for *Aspergillus fumigatus*. *Eukaryotic Cell*, **9**: 1294–1298.

Jones, C.H., Bolken, T.C., Jones, K.F., Zeller, G.O., Hruby, D.E. (2001). Conserved DegP protease in gram-positive bacteria is essential for thermal and oxidative tolerance and full virulence in *Streptococcus pyogenes*. *Infection and Immunity*, **69**: 5538–5545.

Keller, N., Bok, J., Chung, D., Perrin, R.M., Keats Shwab, E. (2006). LaeA, a global regulator of *Aspergillus* toxins. *Medical Mycology*, **44**: S83–S85.

Keown, K., Reid, A., Moore, J.E., Taggart, C.C., Downey, D.G. (2020). Coinfection with *Pseudomonas aeruginosa* and *Aspergillus fumigatus* in cystic fibrosis. *European Respiratory Review*, **29**: 200011.

Kradin, R.L., Mark, E.J. (2008). The pathology of pulmonary disorders due to *Aspergillus* spp. *Archives of Pathology & Laboratory Medicine*, **132**: 606–614.

Lattanzi, C., Messina, G., Fainardi, V., Tripodi, M.C., Pisi, G., Esposito, S. (2020). Allergic Bronchopulmonary Aspergillosis in Children with Cystic Fibrosis: An Update on the Newest Diagnostic Tools and Therapeutic Approaches. *Pathogens*, **9**: 716.

Lau, C.K.Y., Krewulak, K.D., Vogel, H.J. (2016). Bacterial ferrous iron transport: the Feo system. *FEMS microbiology reviews*, **40**: 273–298.

Lee, M.J., Geller, A.M., Bamford, N.C., Liu, H., Gravelat, F.N., Snarr, B.D., Le Mauff, F., Chabot, J., Ralph, B., Ostapska, H., Lehoux, M., Cerone, R.P., Baptista, S.D., Vinogradov, E., Stajich, J.E., Filler, S.G., Howell, P.L., Sheppard, D.C. (2016). Deacetylation of Fungal Exopolysaccharide Mediates Adhesion and Biofilm Formation. *mBio*, **7**: e00252-16.

Leitao Filho, F.S., Alotaibi, N.M., Ngan, D., Tam, S., Yang, J., Hollander, Z., Chen, V., FitzGerald, J.M., Nislow, C., Leung, J.M., Man, S.F.P., Sin, D.D. (2019). Sputum Microbiome Is Associated with 1-Year Mortality after Chronic Obstructive Pulmonary Disease Hospitalizations. *American Journal of Respiratory and Critical Care Medicine*, **199**: 1205–1213.

Lin, H.-C., Chooi, Y.-H., Dhingra, S., Xu, W., Calvo, A.M., Tang, Y. (2013). The fumagillin biosynthetic gene cluster in *Aspergillus fumigatus* encodes a cryptic terpene cyclase involved in the formation of β-trans-bergamotene. *Journal of the American Chemical Society*, **135**: 4616–4619.

Line, L., Alhede, M., Kolpen, M., Kühl, M., Ciofu, O., Bjarnsholt, T., Moser, C., Toyofuku, M., Nomura, N., Høiby, N., Jensen, P.Ø. (2014). Physiological levels of nitrate support anoxic growth by denitrification of *Pseudomonas aeruginosa* at growth rates reported in cystic fibrosis lungs and sputum. *Frontiers in Microbiology*, **5**.

LiPuma, J.J. (2010). The Changing Microbial Epidemiology in Cystic Fibrosis. *Clinical Microbiology Reviews*, **23**: 299–323.

Lu, Z., Huang, W., Wang, L., Xu, N., Ding, Q., Cao, C. (2018). Exhaled nitric oxide in patients with chronic obstructive pulmonary disease: a systematic review and meta-analysis. *International Journal of Chronic Obstructive Pulmonary Disease*, **13**: 2695–2705.

Margalit, A., Carolan, J.C., Sheehan, D., Kavanagh, K. (2020). The *Aspergillus fumigatus* Secretome Alters the Proteome of *Pseudomonas aeruginosa* to Stimulate Bacterial Growth: Implications for Co-infection. *Molecular & cellular proteomics: MCP*, **19**: 1346–1359.

Margalit, A., Sheehan, D., Carolan, J.C., Kavanagh, K. (2022). Exposure to the *Pseudomonas aeruginosa* secretome alters the proteome and secondary metabolite production of *Aspergillus fumigatus*. *Microbiology (Reading, England)*, **168**: 001164.

Navon-Venezia, S., Kondratyeva, K., Carattoli, A. (2017). *Klebsiella pneumoniae*: a major worldwide source and shuttle for antibiotic resistance. *FEMS Microbiology Reviews*, **41**: 252–275.

Neupane, D.P., Kumar, S., Yukl, E.T. (2019). Two ABC Transporters and a Periplasmic Metallochaperone Participate in Zinc Acquisition in *Paracoccus denitrificans*. *Biochemistry*, **58**: 126–136.

Nogueira, M.F., Pereira, L., Jenull, S., Kuchler, K., Lion, T. (2019). *Klebsiella pneumoniae* prevents spore germination and hyphal development of *Aspergillus* species. *Scientific Reports*, **9**: 218.

O'Dwyer, D.N., Dickson, R.P., Moore, B.B. (2016). The Lung Microbiome, Immunity, and the Pathogenesis of Chronic Lung Disease. *The Journal of Immunology*, **196**: 4839–4847.

Perez-Riverol, Y., Bai, J., Bandla, C., García-Seisdedos, D., Hewapathirana, S., Kamatchinathan, S., Kundu, D.J., Prakash, A., Frericks-Zipper, A., Eisenacher, M., Walzer, M., Wang, S., Brazma, A., Vizcaíno, J.A. (2021). The PRIDE database

resources in 2022: a hub for mass spectrometry-based proteomics evidences. *Nucleic Acids Research*, **50**: D543–D552.

Reeves, E.P., Murphy, T., Daly, P., Kavanagh, K. (2004). Amphotericin B enhances the synthesis and release of the immunosuppressive agent gliotoxin from the pulmonary pathogen *Aspergillus fumigatus*. *Journal of Medical Microbiology*, **53**: 719–725.

Sabotić, J., Kos, J. (2012). Microbial and fungal protease inhibitors--current and potential applications. *Applied Microbiology and Biotechnology*, **93**: 1351–1375.

Schweer, K.E., Bangard, C., Hekmat, K., Cornely, O.A. (2014). Chronic pulmonary aspergillosis. *Mycoses*, **57**: 257–270.

Traynor, A.M., Owens, R.A., Coughlin, C.M., Holton, M.C., Jones, G.W., Calera, J.A., Doyle, S. (2021). At the metal-metabolite interface in *Aspergillus fumigatus*: towards untangling the intersecting roles of zinc and gliotoxin. *Microbiology (Reading, England)*, **167**: 001106.

Upadhyay, S.K., Gautam, P., Pandit, H., Singh, Y., Basir, S.F., Madan, T. (2012). Identification of fibrinogen-binding proteins of *Aspergillus fumigatus* using proteomic approach. *Mycopathologia*, **173**: 73–82.

Vicentefranqueira, R., Amich, J., Marín, L., Sánchez, C.I., Leal, F., Calera, J.A. (2018). The Transcription Factor ZafA Regulates the Homeostatic and Adaptive Response to Zinc Starvation in *Aspergillus fumigatus*. *Genes*, **9**: 318.

Vieira, A.T., Rocha, V.M., Tavares, L., Garcia, C.C., Teixeira, M.M., Oliveira, S.C., Cassali, G.D., Gamba, C., Martins, F.S., Nicoli, J.R. (2016). Control of *Klebsiella pneumoniae* pulmonary infection and immunomodulation by oral treatment with the commensal probiotic *Bifidobacterium longum* 51A. *Microbes and Infection*, **18**: 180–189.

Vorapreeda, T., Khongto, B., Thammarongtham, C., Srisuk, T., Laoteng, K. (2021). Metabolic Regulation of Sugar Assimilation for Lipid Production in *Aspergillus oryzae* BCC7051 through Comparative Transcriptome Perspective. *Biology*, **10**: 885.

Wasylnka, J.A., Moore, M.M. (2000). Adhesion of *Aspergillus* Species to Extracellular Matrix Proteins: Evidence for Involvement of Negatively Charged Carbohydrates on the Conidial Surface. *Infection and Immunity*, **68**: 3377–3384.

Webb, B.J., Ferraro, J.P., Rea, S., Kaufusi, S., Goodman, B.E., Spalding, J. (2018). Epidemiology and Clinical Features of Invasive Fungal Infection in a US Health Care Network. *Open Forum Infectious Diseases*, **5**: ofy187.

Zhang, S., Cheng, Y., Ma, J., Wang, Y., Chang, Z., Fu, X. (2019). DegP degrades a wide range of substrate proteins in *Escherichia coli* under stress conditions. *The Biochemical Journal*, **476**: 3549–3564.

Zhang, W., Zhou, H., Jiang, Y., He, J., Yao, Y., Wang, J., Liu, X., Leptihn, S., Hua, X., Yu, Y. (2022). *Acinetobacter baumannii* Outer Membrane Protein A Induces Pulmonary Epithelial Barrier Dysfunction and Bacterial Translocation Through The TLR2/IQGAP1 Axis. *Frontiers in Immunology*, **13**: 927955.

Acknowledgements

Aaron Curtis is the recipient of an Irish Research Council postgraduate studentship GOIPG/2021/860.

Q-exactive mass spectrometer was funded under the SFI Research Infrastructure Call 2012; Grant Number: 12/RI/2346 (3).

Chapter 5

Proteomic characterisation of *Aspergillus fumigatus* – host interactions using the *ex-vivo* pig lung (EVPL) model

Aaron Curtis, Freya Harrison and Kevin Kavanagh

¹Department of Biology, Maynooth University, Maynooth, Co. Kildare,
Ireland

2. School of Life Sciences, University of Warwick, Coventry, UK

Published as:

Curtis, A., Harrison, F., Kavanagh, K. (2025). Proteomic characterization of *Aspergillus fumigatus* – host interactions using the *ex-vivo* pig lung (EVPL) model. *Virulence*, **16**: 2530675.

Author Contributions

Aaron Curtis: Experimental, data analysis, and manuscript preparation. **Freya Harrison:** Experimental design and manuscript review. **Kevin Kavanagh:** Experimental design, manuscript preparation and submission. All authors have read and approved the manuscript.

Abstract

Aspergillus fumigatus is an opportunistic fungal pathogen of the human airway that can cause a variety of chronic infections, typically in the context of pre-existing lung damage. The interaction of *A. fumigatus* with *ex-vivo* pig lung (EVPL) samples was characterized at the proteomic level to provide insights into how the fungus may interact with pulmonary tissue *in vivo*. This model has many advantages, because pigs share 90% immunological homology with humans and display many anatomical similarities. EVPL also retains resident immune cells, has richer cellular complexity compared to *in-vitro* models, and has a microbiome. Label-free quantitative proteomic analysis identified the metabolism and development of *A. fumigatus* on the EVPL alveolar sections; at 48 h, there was an increased abundance of proteins associated with carbon metabolism (e.g., malate dehydrogenase (+ 8.2 fold increase)), and amino acid metabolism and biosynthesis (e.g., 5-methyltetrahydropteroylglutamate--homocysteine S-methyltransferase, (+5.04 fold)) at 72 h. Porcine tissue remained responsive to the pathogen with proteins that increased in abundance associated with innate immune recruitment (e.g., protein S100-A8 (+28.5 fold) and protein S100-A9 (calgranulin-B) (+7.25 fold) at 24 h, while proteins associated with neutrophil degranulation (e.g., elastase, neutrophil (-2.74 fold)) decreased in abundance. At 96 h, the infected tissue demonstrated enhanced abundance of fibrotic markers (e.g., fibrillin 1, collagen type IV alpha 1 chain, and alpha 2 chain, increased by +16.44, +15.42 and +11.95 fold respectively). These results validate the use of this model for studying pathogen-host interactions and highlight how *A. fumigatus* interacts with pulmonary tissue during colonization.

5.1 Introduction

The filamentous fungus *Aspergillus fumigatus* is an environmental saprophyte and opportunistic pathogen in the human airway (van de Veerdonk *et al.*, 2025). Many infections caused by *A. fumigatus* are chronic, with chronic pulmonary aspergillosis affecting approximately 1.8 million patients annually, with an 18.5% mortality rate. Fungal asthma, which has been partially attributed to *Aspergillus* exposure, affects an estimated 11.5 million people, resulting in 46,000 deaths annually (Denning, 2024). A common underlying factor in many chronic infections is pre-existing lung damage, inflammation and cavitation caused by Chronic obstructive pulmonary disease (COPD), pulmonary tuberculosis, cystic fibrosis, bronchiectasis, thoracic radiotherapy, and allergic bronchopulmonary aspergillosis (Janssens *et al.*, 2024). The initial attachment and colonization of the lung by fungi is facilitated by interactions with the components of the host extracellular matrix and basal lamina (Gago *et al.*, 2019). Various conditions, including cystic fibrosis (CF) and asthma, result in the deposition of collagen and fibronectin, which can serve as substrates for fungal conidia adhesion (Lambrecht and Hammad, 2012; Sheppard, 2011). The complex interplay between *A. fumigatus* and its host has been partially elucidated through clinical studies and the utilization of diverse *in vitro* and *in vivo* model systems (Dagenais and Keller, 2009). Despite this, these model systems frequently fail to fully demonstrate the intricacies of human airway infections and, as a result, often fail to achieve the clinical phenotypes observed in the clinic (Cornforth *et al.*, 2020; Roberts *et al.*, 2015). Murine models have been the focus of the majority of aspergillosis *in vivo* studies because of the observed similarities in physiology and pathology in addition to genomic similarities (Resendiz-Sharpe *et al.*, 2022) however, they demonstrate considerable heterogeneity in their susceptibility to infection (Desoubeaux and Cray, 2018). In addition, despite the fact that rodents and human lungs contain many of the same cell types, the anatomy of the lung varies. Human lungs contain basal cells throughout the trachea and bronchi, whereas murine basal cells are only found in the trachea. There is also no evidence that human lungs possess a bronchioalveolar stem cells population as the majority of cells in the human proximal airway are multi-ciliated cells, whereas club cells are more abundant in rodents (Miller and Spence, 2017). Goblet cells are prevalent in the proximal human airway, but they primarily appear in mice following injury (Pardo-Saganta *et al.*, 2013). The chemical composition of murine lung tissue and airway surface liquid is also distinct from that of human airways (Walsh *et al.*, 2024).

The human lung metabolome was distinguishable from the murine metabolome in terms of trimethylamine *N*-oxide, betaine, carnitine, and glycerophosphocholine, which are present in mice but not in the human lung. In addition, fatty acid concentrations are significantly higher in rodent lungs than in human lungs. Acetate, asparagine, glutamate, lactate, lysine, myo-inositol, syllo-inositol, and valine concentrations were considerably lower in murine lungs than in human lungs. The metabolome of pig lungs demonstrated a similar composition to that of humans, with the main difference being the concentration of some components (Benahmed *et al.*, 2014). This difference may contribute to the failure of murine models to replicate pivotal aspects of human diseases and infections such as aberrant abscess formation which occurs in murine lungs during *Staphylococcus aureus* infection (Cigana *et al.*, 2018), but is rarely observed in human CF patients (Patradoon-Ho and Fitzgerald, 2007). Clinically relevant lumen colonization with preferential localization as multicellular aggregates in mucus was observed in bronchiolar pig lung sections, which better recapitulates what is observed in human biopsies (Sweeney *et al.*, 2021).

Many alternative model systems have been employed to study fungal pathogenesis, including insect mini models such as *Galleria mellonella* larvae (Champion *et al.*, 2016), cell culture (Perez-Nadales *et al.*, 2014), and organoid models (Fusco-Almeida *et al.*, 2023). *G. mellonella* is the most utilized insect model for fungal infection studies, and larvae are easy to inoculate and exhibit a dynamic response to pathogens, comparable to the innate immune response in humans (Gallorini *et al.*, 2024). In addition, *G. mellonella* larvae infected with fungal pathogens show structures characteristic of human infection, including granuloma development during *A. fumigatus* infection (Sheehan *et al.*, 2018) and grain formation during *Madurella mycetomatis* infection (Sheehan *et al.*, 2020). The *Galleria* infection model has demonstrated excellent correlation with experiments that assessed the virulence of *Candida albicans* and *Pseudomonas aeruginosa* in mice (Brennan *et al.*, 2002; Miyata *et al.*, 2003). The major limitation of the use of *G. mellonella* larvae is the lack of an adaptive immune response and organs, such as the lungs, which limits the model to the study of invasive and bloodstream infections (Curtis *et al.*, 2022).

Complex tissue models and organoids show a considerable increase in utility compared with 2D cell culture studies (Hoang *et al.*, 2022; Dichtl *et al.*, 2024). Although the complexity of organoids has increased, they are unable to accurately

reproduce the pathological characteristics of the human lung, including angioinvasion. The human lung is composed of over 40 different cell types (Varghese *et al.*, 2022), and current hPSC-derived lung organoids remain incomplete because they lack many lung components, such as vasculature and complex immune cell diversity (Du *et al.*, 2023). In addition to these limitations organoid models require specialist tissue culture facilities and techniques and can be expensive; therefore, they are a relatively low throughput approach for infection studies (Aguilar *et al.*, 2021). Lung damage is a common precursor to many forms of aspergillosis; as many three-dimensional organoids are derived from human pluripotent stem cells they tend to resemble the foetal lung, they may not be suitable to mimic these conditions (Du *et al.*, 2023).

Pig lung models have been developed in an attempt to overcome many of these limitations owing to their immunological and physiological similarities with humans, and the microbiome of healthy pig lungs shows a similar phylum distribution to that found in human lungs (Beck *et al.*, 2012; Huang *et al.*, 2018). The *ex-vivo* lung perfusion model (EVLP) demonstrated pathogen- and virulence factor-specific responses to *Klebsiella pneumoniae* infection in a whole lung system with whole blood perfusion and ventilation over 4 hours postmortem (Dumigan *et al.*, 2019). Despite the successful implementation of this model, it requires a large amount of space and specialized equipment and skills. The *ex-vivo* pig lung model (EVPL) offers a high-throughput, low-cost, and ethical model that closely mimics the lung environment (Harrison *et al.*, 2014). Lungs can be obtained from pigs slaughtered for commercial meat production from butchers or abattoirs and since little or no lung tissue is used in food production, lungs are classified as a waste product whose use does not raise ethical questions (Harrison *et al.*, 2014). This method was first developed by Williams & Gallagher, who collected lungs from commercial abattoirs and used tissue sections to study *Mycoplasma* infection (Williams and Gallagher, 1978; Williams and Gallagher, 1978). This model was then optimized to mimic CF airways and used to study bacterial pathogenicity (Harrison and Diggle, 2016) and antibiotic tolerance (Sweeney *et al.*, 2021; Harrington *et al.*, 2020). This system involves the excision of multiple sections of the bronchiolar or alveolar tissue from the lungs of a single donor. These can be inoculated with pathogens and various endpoints can be examined. This model has demonstrated strain-specific virulence differences, including quorum sensing-deficient mutants of *Pseudomonas aeruginosa* demonstrating reduced damage to alveolar tissue

(Harrison *et al.*, 2014). It has also been demonstrated that the EVPL model shows *in vivo*-like aspects of *P. aeruginosa* gene expression and that the pathogen forms a biofilm using known *in vivo* pathways required during *in vivo* infection, resulting in the formation of clinically realistic structures not seen in other *in vitro* studies (Harrington *et al.*, 2020; Harrington, Allen, *et al.*, 2022).

Once inhaled, *Aspergillus* conidia that are not cleared by mucociliary elevators encounter epithelial cells or alveolar macrophages (Richardson *et al.*, 2019). These conidia are often deposited in the bronchioles and alveolar spaces because of the small size of the fungal conidia (2–3 µm), which is ideal for deep infiltration into alveolar spaces (Dagenais and Keller, 2009). We combined alveolar sections of pig lung tissue with standard tissue culture medium to assess the tractability of this model for working with fungi and to mimic human tissue in the absence of any underlying conditions that radically alters lung chemistry (Ersoy *et al.*, 2017). We examined the development of *A. fumigatus* in this physiologically sustainable and ethical model to gain insight into how the host and the pathogen respond to each other during the early stages of fungal infection.

5.2 Materials and Methods

5.2.1 *Aspergillus fumigatus* culture conditions and conidial preparation

Aspergillus fumigatus ATCC 26933 was cultured for 72 h at 37 °C on malt extract agar (MEA) (Oxoid, Basingstoke, UK) following point inoculation. The conidia were harvested by washing with phosphate-buffered saline supplemented with 0.1% (v/v) Tween-20 (PBS-T), and the suspension was washed three times with PBS. Conidia were enumerated using a haemocytometer and diluted to a final concentration of 1×10^7 conidia/ml

5.2.2 Preparation of *ex-vivo* pig lung sections

Alveolar tissue sections were prepared as described (Harrison *et al.*, 2014), with some modifications. Whole lungs from four individual pigs with attached tracheae were collected from a local abattoir within an hour of slaughter and were transported on ice to Maynooth University. The pleural surface of the caudal lobe was sterilized by briefly touching it with a hot palette knife, and ~5 mm-deep strips of alveolar tissue were cut from the sterilized surface using a mounted razor blade. These were washed in a 50/50 mixture of RPMI 1640 (Gibco) and Dulbecco's modified Eagle medium

[DMEM] (Gibco) supplemented with 10 µg/ml amphotericin B to remove any environmental fungi. The strips were cut to 125 mm³ explants and washed twice in a 50/50 mix of RPMI 1640 and Dulbecco's modified Eagle medium (DMEM) supplemented with 50 µg/mL ampicillin to reduce bacterial load (components of the pig lung microbiome or environmental contaminants). The tissue sections were washed in the RPMI/DMEM mixture and UV sterilized for 5 min before being placed on a pad of 400 µL RPMI/DMEM solidified with 0.8% agarose in a 24 well tissue culture plate. The sections were inoculated using a 25G needle dipped into the prepared *A. fumigatus* conidia suspension (standardised to 1 x 10⁷/ml) and used to inoculate the surface of the section to deposit fungal spores. The sections were suspended in 500µL RPMI/DMEM. The sections were covered with a breathable membrane (Breathe-easy sealing membrane, Diversified Biotech, USA) before incubation in a 6% CO₂ incubator at 37 °C to match the physiological carbon dioxide levels observed in the alveoli (Abolhassani *et al.*, 2009). Sterilized solidified malt extract agar (MEA, Oxoid) was aseptically cut into the same dimensions (5 × 5 × 5 mm) as EVPL tissue and used as a control for fungal growth.

5.2.3 Quantification of fungal burden

Infected tissue sections were removed from the 24 well plate with sterilized forceps at 24-hour intervals and washed in sterile PBS prior to transfer into 2 ml Eppendorf tubes with 1 ml of lysis buffer and a 3 mm chrome stainless steel ball bearing. The tissue was homogenised using a tissue lyser (TissueLyser II, Qiagen, Germany) at 30.0 frequency 1/s for 40 seconds. Lysate (100 µL) was diluted and plated onto MEA plates in triplicate and incubated at 37 °C overnight. The colony-forming units (CFU) were enumerated. The average number of colonies resulting from each treatment was determined and a 2-way ANOVA analysis was performed. Figures were generated using Prism v8.01. Images of infected tissue were viewed at 40x magnification using a brightfield microscope (Olympus CH20).

5.2.4 Proteomic extraction from infected tissue sections

Infected and control EVPL sections were removed from 24 well plate and washed with PBS. The sections were transferred to 2 ml Eppendorf tubes with 1 ml of lysis buffer (8 M urea, 2 M thiourea, and 0.1 M Tris-HCl (pH 8.0) dissolved in HPLC-grade ddH₂O), supplemented with protease inhibitors (aprotinin, leupeptin, pepstatin

A (10 μ g/mL), and phenylmethylsulfonyl fluoride (PMSF) (1 mM/mL)). Tissue sections were homogenized as previously described. The lysates were sonicated (Bandelin Senopuls) three times for 10 s at 50% power. The cell lysate was centrifuged (Eppendorf Centrifuge 5418) for 8 min at 14,500 \times g to pellet cellular debris. Lysate (200 μ L) was precipitated with acetone for 18 hours at -20 °C. Samples were subjected to centrifugation at 14,500 \times g for 10 min to pellet proteins, acetone was removed, and the pellet was resuspended in 50 μ L sample resuspension buffer (8 M urea, 2 M thiourea, and 0.1 M Tris-HCl (pH 8.0) dissolved in HPLC-grade ddH₂O), of which 40 μ L was digested. A 2 μ L aliquot was removed from each sample prior to digestion for quantification using the Qubit quantification system (Invitrogen, Waltham, MA, USA). Ammonium bicarbonate (250 μ L, 50 mM) was added to 40 μ L, which was subjected to reduction *via* the addition of 2 μ L of 0.5 M dithiothreitol and incubated at 56 °C for 20 min, followed by alkylation with 0.55 M iodoacetamide at room temperature in the dark for 15 min. Proteins were digested by adding 2 μ L of sequence- grade trypsin (Promega) (0.5 μ g/ μ L), supplemented with 2 μ L of Protease Max Surfactant Trypsin Enhancer (Promega) (1% w/v), and incubated at 37 °C for 18 h. Digestion was quenched by the addition of 2 μ L of trifluoroacetic acid (TFA) and incubated at room temperature for 5 min. The samples were centrifuged at 14,500 \times g for 10 min prior to clean-up using C18 spin columns (Pierce). The eluted peptides were dried using a SpeedyVac concentrator (Thermo Scientific (Waltham, MA, USA) Savant DNA120) and resuspended in 2% (v/v) acetonitrile and 0.1% (v/v) formic acid to yield a final concentration of 375ng/ μ L aided by sonication in a water bath for 5 min. The samples were centrifuged to pellet debris at 14,500 \times g for 5 min, and 2 μ L of each sample was loaded onto the mass spectrometer.

5.2.5 Mass spectrometry

Purified peptide extracts (2 μ L containing 750 ng protein) were loaded onto a Dionex UltiMate 3000 RSLC nano system equipped with an Easy-Spray C18 HPLC column (Thermoscientific) connected to a Q Exactive Plus Hybrid Quadrupole-orbitrap mass spectrometer (Thermo Fisher Scientific, Waltham, MA, USA) and eluted at a flow rate of 0.3 μ L per minute using a reverse phase 133 minute gradient. A scan range of 200-1600 M/Z with a resolution of 70,000, was used. The top 15 ions were selected from each MS scan with an isolation window of 2 M/Z for fragmentation and an MS/MS scan in the range of 200-2000 M/Z with a resolution of 17,500. Raw

MS/MS data files were processed using the Andromeda search engine in MaxQuant software v.1.6.3.4 110 using a *Neosartorya fumigata* reference proteome obtained from a UniProt-SWISS-PROT (The UniProt Consortium, 2025) database to identify proteins (9647 entries, downloaded July 2022) or the *Sus scrofa* reference proteome (46,174 entries, downloaded December 2023) respectively.

5.2.6 Data analysis

Proteomic data analysis was performed as described (Curtis *et al.*, 2023), with some modifications. Perseus v.1.6.15.0, was used for data analysis, processing, and visualization. Normalized LFQ intensity values were used to quantitatively measure protein abundance. The generated data matrix was filtered to remove contaminants. LFQ intensity values were \log_2 -transformed, and each sample was assigned to its corresponding group matching the time point at which they were collected. Proteins that were not found in all replicates in at least one group were omitted from further analysis. A data-imputation step was conducted to replace missing values with values that simulate signals of low-abundance proteins chosen randomly from a distribution specified by a downshift of 1.8 times the mean standard deviation of all measured values and a width of 0.3 times this standard deviation. Principal component analysis (PCA) was performed using normalized intensity values. The identified proteins were then defined using a Perseus annotation file to assign extract terms for biological process, molecular function, and Kyoto Encyclopaedia of Genes and Genomes (KEGG) names. To visualize the differences between two samples, pairwise Student's *t*-tests were performed using a cut-off of $P < 0.05$ on the post-imputation dataset. Volcano plots were generated by plotting the \log_2 fold change on the x-axis against the log *p*-values on the y-axis for each pairwise comparison. Statistically significant and differentially abundant (SSDA) proteins (ANOVA, $P < 0.05$) with a relative fold change greater than ± 1.5 were retained for analysis. SSDA proteins were z-score-normalized and then used for hierarchical clustering to produce a heat map. Identified SSDAs were then assessed using Uniprot codes generated by Perseus, and pathway analysis was performed using ShinyGO (Ge *et al.*, 2020) to gain insights into their roles within the cells. The mass spectrometry proteomics data were deposited in the ProteomeXchange Consortium *via* the PRIDE (Perez-Riverol *et al.*, 2021) partner repository with the dataset identifier PXD060389.

5.3 Results

5.3.1 Confirmation of *Aspergillus fumigatus* growth on EVPL tissue

MEA cubes ($n = 3$) and EVPL explants ($n = 3$) for each time point were inoculated with *A. fumigatus* conidia and incubated at 37 °C and 6% CO₂. Visual inspection of agar cubes revealed the growth of *A. fumigatus* at 24h and this increased until 96 h when conidiation was evident (Fig 5.1A). In contrast, there was a small amount of visible *A. fumigatus* growth on the EVPL explants at 24 h, but more extensive fungal growth was evident at 48 h. After 96 h, a large *A. fumigatus* colony was observed on the surface. Fungal growth was also assessed by quantifying the number of colony-forming units (CFU) per treatment (Fig 5.1B). The growth on the MEA cubes and EVPL explants was initially comparable, but there was a significantly ($P = 0.002$) lower fungal CFU at 72 h in the EVPL relative to the MEA cubes with 1.2×10^5 CFU on the MEA cube compared to 1.5×10^4 CFU detected in the EVPL section. The growth on the EVPL was comparable to that on the MEA cubes at 96 h, with approximately 1.4×10^5 CFU/section (Fig 5.1). *A. fumigatus* hyphae were visible in the infected tissue (Fig 5.1C).

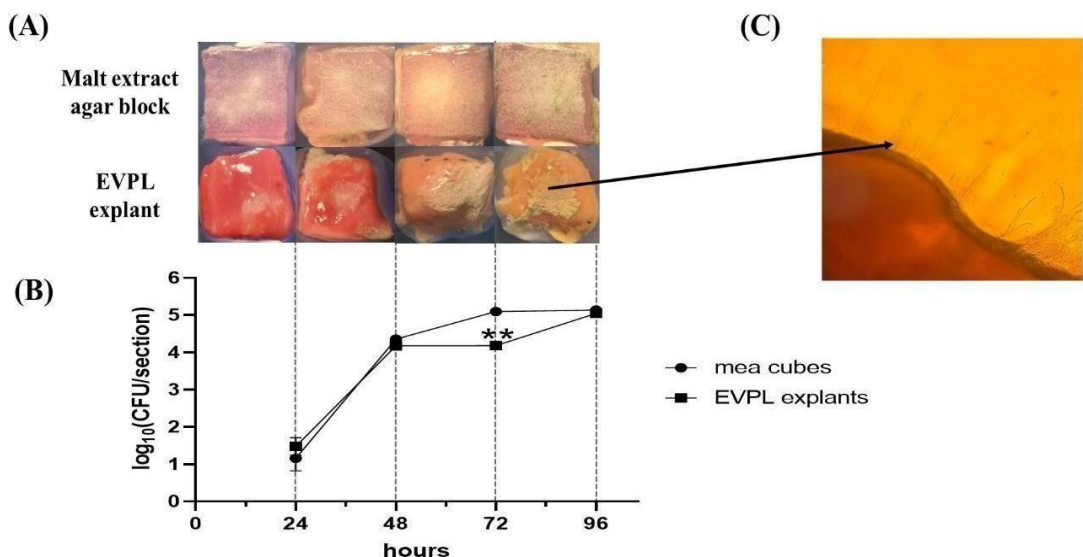


Figure 5.1: Phenotypic analysis and confirmation of fungal growth on agar and *ex-vivo* pig lung explants. (A) Representative image of sections at each 24 hour interval imaged via dissection microscope. (B) Graph of fungal burden calculated from agar and EVPL explants showing a significant decrease in CFU at 72 hours ($P=0.002$) calculated by two-way ANOVA. (C) Microscopy image of hyphal growth on an EVPL section at 40x magnification.

5.3.2 Proteomic analysis of alterations in *A. fumigatus* proteome during growth on EVPL tissue

Quantitative proteomic analysis was used to characterize the changes in the fungal proteome during colonization of EVPL explants. The fungal proteomes ($n = 3$) at each time point were characterized, and these were well separated, as seen in the PCA and heatmap (Fig 5.2 A and B). Changes in the relative abundance of fungal proteins were compared with those of the *A. fumigatus* proteome at 24h. At 48 h post-infection, 15 proteins were significantly increased in abundance and 17 were significantly decreased (Table S1). Many proteins that showed an increase in abundance were associated with carbon metabolism, including glyceraldehyde-3-phosphate dehydrogenase (+10.90 fold). Glyceraldehyde-3-phosphate dehydrogenase expression is associated with conidial germination, is expressed on the hyphal surface, and has been speculated to aid fungal adherence to host tissue (Shankar *et al.*, 2018). Phosphoglycerate kinase (+3.60 fold) is involved in carbon metabolism but is also part of the *Afpes1* NRPS cluster involved in fumigaclavine C biosynthesis (Owens *et al.*, 2014). There was also increased abundance of fungal allergens, such as large ribosomal subunit protein P2 (60S acidic ribosomal protein P2) (AfP2) (allergen Asp f 8) (+6.99 fold) and superoxide dismutase [Mn], mitochondrial (allergen Asp f 6) (+4.40 fold) which may be involved in inducing an immune response within the tissue (Liu *et al.*, 2023). Proteins decreased in abundance at 48 h, including malate synthase and dihydrolipoyl dehydrogenase (-3.47 and -3.86 fold, respectively), which are involved in alternative metabolic processes (Table S1). Gene enrichment analysis indicated that carbon metabolism was enhanced, and amino acid metabolism was decreased at this timepoint (Fig S5.1).

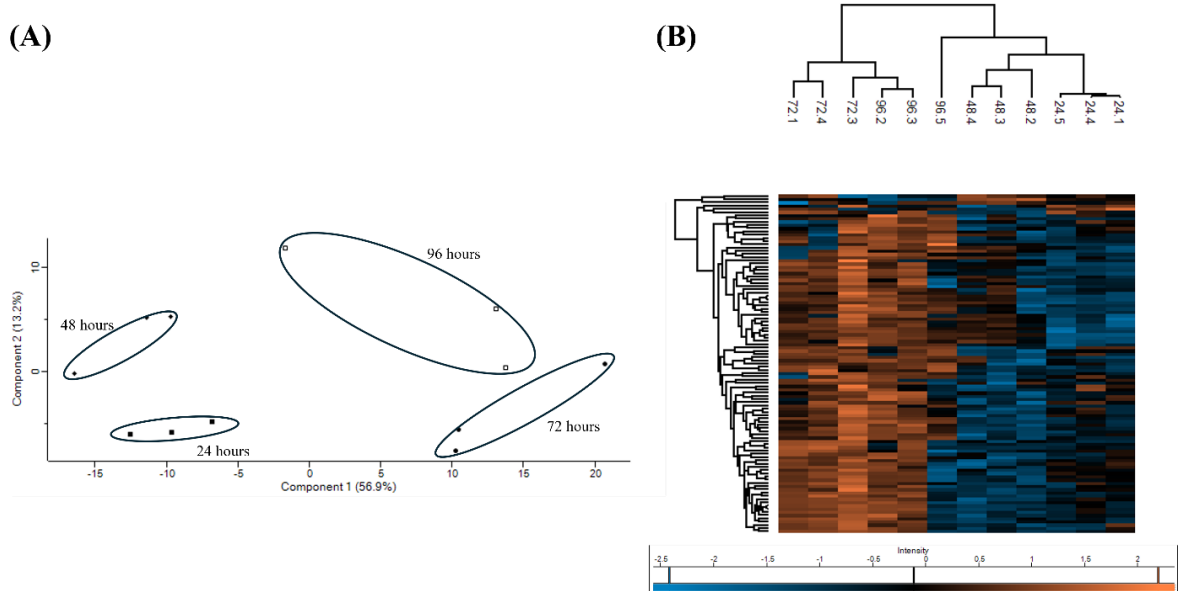


Figure 5.2:(A) Principal component analysis of *A. fumigatus* proteins at 24, 48, 72 and 96 hours demonstrating good separation in the proteome at each timepoint. (B) Heatmap generated through Two-way unsupervised hierarchical clustering of the median protein expression values of all statistically significant differentially abundant proteins.

At 72 h post-infection, 66 proteins were significantly increased in abundance relative to that at 24 h, and no proteins were significantly decreased (Table S2). Many proteins that increased in abundance were associated with amino acid biosynthesis and metabolic processes, including aconitase hydratase, mitochondria (+ 6.26 fold), 5-methyltetrahydropteroyltriglutamate--homocysteine S-methyltransferase (+5.04 fold), 4-aminobutyrate aminotransferase (+2.80 fold), and acetohydroxy-acid reductoisomerase (+1.97 fold), which have also been implicated in fungal iron homeostasis (Fazius *et al.*, 2012; Grynberg *et al.*, 2001; Long *et al.*, 2018). A significant increase in abundance was observed for the 14-3-3 family protein ArtA, putative (+35.63 fold). ArtA is a regulatory protein associated with the response to oxidative stress (Blachowicz *et al.*, 2019). There was also a significant increase in the abundance of large ribosomal subunit protein P1 (60S acidic ribosomal protein P1) (AfP1) (+19.17 fold) and large ribosomal subunit protein P2 (60S acidic ribosomal protein P2) (AfP2) (allergen Asp f 8) (+18.42 fold) indicating enhanced translation and protein biosynthesis (Table S2). Gene enrichment analysis indicated elevated biosynthesis and metabolism of amino acids at this time (Fig S5.2).

At 96 h post-infection, 44 proteins were significantly increased in abundance relative to that at 24 h, and two proteins were significantly decreased (Table S3).

Proteins increased in abundance, including asp-hemolysin (+6.49 fold), and dipeptidyl-peptidase 5 (+11.67 fold) at 72 hours and +9.61 fold at 96 h, and are known to be induced in murine infection (Wartenberg *et al.*, 2011; Guruceaga *et al.*, 2018). Thioredoxin reductase gliT, involved in self-protection during gliotoxin production and oxidative stress mitigation (Ries *et al.*, 2020) was increased (+5.97 fold). Short-chain dehydrogenase, which was previously shown to be induced by gliotoxin exposure (Doyle *et al.*, 2018), increased by +9.21 fold at 72 hours and +17.37 fold at 96 h. Woronin body major protein hexA, involved in physical stress meditation through septal pore formation and virulence (Beck *et al.*, 2013), increased in abundance at 72 (+11.73 fold) and 96 (+9.86 fold) hours, indicating the occurrence of host-induced damage. Proteins that decreased in abundance at 96 h were triosephosphate isomerase (-2.09 fold), involved in glucose metabolism, and phytanoyl-CoA dioxygenase family protein (-2.31 fold), and similar proteins are known to be involved in the production of fungal toxins, including verruculogen (Owens *et al.*, 2014), typically expressed during the early stages of infection. Gene enrichment analysis (Fig S5.3) highlighted the increased expression of proteins associated with ascorbate and aldarate metabolism, beta-alanine metabolism, fatty acid degradation, glycolysis/gluconeogenesis, tryptophan metabolism, and degradation of valine, leucine, and isoleucine, all of which have been demonstrated to be enhanced following *A. fumigatus* exposure to human dendritic cells (Srivastava *et al.*, 2019).

Some *A. fumigatus* proteins were detected at two or more sampling timepoints (Table 5.1). These proteins including the suspected allergen 60S ribosomal protein L12 (Saxena *et al.*, 2003), detected at 48 and 72 hours post infection. Other proteins were consistently increased in abundance at all three time points and included cyanovirin-N domain-containing protein, which increased +13.14-, +18.00 and +23.01 fold at 48, 72, and 96 h, respectively. This protein belongs to a family of highly conserved proteins that are known to bind strongly to mannose, potentially enhancing fungal attachment to the host (Koharudin *et al.*, 2008) and affecting the morphology of PBMCs (Huskens *et al.*, 2008). Mannose-dependent C type lectin interactions have been shown to be impeded by cyanovirin-N (Driessens *et al.*, 2012) and as such consistent expression of this protein could indicate its role in immune evasion by *A. fumigatus*.

Table 5.1: Statistically significantly and differentially abundant *Aspergillus fumigatus* proteins associated with virulence or involvement in eliciting an immunological response within the host detected at two or more timepoints relative to a 24-hour sample.

protein ID	Protein name	48 hours	72 hours	96 hours
Superoxide dismutase [Mn], mitochondrial (EC 1.15.1.1) (allergen Asp f 6)	Q92450	4.40	9.29	N/A
14-3-3 family protein ArtA, putative	Q4WI29	-2.14	35.63	N/A
60S ribosomal protein L12	Q4WK81	-3.15	3.15	N/A
Malate synthase (EC 2.3.3.9)	Q4WD53	-3.47	3.47	N/A
Phytanoyl-CoA dioxygenase family protein	Q4WZT3	-4.03	N/A	-2.31
Acyl CoA binding protein family	Q4X164	N/A	13.93	11.24
Woronin body major protein hexA	Q4WUL0	N/A	11.73	9.86
Dipeptidyl-peptidase 5 (EC 3.4.14.-) (Dipeptidyl-peptidase V) (DPP V) (DppV)	P0C959	N/A	11.67	9.61
Short chain dehydrogenase, putative (EC 1.-.-.-)	Q4WPB8	N/A	9.21	17.37
Thioredoxin	Q4WV97	N/A	3.21	5.26
Cyanovirin-N domain-containing protein	Q4WKJ1	13.14	18.00	23.01
Glyceraldehyde-3-phosphate dehydrogenase (EC 1.2.1.12)	Q4WE70	10.90	30.96	33.92
Malate dehydrogenase (EC 1.1.1.37)	Q4WE70	8.20	23.43	11.52
Large ribosomal subunit protein P2 (60S acidic ribosomal protein P2) (AfP2) (allergen Asp f 8)	Q9UUZ6	6.99	18.42	12.60
Enolase (EC 4.2.1.11) (2-phospho-D-glycerate hydro-lyase) (2-phosphoglycerate dehydratase) (allergen Asp f 22)	Q96X30	6.08	12.98	13.54
Methyltransferase psoC (EC 2.1.1.-) (Pseurotin biosynthesis protein C)	Q4WB00	5.63	6.80	6.77
Alanine transaminase (EC 2.6.1.2)	Q4WN34	3.81	8.60	4.92
G-protein complex beta subunit CpcB	Q4WQK8	3.73	6.12	4.40

The G-protein complex beta subunit CpcB was also detected at all time points (+3.73-, +6.12 and +4.40 fold, at 48, 72, and 96 h, respectively) and plays an essential role in cellular growth, spore germination, and conidiation (Cai *et al.*, 2015). Methyltransferase psoC increased +5.63-, +6.80 and +6.77 fold, respectively, and is involved in the synthesis of pseurotin A, which can suppress RankL-induced oxidative stress (Chen *et al.*, 2019). Enolase was increased by +6.08-, +12.98 and +13.54 fold, respectively, and is involved in glycolysis. It has been identified as a potential inhibitor of the human complement cascade by binding to Factor H, FHL-1, C4BP, and plasminogen (Dasari *et al.*, 2019).

5.3.3 Characterisation of proteomic alterations in EVPL tissue during *A. fumigatus* colonisation

The pig proteome ($n = 3$) at each time point during infection was characterized, and these were well separated, with clear differences between infected and uninfected tissue, as shown in the PCA and heatmap with some overlap observed at later time points (Fig 5.3 A and B). The early response to infection elicited many changes in the porcine proteome, indicating a dynamic response to *A. fumigatus* (Fig 5.4 A and B). At 24 h post-infection, 123 proteins were significantly increased in abundance in infected EVPL tissue, and 212 were decreased relative to uninfected tissue (Table S4). Protein S100-A8 and protein S100-A9 (calgranulin-B) were increased in abundance (+28.25 and +7.25 fold, respectively), and S100A8/A9 plays a critical role in modulating the proinflammatory response by stimulating leukocyte recruitment and inducing cytokine secretion (Wang *et al.*, 2018; Singh and Ali, 2022; Xia *et al.*, 2024). Costar family protein ABRACL was increased in abundance in the infected tissue (+18.58 fold) and is associated with immune cell infiltration (Liu *et al.*, 2022). Carbonic anhydrase 4 was also increased +10.09 fold and was expressed on IL-5- activated eosinophils, indicating that an allergic response could be elicited at this timepoint (Wen *et al.*, 2014). Tetraspanin was increased in abundance +5.49 fold in the infected tissue and is involved in forming functional interactions with prominent leukocyte receptors including MHC molecules (Lu *et al.*, 2020; van Spriel and Figdor, 2010). Gene enrichment analysis indicated enrichment in antigen processing and presentation, particularly through MHC class II, phagosome, and neutrophil extracellular trap formation, indicating that an active immune response was induced within the infected tissue (Strickland *et al.*, 2022; Thrikawala *et al.*, 2024) (Fig S5.4). Proteins decreased in abundance, including pulmonary surfactant-associated protein A1 isoform X2 (-115.77 fold) which is integral to prevent airway collapse and is known to bind to fungal carbohydrates, enhancing fungal phagocytosis (Carreto- Binaghi *et al.*, 2016). The levels of surfactant protein A are decreased in the lungs of patients with CF, Acute respiratory distress syndrome and further chronic lung diseases (Heinrich, 2011). This can be attributed to neutrophilic recruitment factors including cathepsins which can degrade pulmonary surfactant A (Rubio *et al.*, 2004). Dipeptidyl peptidase 1 (cathepsin C) and cathepsin S were increased 1.53 and 1.71 fold respectively at 24 hours post infection. Cathepsin C has been demonstrated to be involved in inflammation and pathogenesis in both acute and chronic disease (Aghdassi *et al.*, 2024).

Cathepsin S has been demonstrated to directly cleave surfactant protein A and has been implicated in lung injuries and tissue remodelling associated with CF (Lecaille *et al.*, 2013). Prophenin and tritrpticin precursor (C6) (- 26.95 fold), antibacterial protein (cathelicidin antimicrobial peptide preproprotein) (- 18.02 fold), lipocalin 2 (- 13.68 fold), proteinase 3 (-12.00 fold) and elastase, neutrophil expressed (- 2.74 fold) were decreased in abundance in the infected tissue and are involved in neutrophil activity and degranulation (Wessely-Szponder *et al.*, 2010; Liu *et al.*, 2021; Du *et al.*, 2021; Espinosa and Rivera, 2016; Stockley *et al.*, 2013). Gene enrichment analysis (Fig S5.4) also highlighted decreases in proteins associated with the citrate cycle and amino acid degradation indicating the infected tissue is less metabolically active which is similar to that observed in murine models of invasive pulmonary Aspergillosis (Kale *et al.*, 2017).

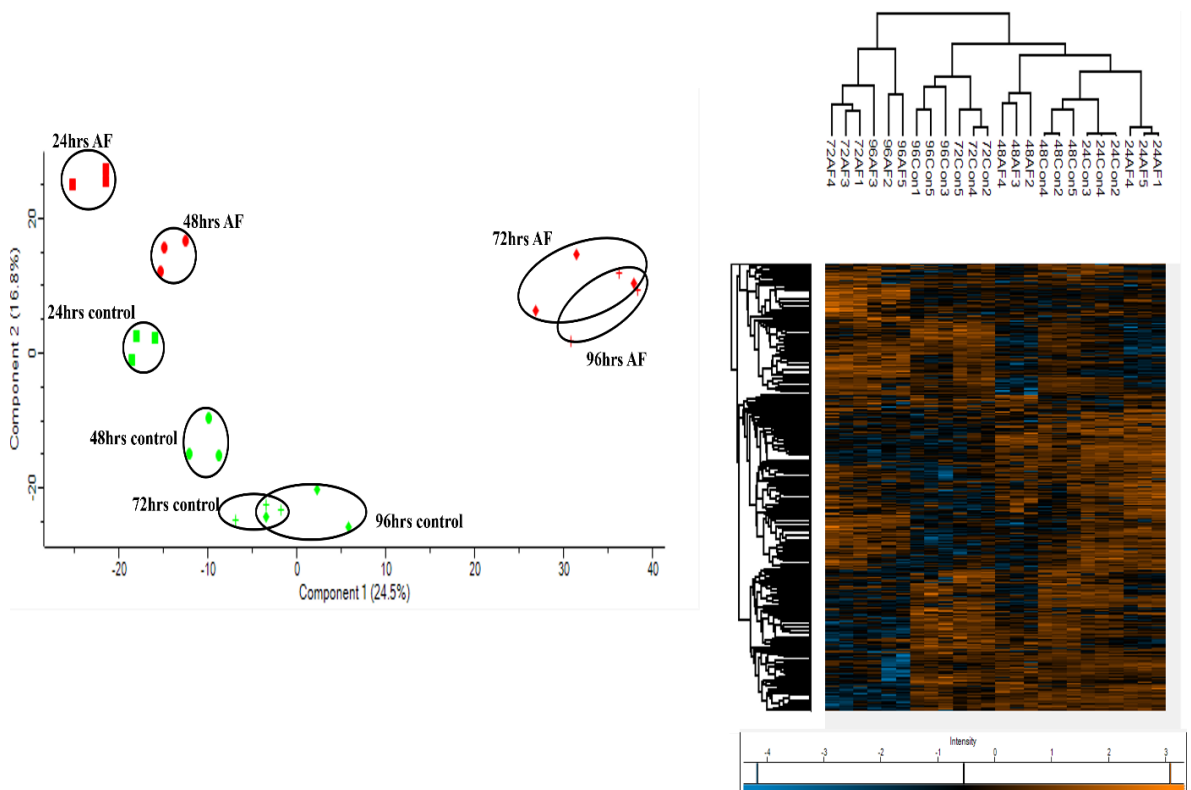


Figure 5.3:(A) Principal component analysis of *Sus scrofa* proteins at 24, 48,72 and 96 hours demonstrating good separation in the proteome at each timepoint (B) Heatmap generated through Two-way unsupervised hierarchical clustering of the median protein expression values of all statistically significant differentially abundant proteins.

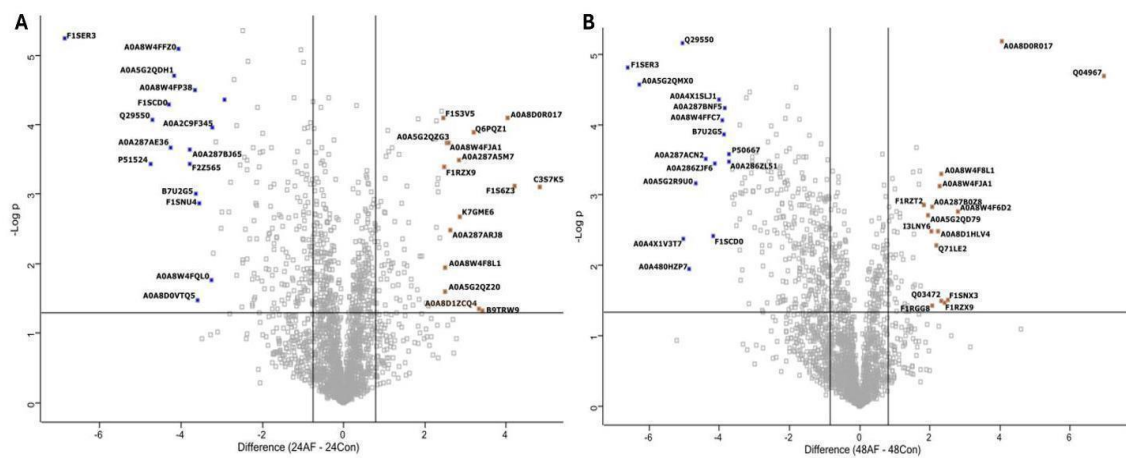


Figure 5.4: Volcano plots showing the distribution of statistically significant and differentially abundant (SSDA) proteins which have a $-\log$ (p-value) > 1.3 and difference $+/-0.58$. (A) *Sus scrofa* infected lung explants with *A. fumigatus* compared to uninfected lung explants at 24 hours and (B) *Sus scrofa* infected lung explants with *A. fumigatus* compared to uninfected lung explants at 48 hours.

At 48 h, 88 proteins were increased in abundance, and 351 proteins were decreased in abundance in the infected tissue (Table S5). Heat shock 70 kDa protein 6 was increased by +125.30 fold, and this protein is induced during stress and has been associated with the infiltration of immune cells (Llewellyn *et al.*, 2023; Zhou *et al.*, 2022). Importin subunits alpha, KPNA3 and KPNA4 were increased by +6.92 and +4.99 fold, respectively, and are essential for TNF-alpha-stimulated NF-kappaB p50/p65 heterodimer translocation into the nucleus (Fagerlund *et al.*, 2005). KPNA4 expression was also positively correlated with the infiltration of CD8+ T cells, B cells, dendritic cells, CD4+ T cells, neutrophils and macrophages (Xu *et al.*, 2021). Marginal zone B-and B1-cell-specific protein (MZB1) and Histone H3.3 also increased in abundance (+4.10 and +4.52 fold, respectively), and these proteins play a role in the humoral immune response and are involved in differentiation to plasma cells. Histone H3.3 is involved in maintaining B-cell and CD8+ T-cell function and prevents premature hematopoietic stem cell exhaustion and differentiation into granulocyte-macrophage progenitors (Guo *et al.*, 2022). The first markers of pulmonary fibrosis were detected at this timepoint, including indoleethylamine N-methyltransferase (+4.17 fold), associated with myofibroblast formation (Zabihi *et al.*, 2024; Schipke *et al.*, 2021), nestin (+4.17 fold), which is expressed in myofibroblasts and has a pro-fibrotic function by facilitating Rab11-dependent recycling of TGF- β receptor I (Wang *et al.*, 2022). TGF- β was significantly enhanced at 24 h post-infection (+2.70 fold).

Proteins decreased in abundance at 48 h, including histone H2A (-78.18 fold) which plays a role in double-strand break repair (Dickey *et al.*, 2009). FLII actin remodelling protein was also decreased -29.04 fold, and knockouts of this protein have been associated with increased numbers of myofibroblasts (Cameron *et al.*, 2016) (Table S5). There is also evidence of disruption of the epithelial tight junction with reduced abundance of junctional adhesion molecule A (-3.54 fold) and claudin 18 (-2.97 fold) both integral to epithelial integrity (Czubak-Prowizor *et al.*, 2022; Kotton, 2018). Complement factor B (C3/C5 convertase) and Complement C3 decreased in abundance (-2.58 and -2.04 fold, respectively), indicating that immune evasion induced by the fungus could be occurring (Dasari *et al.*, 2019). Other known complement evasion mechanisms observed in *A. fumigatus* include recruitment of the human plasma regulators factor H, FHL-1, C4BP, and plasminogen and pentraxin-3 and ficolin-2 (Dasari *et al.*, 2018), none of which were significantly altered in our analysis. The secretion of proteases alp1 and mep1 has also been shown to degrade or cleave complement factors (Shende *et al.*, 2018). These were also not detected in either the host or pathogen analysis presented. This implies enolase is a potent inhibitor of this cascade or other factors yet to be identified are involved in the evasion observed in this study. Gene enrichment analysis (Fig S5.5) demonstrated a response to fungal infection with enriched pathways, including leukocyte transendothelial migration and chemokine signalling pathways, while metabolism was decreased (i.e., 2-oxocarboxylic acid metabolism and propanoate metabolism). Elevated levels of propanoate and its byproduct methylmalonic acid can induce a pro-fibrotic phenotype in both epithelial cells and fibroblasts by activating the canonical transforming growth factor- β /Smad pathway (Xu *et al.*, 2024).

The later response to infection elicited many changes in the tissue proteome, supporting the impact *A. fumigatus* primarily associated with tissue remodelling and fibrosis (Fig 5.5 A and B) (Table S6). At 72 h post-infection, 346 proteins were increased in abundance and 356 were decreased in abundance. There is further evidence of tissue remodelling and fibrosis with transforming growth factor beta-1-induced transcript 1 protein increased +7.06 fold, indicating that TGF- β could drive fibrosis following fungal infection. Many components of the extracellular matrix associated with fibrosis were significantly increased in abundance, including fibrillin 1 (+151.93 fold), collagen type IV alpha 2 chain (+26.94), alpha 1 chain (+24.92),

alpha 4 chain (+21.14), and alpha 3 chain (+10.67) (Olivieri *et al.*, 2010). There is evidence of an immune response to fungal infection due to the increased abundance of proteins associated with MHC class II signalling, including SLA class II histocompatibility antigen DQ haplotype C alpha chain (+7.04 fold) (Techakriengkrai *et al.*, 2021). MHC class II, DM beta (major histocompatibility complex, class II, DM beta) (+2.83 fold), and ABC-type antigen peptide transporter (TAP2) (+2.71 fold) are involved in antigen processing and presentation and T cell activation (Mantel *et al.*, 2022).

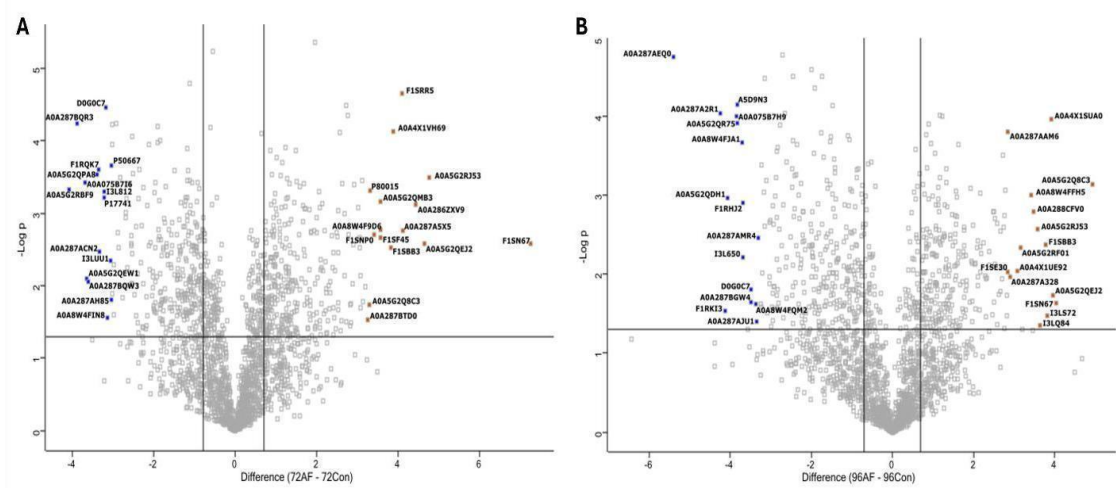


Figure 5.5: Volcano plots showing the distribution of statistically significant and differentially abundant (SSDA) proteins which have a $-\log$ (p-value) > 1.3 and difference $+/-0.58$. (A) *Sus scrofa* infected lung explants with *A. fumigatus* compared to uninfected lung explants at 72 hours and (B) *Sus scrofa* infected lung explants with *A. fumigatus* compared to uninfected lung explants at 96 hours.

Glutathione-S transferase (-16.87 fold) was decreased in abundance at 72 h and is involved in phase II metabolism and is also an important mediator of normal lung growth (van de Wetering *et al.*, 2021). The complement system was again observed to be compromised, with a variety of associated proteins reduced in abundance, including ficolin 2 (-14.64 fold), complement C3 (-1.97 fold), complement C4A (Rodgers blood group) (-2.46 fold), complement factor H (-2.97 fold), complement C5 (-3.42 fold) and complement factor B (C3/C5 convertase) (-6.76 fold). Gene enrichment analysis (Fig S5.6) highlighted an increase in ECM receptor expression, indicating fibrosis and tissue remodelling, in addition to increased expression of proteins associated with gap junctions, indicating recovery from increased permeability. Gene enrichment analysis also indicated a decrease in the abundance of proteins associated with glyoxylate

and dicarboxylate metabolism, glycolysis/gluconeogenesis, and the pentose phosphate pathway, supporting the fact that the infected tissue was less metabolically active than the healthy control (Fig S5.6).

At 96 h post-infection, 258 proteins were increased in abundance and 308 were decreased (Table S7). Proteins associated with fibrosis, such as fibrillin 1, collagen type IV alpha 1 chain, and alpha 2 chain, were increased by +16.44, +15.42, and +11.95, respectively, at 96 h. Collagen type VI alpha 1 chain (+14.16 fold), and alpha 2 chain (+12.37 fold) are associated with pulmonary fibrosis and tissue remodelling, and are elevated in numerous fibrotic conditions (Schaefer *et al.*, 2020; Mouraux *et al.*, 2018). In addition, laminin subunit alpha 3, detected at +14.17 fold and +13.78 fold at 72 and 96 h, respectively, is increased in pulmonary fibrosis (Morales-Nebreda *et al.*, 2015). Proteins associated with immune activity include serine- and arginine- rich splicing factor 3 (+15.10 fold) and expression of which is associated with immune infiltration (Li *et al.*, 2023). SLA class II histocompatibility antigen, DQ haplotype C alpha chain (+6.34 fold) and ABC-type antigen peptide transporter (tap2) (+5.18 fold), MHC class II histocompatibility antigen SLA-DRB1 (+2.43 fold) and SLA-DRA (+2.12) involved in antigen presentation which were also detected at the 72 hours. Mesencephalic astrocyte-derived neurotrophic factor was found to be decreased - 19.02 fold, deficiency of this protein in macrophages promoted macrophages to M1 differentiation in lung tissue, contributing to inflammation and aggravated lung injury in mice (Shen *et al.*, 2022). Despite this, other protein changes indicate fungal antagonism of the inflammatory response, with a decrease in allograft inflammatory factor 1 (-14.12 fold). AIF1 promotes macrophage activation and regulates immunity by mediating the differentiation and function of dendritic cells (Elizondo *et al.*, 2019). Syntaxin 3 was also decreased by -14.21 fold and is required for the maximal release of IL-1 α , IL-1 β , and IL-12, and is involved in MMP-9 exocytosis during gelatinase degranulation (Naegelen *et al.*, 2015), again indicating that neutrophil activity is impaired by *A. fumigatus*. In addition, copper transport protein ATOX1 was decreased 11.25 fold, deficiency of this protein was shown to reduce recruitment of monocytes/macrophages and is associated with impaired angiogenesis and wound healing (Das *et al.*, 2016). Gene enrichment analysis (Fig S5.7) also highlighted increased ECM alterations and proteins associated with focal adhesion, indicating

tissue damage. Aspects of the complement cascade are also observed as being compromised in addition to the phagosome, both of which are immune mechanisms known to be inhibited by *A. fumigatus* through the action of enolase and gliotoxin, respectively.

5.4 Discussion

The initial establishment of *A. fumigatus* infection and host adaptation processes have not been fully characterized. Understanding these processes could shed light on the diverse spectrum of infections caused by *A. fumigatus* and may provide insights into how to detect and treat these infections more effectively. A variety of model systems have been developed to characterize the development of *A. fumigatus* *in vitro* and the results have been useful for understanding how the fungus may interact with pulmonary tissue *in vivo*. Compared to the more commonly used model organisms, pig lungs demonstrate a higher degree of similarity to human lungs, sharing similarities in metabolic composition, overall physiology, anatomy, and immunology (Benahmed *et al.*, 2014; Meurens *et al.*, 2012). The EVPL system has previously been developed to mimic human airways in CF and has successfully demonstrated clinically realistic biofilm structures (Harrington *et al.*, 2020; Harrington, Littler, *et al.*, 2022), providing insight into how antibiotic tolerance is affected by growth on a realistic lung substrate (Harrington *et al.*, 2021). The EVPL model is best suited to study saprophytic or chronic infections such as chronic pulmonary aspergillosis but may not be suitable for studying invasive infections as there are no other tissues to disseminate into. In addition, proteomic signals indicate adaptive immune activation but as the tissue is isolated and non-resident recruitment cannot occur, understanding the impact of these signals later in the infection process remains elusive. The timeframe in which the experiments can be conducted is also limited as the tissue cannot be kept for long periods while murine studies can be conducted over a longer timeframe. The EVPL model offers a greater cellular complexity to that observed in epithelial models while demonstrating similar responses including TGF- β production in human primary bronchial epithelial cells following exposure to *A. fumigatus* (Barros *et al.*, 2022). Epithelial cell models lack the cellular complexity and cell-cell interaction that were observed in the explant model. Most *in vitro* studies on *A. fumigatus* pathogenesis have focused on one host cell type, but rarely capture the interactions that

would occur in a multi-cell system as present in the host lung (Bouyssi *et al.*, 2023).

In this study, the EVPL model was successfully adapted for studying *A. fumigatus* colonisation. Alveolar tissue sections were combined with commonly available tissue culture media (1:1 mixture of RPMI and DMEM). This medium was used in the first publications exploring the potential use of post-slaughter pig lung tissue as an *ex-vivo* infection model and was shown to allow long-term culture of pig tissue (Williams and Gallagher, 1978). Furthermore, tissue culture media has been proposed as an improved medium for clinically predictive antimicrobial susceptibility testing (Ersoy *et al.*, 2017). There is a plethora of more tailored, chemically defined media available that have been designed to mimic human airway secretions in health and diseases, including conditions that predispose individuals to *A. fumigatus* infection, such as CF with various media developed to mimic this condition (Ruhluel *et al.*, 2022; Aiyer and Manos, 2022) and future work could combine these with EVPL to study *A. fumigatus* in conditions that mimic the host environment found in specific infection contexts. However, in the first exploration of *A. fumigatus* growth and metabolism in EVPL, we elected to use a general-purpose, widely accessible, and cheap growth medium to facilitate model adoption and gain a first look at how this pathogen acts in settings that are more human-like than *in vitro* or mouse models.

Visual inspection of the tissue and agar sections confirmed the ability of the fungus to grow on both the substrates. There was a significant reduction in the growth on the tissue explant compared to the agar control and this is likely to have occurred as a result of immune antagonism occurring within the tissue as observed in the proteomic results, which would not be present in the agar control. In addition, the increased complexity of the metabolic profile between the two substrates could have delayed the growth at this timepoint. Proteomic analysis of the fungus indicated an increased abundance of proteins associated with growth and carbohydrate metabolism at 48 h, whereas at 72 and 96 h, proteins associated with amino acid metabolism were increased in abundance. Glyceraldehyde-3-phosphate dehydrogenase expression is associated with conidial germination, is expressed on the hyphal surface, and phosphoglycerate kinase is also involved in carbon metabolism, but is also involved in fumigaclavine C biosynthesis (Owens *et al.*, 2014). Amino acid metabolism and biosynthesis

were more prevalent at 72 h post-infection with aconitase hydratase, 5-methyltetrahydropteroylreiglutamate-homocysteine S-methyltransferase, 4-aminobutyrate aminotransferase, and acetohydroxy-acid reductoisomerase involved in the biosynthesis of lysine, methionine, and glutamate L-isoleucine, respectively, all of which were significantly increased in abundance. Amino acid metabolism and the shikimate pathway have been identified as markers of clinical isolates (Mirhakkak *et al.*, 2023) indicating EVPL induces *A. fumigatus* to behave in a manner similar to that observed in clinical isolates. Malate dehydrogenase detected at 48, 72, and 96 h, is involved in carbon metabolism and is a component of the methylcitrate cycle, an alternative metabolic pathway that plays an important role in the metabolism of propionyl-CoA, a byproduct of amino acids, odd-chain fatty acids, and certain intermediate metabolites (Silva *et al.*, 2023). This pathway is the link between the TCA and glyoxylate cycles in fungi and carbon assimilation by *A. fumigatus* *in vivo* (Huang *et al.*, 2023). This pathway is required for fungal survival and pathogenicity, the deletion of which reduces virulence in murine and insect models (Ibrahim-Granet *et al.*, 2008; Maerker *et al.*, 2005).

A range of virulence factors and potential host antagonistic mechanisms were increased in abundance, including fungal allergens at 48 h, such as large ribosomal subunit protein P2 (60S acidic ribosomal protein P2) (AfP2) (allergen Asp f 8) and mitochondrial superoxide dismutase [Mn] (allergen Asp f 6), which may induce the immune response observed within the tissue (Liu *et al.*, 2023). These allergens can directly disrupt the integrity of the epithelium and elicit the production of pro-inflammatory cytokines and fibrogenic growth factors. Several cytokines and chemokines have been implicated in the immune response to *Aspergillus* infection (Shankar *et al.*, 2024) and this model may have applications in characterising which may shed new insight into their roles in the response to fungal infection. The ensuing recruitment of immune cells and further leakage of plasma proteins would support the development of a cycle of inflammation, fibrin deposition and structural changes (Namvar *et al.*, 2022). Mycotoxin production can also impact the host invasion process, as evidenced by thioredoxin reductase gliT, detected at 96 hours, and methyltransferase psoC, detected at all time points, involved in gliotoxin and pseurotin A production, respectively. Interestingly, fungal enolase, which increased in abundance at all time points, acts as an inhibitor of the human complement cascade (Dasari *et al.*, 2019).

This pathway has been demonstrated to be compromised within the pig proteome, supporting the role of this protein in immune evasion. The results indicate that the fungus is capable of growing on the EVPL tissue and metabolizing the substrate, but the fungus is under stress with evidence of hyphal damage, as evidenced by the formation of the Woronin body and the production of numerous detoxification enzymes.

Proteomic changes in infected EVPL tissues indicate the induction of an immune response. S100-A8 and protein S100-A9 (Calgranulin-B) were increased in abundance at 24 h, which stimulate leukocyte recruitment and induced cytokine secretion (Wang *et al.*, 2018; Singh and Ali, 2022; Xia *et al.*, 2024). There is also evidence of an initial allergic response possibly induced by the expression of allergens, as carbonic anhydrase 4 was also increased in abundance and expressed in IL-5-activated eosinophils. In murine studies, carbonic anhydrase 4 was enhanced following an allergic insult with *A. fumigatus*, resulting in increased airway epithelial cell differentiation, anion exchange, and keratinization (Wen *et al.*, 2014). Proteins associated with degranulation decreased in abundance in the infected cohort, including prophenin and tritrypticin precursor (C6), proteinase 3, elastase, and neutrophil expression, indicating specific immune evasion induced by the fungus. At 48 h, there is further evidence of a mounted immune response as importin subunit alpha KPNA3 and KPNA4 were increased in abundance and are essential for TNF-alpha-stimulated NF-kappaB p50/p65 heterodimer translocation into the nucleus (Fagerlund *et al.*, 2005). *A. fumigatus* can be detected by Dectin-2 expressed on alveolar macrophages via Syk, which results in Nf-KB activation (Sun *et al.*, 2014). MZB1 was also increased in abundance and was expressed on plasmacytoid dendritic cells, which facilitates interferon alpha production following TLR9 stimulation (Kapoor *et al.*, 2020).

The first markers of pulmonary fibrosis were detected at 48 hours including indoleethylamine N-methyltransferase and nestin (Wang *et al.*, 2022). At later time points, there were more prominent markers of pulmonary fibrosis and tissue remodelling, consistent with the situation in immunocompetent mice, where collagen accumulation is reported following infection (Guirao-Abad *et al.*, 2024; Labram, 2017). This may be driven by transforming growth factor beta-1-induced transcript 1

protein increased +7.06 fold as overexpression of TGF- β is known to induce collagen deposition in mice (Hillege *et al.*, 2020). Many components of the extracellular matrix increased in abundance during fibrosis and are associated with the establishment of invasive fungal diseases. The increased expression of ECM components could also facilitate the covering of fungal hyphae by the extracellular matrix (Loussert *et al.*, 2010). This can lead to the formation of aspergillomas where the hyphae are embedded together in this dense extracellular matrix whereas in invasive aspergillosis hyphae are individually engulfed in the matrix (Müller *et al.*, 2011). The extracellular matrix coating protects the fungus against host immune effectors as well as antifungal drugs (Muszkieta *et al.*, 2013). Protein associated with T cell activation was also found to be increased in abundance, possibly mediated by the NF-KB activation observed previously. This indicates that both innate and adaptive immune responses are active within the tissue. The complement system was compromised, with a variety of associated proteins being reduced in abundance relative to the control. There is further evidence of fibrosis at 96 h post infection with fibrillin 1, collagen type IV, and type VI being significantly increased in abundance (Klingberg *et al.*, 2013; Hansen *et al.*, 2022). Aspects of an adaptive immune response are present, including SLA class II histocompatibility antigen, DQ haplotype C alpha chain, and ABC-type antigen peptide transporter (TAP2) involved in antigen presentation at 96 hours. Prothymosin alpha was decreased in abundance by -42.09 fold potentially occurring as a result of cleavage to its bioactive form, thymosin α 1, which has also been shown to enhance maturation of dendritic cells exposed to *A. fumigatus*. This effect was shown to be p38 MAP kinase/NF- κ B-dependent and required Toll-like receptor 9 signalling (Armstrong-James and Harrison, 2012). Some aspects of the immune response appeared to be inhibited by the presence of *A. fumigatus* evidenced by the decreased abundance of allograft inflammatory factor 1 (-14.12 fold). AIF1 promotes macrophage activation and NO production and regulates immunity by mediating the differentiation and function of dendritic cells (De Leon-Oliva *et al.*, 2023). *Leishmania* parasites inhibit AIF1 to effectively evade immune responses and avoid an inflammatory response (da Silva *et al.*, 2021), and it is possible *Aspergillus* may utilize a similar mechanism to protect itself from inflammatory markers. Syntaxin 3 also decreased by-14.21 fold and was involved in degranulation (Naegelen *et al.*, 2015), again indicating that neutrophil activity is impaired by *A. fumigatus*.

In a previous study of *P. aeruginosa* infection of bronchioles using EVPL with medium that mimics CF mucus, transcriptomic analysis showed an absence of pig mRNA (Harrington *et al.*, 2022). This suggests that, in that study, the host tissue was unresponsive to infection. There are two key differences in the present study that may explain this active host response. First, we used alveolar tissue, which provides a much greater number of host cells than bronchiolar epithelium and may contain alveolar immune cells. Second, in the present study, we were able to obtain lungs immediately after slaughter from the abattoir, rather than *via* a commercial butcher, which necessitates a delay between slaughter and lab use of at least 24-48 hours.

The results presented here highlight the response of porcine lung tissue to *A. fumigatus* infection in a complex biologically relevant model that demonstrates many of the patterns observed in *in vivo* models, as well as clinically. The model demonstrates both innate and adaptive immune responses, tissue remodelling, and fibrosis in response to fungal infection and demonstrates responses observed in allergic and invasive aspergillosis. This study provides insights into the initial host- pathogen interactions and highlights the importance of various metabolic processes for *A. fumigatus* colonization of the host, as well as supporting the role of various virulence factors in the establishment of infection. The tissue response to infection provides information on the importance of various immunological effectors and potential targets for fungal antagonism and demonstrates the role of *A. fumigatus* in the establishment of lung remodelling and fibrosis within the airways. These molecular patterns may provide insight into the initial host-pathogen interactions occurring in the human host and provide molecular targets for therapeutics in the future.

5.5 References

Abolhassani, M., Guais, A., Chaumet-Riffaud, P., Sasco, A. J. and Schwartz, L., 2009. Carbon dioxide inhalation causes pulmonary inflammation. *American Journal of Physiology-Lung Cellular and Molecular Physiology*, 296 (4), L657–L665.

Aghdassi, A. A., Pham, C., Zierke, L., Mariaule, V., Korkmaz, B. and Rhimi, M., 2024. Cathepsin C role in inflammatory gastroenterological, renal, rheumatic, and pulmonary disorders. *Biochimie*, 216, 175–180.

Aguilar, C., Alves da Silva, M., Saraiva, M., Neyazi, M., Olsson, I. A. S. and Bartfeld, S., 2021. Organoids as host models for infection biology – a review of methods. *Experimental & Molecular Medicine*, 53 (10), 1471–1482.

Aiyer, A. and Manos, J., 2022. The Use of Artificial Sputum Media to Enhance Investigation and Subsequent Treatment of Cystic Fibrosis Bacterial Infections. *Microorganisms*, 10 (7), 1269.

Armstrong-James, D. and Harrison, T. S., 2012. Immunotherapy for fungal infections. *Current Opinion in Microbiology*, 15 (4), 434–439.

Barros, B. C. S. C., Almeida, B. R., Barros, D. T. L., Toledo, M. S. and Suzuki, E., 2022. Respiratory Epithelial Cells: More Than Just a Physical Barrier to Fungal Infections. *Journal of Fungi*, 8 (6), 548.

Beck, J., Echtenacher, B. and Ebel, F., 2013. Woronin bodies, their impact on stress resistance and virulence of the pathogenic mould *Aspergillus fumigatus* and their anchoring at the septal pore of filamentous Ascomycota. *Molecular Microbiology*, 89 (5), 857–871.

Beck, J. M., Young, V. B. and Huffnagle, G. B., 2012. The microbiome of the lung. *Translational Research: The Journal of Laboratory and Clinical Medicine*, 160 (4), 258–266.

Benahmed, M. A., Elbayed, K., Daubeuf, F., Santelmo, N., Frossard, N. and Namer, I. J., 2014. NMR HRMAS spectroscopy of lung biopsy samples: Comparison study between human, pig, rat, and mouse metabolomics. *Magnetic Resonance in Medicine*, 71 (1), 35–43.

Blachowicz, A., Chiang, A. J., Romsdahl, J., Kalkum, M., Wang, C. C. C. and Venkateswaran, K., 2019. Proteomic characterization of *Aspergillus fumigatus* isolated from air and surfaces of the International Space Station. *Fungal genetics and biology : FG & B*, 124, 39–46.

Bouyssi, A., Déméautis, T., Trecourt, A., Delles, M., Agostini, F., Monneret, G., Glehen, O., Wallon, M., Persat, F., Devouassoux, G., Bentaher, A. and Menotti, J., 2023. Characterization of Lung Inflammatory Response to *Aspergillus fumigatus* Spores. *Journal of Fungi*, 9 (6), 682.

Brennan, M., Thomas, D. Y., Whiteway, M. and Kavanagh, K., 2002. Correlation between virulence of *Candida albicans* mutants in mice and *Galleria mellonella* larvae. *FEMS Immunology & Medical Microbiology*, 34 (2), 153–157.

Cai, Z., Chai, Y., Zhang, C., Qiao, W., Sang, H. and Lu, L., 2015. The G β -like protein CpcB is required for hyphal growth, conidiophore morphology and pathogenicity in *Aspergillus fumigatus*. *Fungal genetics and biology: FG & B*, 81, 120–131.

Cameron, A. M., Turner, C. T., Adams, D. H., Jackson, J. E., Melville, E., Arkell, R. M., Anderson, P. J. and Cowin, A. J., 2016. Flightless I is a key regulator of the fibroproliferative process in hypertrophic scarring and a target for a novel antiscarring therapy. *The British Journal of Dermatology*, 174 (4), 786–794.

Carreto-Binaghi, L. E., Aliouat, E. M. and Taylor, M. L., 2016. Surfactant proteins, SP-A and SP-D, in respiratory fungal infections: their role in the inflammatory response. *Respiratory Research*, 17 (1), 66.

Champion, O. L., Wagley, S. and Titball, R. W., 2016. *Galleria mellonella* as a model host for microbiological and toxin research. *Virulence*, 7 (7), 840–845.

Chen, K., Qiu, P., Yuan, Y., Zheng, L., He, J., Wang, C., Guo, Q., Kenny, J., Liu, Q., Zhao, J., Chen, J., Tickner, J., Fan, S., Lin, X. and Xu, J., 2019. Pseurotin A Inhibits

Osteoclastogenesis and Prevents Ovariectomized-Induced Bone Loss by Suppressing Reactive Oxygen Species. *Theranostics*, 9 (6), 1634–1650.

Cigana, C., Bianconi, I., Baldan, R., De Simone, M., Riva, C., Sipione, B., Rossi, G., Cirillo, D. M. and Bragonzi, A., 2018. *Staphylococcus aureus* Impacts *Pseudomonas aeruginosa* Chronic Respiratory Disease in Murine Models. *The Journal of Infectious Diseases*, 217 (6), 933–942.

Cornforth, D. M., Diggle, F. L., Melvin, J. A., Bomberger, J. M. and Whiteley, M., 2020. Quantitative Framework for Model Evaluation in Microbiology Research Using *Pseudomonas aeruginosa* and Cystic Fibrosis Infection as a Test Case. *mBio*, 11 (1), 10.1128/mbio.03042-19.

Curtis, A., Binder, U. and Kavanagh, K., 2022. *Galleria mellonella* Larvae as a Model for Investigating Fungal—Host Interactions. *Frontiers in Fungal Biology* [online], 3. Available from: <https://www.frontiersin.org/articles/10.3389/ffunb.2022.893494> [Accessed 31 Jan 2023].

Curtis, A., Walshe, K. and Kavanagh, K., 2023. Prolonged Subculturing of *Aspergillus fumigatus* on *Galleria* Extract Agar Results in Altered Virulence and Sensitivity to Antifungal Agents. *Cells*, 12 (7), 1065.

Czubak-Prowizor, K., Babinska, A. and Swiatkowska, M., 2022. The F11 Receptor (F11R)/Junctional Adhesion Molecule-A (JAM-A) (F11R/JAM-A) in cancer progression. *Molecular and Cellular Biochemistry*, 477 (1), 79–98.

Dagenais, T. R. T. and Keller, N. P., 2009. Pathogenesis of *Aspergillus fumigatus* in Invasive Aspergillosis. *Clinical Microbiology Reviews*, 22 (3), 447–465.

Das, A., Sudhahar, V., Chen, G.-F., Kim, H. W., Youn, S.-W., Finney, L., Vogt, S., Yang, J., Kweon, J., Surenkhuu, B., Ushio-Fukai, M. and Fukai, T., 2016. Endothelial Antioxidant-1: a Key Mediator of Copper-dependent Wound Healing in vivo. *Scientific Reports*, 6, 33783.

Dasari, P., Koleci, N., Shopova, I. A., Wartenberg, D., Beyersdorf, N., Dietrich, S., Sahagún-Ruiz, A., Figge, M. T., Skerka, C., Brakhage, A. A. and Zipfel, P. F., 2019. Enolase From *Aspergillus fumigatus* Is a Moonlighting Protein That Binds the Human Plasma Complement Proteins Factor H, FHL-1, C4BP, and Plasminogen. *Frontiers in Immunology* [online], 10. Available from: <https://www.frontiersin.org/journals/immunology/articles/10.3389/fimmu.2019.02573/full> [Accessed 18 Dec 2024].

Dasari, P., Shopova, I. A., Stroe, M., Wartenberg, D., Martin-Dahse, H., Beyersdorf, N., Hortschansky, P., Dietrich, S., Cseresnyés, Z., Figge, M. T., Westermann, M., Skerka, C., Brakhage, A. A. and Zipfel, P. F., 2018. Aspf2 From *Aspergillus fumigatus* Recruits Human Immune Regulators for Immune Evasion and Cell Damage. *Frontiers in Immunology*, 9, 1635.

De Leon-Oliva, D., Garcia-Montero, C., Fraile-Martinez, O., Boaru, D. L., García-Puente, L., Rios-Parra, A., Garrido-Gil, M. J., Casanova-Martín, C., García-Honduvilla, N., Bujan, J., Guijarro, L. G., Alvarez-Mon, M. and Ortega, M. A., 2023. AIF1: Function and Connection with Inflammatory Diseases. *Biology*, 12 (5), 694.

Denning, D. W., 2024. Global incidence and mortality of severe fungal disease. *The Lancet Infectious Diseases*, 24 (7), e428–e438.

Desoubeaux, G. and Cray, C., 2018. Animal Models of Aspergillosis. *Comparative Medicine*, 68 (2), 109–123.

Dichtl, S., Posch*, W. and Wilflingseder, D., 2024. The breathtaking world of human respiratory in vitro models: Investigating lung diseases and infections in 3D models, organoids, and lung-on-chip. *European Journal of Immunology*, 54 (3), 2250356.

Dickey, J. S., Redon, C. E., Nakamura, A. J., Baird, B. J., Sedelnikova, O. A. and Bonner, W. M., 2009. H2AX: functional roles and potential applications. *Chromosoma*, 118 (6), 683–692.

Doyle, S., Jones, G. W. and Dolan, S. K., 2018. Dysregulated gliotoxin biosynthesis attenuates the production of unrelated biosynthetic gene cluster-encoded metabolites in *Aspergillus fumigatus*. *Fungal Biology*, 122 (4), 214–221.

Driessen, N. N., Boshoff, H. I. M., Maaskant, J. J., Gilissen, S. A. C., Vink, S., van der Sar, A. M., Vandebroucke-Grauls, C. M. J. E., Bewley, C. A., Appelmelk, B. J. and Geurtzen, J., 2012. Cyanovirin-N inhibits mannose-dependent *Mycobacterium*-C-type lectin interactions but does not protect against murine tuberculosis. *Journal of Immunology (Baltimore, Md.: 1950)*, 189 (7), 3585–3592.

Du, H., Liang, L., Li, J., Xiong, Q., Yu, X. and Yu, H., 2021. Lipocalin-2 Alleviates LPS-Induced Inflammation Through Alteration of Macrophage Properties. *Journal of Inflammation Research*, 14, 4189–4203.

Du, X., Dong, Y., Li, W. and Chen, Y., 2023. hPSC-derived lung organoids: Potential opportunities and challenges. *Heliyon*, 9 (2), e13498.

Dumigan, A., Fitzgerald, M., Santos, J. S.-P. G., Hamid, U., O’Kane, C. M., McAuley, D. F. and Bengoechea, J. A., 2019. A Porcine Ex Vivo Lung Perfusion Model To Investigate Bacterial Pathogenesis. *mBio*, 10 (6), 10.1128/mbio.02802-19.

Elizondo, D. M., Brandy, N. Z. D., da Silva, R. L. L., Haddock, N. L., Kacsinta, A. D., de Moura, T. R. and Lipscomb, M. W., 2019. Allograft Inflammatory Factor-1 Governs Hematopoietic Stem Cell Differentiation Into cDC1 and Monocyte-Derived Dendritic Cells Through IRF8 and RelB in vitro. *Frontiers in Immunology*, 10, 173.

Ersoy, S. C., Heithoff, D. M., Barnes, L., Tripp, G. K., House, J. K., Marth, J. D., Smith, J. W. and Mahan, M. J., 2017. Correcting a Fundamental Flaw in the Paradigm for Antimicrobial Susceptibility Testing. *EBioMedicine*, 20, 173–181.

Espinosa, V. and Rivera, A., 2016. First Line of Defense: Innate Cell-Mediated Control of Pulmonary Aspergillosis. *Frontiers in Microbiology* [online], 7. Available from: <https://www.frontiersin.org/journals/microbiology/articles/10.3389/fmicb.2016.00272/full> [Accessed 18 Dec 2024].

Fagerlund, R., Kinnunen, L., Köhler, M., Julkunen, I. and Melén, K., 2005. NF-κB Is Transported into the Nucleus by Importin $\alpha 3$ and Importin $\alpha 4^*$. *Journal of Biological Chemistry*, 280 (16), 15942–15951.

Fazius, F., Shelest, E., Gebhardt, P. and Brock, M., 2012. The fungal α -amino adipate pathway for lysine biosynthesis requires two enzymes of the aconitase family for the isomerization of homocitrate to homoisocitrate. *Molecular Microbiology*, 86 (6), 1508–1530.

Fusco-Almeida, A. M., de Matos Silva, S., dos Santos, K. S., de Lima Gualque, M. W., Vaso, C. O., Carvalho, A. R., Medina-Alarcón, K. P., Pires, A. C. M. da S., Belizario, J. A., de Souza Fernandes, L., Moroz, A., Martinez, L. R., Ruiz, O. H., González, Á. and Mendes-Giannini, M. J. S., 2023. Alternative Non-Mammalian Animal and Cellular Methods for the Study of Host–Fungal Interactions. *Journal of Fungi*, 9 (9), 943.

Gago, S., Denning, D. W. and Bowyer, P., 2019. Pathophysiological aspects of *Aspergillus* colonization in disease. *Medical Mycology*, 57 (Supplement_2), S219–S227.

Gallorini, M., Marinacci, B., Pellegrini, B., Cataldi, A., Dindo, M. L., Carradori, S. and Grande, R., 2024. Immunophenotyping of hemocytes from infected *Galleria mellonella* larvae as an innovative tool for immune profiling, infection studies and drug screening. *Scientific Reports*, 14 (1), 759.

Ge, S. X., Jung, D. and Yao, R., 2020. ShinyGO: a graphical gene-set enrichment tool for animals and plants. *Bioinformatics (Oxford, England)*, 36 (8), 2628–2629.

Grynpberg, M., Piotrowska, M., Pizzinini, E., Turner, G. and Paszewski, A., 2001. The *Aspergillus nidulans* metE gene is regulated by a second system independent from sulphur metabolite repression. *Biochimica Et Biophysica Acta*, 1519 (1–2), 78–84.

Guirao-Abad, J. P., Shearer, S. M., Bowden, J., Kasprovic, D. A., Grisham, C., Ozdemir, M., Tranter, M., Wang, Y., Askew, D. S. and Kanisicak, O., 2024. Pulmonary fibroblast activation during *Aspergillus fumigatus* infection enhances lung defense via immunomodulation and tissue remodeling. [online]. Available from: <https://www.biorxiv.org/content/10.1101/2024.12.19.629499v1> [Accessed 7 Jan 2025].

Guo, P., Liu, Y., Geng, F., Daman, A. W., Liu, X., Zhong, L., Ravishankar, A., Lis, R., Durán, J. G. B., Itkin, T., Tang, F., Zhang, T., Xiang, J., Shido, K., Ding, B., Wen, D.,

Josefowicz, S. Z. and Rafii, S., 2022. Histone variant H3.3 maintains adult haematopoietic stem cell homeostasis by enforcing chromatin adaptability. *Nature cell biology*, 24 (1), 99–111.

Guruceaga, X., Ezpeleta, G., Mayayo, E., Sueiro-Olivares, M., Abad-Diaz-De-Cerio, A., Aguirre Urízar, J. M., Liu, H. G., Wiemann, P., Bok, J. W., Filler, S. G., Keller, N. P., Hernando, F. L., Ramirez-Garcia, A. and Rementeria, A., 2018. A possible role for fumagillin in cellular damage during host infection by *Aspergillus fumigatus*. *Virulence*, 9 (1), 1548–1561.

Hansen, A. H., Prior, T. S., Leeming, D. J., Karsdal, M. A., Sand, J. M. B. and Bendstrup, E., 2022. A lung and kidney specific fragment of type IV collagen is associated with increased mortality in idiopathic pulmonary fibrosis. *European Respiratory Journal* [online], 60 (suppl 66). Available from: https://publications.ersnet.org/content/erj/60/suppl_66/1703 [Accessed 8 Jan 2025].

Harrington, N. E., Allen, F., Garcia-Maset, R. and Harrison, F., 2022. *Pseudomonas aeruginosa* transcriptome analysis in a cystic fibrosis lung model reveals metabolic changes accompanying biofilm maturation and increased antibiotic tolerance over time. [online]. Available from: <https://www.biorxiv.org/content/10.1101/2022.06.30.498312v1> [Accessed 29 Jan 2025].

Harrington, N. E., Littler, J. L. and Harrison, F., 2022. Transcriptome Analysis of *Pseudomonas aeruginosa* Biofilm Infection in an Ex Vivo Pig Model of the Cystic Fibrosis Lung. *Applied and Environmental Microbiology*, 88 (3), e01789-21.

Harrington, N. E., Sweeney, E., Alav, I., Allen, F., Moat, J. and Harrison, F., 2021. Antibiotic Efficacy Testing in an Ex vivo Model of *Pseudomonas aeruginosa* and *Staphylococcus aureus* Biofilms in the Cystic Fibrosis Lung. *Journal of Visualized Experiments: JoVE*, (167).

Harrington, N. E., Sweeney, E. and Harrison, F., 2020. Building a better biofilm - Formation of in vivo-like biofilm structures by *Pseudomonas aeruginosa* in a porcine model of cystic fibrosis lung infection. *Biofilm*, 2, 100024.

Harrison, F. and Diggle, S. P., 2016. An ex vivo lung model to study bronchioles infected with *Pseudomonas aeruginosa* biofilms. *Microbiology*, 162 (10), 1755–1760.

Harrison, F., Muruli, A., Higgins, S. and Diggle, S. P., 2014. Development of an Ex Vivo Porcine Lung Model for Studying Growth, Virulence, and Signaling of *Pseudomonas aeruginosa*. *Infection and Immunity*, 82 (8), 3312–3323.

Heinrich, S. M., 2011. Human SP-A- genes, structure, function- and lung diseases. Text.PhDThesis. [online]. Ludwig-Maximilians-Universität München. Available from: <https://edoc.ub.uni-muenchen.de/13834/> [Accessed 12 May 2025].

Hillege, M. M. G., Galli Caro, R. A., Offringa, C., de Wit, G. M. J., Jaspers, R. T. and Hoogaars, W. M. H., 2020. TGF- β Regulates Collagen Type I Expression in Myoblasts and Myotubes via Transient Ctgf and Fgf-2 Expression. *Cells*, 9 (2), 375.

Hoang, T. N. M., Cseresnyés, Z., Hartung, S., Blickensdorf, M., Saffer, C., Rennert, K., Mosig, A. S., von Lilienfeld-Toal, M. and Figge, M. T., 2022. Invasive aspergillosis- on-chip: A quantitative treatment study of human *Aspergillus fumigatus* infection. *Biomaterials*, 283, 121420.

Huang, T., Zhang, M., Tong, X., Chen, J., Yan, G., Fang, S., Guo, Y., Yang, B., Xiao, S., Chen, C., Huang, L. and Ai, H., 2018. Microbial communities in swine lungs and their association with lung lesions. *Microbial Biotechnology*, 12 (2), 289–304.

Huang, Z., Wang, Q., Khan, I. A., Li, Y., Wang, J., Wang, J., Liu, X., Lin, F. and Lu, J., 2023. The Methylcitrate Cycle and Its Crosstalk with the Glyoxylate Cycle and Tricarboxylic Acid Cycle in Pathogenic Fungi. *Molecules*, 28 (18), 6667.

Huskens, D., Vermeire, K., Vandemeulebroucke, E., Balzarini, J. and Schols, D., 2008. Safety concerns for the potential use of cyanovirin-N as a microbicidal anti-HIV agent. *The International Journal of Biochemistry & Cell Biology*, 40 (12), 2802–2814.

Ibrahim-Granet, O., Dubourdeau, M., Latgé, J.-P., Ave, P., Huerre, M., Brakhage, A. A. and Brock, M., 2008. Methylcitrate synthase from *Aspergillus fumigatus* is essential for manifestation of invasive aspergillosis. *Cellular Microbiology*, 10 (1), 134–148.

Janssens, I., Lambrecht, B. N. and Van Braeckel, E., 2024. *Aspergillus and the Lung. Seminars in Respiratory and Critical Care Medicine*, 45 (1), 3–20.

Kale, S. D., Ayubi, T., Chung, D., Tubau-Juni, N., Leber, A., Dang, H. X., Karyala, S., Hontecillas, R., Lawrence, C. B., Cramer, R. A. and Bassaganya-Riera, J., 2017. Modulation of Immune Signaling and Metabolism Highlights Host and Fungal Transcriptional Responses in Mouse Models of Invasive Pulmonary Aspergillosis. *Scientific Reports*, 7 (1), 17096.

Kapoor, T., Corrado, M., Pearce, E. L., Pearce, E. J. and Grosschedl, R., 2020. MZB1 enables efficient interferon α secretion in stimulated plasmacytoid dendritic cells. *Scientific Reports*, 10 (1), 21626.

Klingberg, F., Hinz, B. and White, E. S., 2013. The myofibroblast matrix: implications for tissue repair and fibrosis. *The Journal of Pathology*, 229 (2), 298–309.

Koharudin, L. M. I., Visconti, A. R., Jee, J.-G., Ottonello, S. and Gronenborn, A. M., 2008. The Evolutionarily Conserved Family of Cyanovirin-N Homologs: Structures and Carbohydrate Specificity. *Structure*, 16 (4), 570–584.

Kotton, D. N., 2018. Claudin-18: unexpected regulator of lung alveolar epithelial cell proliferation. *The Journal of Clinical Investigation*, 128 (3), 903–905.

Labram, B., 2017. Defining the molecular and cellular mechanisms regulating *Aspergillus fumigatus* regulated airway wall remodelling in asthma.

Lambrecht, B. N. and Hammad, H., 2012. The airway epithelium in asthma. *Nature Medicine*, 18 (5), 684–692.

Lecaille, F., Naudin, C., Sage, J., Joulin-Giet, A., Courty, A., Andrault, P.-M., Veldhuizen, R. A. W., Possmayer, F. and Lalmanach, G., 2013. Specific cleavage of the lung surfactant protein A by human cathepsin S may impair its antibacterial properties. *The International Journal of Biochemistry & Cell Biology*, 45 (8), 1701–1709.

Li, D., Yu, W. and Lai, M., 2023. Towards understandings of serine/arginine-rich splicing factors. *Acta Pharmaceutica Sinica B*, 13 (8), 3181–3207.

Liu, B., Guan, Y., Wang, M., Han, Y., Wang, W., Wang, Y. and Wu, P., 2022. ABRACL as a potential prognostic biomarker and correlates with immune infiltration in low-grade gliomas. *Interdisciplinary Neurosurgery*, 30, 101618.

Liu, T., Wang, Y., Zhang, Z., Jia, L., Zhang, J., Zheng, S., Chen, Z., Shen, H., Piao, C. and Du, J., 2023. Abnormal adenosine metabolism of neutrophils inhibits airway inflammation and remodeling in asthma model induced by *Aspergillus fumigatus*. *BMC Pulmonary Medicine*, 23, 258.

Liu, Y., Shen, T., Chen, L., Zhou, J. and Wang, C., 2021. Analogs of the Cathelicidin-Derived Antimicrobial Peptide PMAP-23 Exhibit Improved Stability and Antibacterial Activity. *Probiotics and Antimicrobial Proteins*, 13 (1), 273–286.

Llewellyn, J., Mallikarjun, V., Appleton, E., Osipova, M., Gilbert, H. T. J., Richardson, S. M., Hubbard, S. J. and Swift, J., 2023. Loss of regulation of protein synthesis and turnover underpins an attenuated stress response in senescent human mesenchymal stem cells. *Proceedings of the National Academy of Sciences*, 120 (14), e2210745120.

Long, N., Orasch, T., Zhang, S., Gao, L., Xu, X., Hortschansky, P., Ye, J., Zhang, F., Xu, K., Gsaller, F., Straßburger, M., Binder, U., Heinekamp, T., Brakhage, A. A., Haas, H. and Lu, L., 2018. The Zn2Cys6-type transcription factor LeuB cross-links regulation of leucine biosynthesis and iron acquisition in *Aspergillus fumigatus*. *PLOS Genetics*, 14 (10), e1007762.

Loussert, C., Schmitt, C., Prevost, M.-C., Balloy, V., Fadel, E., Philippe, B., Kauffmann-Lacroix, C., Latgé, J. P. and Beauvais, A., 2010. In vivo biofilm composition of *Aspergillus fumigatus*. *Cellular Microbiology*, 12 (3), 405–410.

Lu, Z., Pang, T., Yin, X., Cui, H., Fang, G., Xue, X. and Luo, T., 2020. Delivery of TSPAN1 siRNA by Novel Th17 Targeted Cationic Liposomes for Gastric Cancer Intervention. *Journal of Pharmaceutical Sciences*, 109 (9), 2854–2860.

Maerker, C., Rohde, M., Brakhage, A. A. and Brock, M., 2005. Methylcitrate synthase from *Aspergillus fumigatus*. Propionyl-CoA affects polyketide synthesis, growth and morphology of conidia. *The FEBS journal*, 272 (14), 3615–3630.

Mantel, I., Sadiq, B. A. and Blander, J. M., 2022. Spotlight on TAP and its vital role in antigen presentation and cross-presentation. *Molecular immunology*, 142, 105–119.

Meurens, F., Summerfield, A., Nauwynck, H., Saif, L. and Gerdts, V., 2012. The pig: a model for human infectious diseases. *Trends in Microbiology*, 20 (1), 50–57.

Miller, A. J. and Spence, J. R., 2017. In Vitro Models to Study Human Lung Development, Disease and Homeostasis. *Physiology*, 32 (3), 246–260.

Mirhakkak, M. H., Chen, X., Ni, Y., Heinekamp, T., Sae-Ong, T., Xu, L.-L., Kurzai, O., Barber, A. E., Brakhage, A. A., Boutin, S., Schäuble, S. and Panagiotou, G., 2023. Genome-scale metabolic modeling of *Aspergillus fumigatus* strains reveals growth dependencies on the lung microbiome. *Nature Communications*, 14 (1), 4369.

Miyata, S., Casey, M., Frank, D. W., Ausubel, F. M. and Drenkard, E., 2003. Use of the *Galleria mellonella* caterpillar as a model host to study the role of the type III secretion system in *Pseudomonas aeruginosa* pathogenesis. *Infection and Immunity*, 71 (5), 2404–2413.

Morales-Nebreda, L. I., Rogel, M. R., Eisenberg, J. L., Hamill, K. J., Soberanes, S., Nigdelioglu, R., Chi, M., Cho, T., Radigan, K. A., Ridge, K. M., Misharin, A. V., Woychek, A., Hopkinson, S., Perlman, H., Mutlu, G. M., Pardo, A., Selman, M., Jones, J. C. R. and Budinger, G. R. S., 2015. Lung-Specific Loss of α 3 Laminin Worsens Bleomycin-Induced Pulmonary Fibrosis. *American Journal of Respiratory Cell and Molecular Biology*, 52 (4), 503–512.

Mouraux, S., Bernasconi, E., Pattaroni, C., Koutsokera, *et al*, 2018. Airway microbiota signals anabolic and catabolic remodeling in the transplanted lung. *Journal of Allergy and Clinical Immunology*, 141 (2), 718–729.e7.

Müller, F.-M. C., Seidler, M. and Beauvais, A., 2011. *Aspergillus fumigatus* biofilms in the clinical setting. *Medical Mycology*, 49 (Supplement_1), S96–S100.

Muszkieta, L., Beauvais, A., Pähtz, V., Gibbons, J., Anton Leberre, V., Beau, R., Shibuya, K., Rokas, A., Francois, J. M., Kniemeyyer, O., Brakhage, A. A. and Latge, J. P., 2013. Investigation of *Aspergillus fumigatus* biofilm formation by various “omics” approaches. *Frontiers in Microbiology* [online], 4. Available from: <https://www.frontiersin.org/journals/microbiology/articles/10.3389/fmicb.2013.00013/full> [Accessed 8 Jan 2025].

Naegelen, I., Plancon, S., Nicot, N., Kaoma, T., Muller, A., Vallar, L., Tschirhart, E. J. and Bre'chard, S., 2015. An essential role of syntaxin 3 protein for granule exocytosis and secretion of IL-1 α , IL-1 β , IL-12b, and CCL4 from differentiated HL-60 cells. *Journal of Leukocyte Biology*, 97 (3), 557–571.

Namvar, S., Labram, B., Rowley, J. and Herrick, S., 2022. *Aspergillus fumigatus*—Host Interactions Mediating Airway Wall Remodelling in Asthma. *Journal of Fungi*, 8 (2), 159.

Olivieri, J., Smaldone, S. and Ramirez, F., 2010. Fibrillin assemblies: extracellular determinants of tissue formation and fibrosis. *Fibrogenesis & Tissue Repair*, 3 (1), 24.

Owens, R. A., Hammel, S., Sheridan, K. J., Jones, G. W. and Doyle, S., 2014. A Proteomic Approach to Investigating Gene Cluster Expression and Secondary Metabolite Functionality in *Aspergillus fumigatus*. *PLoS ONE*, 9 (9), e106942.

Pardo-Saganta, A., Law, B. M., Gonzalez-Celeiro, M., Vinarsky, V. and Rajagopal, J., 2013. Ciliated cells of pseudostratified airway epithelium do not become mucous cells after ovalbumin challenge. *American Journal of Respiratory Cell and Molecular Biology*, 48 (3), 364–373.

Patradoon-Ho, P. and Fitzgerald, D. A., 2007. Lung abscess in children. *Paediatric Respiratory Reviews*, 8 (1), 77–84.

Perez-Nadale, E., Almeida Nogueira, M. F., Baldin, C., Castanheira, S., El Ghalid, M., Grund, E., Lengeler, K., Marchegiani, E., Mehrotra, P. V., Moretti, M., Naik, V.,

Osés-Ruiz, M., Oskarsson, T., Schäfer, K., Wasserstrom, L., Brakhage, A. A., Gow, N. A. R., Kahmann, R., Lebrun, M.-H., Perez-Martin, J., Di Pietro, A., Talbot, N. J., Toquin, V., Walther, A. and Wendland, J., 2014. Fungal model systems and the elucidation of pathogenicity determinants. *Fungal Genetics and Biology*, 70, 42–67.

Perez-Riverol, Y., Bai, J., Bandla, C., García-Seisdedos, D., Hewapathirana, S., Kamatchinathan, S., Kundu, D. J., Prakash, A., Frericks-Zipper, A., Eisenacher, M., Walzer, M., Wang, S., Brazma, A. and Vizcaíno, J. A., 2021. The PRIDE database resources in 2022: a hub for mass spectrometry-based proteomics evidences. *Nucleic Acids Research*, 50 (D1), D543–D552.

Resendiz-Sharpe, A., da Silva, R. P., Geib, E., Vanderbeke, L., Seldeslachts, L., Hupko, C., Brock, M., Lagrou, K. and Vande Velde, G., 2022. Longitudinal multimodal imaging-compatible mouse model of triazole-sensitive and -resistant invasive pulmonary aspergillosis. *Disease Models & Mechanisms*, 15 (3), dmm049165.

Richardson, M., Bowyer, P. and Sabino, R., 2019. The human lung and Aspergillus: You are what you breathe in? *Medical Mycology*, 57 (Suppl 2), S145–S154.

Ries, L. N. A., Pardeshi, L., Dong, Z., Tan, K., Steenwyk, J. L., Colabardini, A. C., Filho, J. A. F., Castro, P. A. de, Silva, L. P., Preite, N. W., Almeida, F., Assis, L. J. de, Santos, R. A. C. dos, Bowyer, P., Bromley, M., Owens, R. A., Doyle, S., Demasi, M., Hernández, D. C. R., Netto, L. E. S., Pupo, M. T., Rokas, A., Loures, F. V., Wong, K. H. and Goldman, G. H., 2020. The Aspergillus fumigatus transcription factor RglT is important for gliotoxin biosynthesis and self-protection, and virulence. *PLOS Pathogens*, 16 (7), e1008645.

Roberts, A. E. L., Kragh, K. N., Bjarnsholt, T. and Diggle, S. P., 2015. The Limitations of *In Vitro* Experimentation in Understanding Biofilms and Chronic Infection. *Journal of Molecular Biology*, 427 (23), 3646–3661.

Rubio, F., Cooley, J., Accurso, F. J. and Remold-O'Donnell, E., 2004. Linkage of neutrophil serine proteases and decreased surfactant protein-A (SP-A) levels in inflammatory lung disease. *Thorax*, 59 (4), 318–323.

Ruhluel, D., O'Brien, S., Fothergill, J. L. and Neill, D. R., 2022. Development of liquid culture media mimicking the conditions of sinuses and lungs in cystic fibrosis and health. *F1000Research*, 11, 1007.

Saxena, S., Madan, T., Muralidhar, K. and Sarma, P. U., 2003. cDNA cloning, expression and characterization of an allergenic L3 ribosomal protein of Aspergillus fumigatus. *Clinical and Experimental Immunology*, 134 (1), 86–91.

Schaefer, A. L., Ceesay, M., Leier, J. A., Tesch, J., Wisenden, B. D. and Pandey, S., 2020. Factors Contributing to Sex Differences in Mice Inhalng Aspergillus fumigatus. *International Journal of Environmental Research and Public Health*, 17 (23), 8851.

Schipke, J., Kuhlmann, S., Hegermann, J., Fassbender, S., Kühnel, M., Jonigk, D. and Mühlfeld, C., 2021. Lipofibroblasts in Structurally Normal, Fibrotic, and Emphysematous Human Lungs. *American Journal of Respiratory and Critical Care Medicine*, 204 (2), 227–230.

Shankar, J., Thakur, R., Clemons, K. V. and Stevens, D. A., 2024. Interplay of Cytokines and Chemokines in Aspergillosis. *Journal of Fungi*, 10 (4), 251.

Shankar, J., Tiwari, S., Shishodia, S. K., Gangwar, M., Hoda, S., Thakur, R. and Vijayaraghavan, P., 2018. Molecular Insights Into Development and Virulence Determinants of Aspergilli: A Proteomic Perspective. *Frontiers in Cellular and Infection Microbiology*, 8, 180.

Sheehan, G., Clarke, G. and Kavanagh, K., 2018. Characterisation of the cellular and proteomic response of Galleria mellonella larvae to the development of invasive aspergillosis. *BMC Microbiology*, 18 (1), 63.

Sheehan, G., Konings, M., Lim, W., Fahal, A., Kavanagh, K. and Van De Sande, W. W. J., 2020. Proteomic analysis of the processes leading to Madurella mycetomatis grain formation in Galleria mellonella larvae. *PLOS Neglected Tropical Diseases*, 14 (4), e0008190.

Shen, Q., Wang, D., Xu, H., Wei, C., Xiao, X., Liu, J., Shen, Y., Fang, L., Feng, L. and Shen, Y., 2022. Mesencephalic astrocyte-derived neurotrophic factor attenuates acute lung injury via inhibiting macrophages' activation. *Biomedicine & Pharmacotherapy*, 150, 112943.

Shende, R., Wong, S. S. W., Rapole, S., Beau, R., Ibrahim-Granet, O., Monod, M., Gührs, K.-H., Pal, J. K., Latgé, J.-P., Madan, T., Aimanianda, V. and Sahu, A., 2018. *Aspergillus fumigatus* conidial metalloprotease Mep1p cleaves host complement proteins. *The Journal of Biological Chemistry*, 293 (40), 15538–15555.

Sheppard, D. C., 2011. Molecular mechanism of *Aspergillus fumigatus* adherence to host constituents. *Current Opinion in Microbiology*, 14 (4), 375–379.

Silva, L. do C., Rocha, O. B., Portis, I. G., Santos, T. G., Freitas e Silva, K. S., dos Santos Filho, R. F., Cunha, S., Alonso, A., Soares, C. M. de A. and Pereira, M., 2023. Proteomic Profiling of *Paracoccidioides brasiliensis* in Response to Phenacylideneoxindol Derivative: Unveiling Molecular Targets and Pathways. *Journal of Fungi*, 9 (8), 854.

da Silva, R. L., Elizondo, D. M., Brandy, N. Z. D., Haddock, N. L., Boddie, T. A., de Oliveira, L. L., de Jesus, A. R., de Almeida, R. P., de Moura, T. R. and Lipscomb, M. W., 2021. *Leishmania donovani* infection suppresses Allograft Inflammatory Factor-1 in monocytes and macrophages to inhibit inflammatory responses. *Scientific Reports*, 11 (1), 946.

Singh, P. and Ali, S. A., 2022. Multifunctional Role of S100 Protein Family in the Immune System: An Update. *Cells*, 11 (15), 2274.

van Spriel, A. B. and Figdor, C. G., 2010. The role of tetraspanins in the pathogenesis of infectious diseases. *Microbes and Infection*, 12 (2), 106–112.

Srivastava, M., Bencurova, E., Gupta, S. K., Weiss, E., Löffler, J. and Dandekar, T., 2019. *Aspergillus fumigatus* Challenged by Human Dendritic Cells: Metabolic and Regulatory Pathway Responses Testify a Tight Battle. *Frontiers in Cellular and Infection Microbiology*, 9, 168.

Stockley, J. A., Walton, G. M., Lord, J. M. and Sapey, E., 2013. Aberrant neutrophil functions in stable chronic obstructive pulmonary disease: the neutrophil as an immunotherapeutic target. *International Immunopharmacology*, 17 (4), 1211–1217.

Strickland, A. B., Sun, D., Sun, P., Chen, Y., Liu, G. and Shi, M., 2022. IL-27 Signaling Promotes Th1 Responses and Is Required to Inhibit Fungal Growth in the Lung during Repeated Exposure to *Aspergillus fumigatus*. *ImmunoHorizons*, 6 (1), 78–89.

Sun, H., Xu, X., Tian, X., Shao, H., Wu, X., Wang, Q., Su, X. and Shi, Y., 2014. Activation of NF-κB and respiratory burst following *Aspergillus fumigatus* stimulation of macrophages. *Immunobiology*, 219 (1), 25–36.

Sweeney, E., Harrington, N. E., Harley Henriques, A. G., Hassan, M. M., Crealock-Ashurst, B., Smyth, A. R., Hurley, M. N., Tormo-Mas, M. Á. and Harrison, F., 2021. An ex vivo cystic fibrosis model recapitulates key clinical aspects of chronic *Staphylococcus aureus* infection. *Microbiology (Reading, England)*, 167 (1).

Techakriengkrai, N., Nedumpun, T., Golde, W. T. and Suradhat, S., 2021. Diversity of the Swine Leukocyte Antigen Class I and II in Commercial Pig Populations. *Frontiers in Veterinary Science* [online], 8. Available from: <https://www.frontiersin.org/journals/veterinary-science/articles/10.3389/fvets.2021.637682/full> [Accessed 20 Dec 2024].

The UniProt Consortium, 2025. UniProt: the Universal Protein Knowledgebase in 2025. *Nucleic Acids Research*, 53 (D1), D609–D617.

Thrikawala, S. U., Anderson, M. H. and Rosowski, E. E., 2024. Glucocorticoids Suppress NF-κB–Mediated Neutrophil Control of *Aspergillus fumigatus* Hyphal Growth. *The Journal of Immunology*, 213 (7), 971–987.

Varghese, B., Ling, Z. and Ren, X., 2022. Reconstructing the pulmonary niche with stem cells: a lung story. *Stem Cell Research & Therapy*, 13 (1), 161.

van de Veerdonk, F. L., Carvalho, A., Wauters, J., Chamilos, G. and Verweij, P. E., 2025. *Aspergillus fumigatus* biology, immunopathogenicity and drug resistance. *Nature Reviews Microbiology*, 1–15.

Walsh, D., Bevan, J. and Harrison, F., 2024. How Does Airway Surface Liquid Composition Vary in Different Pulmonary Diseases, and How Can We Use This Knowledge to Model Microbial Infections? *Microorganisms*, 12 (4), 732.

Wang, J., Lai, X., Yao, S., Chen, H., Cai, J., Luo, Y., Wang, Y., Qiu, Y., Huang, Y., Wei, X., Wang, B., Lu, Q., Guan, Y., Wang, T., Li, S. and Xiang, A. P., 2022. Nestin promotes pulmonary fibrosis via facilitating recycling of TGF- β receptor I. *The European Respiratory Journal*, 59 (5), 2003721.

Wang, S., Song, R., Wang, Z., Jing, Z., Wang, S. and Ma, J., 2018. S100A8/A9 in Inflammation. *Frontiers in Immunology* [online], 9. Available from: <https://www.frontiersin.org/journals/immunology/articles/10.3389/fimmu.2018.01298/full> [Accessed 24 Sep 2024].

Wartenberg, D., Lapp, K., Jacobsen, I. D., Dahse, H.-M., Kniemeyer, O., Heinekamp, T. and Brakhage, A. A., 2011. Secretome analysis of *Aspergillus fumigatus* reveals Asp-hemolysin as a major secreted protein. *International journal of medical microbiology: IJMM*, 301 (7), 602–611.

Wen, T., Mingler, M. K., Wahl, B., Khorki, M. E., Pabst, O., Zimmermann, N. and Rothenberg, M. E., 2014. Carbonic Anhydrase IV Is Expressed on IL-5-Activated Murine Eosinophils. *The Journal of Immunology*, 192 (12), 5481–5489.

Wessely-Szponder, J., Majer-Dziedzic, B. and Smolira, A., 2010. Analysis of antimicrobial peptides from porcine neutrophils. *Journal of Microbiological Methods*, 83 (1), 8–12.

van de Wetering, C., Elko, E., Berg, M., Schiffrers, C. H. J., Stylianidis, V., van den Berge, M., Nawijn, M. C., Wouters, E. F. M., Janssen-Heininger, Y. M. W. and Reynaert, N. L., 2021. Glutathione S-transferases and their implications in the lung diseases asthma and chronic obstructive pulmonary disease: Early life susceptibility? *Redox Biology*, 43, 101995.

Williams, P. P. and Gallagher, J. E., 1978a. Preparation and long-term cultivation of porcine tracheal and lung organ cultures by alternate exposure to gaseous and liquid medium phases. *In Vitro*, 14 (8), 686–696.

Williams, P. P. and Gallagher, J. E., 1978b. Cytopathogenicity of *Mycoplasma hyopneumoniae* in porcine tracheal ring and lung explant organ cultures alone and in combination with monolayer cultures of fetal lung fibroblasts. *Infection and Immunity*, 20 (2), 495–502.

Xia, P., Ji, X., Yan, L., Lian, S., Chen, Z. and Luo, Y., 2024. Roles of S100A8, S100A9 and S100A12 in infection, inflammation and immunity. *Immunology*, 171 (3), 365–376.

Xu, K., Ding, L., Li, W., Wang, Y., Ma, S., Lian, H., Pan, X., Wan, R., Zhao, W., Yang, J., Rosas, I., Wang, L. and Yu, G., 2024. Aging-Associated Metabolite Methylmalonic Acid Increases Susceptibility to Pulmonary Fibrosis. *The American Journal of Pathology*, 194 (8), 1478–1493.

Xu, M., Liang, H., Li, K., Zhu, S., Yao, Z., Xu, R. and Lin, N., 2021. Value of KPNA4 as a diagnostic and prognostic biomarker for hepatocellular carcinoma. *Aging*, 13 (4), 5263–5283.

Zabihi, M., Shahriari Felordi, M., Lingampally, A., Bellusci, S., Chu, X. and El Agha, E., 2024. Understanding myofibroblast origin in the fibrotic lung. *Chinese Medical Journal Pulmonary and Critical Care Medicine*, 2 (3), 142–150.

Zhou, X., Ji, Q., Li, Q., Wang, P., Hu, G., Xiao, F., Ye, M., Lin, L., Luo, M., Guo, Y., Wu, W., Huang, K. and Guo, H., 2022. HSPA6 is Correlated With the Malignant Progression and Immune Microenvironment of Gliomas. *Frontiers in Cell and Developmental Biology*, 10, 833938.

Chapter 6

More potent together: *Aspergillus fumigatus* facilitates the dominance of *Pseudomonas aeruginosa* during coinfection of an *ex-vivo* pig lung model

Aaron Curtis, David Fitzpatrick, Freya Harrison and Kevin Kavanagh

¹Department of Biology, Maynooth University, Maynooth, Co. Kildare,
Ireland

2. School of Life Sciences, University of Warwick, Coventry, UK

Submitted as:

Curtis, A., FitzPatrick, D., Harrison, F., Kavanagh, K. More potent together: *Aspergillus fumigatus* facilitates the dominance of *Pseudomonas aeruginosa* during coinfection of an *ex-vivo* pig lung model mBio mBio02571-25 (submitted)

Author Contributions

Aaron Curtis: Experimental, data analysis, and manuscript preparation. **David Fitzpatrick** data analysis, and manuscript preparation and review. **Freya Harrison:** Experimental design and manuscript review. **Kevin Kavanagh:** Experimental design, manuscript preparation and submission. All authors have read and approved the manuscript.

Abstract

Pseudomonas aeruginosa and *Aspergillus fumigatus* represent the dominant bacterial and fungal pathogen in the airways of adults with cystic fibrosis. Understanding how these species interact with the host and with each other may provide insight into pathology and microbial succession and potentially highlight more efficient therapeutics. The *ex-vivo* pig lung model is suitable for studying host responses to pathogens in an ethical and high-throughput manner due to its rich cell complexity and anatomical and immunological similarity to humans. Proteomic analysis of coinfecting alveolar lung explants identified reduced virulence capacity of *A. fumigatus* in competition with *P. aeruginosa* with reductions in abundance of dipeptidyl-peptidase 5 (-10.30 fold) and thioredoxin reductase gliT (-11.72 fold) and a reduction in amide biosynthetic processes. *P. aeruginosa* flourished in coinfection proliferating in the tissue and increasing protein translation and amino acid biosynthesis and cellular nitrogen utilisation. This is supported by metataxonomic analysis which demonstrates that *A. fumigatus* promotes proliferation of pseudomonadota and *P. aeruginosa* specifically in coinfecting explants. Examination of changes in the host proteome indicated specific nutritional utilisation with *A. fumigatus* inducing greater complement activation and potential utilisation of amino acids to fuel growth. *P. aeruginosa* infection induced greater natural killer cell toxicity and potential butanoate metabolism from the host. Greater inflammation and immune activation were observed in coinfecting samples relative to their respective mono-infected tissue explants, potentially driven by the loss of elastase LasB in coinfection. Coinfection also resulted in the reduction of iron sequestering molecules such as ferritin and lactotransferrin indicating elevated bioavailability of iron which can further fuel *P. aeruginosa* virulence.

Importance:

The lungs of cystic fibrosis (CF) patients are frequently colonised by the fungus *Aspergillus fumigatus* and the bacterium *Pseudomonas aeruginosa*. Previous work has shown that *P. aeruginosa* predominates when co-cultured with *A. fumigatus* in cell culture and murine systems. In this work the interaction of these pathogens while coinfecting *ex vivo* pig lung samples was characterised and demonstrated the proliferation of *P. aeruginosa* populations during infection. Quantitative proteomic analysis revealed greater tissue inflammation and immune activation in coinfecting samples relative to mono-infected samples. The results presented here give an insight into how these two pathogens may interact in the CF lung and highlight potential targets for novel antimicrobial therapies.

6.1 Introduction

The human lung is constantly exposed to microbial colonisation through inhalation of various viruses, bacteria and fungi (Invernizzi *et al.*, 2020). In most cases these microbes are eliminated or inactivated by the host's defences including clearance by coughing, pulmonary macrophages, the ciliary beat of respiratory tract cells, and inhibition by alveolar surfactants (Li *et al.*, 2024). However, in vulnerable patients including immunocompromised individuals and patients with cystic fibrosis (CF), the airway can be colonised by a range of microbial pathogens which are in dynamic competition with the host and each other for dominance in the niche (Gannon and Darch, 2021). *Pseudomonas aeruginosa* and *Aspergillus fumigatus* are ubiquitous microorganisms found in soil, water and plants (Nazik *et al.*, 2020). These species are opportunistic pathogens and are equipped with various virulence factors to aid in colonisation of the airway by suppressing or evading aspects of the host immune defences and dominate other species attempting to do the same. These species represent the principal bacterial and fungal pathogen in the airways of CF adults and neutropenic individuals (Keown *et al.*, 2020) and are considered to have the most devastating impacts on a patient's health (Mayer-Hamblett *et al.*, 2014; Amin *et al.*, 2010). Approximately 15.8% of CF patients are coinfecte with *A. fumigatus* and *P. aeruginosa* (Zhao *et al.*, 2018) and these patients have a poorer prognosis and a greater requirement for intravenous antibiotics (Hughes *et al.*, 2022).

Both species can adopt acute, high-virulence infection phenotypes, resulting in severe host tissue damage and inflammation, but are also capable of switching to a chronic infection phenotype characterised by reduced virulence but tenacious persistence and drug tolerance. Understanding how this switch happens is important in the context of CF lung disease, especially with relevance to the acute exacerbations that punctuate periods of stable infection and result in severe reductions in lung function (Stanford *et al.*, 2021), and with relevance to the ability of *A. fumigatus* to trigger a hypersensitive allergic response (Bouyssi *et al.*, 2023). The role of interactions between coinfecting pathogens in determining overall infection phenotype has long been a matter of investigation in CF microbiology (Zhao *et al.*, 2012; O'Brien and Fothergill, 2017).

Interactions between these two pathogens have been examined in culture, revealing that secreted products from *A. fumigatus* result in *P. aeruginosa* proliferation

and increased expression of proteins associated with denitrification, stress response, replication, amino acid metabolism and efflux pumps (Margalit *et al.*, 2020). Exposure of *A. fumigatus* hyphae to *P. aeruginosa* cells induced increased production of gliotoxin and a decrease in fungal growth. In contrast, exposure of *A. fumigatus* hyphae to *P. aeruginosa* culture filtrate led to increased growth and decreased gliotoxin production (Margalit *et al.*, 2022). This interaction has been studied in *Galleria mellonella* larvae where sublethal *A. fumigatus* infection resulted in increased mortality in subsequent *P. aeruginosa* infection and there was a strain specific response in human bronchial epithelial cells when coinfected with the two pathogens resulting in increased proinflammatory IL-6 and IL-8 production (Reece *et al.*, 2018). Coinfection in an immunocompetent murine model with both pathogens isolated in agar beads demonstrated close proximity of the pathogens is disadvantageous for *A. fumigatus* whereas a larger separation had no effect on fungal burden (Sass and Stevens, 2023). The aim of the work presented here was to establish whether *A. fumigatus* influences *P. aeruginosa* virulence in an *ex-vivo* tissue model with a resident microbiome.

The *ex vivo* pig lung (EVPL) model offers an ethical, high-throughput approach to examine microbial response to host tissue and resulting pathogenesis (Harrington *et al.*, 2020). Sections of pig alveolar tissue combined with synthetic CF mucus have been employed to demonstrate that *LasR* mutant *P. aeruginosa* grows as well as or better than the wild-type strain in the explant replicating results from the clinic where this mutant is frequently isolated in chronically infected CF lungs (Harrison *et al.*, 2014). The EVPL model, combining pig bronchiolar tissue with synthetic CF mucus, also gives a better representation of *Staphylococcus aureus* pathology compared to murine models as mice typically develop *S. aureus* induced abscesses which are rare in human patients and these do not occur in the EVPL explants (Sweeney *et al.*, 2021). The microbiome of healthy pig lungs shows a similar phylum distribution to that found in human lungs (Huang *et al.*, 2018). The microbiome remains difficult to produce in many models employed to study microbial virulence including 2D culture and organoids (Poletti *et al.*, 2020) but it plays a crucial role in shaping both *P. aeruginosa* and *A. fumigatus* development and virulence (Nguyen *et al.*, 2016; Popovic *et al.*, 2023; Nikitashina *et al.*, 2025) including the degradation of host factors such as mucin which can impact *P. aeruginosa* attachment (Flynn *et al.*, 2016; Herrmann *et al.*, 2024).

Understanding how *P. aeruginosa* and *A. fumigatus* influence microbiota dysbiosis alone and in combination may provide key insight into the impacts these species can have in isolation and in combination on the host. In this work label free quantitative proteomic analysis was utilised to examine the interaction of *P. aeruginosa* and *A. fumigatus* with host tissue in pig alveolar tissue sections in tissue culture media, and to characterise the host response to each pathogen in mono-infection and coinfection. In addition, the proteomic response of *A. fumigatus* and *P. aeruginosa* during coinfection was also assessed. Metataxonomic analysis was also employed to assess alterations in the host microbiome as a result of mono and co- infection.

6.2 Results

6.2.1 Visual confirmation of tissue pathology

EVPL sections mono-infected with *P. aeruginosa* at 96 h displayed a green colour indicating production of pyocyanin (Figure 6.1). Tissue mono-infected with *A. fumigatus* displayed fungal growth on the surface. There was less visible fungal growth and green pigmentation on the co-infected tissue sections indicating a distinct pathology relative to the mono-infected explants.

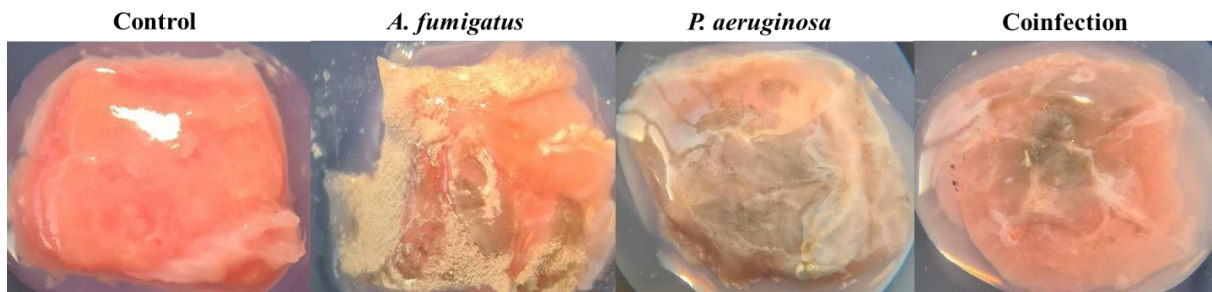


Figure 6.1: Representative image of various treatments at 96 hours post inoculation; uninfected control, *A. fumigatus* mono-infected, *P. aeruginosa* mono-infected and *A. fumigatus* and *P. aeruginosa* coinfecting explants at 20x magnification.

6.2.2 Initial amplicon analysis

The lung microbial community diversity was examined by amplifying the V3-V4 region of the 16S rRNA gene and the eukaryotic ITS2 region. There was a single time point (96 hours) and five treatments in total. (A) Unwashed control, (B) washed control, (C) *P. aeruginosa* mono-infected, (D) *A. fumigatus* mono-infected and (E) *P. aeruginosa* and *A. fumigatus* coinfection. Each treatment was sequenced in triplicate

resulting in 15 individual samples for the downstream 16S and ITS2 analysis respectively. To ensure sampling depth was sufficient to capture the full community diversity Alpha rarefaction curves were undertaken. Both 16S and ITS2 rarefaction curves were close to reaching a plateau suggesting that our samples contained most of the potential community richness (Figure S1).

After filtering, the number of Tags across all fifteen 16S samples ranged from 54,299 to 63,876 and after OTU clustering, the OTU number ranged from 108 to 213 (Table 6.1). Across all 16S samples, 18 Bacterial phyla corresponding to 17 Genera were identified (Table S6.1). Only 8 unique Bacterial species were identified, with the majority of OTUs being unassigned at the species level (except in treatments C and E (Table S6.1). When examining the corresponding samples for high quality ITS2 Tags only samples D and E reported ITS2 Tags (samples D3 and E2 did not have tags). The number of tags ranged from 66,110 to 66,147 and after OTU clustering, the OTU number ranged from 19 to 48 (Table 6.1). The vast majority (>99.99%) of Tags were mapped back to *A. fumigatus* (Table S6.2). Overall, the lack of ITS2 Tags in treatments A, B and C indicates that no Fungal species were found in the lung tissue prior to infection with *A. fumigatus*.

Table 6.1: OTU statistics

16S Samples	Sample	Tag number	OTU number
Unwashed Control	A1	59981	163
	A2	60006	164
	A3	61045	160
Control	B1	63876	165
	B2	56647	151
	B3	62257	108
<i>P. aeruginosa</i> infection	C1	63241	139
	C2	59125	213
	C3	60142	139
<i>A. fumigatus</i> infection	D1	63495	183
	D2	61589	145
	D3	54961	171
Coinfection	E1	56894	168
	E2	60026	147
	E3	54299	209
ITS2 Samples	Sample	Tag number	OTU number
<i>A. fumigatus</i> infection	D1	66147	19
	D2	66132	28
Coinfection	E1	66138	30
	E3	66110	48

6.2.3 *Sus scrofa* lung tissue microbiome

Below we report the relative abundance of Bacterial phyla and genera for five different lung tissue treatments in triplicate. The visualisation of these can be seen in Figure 6.2 and the raw data is located in (Table S6.1). For clarity, relative abundance is a quantitative measure and corresponds to the total number (abundance) of OTUs of a particular kind which is present in a sample, relative to the total number of OTUs in that sample.

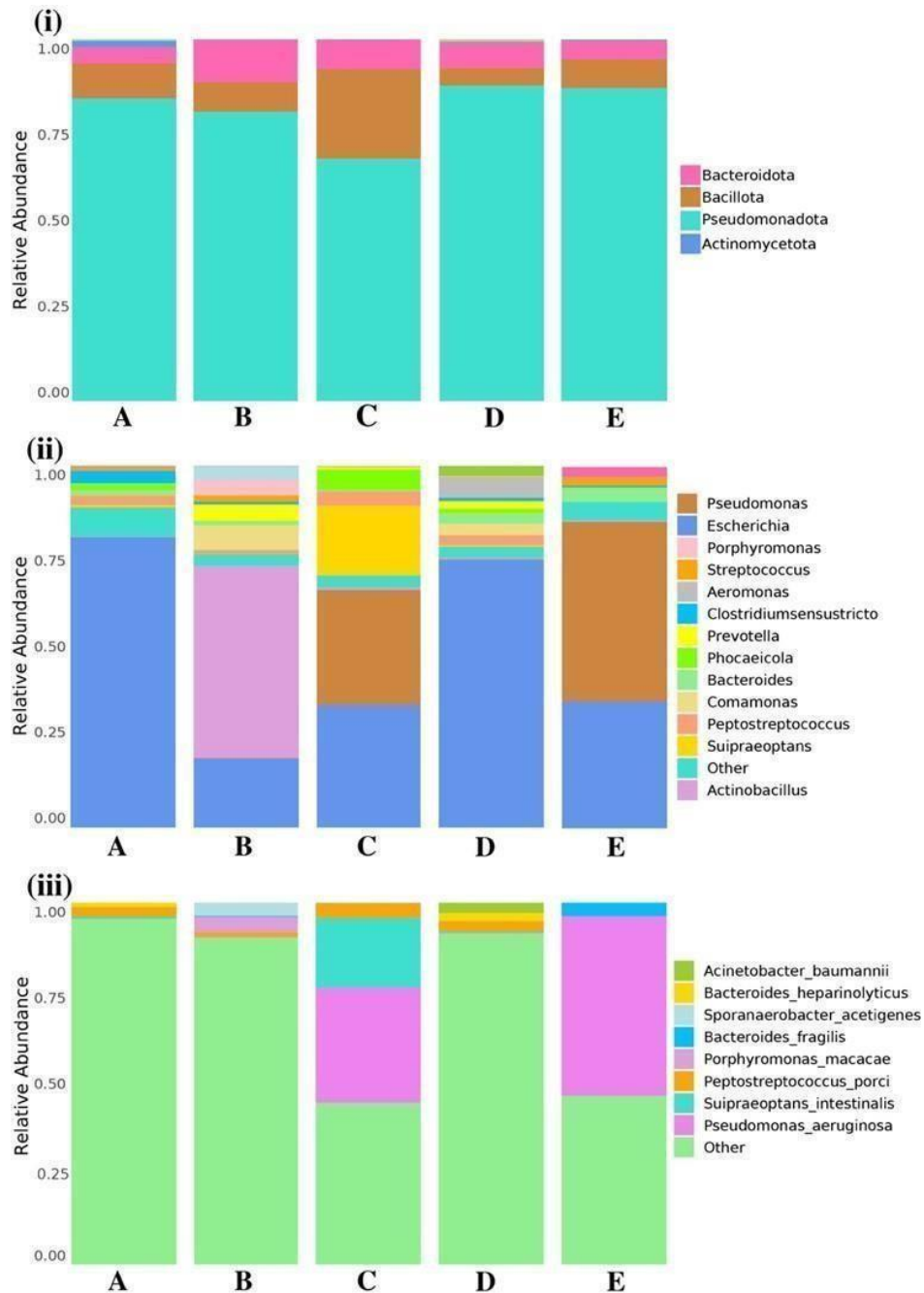


Figure 6.2: Metataxonomic analysis of infected explants (i) Phylum level relative abundance of Bacterial OTUs found in five lung tissue treatments A: unwashed tissue, B: washed tissue, C: *P. aeruginosa* infection, D: *A. fumigatus* infection, E: coinfection. Note only top 4 phyla are shown (>99% of OTUs). Corresponding (ii) Genus level relative abundance and (iii) Species level relative abundance are also shown

In all five treatment types, three Bacterial phyla represent the majority (>99%) of observed OTUs (Figure 6.2(i)) and (Table S6.1). The Pseudomonadota phylum dominates representing 83.61%, 80.04%, 66.96%, 87.22% and 86.51% of all OTUs in treatments A, B, C, D and E respectively. The next two abundant phyla are the

Bacillota (9.75%, 8.14%, 24.83%, 4.83%, 7.97%) and the Bacteroidota (4.48%, 11.68%, 8.06%, 7.14%, 5.12%). The relatively lower abundance of Pseudomonadota species (66.96%) in treatment C is noteworthy as it shows a decrease in the overall abundance of Pseudomonadota species when *P. aeruginosa* is added to the tissue indicating that it may be suppressing the growth of other closely related species (genus-level identification confirms that *Pseudomonas* was only present in appreciable amounts when we inoculated it, see below). Similarly, the relative higher abundance (24.83%) of Bacillota species is also of interest as it indicates that infection with *P. aeruginosa* alone, promotes outgrowth of members of the Bacillota phylum.

Although the relative abundance of phyla between treatments is relatively stable, different genera within phyla seem to be favoured under certain treatment conditions. For example, when comparing the two controls (A vs B), we see that the *Escherichia* genus is most abundant (80.25%) in the unwashed control (A) relative to the washed control (B) where it only accounts for 19.06% of species whereas members of the *Actinobacillus* genus are now the most abundant (53.13%) (Figure 6.2(ii)) and (Table S6.1). The *Escherichia* genus is also most abundant (73.99%) in treatment D (infection with *A. fumigatus* alone). When tissue is mono-infected with *P. aeruginosa* (treatment C), unsurprisingly we see an increase in the relative abundance of members of the *Pseudomonas* genus (31.81%) relative to the controls (0.02%, 0.17%) although it is still not the most abundant genus (*Escherichia*, 33.92%). There is also a marked increase in the relative abundance of members of the *Supraeoptans* genus (Phylum Bacillota) indicating that *P. aeruginosa* infection alone promotes the growth of members of this genus. Significantly, when examining treatment E (coinfection) we observe that the relative abundance of *Pseudomonas* species increases to 49.69% and outcompetes all other genera (Figure 6.2(iii)) and (Table S6.1). The relative abundance of *Supraeoptans* is also significantly reduced (0.04%). Therefore, there appears to be a synergistic effect in coinfections where the presence of *A. fumigatus* promotes the growth of *Pseudomonas* species and allows it to become the dominant genus. Closer inspection of the species level taxonomy of our OTUs shows that all members of the *Pseudomonas* genera are *P. aeruginosa*.

6.2.4 Characterisation of *A. fumigatus* Proteome from coinfecting explants relative to that from mono-infected tissue

Proteomic analysis of *A. fumigatus* from tissue coinfecting with *P. aeruginosa* relative to tissue mono-infected with *A. fumigatus* demonstrated clear separation between the groups (Figure 6.3a) and identified 379 fungal proteins of which 41 proteins were classified as statistically significant and differentially abundant (SSDA) (Figure 6.3b). Only one protein was significantly increased in abundance, 60S ribosomal protein L30, putative (+13.12 fold) in the coinfection *A. fumigatus* sample relative to the mono-infection. 60S ribosomal protein L30 was increased in early-stage hyphal germination (Jia *et al.*, 2020) and was highly detected in murine models and human invasive pulmonary aspergillosis (Machata *et al.*, 2020). Thirty nine fungal proteins were significantly decreased in abundance including aldehyde dehydrogenase (-40.48 fold) associated with response to hypoxia and heat shock (Escobar *et al.*, 2018) and was mutated in azole resistant strains isolated from chronically infected patients (Hagiwara *et al.*, 2014). In addition, proteins associated with virulence were decreased in abundance including dipeptidyl-peptidase 5 (-10.30 fold) and thioredoxin reductase gliT (-11.72 fold). Gene enrichment analysis of the *A. fumigatus* database indicated biological processes associated with nitrogen including S-adenosylmethionine metabolism, protein peptidyl-prolyl isomerisation and amide biosynthetic processes are compromised following coinfection with *P. aeruginosa*, all indicating reduced fitness of *A. fumigatus* as a result of this interaction (Figure S2).

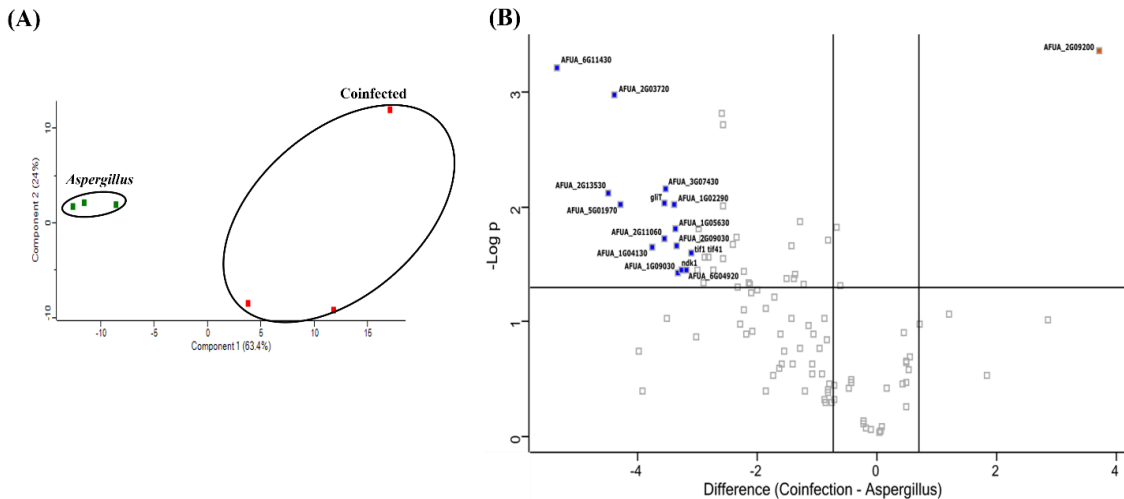


Figure 6.3: (A) Principal component analysis of *A. fumigatus* proteins grown on *ex-vivo* pig lung explants in mono-infection (Green) and coinfection (Red) demonstrating good separation in the proteome between conditions. (B) Volcano plots showing the distribution of statistically significant and differentially abundant (SSDA) proteins which have a $-\log$ (p-value) > 1.3 and difference $+/- 0.58$.

6.2.5 Analysis of changes in *P. aeruginosa* Proteome from coinfecting explants relative to mono-infected samples

Proteomic analysis of *P. aeruginosa* in a coinfection with *A. fumigatus* and *P. aeruginosa* from mono-infected explants show clear distinction from one another (Figure 6.4a) and identified 642 proteins of which 40 proteins were SSDA (Figure 6.4b). Thirty-two *P. aeruginosa* proteins were significantly increased in abundance in the coinfection group compared to mono-infection and these included a large number of small ribosomal subunit proteins including bS16 (+ 3.11 fold), uS17 (+ 2.92 fold), uS5 (+ 2.66 fold) and bS6 (+ 2.30), indicating elevated translation occurring as a result of exposure to *A. fumigatus*. In addition, proteins involved with regulation of amino acids and their amide derivatives in *P. aeruginosa* were increased in abundance including glutathione hydrolase proenzyme (+1.73 fold). Serine hydromethyltransferase 3 (GlyA3) (+2.32 fold) catalyses the reversible conversion of serine and glycine and is the main source of single carbon atoms required for synthesis of purine and methionine (Wang *et al.*, 2023). Pterin-4-alpha-carbinolamine dehydratase (phhB) (+2.93 fold) which catalyses the dehydration step in the cyclic regeneration of tetrahydrobiopterin (BH₄), an essential cofactor required for the phenylalanine hydroxylase reaction (Song *et al.*, 1999). Gene enrichment analysis of *P. aeruginosa* in coinfecting explants highlighted an increase in pathways associated with nitrogen metabolism and utilisation including translation, amide biosynthetic

processes and cellular nitrogen compound biosynthetic processes, suggesting increased cellular activity related to protein synthesis and nitrogen utilisation (Figure S3).

Eight proteins were significantly decreased in abundance in *P. aeruginosa* during coinfection and these included elastase LasB (-6.04) which is associated with virulence. Elastase LasB is capable of degrading the extracellular matrix including elastin, collagen types III and IV, laminin, fibronectin, and vitronectin of host cells (Yang *et al.*, 2015). Additionally, 5-aminovalerate aminotransferase DavT was decreased -4.35 fold in coinfection relative to mono-infection, and is involved in lysine catabolism (Yamanishi *et al.*, 2007), potentially indicating competition during coinfection for host amino acids such as lysine whose bioavailability is limited in the lung, and its presence fuels *A. fumigatus* virulence (Schöbel *et al.*, 2010).

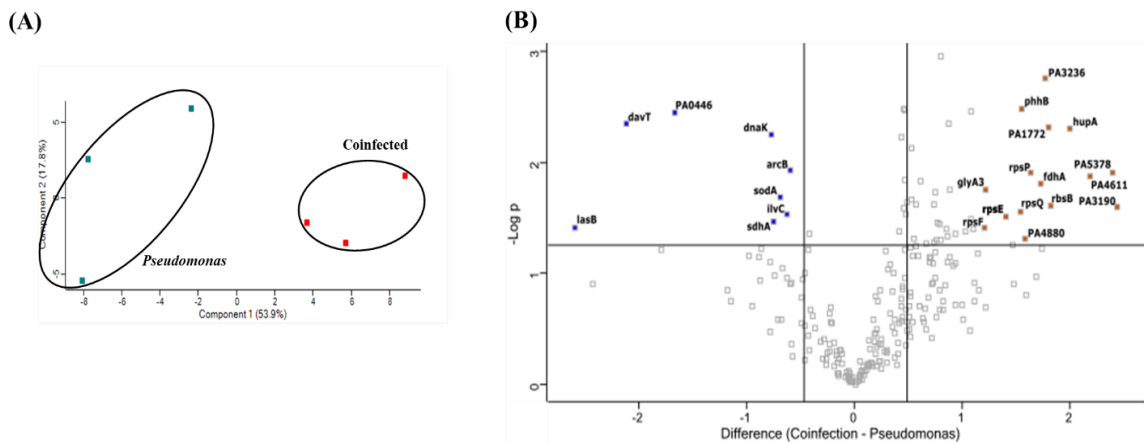


Figure 6.4: (A) Principal component analysis of *P. aeruginosa* proteins grown on *ex-vivo* pig lung explants in mono-infection (Blue) and coinfection (Red) demonstrating good separation in the proteome between conditions. (B) Volcano plots showing the distribution of statistically significant and differentially abundant (SSDA) proteins which have a $-\log$ (p-value) > 1.3 and difference $+/- 0.58$.

6.2.6 *Sus scrofa* proteome in various infection states relative to control

Proteomic analysis of the EVPL explants identified 3183 proteins in total, 130 *S. scrofa* proteins were significantly altered in abundance in the *A. fumigatus* mono-infected tissues relative to the control, 371 were significantly altered in the *P. aeruginosa* mono-infected tissues relative to the control and 133 were significantly altered in abundance in the coinfected tissues relative to the control (Figure 6.5a and b).

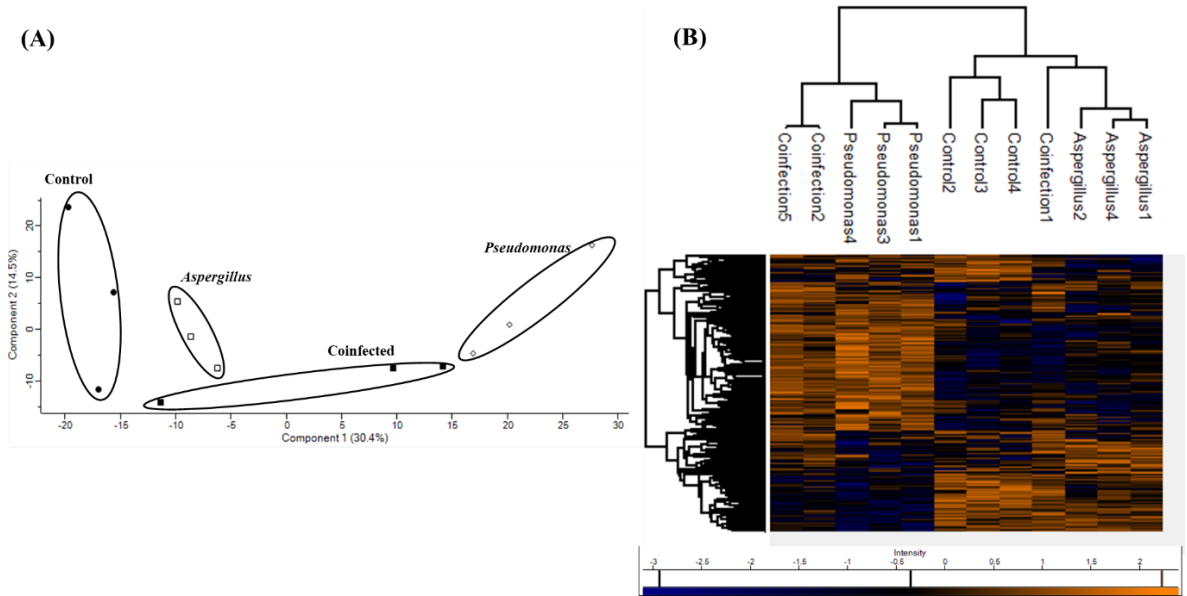


Figure 6.5: (A) Principal component analysis of *S. scrofa* proteins in control (Black circle) or infected with *A. fumigatus* mono-infection (white square), *P. aeruginosa* mono-infection (White Square) and coinfection (Black Square) demonstrating good separation in the proteome between conditions. (B) Heatmap generated through Two-way unsupervised hierarchical clustering of the median protein expression values of all statistically significant differentially abundant proteins.

6.2.7 Proteomic response of *Sus scrofa* to *A. fumigatus* mono-infection relative to control

Proteomic analysis demonstrated significant differences between *A. fumigatus* mono-infected explants compared to the control (Figure 6.6a). Fifty five *S. scrofa* proteins were increased in abundance and these included many proteins associated with fibrosis and tissue remodelling such as collagen type VI alpha 1,2,3 and 6 chains increased +6.11, +5.75, +4.02, +13.97 and +10.55 fold, respectively, and these have been identified as inducing fibrosis (Williams *et al.*, 2022). Plasminogen activator inhibitor 1 (+3.67 fold) is the main inhibitor of the plasminogen activator system, which blocks fibrinolysis and promotes extracellular matrix accumulation in tissues (Ghosh and Vaughan, 2012). There was increased abundance of CD9 molecule (+2.54) which is associated with antifungal extracellular vesicles released by polymorphonuclear leukocytes during *A. fumigatus* infection (Visser *et al.*, 2024). Complement factor H (+2.45 fold) and complement factor B (+2.05 fold), both of which are involved in the alternative pathway indicate some activation during infection (Kang *et al.*, 2024; Kavanagh *et al.*, 2025). Gene enrichment analysis of *A. fumigatus* mono-infected explants (Figure 6.6b) indicates alterations to the extracellular matrix and highlights the activation of the complement and coagulation cascade.

Seventy five proteins were significantly decreased in abundance relative to the control, and included arachidonate 5-lipoxygenase (Alox5) (- 4.15 fold) which is a key regulator of leukotriene biosynthesis and is required for neutrophil recruitment activation in the lungs during invasive pulmonary aspergillosis (Caffrey-Carr *et al.*, 2018). Gene enrichment analysis also highlighted decreased metabolic activity in fungal infected tissue including the citrate cycle and valine, leucine and isoleucine degradation and propanoate metabolism indicating reduced metabolic activity in the host tissue following fungal infection. 2-oxocarboxylic acid metabolism was also decreased in abundance which is involved in branched amino acid biosynthesis (Figure 6.6b).

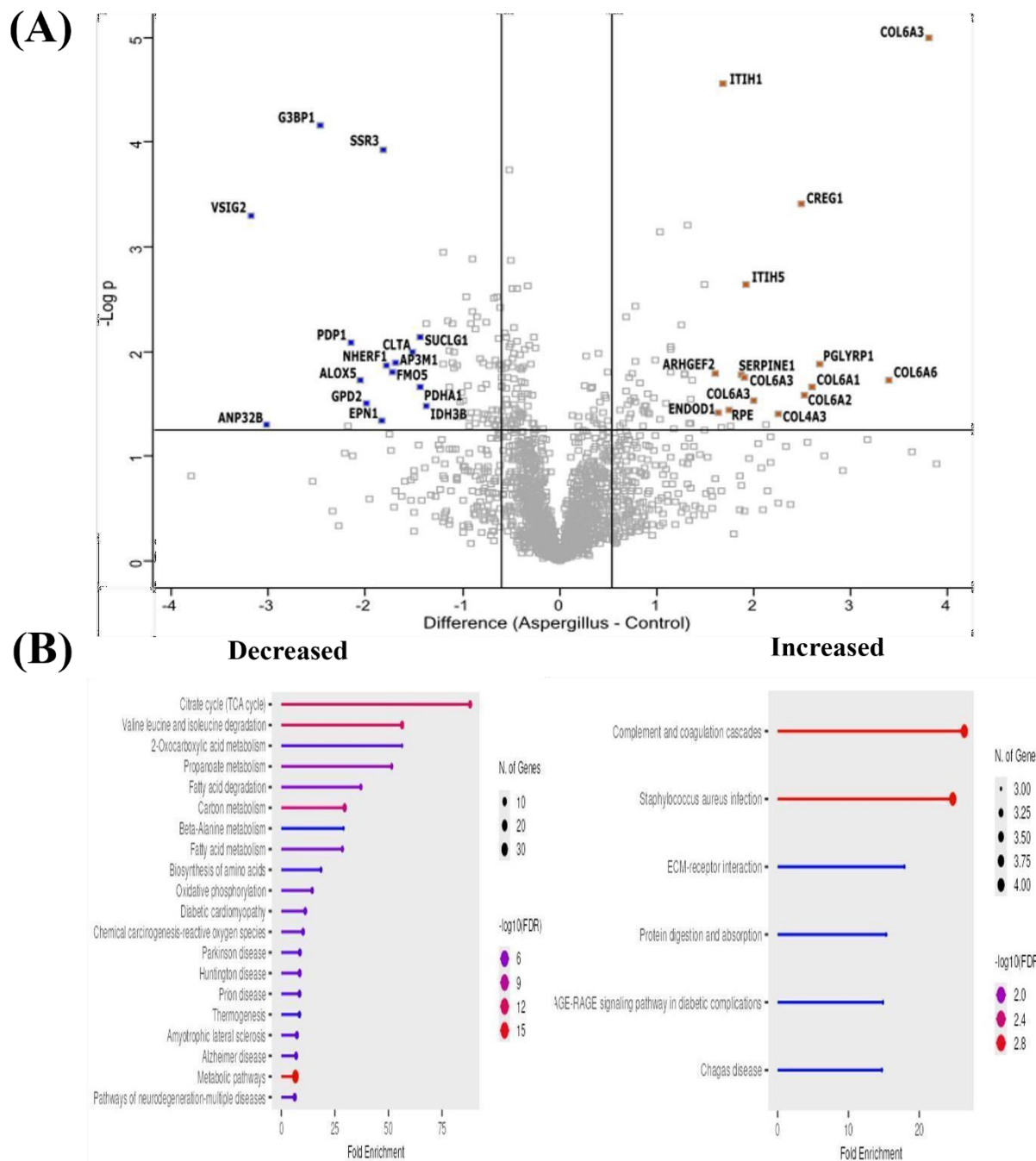
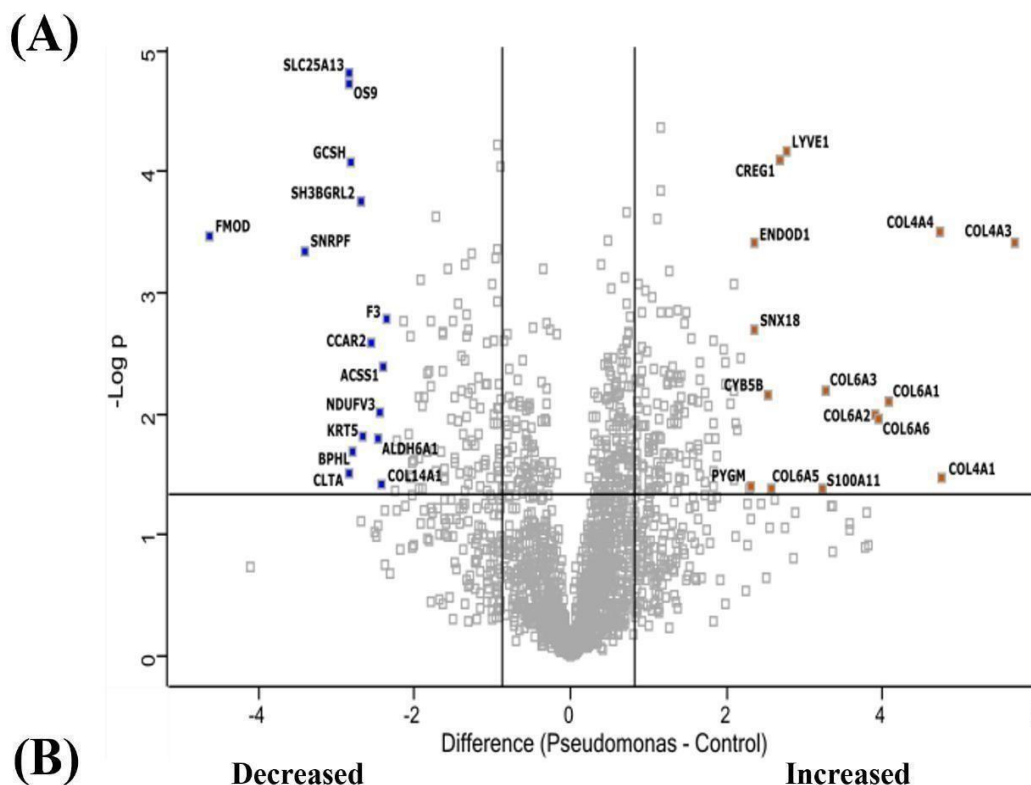


Figure 6.6: (A) Volcano plot of *S. scrofa* proteins in response to *A. fumigatus* mono-infection relative to uninfected explants showing the distribution of statistically significant and differentially abundant (SSDA) proteins which have a $-\log$ (p-value) > 1.3 and difference $+/- 0.58$. (B) Gene enrichment analysis highlight KEGG pathways increased and decreased in response to *A. fumigatus* infection relative to healthy control

6.2.8 Proteomic response of *Sus scrofa* to *P. aeruginosa* mono- infection relative to control

Proteomic analysis demonstrated significant differences between *P. aeruginosa* mono-infected explants compared to the control (Figure 6.7a). Two hundred and twenty-two *S. scrofa* proteins were increased in abundance in the infected tissue compared to the control. There was a significant increase in the abundance of extracellular matrix proteins indicative of tissue fibrosis with collagen type VI alpha chains 1, 2, 3 and 6 increased +16.97, 14.93, 9.78 and 15.57 fold, respectively. In addition, collagen type IV alpha chains 1, 3 and 4 were also increased +27.27, +52.19 and +26.63 fold, respectively. There is evidence of immune antagonism occurring as a result of bacterial infection with a + 9.32 fold increase of protein S100-A11 (Calgizzarin) (Protein S100-C) which is released by neutrophils *via* NETosis and stimulates an inflammatory response through stimulation of IL-6 and Tumour necrosis factor (Navrátilová *et al.*, 2021). Gene enrichment analysis of *P. aeruginosa* mono-infected EVPL tissue (Figure 6.7b) also indicated natural killer cell mediated cytotoxicity. Natural killer cell cytotoxicity was supported by detection of integrin subunit alpha L (+2.31 fold), a gene specifically associated with natural killer cell tissue residency (Hegewisch-Solloa *et al.*, 2021) and cellular repressor of E1A stimulateds 1 (Creg1) increased + 6.39 fold which is localised to the endosomal-lysosomal compartment where it promotes lysosomal biogenesis, acidification and degradation (Liu *et al.*, 2021).



(B)

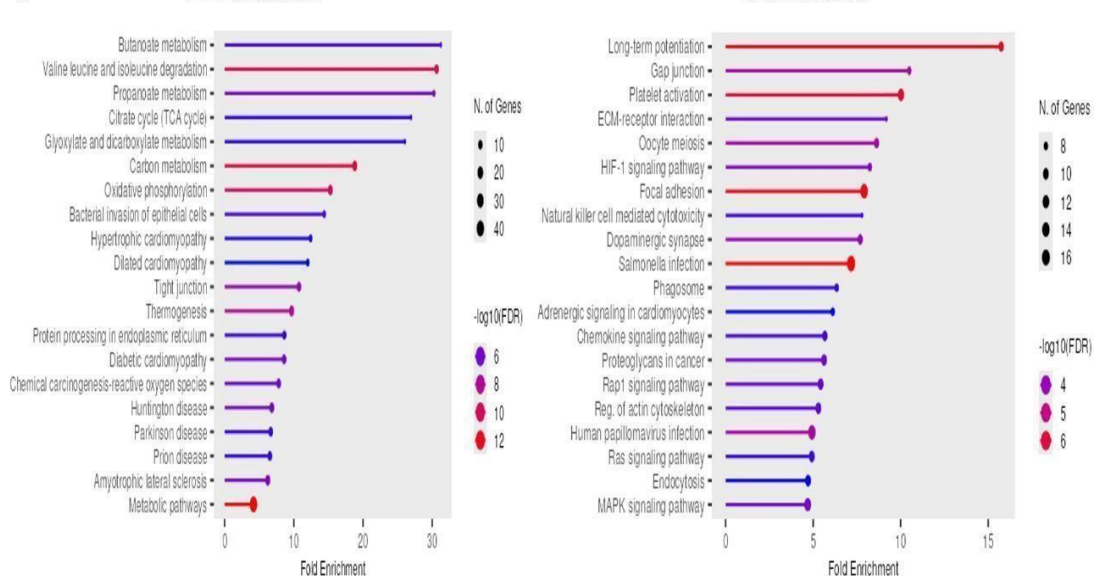


Figure 6.7: (A) Volcano plot of *S. scrofa* proteins in response to *P. aeruginosa* mono-infection relative to uninfected explants showing the distribution of statistically significant and differentially abundant (SSDA) proteins which have a $-\log$ (p-value) > 1.3 and difference $+/- 0.58$. (B) Gene enrichment analysis highlight KEGG pathways increased and decreased in response to *P. aeruginosa* infection relative to healthy control

P. aeruginosa can induce a hypoxic microenvironment (Schaible *et al.*, 2012). This may be occurring as gene enrichment analysis highlights HIF-1 α signalling, which is known to be upregulated in response to bacterial infection (Kiani *et al.*, 2021). This is supported by detection of signal transducer and activator of transcription 3 (STAT3) (+1.72 fold) which in combination with HIF-1 α cooperatively mediate the transcriptional and physiological responses to hypoxia (Dinarello *et al.*, 2023). Heme oxygenase 1 (+1.68 fold) a stress induced enzyme that is induced by HIF-1 α in hypoxic conditions (Dunn *et al.*, 2021) was also detected supporting the induction of hypoxia as a result of bacterial infection.

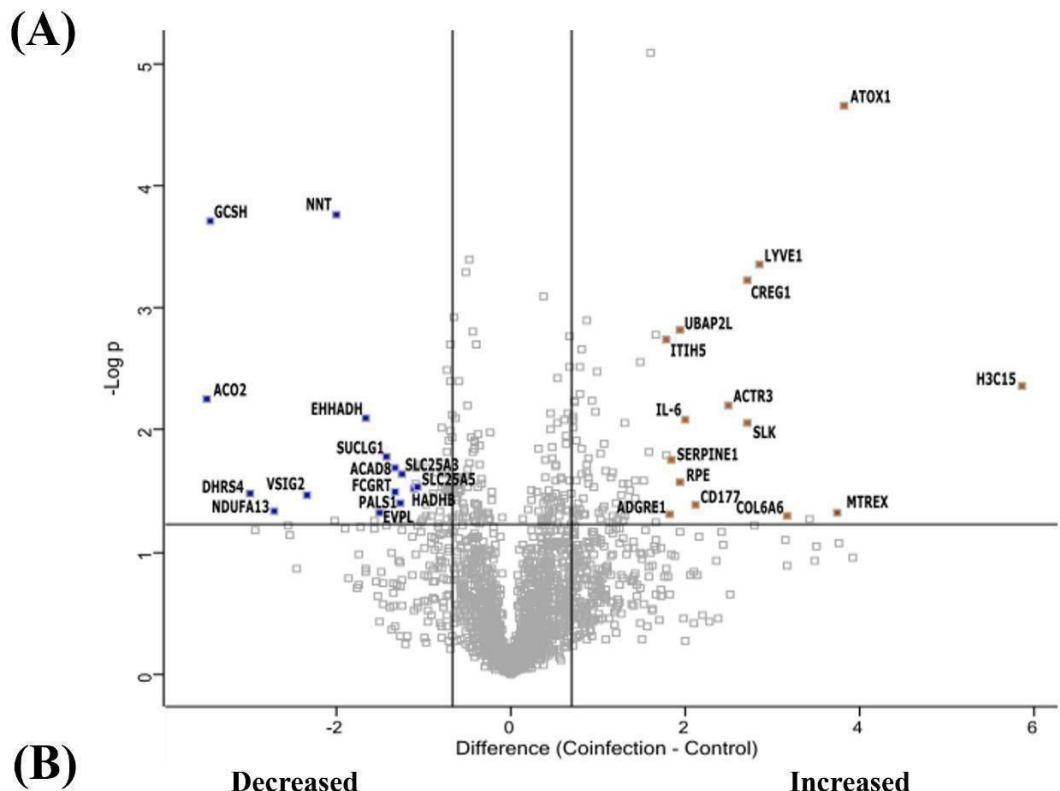
One hundred and forty-nine *S. scrofa* proteins were significantly decreased in abundance during *P. aeruginosa* mono-infection relative to the controls. Fibromodulin (keratan sulfate proteoglycan fibromodulin) was decreased -24.87 fold and this has an important role in regulating TGF- β 1 signalling by sequestering the active form of this growth factor in the extracellular matrix and the complement cascade. Complement component 1 Q subcomponent-binding protein, mitochondrial was decreased in abundance -2.15 fold. Fibromodulin also interacts with the complement factor H (-2.41 fold) and C4b-binding protein (C4BP) (-4.21), inhibitors of the complement system, limiting complement activation to the early part of the classical pathway. Gene enrichment analysis of the proteomic response of host tissue to *P. aeruginosa* mono-infection indicated reduced metabolic activity including butanoate metabolism, valine leucine and isoleucine degradation, propanoate metabolism and citrate cycle. Butanoate metabolism is associated with chronic persistence of *P. aeruginosa* in hypoxic biofilm as it is required for promoting planktonic cells to the biofilm state and could serve as a marker for biofilm development (Abdelhamid and Yousef, 2024) (Figure 6.7b).

6.2.9 Proteomic response of *Sus scrofa* to co-infection infection relative to control

Proteomic analysis demonstrated significant differences between *A. fumigatus* and *P. aeruginosa* coinfecting explants compared to the control (Figure 6.8a). Eighty-three *S. scrofa* proteins were increased in abundance including histone H3 (+58.27 fold), which is known to be released during NETosis (Grilz *et al.*, 2019) a process induced by both *P. aeruginosa* (Yoo *et al.*, 2014) and *A. fumigatus* (McCormick *et al.*, 2010). Complement factor B and H were increased +1.84 fold and +1.83 fold,

respectively, in coinfecting explants relative to the control, indicating activation of the alternative complement cascade. Natural killer cell mediated cytotoxicity may also be activated in coinfection as cellular repressor of E1A stimulated 1 (Creg1) was increased +6.54 fold in coinfecting EVPL explants. In addition, protein-tyrosine-phosphatase (EC 3.1.3.48) encoded by the gene PTPN6 was increased +1.78 fold in *P. aeruginosa* mono-infection and + 1.70 fold in coinfecting EVPL respectively. PTPN6 has been identified as playing a role in natural killer cells, T cell regulation and differentiation, and the JAK-STAT pathway (Zhong *et al.*, 2025).

Fifty *S. scrofa* proteins were significantly decreased in abundance in the coinfecting EVPL explants relative to the controls. Many of these proteins are involved in metabolic processes including valine leucine and isoleucine degradation including 3-hydroxyisobutyrate dehydrogenase (-1.52 fold) and acyl-CoA dehydrogenase family member 8 (-2.49 fold) (Meyer *et al.*, 2021; Sabbagh *et al.*, 2011). Gene enrichment analysis of coinfecting explants (Figure 6.8b) highlighted 2-oxocarboxylic acid metabolism, only detected in *A. fumigatus* mono-infection and glyoxylate and dicarboxylate metabolism, only detected in *P. aeruginosa* mono-infection were also detected in coinfecting EVPL indicating a combined impact on the host tissue when both species are present and a unique pathology with shared attributes of both components has been identified.



(B) Decreased Increased

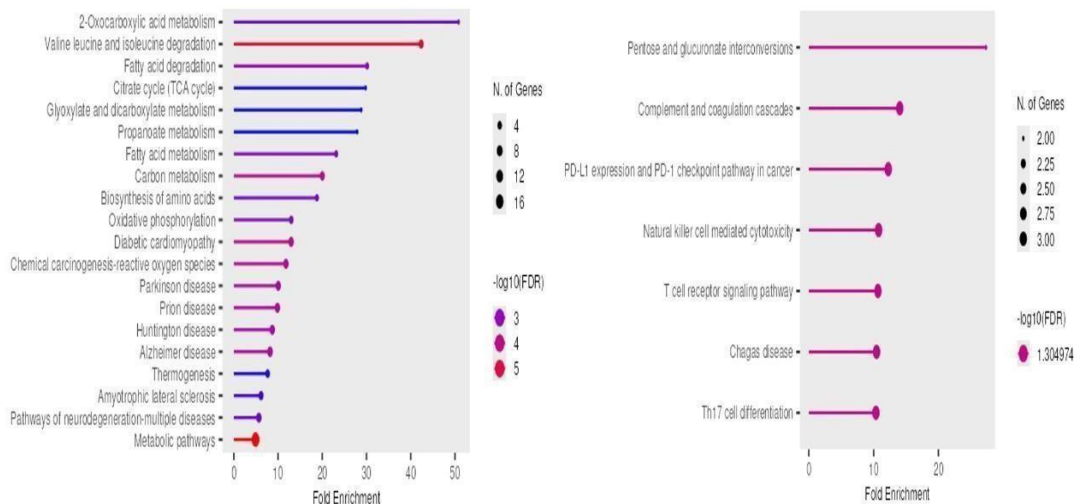


Figure 6.8: (A) Volcano plot of *S. scrofa* proteins in response to *A. fumigatus* and *P. aeruginosa* coinfection relative to uninjected explants showing the distribution of statistically significant and differentially abundant (SSDA) proteins which have a $-\log$ (p-value) > 1.3 and difference $+/- 0.58$. (B) Gene enrichment analysis highlight KEGG pathways increased and decreased in response to coinfection relative to healthy control

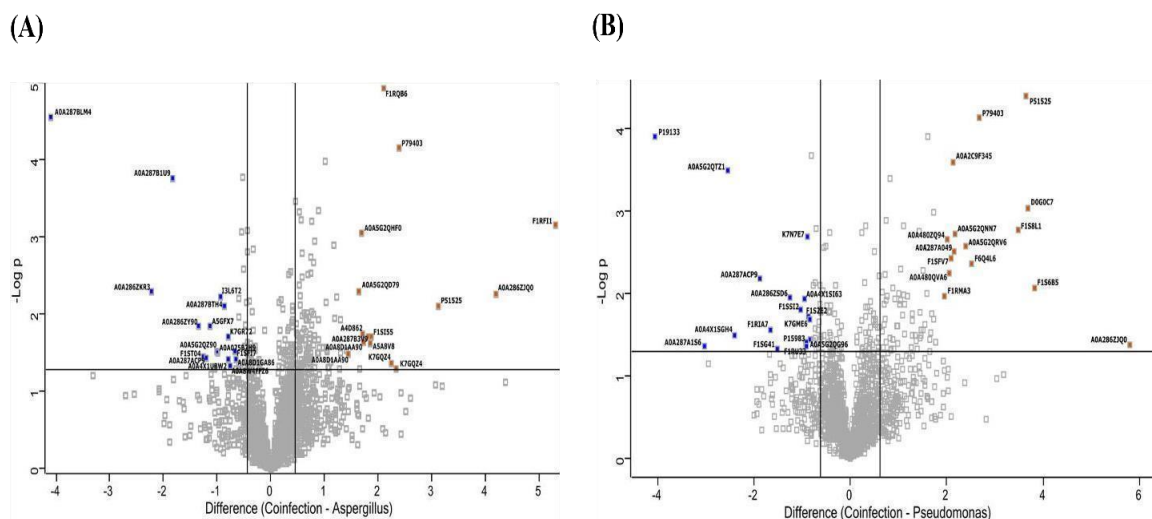
6.2.10 Analysis of *Sus scrofa* proteome in coinfecte dEVPL relative to mono-infected explants

When comparing the *S. scrofa* proteome in the coinfecte dEVPL explants to *A. fumigatus* mono-infected samples, 79 *S. scrofa* proteins were significantly increased in abundance and 19 proteins were significantly decreased (Figure 6.9a). Arachidonate 5-lipoxygenase was increased (+4.77 fold), and the production of arachidonate 5-lipoxygenase may induce a proinflammatory state (Steinhilber *et al.*, 2010). Myeloperoxidase was increased +1.96 fold. Collagen type VI alpha 3 chain (-17.16 fold) is a microfibrillar component of the extracellular matrix and is essential for the stable assembly process of collagen VI (Wang and Pan, 2020). Cingulin was decreased -2.38 fold relative to that in *A. fumigatus* mono-infected EVPL tissue. Cingulin is an adaptor protein, involved in the organization of the tight junctions and participates in endothelial barrier function (Tian *et al.*, 2016; Schossleitner *et al.*, 2016).

Seventy-four proteins were significantly increased in abundance, and 35 proteins were significantly decreased in the coinfection EVPL tissue relative to *P. aeruginosa* mono-infection (Figure 6.9b). Fibromodulin (keratan sulfate proteoglycan fibromodulin), involved in complement activation increased +14.27 fold in the coinfection tissue. There is also evidence of a more potent activation of the adaptive immune response with Janus kinase and microtubule interacting protein 1 increased + 11.15 fold (Libri *et al.*, 2008). In addition, basal cell adhesion molecule was increased +5.23 fold relative to that *P. aeruginosa* mono-infected tissue, and it induces leukocyte recruitment resulting in a proinflammatory microenvironment (Huang *et al.*, 2014). There is also evidence that fibrosis is occurring more prominently in coinfecte dEVPL tissue relative to *P. aeruginosa* mono-infection with fibrinogen beta and gamma chains increased +2.05 and +2.04 fold, respectively. These proteins polymerise with fibrinogen alpha chain following to produce an insoluble fibrin matrix and are known to be elevated in murine models of pulmonary fibrosis (Lu *et al.*, 2021; Principi *et al.*, 2023). Proteins decreased in abundance in the coinfecte dEVPL tissue relative to *P. aeruginosa* mono-infection indicate reduction in proteins associated with iron sequestering and storage. Ferritin light chain (Ferritin L subunit) and lactotransferrin (lactoferrin), were decreased -16.50 fold and -1.55 fold, respectively.

Eleven proteins were SSDA in the coinfecte dEVPL tissue relative to both mono-infected samples, 10 proteins increased and 1 decreased in abundance. Histone

H3 was increased + 18.37 fold and this protein is known to be released during NETosis (Grilz *et al.*, 2019) a process induced by both *P. aeruginosa* (Yoo *et al.*, 2014) and *A. fumigatus* (McCormick *et al.*, 2010). Prophenin-2 (C12) (PF-2) (PR-2) (Prophenin-1-like) increased +8.77 and +12.54 fold relative to that in EVPL *A. fumigatus* and *P. aeruginosa* mono-infected, respectively. Prophenin 2 is released by leukocytes during degranulation. Interleukin-6 was also increased + 3.28 fold relative to that in *A. fumigatus* infected EVPL and + 2.44 fold relative to *P. aeruginosa* infection. IL-6 has a pivotal role in protective immunity against *Aspergillus* in mice (Heldt *et al.*, 2017). The only protein decreased in abundance in the coinfecting EVPL tissue compared to both mono-infected samples was peroxisomal bifunctional enzyme (multifunctional enzyme 1, coded by EHHADH), and this was decreased -2.30 fold relative to that in *A. fumigatus* mono-infection and -3.66 fold relative to that in *P. aeruginosa* mono-infection. EHHADH is primarily expressed on macrophages and was downregulated in patients with neutrophilic asthma and was significantly decreased in non-eosinophilic asthma patients and positively correlates with airflow limitation (Chen *et al.*, 2024).



6.3 Discussion

In CF patients *P. aeruginosa* and *A. fumigatus* are the dominant species of their respective kingdoms and can have detrimental impacts on the host. Their prevalence and the frequency of co-colonisation suggest they can potentially interact in the CF lung (Amin *et al.*, 2010; Al Shakirchi *et al.*, 2021; Chesshyre *et al.*, 2024; Hong *et al.*, 2020; Nayir Buyuksahin *et al.*, 2022), but the available literature does not present a clear picture of how co-colonisation affects infection virulence. The work presented here provides novel insights into how these pathogens interact in an *ex-vivo* pig lung model with a resident microbiome. A major advantage of *ex vivo* models to study the interactions of these pathogens is their ability to reflect the complex architecture of the lung both in terms of topography and richness of cell types (Grassi and Crabbé, 2024). The general anatomic features of the porcine airways are similar to those in the human, with some minor exceptions (Rogers *et al.*, 2008). For these reasons the EVPL model serves as a promising model to characterise host factors that form the environment in which *P. aeruginosa* and *A. fumigatus* compete for dominance and can influence their interactions. In a previous study, we used alveolar tissue sections from freshly-slaughtered pigs to reflect the ability of *A. fumigatus* to infect the lower airways and showed that combining this with tissue culture media supported the survival of the tissue for the duration of lab experiments, allowing us to assess the changes in both host and pathogen proteome over 96 hours (Curtis *et al.*, 2025). We have now built on this work by exploring co-culture of *A. fumigatus* and *P. aeruginosa* in the same model conditions.

Visual assessment of infected explants indicated competition between pathogens in the co-infected samples (Fig 1). Metataxonomic analysis of these explants identified a dynamic microbial community resident within the tissue and demonstrated that both pathogens alter the host microbiome when present in isolation and in combination. *P. aeruginosa* mono-infection results in decreased abundance of Pseudomonadota species indicating it outcompetes closely related species while promoting colonisation of Bacillota (formerly firmicutes) species. *A. fumigatus* mono-infection also alters the host microbiome resulting in promotion of Pseudomonadota phylum, but more specifically the genus Escherichia. Further work would be needed to assess how changes in relative abundance of the endogenous microbiota constituents relate to increases *versus* decreases in cell numbers. Despite this, we can clearly

conclude that when in coinfection, *P. aeruginosa* dominates much more prominently than it does in mono-infection. This confirms that *A. fumigatus* can facilitate *P. aeruginosa* dominance in the airway. The mechanism behind this dominance can be elucidated by examining the proteomic changes elicited in each species during their interaction.

Proteomic analysis of *A. fumigatus* in coinfection relative to mono-infection revealed a reduction in the abundance of proteins associated with virulence. Virulence-associated *A. fumigatus* proteins that altered in abundance included di-peptidyl-peptidase 5 (-10.30 fold) and thioredoxin reductase gliT (-11.72 fold). Dipeptidyl-peptidase 5 is not essential for pathogenicity but may function as part of a concerted action or contributing to the infection process and was induced during infection (Wartenberg *et al.*, 2011; Guruceaga *et al.*, 2018). Thioredoxin reductase gliT is associated with self-protection against Gliotoxin was decreased in abundance which could indicate reduced gliotoxin production as deletion of this gene has been shown to completely disrupt gliotoxin secretion (Schrettl *et al.*, 2010). In addition enolase, previously demonstrated to inhibit the complement cascade (Dasari *et al.*, 2019) was decreased (-4.63 fold) in *A. fumigatus* in coinfecting sections. Proteins associated with numerous processes involving nitrogen utilisation were also decreased in abundance in coinfection as identified by gene enrichment analysis including, S-adenosylmethionine metabolism including adenosylhomocysteinase (-2.85 fold) and S-adenosylmethionine synthase (-4.40 fold) indicating competition for sulphur containing amino acids cysteine and methionine, both of which have been associated with fungal growth and virulence in the host (Amich *et al.*, 2016).

P. aeruginosa cysteine metabolism was enhanced in coculture with *A. fumigatus* (Margalit *et al.*, 2020). Amide biosynthetic processes were also compromised following coinfection with *P. aeruginosa* indicating reduced nitrogen availability for the fungus which is crucial to protein synthesis and fungal development and virulence (Krappmann and Braus, 2005). All of these factors indicate reduced availability of key nutrients, potentially because of competition from *P. aeruginosa*, possibly weakening *A. fumigatus*. This is supported by an increase in similar processes in *P. aeruginosa* in coinfection relative to mono-infection such as small ribosomal subunit proteins, indicating elevated translation occurring as a result of exposure to *A. fumigatus*. In addition, proteins involved with regulation of amino acids and their

amide derivatives in *P. aeruginosa* were increased in abundance including serine hydromethytransferase 3 (GlyA3) (+2.32 fold) and glutathione hydrolase proenzyme (+1.73 fold) also annotated as periplasmic gamma-glutamyltranspeptidase encoded by the *ggt* gene. This enzyme catalyzes the transfer of γ -glutamyl groups from donor molecules to target or acceptor substrates including amino acids and peptides. This enzyme may have a role in glutamate-related metabolism in *Pseudomonas* (Lundgren *et al.*, 2021).

In Coinfection with *A. fumigatus* there was a significant decrease in elastase LasB (-6.04 fold) which is associated with acute virulence and is the most abundant protease produced by *P. aeruginosa* (Sun *et al.*, 2020). LasB is also a potent immune evasion molecule in chronic infections through its ability to manipulate host responses (Suarez-Cuartin *et al.*, 2017). Paradoxically, the strong inflammatory responses to *P. aeruginosa* are often associated with bacterial persistence and tissue damage (Lin and Kazmierczak, 2017) and *lasR*, which regulates LasB loss of function mutants frequently arise in chronically infected CF patients and are associated with greater neutrophilic inflammation and immunopathology in both murine models and human patients (LaFayette *et al.*, 2015). The decreased abundance of elastase (LasB) (-6.04 fold) in the coinfection group indicates this phenomenon could be occurring in the lung explants, driving inflammatory responses at the expense of *A. fumigatus* clearance. This is supported by the increased detection of arachidonate 5- lipoxygenase, a key regulator of leukotriene biosynthesis and is required for neutrophil recruitment activation in the lungs during invasive pulmonary aspergillosis (Caffrey- Carr *et al.*, 2018). This protein was increased in abundance in coinfecting (+4.77 fold) tissue relative to *A. fumigatus* mono-infected explants. This protein was identified as being decreased in *A. fumigatus* mono-infected explants (-4.15 fold) relative to control and is a target of immune evasion by *A. fumigatus* through production of gliotoxin which has been shown to inhibit Leukotriene A4 Hydrolase (Günther *et al.*, 2024; König *et al.*, 2019).

In response to *A. fumigatus* mono-infection many porcine proteins associated with lung fibrosis were increased in abundance including collagen type VI alpha chains which are known to be deposited during tissue fibrosis (Mereness and Mariani, 2021). This is further supported by the increase in transforming growth factor-beta- induced protein ig-h3 (+1.71 fold), a pro-inflammatory marker (Kim *et al.*, 2016) which

is induced by TGF- β . This suggests *A. fumigatus* infection is inducing tissue remodelling and an inflammatory environment within the host. The reduction in numerous metabolic processes in the host including valine, leucine and isoleucine degradation including methylmalonate-semialdehyde dehydrogenase (-1.91 fold) and 3-Hydroxyisobutyryl-CoA hydrolase (-2.22 fold), crucial for valine degradation (Dobrowolski *et al.*, 2020; Çakar and Görükmez, 2021) indicated reduced metabolic activity in the host tissue following fungal infection. 2-Oxocarboxylic acid metabolism was also compromised including Branched-chain-amino-acid aminotransferase (-1.75 fold), involved in the initial catalysis of branched-chain amino acid (Cao *et al.*, 2024) and Isocitrate dehydrogenase [NAD] subunit (-2.20 fold) which catalyses the conversion of isocitrate to α -ketoglutarate to fuel the TCA cycle (Chotirat *et al.*, 2012). The biosynthesis of the branched aliphatic proteinogenic amino acids valine, leucine, and isoleucine also depend on precursors produced from 2-oxocarboxylic acid metabolism (Kirschning, 2022). Amino acid metabolism is known to stimulate *A. fumigatus* virulence and this would suggest that *A. fumigatus* degrades host proteins to scavenge for nutrients (Hartmann *et al.*, 2011). *A. fumigatus* relies heavily on the amino acids valine, isoleucine, and methionine as carbon sources during invasive aspergillosis (Ibrahim-Granet *et al.*, 2008), which was also decreased in abundance in the infected explants. The catabolism of host amino acids leads to the accumulation of propionyl-CoA, which is incorporated as pyruvate into the primary metabolism *via* the methylcitrate cycle-a pathway closely linked to the TCA cycle (Garbe and Vylkova, 2019).

Many extracellular matrix component proteins were increased in abundance in *P. aeruginosa* mono-infected tissue including type VI but also type IV collagen chains which are elevated in response to epithelial damage (Urushiyama *et al.*, 2015). Fibroblasts enhanced the expression of α 1 and α 2 chains of type IV collagen after transforming growth factor- β 1 stimulation (Urushiyama *et al.*, 2015). There was also evidence of Natural killer cell mediated toxicity. Natural killer cells directly kill extracellular *P. aeruginosa* through a contact-dependent process that requires granzyme induced ROS production (Feehan *et al.*, 2022). Host proteins decreased in abundance during *P. aeruginosa* mono-infection indicate utilisation of host nutrients in a similar manner to *A. fumigatus* infection but also displays elements of immune evasion with evidence of degradation of complement factors including complement

component 1 Q subcomponent-binding protein, mitochondrial was decreased in abundance -2.15 fold, complement factor H (-2.41 fold) and C4b-binding protein (C4BP) (-4.21). *P. aeruginosa* elastase can destroy several complement proteins, including cell-bound C3 and fluid phase C9, and inactivate others, including fluid phase C2, C4, C6, and C7. C1q and C3 were degraded by both elastase and alkaline protease derived from *P. aeruginosa* (Hastings *et al.*, 2023). Fibromodulin (keratan sulfate proteoglycan fibromodulin) was also decreased -24.87 fold and activates the classical and alternative pathways of complement *via* direct binding to complement elements C1q and C3b. Mice lacking fibromodulin displayed abnormal wound healing, which correlates with elevated inflammatory cell infiltration and accelerated epithelial cell migration and increased type I TGF- β receptor levels in individual inflammatory cells at wound sites (Zheng *et al.*, 2016).

The decrease in the abundance of LasB was specific to coinfection with *A. fumigatus* indicating specific response and consequences within the host. This suggests that *P. aeruginosa* could be manipulating the host immune response to outcompete *A. fumigatus*. Decreased expression of valine degradation methylmalonate-semialdehyde dehydrogenase (-5.55 fold) and 3-hydroxyisobutyryl- CoA hydrolase (-2.71 fold) similarly to *A. fumigatus* infection but to a more significant factor. *P. aeruginosa* mono-infected tissue also highlights butanoate metabolism including a decrease in Succinate-semialdehyde dehydrogenase (-4.13 fold) and Succinyl-CoA:3-ketoacid coenzyme A transferase 1 is annotated as part of the pathway (Zhang and Yang, 2022). Butanoate metabolites, particularly acetoin, is associated with chronic persistence of *P. aeruginosa* in hypoxic biofilm as it is required for promoting planktonic cells to the biofilm state (Abdelhamid and Yousef, 2024). Reduction in host Butanoate metabolism could indicate leaching specific nutrients from the host to fuel its own chronicity.

Histone H3 was significantly increased in abundance in coinfecting explants relative to uninfected controls (+58.27 fold) and is known to be released during NETosis (Grilz *et al.*, 2019) a process induced by both *P. aeruginosa* and *A. fumigatus*. There was less prominent expression of collagen subunits potentially indicating reduced remodelling occurring in the coinfection when compared to each species colonisation in isolation. The proteome of the coinfecting explants also indicated a mixed phenotype when compared to mono-infection with complement activation, as

observed in *A. fumigatus* infection and Natural killer cell cytotoxicity, as observed in *P. aeruginosa* infection, both occurring when the species coinfect the lung. The decrease in metabolic processes indicate competition over some nutrients including propanoate and Valine leucine and isoleucine but also specific alterations including 2-Oxocarboxylic acid metabolism, only detected in *A. fumigatus* infection and Glyoxylate and dicarboxylate metabolism, only detected in *P. aeruginosa* infection were also detected indicating a combination impact on the host tissue when both species are present and a unique pathology with shared attributes of both components has been identified. 2-Oxocarboxylic acid metabolism can stimulate *A. fumigatus* development and the glyoxylate and dicarboxylate metabolism pathway allows *P. aeruginosa* to grow on limited carbon sources by synthesizing macromolecules from two-carbon compounds such as ethanol and acetate. Additionally, the glyoxylate cycle is up-regulated in *P. aeruginosa* under conditions of oxidative stress and antibiotic stress, which induces oxidative stress (D'Arpa *et al.*, 2021).

When comparing coinfecting explants to *A. fumigatus* mono-infection there is further evidence of elevated inflammation including increased abundance of myeloperoxidase (+1.96 fold), also detected to be increased +2.92 fold in *P. aeruginosa* mono-infected explants but decreased -3.62 fold in *A. fumigatus* mono-infected explants relative to the control. Myeloperoxidase is a potent inhibitor of both *A. fumigatus* (Balloy and Chignard, 2009) and *P. aeruginosa* (Dickerhof *et al.*, 2019). There was a decrease in proteins associated with tissue structure in the coinfecting tissue relative to *A. fumigatus* mono-infected tissue. Collagen type VI alpha 3 chain (- 17.16) is a microfibrillar component of the extracellular matrix and is essential for the stable assembly process of collagen VI (Wang and Pan, 2020).

There is evidence of potent activation of the adaptive immune response in coinfecting explants. Janus kinase and microtubule interacting protein 1 was increased +11.15 fold relative to *P. aeruginosa* mono-infection. Induction of Jakmip1 occurs upon TCR/CD28 stimulation and parallels induction of effector proteins, such as granzyme B and perforin (Libri *et al.*, 2008). In addition, basal cell adhesion molecule was increased +5.23 fold relative to *P. aeruginosa* mono-infected tissue, which was also increased +1.69 fold in *A. fumigatus* mono-infected tissue and decreased -4.43 fold in *P. aeruginosa* mono-infected explants relative to uninfected controls, respectively. This protein drives leukocyte recruitment resulting in a proinflammatory

microenvironment (Huang *et al.*, 2014) indicating increased inflammation and immune recruitment during coinfection. In coinfection EVPL samples Interleukin-6 was also increased in abundance relative to both mono-infections, increased +3.28 fold relative to *A. fumigatus* mono-infection and +2.44 fold relative to *P. aeruginosa* mono-infection. IL-6 has a pivotal role in protective immunity against *A. fumigatus* infection in mice (Heldt *et al.*, 2017). Elevated IL-6, high local neutrophil counts and lung oedema were characteristic signs of a temporary decline in lung function and correlate with signs of histologic inflammation in response to *P. aeruginosa* infection (Wölbeling *et al.*, 2011).

Proteins decreased in abundance in the coinfecting EVPL tissue relative to *P. aeruginosa* mono-infected tissue include proteins associated with iron sequestering and storage. Ferritin light chain (Ferritin L subunit) (-16.50 fold), an iron-binding protein was found to be decreased in *A. fumigatus* infection in air-liquid interface models, which results in an increased amount of free iron available to the fungus (Toor *et al.*, 2018). Lactotransferrin was also decreased -1.55 fold and it is released by neutrophils typically in response to inflammation and has potent antifungal activity *via* iron and fungal siderophore sequestration (Zaremba *et al.*, 2007; Leal *et al.*, 2013). Lactoferrin levels were found to be decreased in CF patients with *P. aeruginosa* infection (Rogan *et al.*, 2004). This would suggest elevated iron availability during coinfection relative to *P. aeruginosa* mono-infection and weakening of host defences against both pathogens. Iron availability has been identified as being crucial for *A. fumigatus* proliferation and plays a pivotal role in fungal virulence (Moore, 2013). There is evidence suggesting that immunocompromised patients with iron-overload after transplantation are at high risk of developing invasive aspergillosis (Matthaiou *et al.*, 2018).

6.4 Conclusion

Proteomic analysis of coinfection between *A. fumigatus* and *P. aeruginosa* in a realistic host model provides new insight into how the species interact and the consequences of these interactions for the host. *P. aeruginosa* dominates in coinfection at the expense of *A. fumigatus* as supported by metataxonomic analysis where *A. fumigatus* induces dysbiosis favouring growth of Pseudomonadota and *P. aeruginosa* specifically. This seems to be driven by competition over nitrogen, sulphur and iron nutrient sources. *P. aeruginosa* appears to induce a more potent

pro-inflammatory microenvironment through loss of *LasB* expression which can aid in the clearance of their fungal competitor. Our work clearly demonstrates that single and dual infections of these two important pathogens have distinct pathologies within the EVPL tissue, inducing fibrosis and distinct immune responses. A mixed result was observed in coinfecting explants indicating dynamic interactions between the host and the pathogens in isolation or in combination.

6.5 Materials and Methods

6.5.1 *Aspergillus fumigatus* culture conditions and conidial preparation

Aspergillus fumigatus ATCC 26933 was cultured for 72 h at 37 °C on malt extract agar (MEA) (Oxoid, Basingstoke, UK) following point inoculation. The conidia were harvested by washing with phosphate-buffered saline supplemented with 0.1% (v/v) Tween-20 (PBS-T), and the suspension was washed three times with PBS. Conidia were enumerated using a haemocytometer and diluted to a final concentration of 1×10^7 conidia/ml

6.5.2 *Pseudomonas aeruginosa* culture conditions and liquid suspension preparation

Pseudomonas aeruginosa (PAO1) was cultured for 24 h at 37 °C on Nutrient agar plates (Oxoid, Basingstoke, UK). A single colony from the plate was isolated with an inoculating loop and placed into 1ml of sterile PBS to generate a bacterial suspension with a density of approximately 1.1×10^9 cells/ml.

6.5.3 Preparation of *ex-vivo* pig lung sections

Lungs from a single pig were collected from a local abattoir within an hour of slaughter and transported on ice to Maynooth University. The respiratory zone of the lung (tissue rich in alveolae) was processed into tissue explants (5×5×5 mm) as previously described (Harrison *et al.*, 2014) with the following changes. Unprocessed control sections (n=3) were removed following surface sterilisation of the pleura, which served as untreated controls for metataxonomic analysis. Control EVPL explants (n=3) were sham inoculated with a needle dipped into PBS. Infected EVPL sections (n=3) were inoculated with *A. fumigatus* conidia *via* a needle dipped in a 1×10^7 conidia/ml suspension, and other tissue samples (n=3) were inoculated with *P. aeruginosa* suspension (approximately 1.1×10^9 /ml) in a similar manner. Coinfected explants (n=3) were inoculated with two single inoculations with each pathogen immediately adjacent to each other. All sections were suspended in 50/50 mixture of

RPMI (Gibco, UK) and DMEM (Gibco, Miami) and incubated at 6% CO₂ and 37 °C for 96 hours. RPMI/DMEM was used for this experiment for consistency with our previous work (Curtis *et al.*, 2025).

6.5.4 Visualisation of tissue pathology

Infected tissue explants were removed from the 24 well plate with sterilized forceps at 96 hours post infection. The explants were washed in sterile PBS prior to visualisation at 40x magnification using a brightfield microscope (Olympus CH20).

6.5.5 DNA Extraction, Library Preparation, and Sequencing

Genomic DNA was extracted from 200 µl of EVPL lysate from unprocessed and processed control lung isolates as well as mono-infected *P. aeruginosa* sections, mono-infected *A. fumigatus* sections and sections coinfecte^d with *P. aeruginosa* and *A. fumigatus*. The extraction was conducted using the DNeasy PowerSoil Pro Kit (QIAGEN) according to manufacturer's instructions. DNA concentration and purity values were analysed with a Nanodrop 2000 Spectrophotometer (ThermoFisher Scientific). A total of 30 ng of qualified genomic DNA was used as input for PCR amplification using either 16S rRNA gene or ITS2 region fusion primers. Amplified products were purified using Agencourt AMPure XP beads, eluted in Elution Buffer, and subsequently labelled for library construction. The quality and concentration of the libraries were assessed using an Agilent 2100 Bioanalyzer. Libraries that met the quality thresholds were sequenced on the DNBSEQ platform by BGI. The resultant sequences were filtered and classified using their standard bioinformatics pipeline described below. All raw sequences have been deposited to the NCBI under Bioproject accession PRJNA1279114, Biosample accession SAMN49395613 and SRA accessions SRX29229626- SRX29229644.

6.5.6 Sequence Data Processing and Quality Control

Raw reads were processed to obtain high-quality clean sequences. Filtering was carried out using iTools Fqtools fqcheck (v0.25) (Dinov *et al.*, 2008), readfq (v1.0), and Cutadapt (v2.6) (Martin, 2011), with the following criteria. Reads with an average Phred quality score below 20 across a 25 bp sliding window were truncated, subsequent reads trimmed to less than 75% of their original length were discarded. Adapter-contaminated reads (≥ 15 bp overlap with ≤ 3 mismatches) were also removed. Any reads containing ambiguous bases (N) or low-complexity reads (≥ 10 consecutive identical

bases) were excluded. Demultiplexing was completed using in-house BGI scripts. For both 16S and ITS2 libraries, paired-end reads with overlapping regions were merged into consensus tags using FLASH (v1.2.11) (Magoč and Salzberg, 2011). The merging required a minimum overlap of 15 bp overlap and a maximum mismatch rate of 10%.

6.5.7 OTU Clustering and Chimera Removal

High-quality tags were clustered into Operational Taxonomic Units (OTUs) at a 97% similarity threshold using USEARCH (v7.0.1090) (Zhou *et al.*, 2024) with the UPARSE algorithm. Representative sequences were identified for each OTU. Chimeric sequences were identified and filtered using UCHIME (v4.2.40) (Edgar *et al.*, 2011). 16S sequence chimeras were screened against the GOLD database (v20110519) (Mukherjee *et al.*, 2017). ITS2 chimeras were removed based on comparisons to the UNITE database (v20140703) (Abarenkov *et al.*, 2024). The remaining clean tags were mapped back to the OTU representative sequences using the USEARCH GLOBAL algorithm to quantify OTU abundances.

6.5.8 Taxonomic Annotation

Taxonomic classification of representative OTU sequences was performed using the **RDP Classifier (v2.2)** (Wang *et al.*, 2007) with a confidence threshold of 0.6. Bacteria and Archaea (16S) were classified using Greengenes (v202210) (DeSantis *et al.*, 2006) and RDP (Release 19) (Wang and Cole, 2024). **Fungi (ITS2) were classified using the UNITE database (Version 10)** (Abarenkov *et al.*, 2024). OTUs without taxonomic assignment were excluded from further analysis.

6.5.9 Proteomic extraction

Control, mono-infected and co-infected EVPL explants (n = 3 of each) were washed in PBS following incubation for 96 hours at 6% CO₂ at 37 °C. Proteins were extracted and purified as previously described (Curtis *et al.*, 2025).

6.5.10 Mass spectrometry

Proteomic analysis was conducted using a Vanquish Neo UHPLC system (Thermo Fisher Scientific), equipped with an EASY-Spray PepMap Neo column (2 µm, C18, 0.075 x 500 mm) and coupled with an EASY-Spray source to an Orbitrap Ascend mass spectrometer (Thermo Fisher Scientific, San Jose, CA, USA). Dried

peptides were dissolved in Mobile Phase A (2% acetonitrile, 0.5% Trifluoracetic acid and 97.5% water) to give a final concentration of 375ng/μl. The injection volume was set to 2 μl. After ‘Automatic’ loading, peptides were eluted using a 90-minute gradient with Mobile Phase A and Mobile Phase B (80% acetonitrile in water and 0.1 % formic acid) at a flow rate of 300 nL/min. The linear gradient was delivered from 2% to 40% Mobile Phase B over 80 minutes and from 40% to 90% Mobile Phase B over 10 minutes followed by column wash and equilibration. Data-dependent acquisition was performed using Xcalibur (v4.7) and Orbitrap Tribrid Series instrument control software v4.2. The mass spectrometry parameters were set as follows: for the MS¹ full scan, an Orbitrap resolution of 120,000 (at *m/z* 200), a scan range of *m/z* 375 to 1500, Automatic gain control (AGC) of 8×10^5 , and maximum injection time Auto were used. Filters included MIPS, minimum intensity threshold of 5×10^3 , include charge states 2-6, and dynamic exclusion of 60 seconds. For MS² scans, Precursor ions were quadrupole isolated (*m/z* 1.6) and fragmented with an HCD (higher-energy collisional dissociation) NCE of 30%. Fragment ions were detected in the ion trap set to scan rate of Rapid, a scan range of *m/z* 110 to 2000, AGC target of 1×10^4 , and a maximum injection time set to Auto. Precursor ions were fragmented using high-energy collisional dissociation (HCD) mode with a normalized collision energy of 30%. The AGC and maximum injection time were set to 1×10^4 , respectively. Additionally, dynamic exclusion was set to 60s, and the isolation window was set to 1.6 *m/z*. The duty cycle was set to max cycle time of 2 seconds

6.5.11 Data analysis

A quantitative analysis of EVPL tissue, *A. fumigatus* and *P. aeruginosa* was conducted using MaxQuant version 2.5.2.0 (<http://www.maxquant.org>). Raw MS/MS datafiles were processed using the Andromeda search engine in MaxQuant software v.1.6.3.4 110 using the *Sus scrofa* reference proteome (46,174 entries, downloaded December 2023), a *Neosartorya fumigata* reference proteome obtained from a UniProt-SWISS-PROT (The UniProt Consortium, 2025) database to identify proteins (9647 entries, downloaded July 2022) or the *P. aeruginosa* reference proteome (5563 entries, downloaded October 2024) respectively. The following search parameters were used: first search peptide tolerance of 20 ppm, second search peptide tolerance of 4.5 ppm with cysteine carbamidomethylation as a fixed modification and N-acetylation of protein and oxidation of methionine were set as variable modifications

and a maximum of two missed cleavage sites were allowed. The False discovery rate (FDR) for peptides and proteins was set to 1% and was estimated following searches against a target-decoy database. Peptides with minimum length of 7 amino acids were considered for identification and proteins were only considered identified when observed in three replicates of one sample group. Proteomic data analysis was performed in Perseus v.1.6.15.0, for data analysis, processing, and visualization as described (Margalit *et al.*, 2020). The mass spectrometry proteomics data have been deposited to the ProteomeXchange Consortium *via* the PRIDE (Perez-Riverol *et al.*, 2021) partner repository with the dataset identifier (PXD065657).

6.6 References

Abarenkov, K., Nilsson, R. H., Larsson, K.-H., Taylor, A. F. S., May, T. W., Frøslev, T. G., Pawlowska, J., Lindahl, B., Pöldmaa, K., Truong, C., Vu, D., Hosoya, T., Niskanen, T., Piirmann, T., Ivanov, F., Zirk, A., Peterson, M., Cheeke, T. E., Ishigami, Y., Jansson, A. T., Jeppesen, T. S., Kristiansson, E., Mikryukov, V., Miller, J. T., Oono, R., Ossandon, F. J., Paupério, J., Saar, I., Schigel, D., Suija, A., Tedersoo, L. and Köljalg, U., 2024. The UNITE database for molecular identification and taxonomic communication of fungi and other eukaryotes: sequences, taxa and classifications reconsidered. *Nucleic Acids Research*, 52 (D1), D791–D797.

Abdelhamid, A. G. and Yousef, A. E., 2024. Untargeted metabolomics unveiled the role of butanoate metabolism in the development of *Pseudomonas aeruginosa* hypoxic biofilm. *Frontiers in Cellular and Infection Microbiology* [online], 14. Available from: <https://www.frontiersin.org/journals/cellular-and-infection-microbiology/articles/10.3389/fcimb.2024.1346813/full> [Accessed 21 May 2025].

Al Shakirchi, M., Sorjonen, K., Klingspor, L., Bergman, P., Hjelte, L. and de Monestrol, I., 2021. The Effects of *Aspergillus fumigatus* Colonization on Lung Function in Patients with Cystic Fibrosis. *Journal of Fungi*, 7 (11), 944.

Amich, J., Dümig, M., O'Keefe, G., Binder, J., Doyle, S., Beilhack, A. and Krappmann, S., 2016. Exploration of Sulfur Assimilation of *Aspergillus fumigatus* Reveals Biosynthesis of Sulfur-Containing Amino Acids as a Virulence Determinant. *Infection and Immunity*, 84 (4), 917–929.

Amin, R., Dupuis, A., Aaron, S. D. and Ratjen, F., 2010. The effect of chronic infection with *Aspergillus fumigatus* on lung function and hospitalization in patients with cystic fibrosis. *Chest*, 137 (1), 171–176.

Balloy, V. and Chignard, M., 2009. The innate immune response to *Aspergillus fumigatus*. *Microbes and Infection*, 11 (12), 919–927.

Bouyssi, A., Déméautis, T., Trecourt, A., Delles, M., Agostini, F., Monneret, G., Glehen, O., Wallon, M., Persat, F., Devouassoux, G., Bentaher, A. and Menotti, J., 2023. Characterization of Lung Inflammatory Response to *Aspergillus fumigatus* Spores. *Journal of Fungi*, 9 (6), 682.

Caffrey-Carr, A. K., Hilmer, K. M., Kowalski, C. H., Shepardson, K. M., Temple, R. M., Cramer, R. A. and Obar, J. J., 2018. Host-Derived Leukotriene B4 Is Critical for Resistance against Invasive Pulmonary Aspergillosis. *Frontiers in Immunology* [online], 8. Available from: <https://www.frontiersin.org/journals/immunology/articles/10.3389/fimmu.2017.01984/full> [Accessed 20 May 2025].

Çakar, N. E. and Görükmez, O., 2021. 3-Hydroxyisobutyryl-CoA Hydrolase (HIBCH) Deficiency Cases Diagnosed by Only HIBCH Gene Analysis and Novel Pathogenic Mutation. *Annals of Indian Academy of Neurology*, 24 (3), 372–378.

Cao, Q., Fan, J., Zou, J. and Wang, W., 2024. Multi-omics analysis identifies BCAT2 as a potential pan-cancer biomarker for tumor progression and immune microenvironment modulation. *Scientific Reports*, 14 (1), 23371.

Chen, G., Gu, W., Huang, C., Kong, W., Zhao, L., Jie, H. and Zhen, G., 2024. Peroxisome Metabolism Pathway and EHHADH Expression are Downregulated in Macrophages in Neutrophilic Asthma. *Allergy, Asthma & Immunology Research*, 17 (1), 111–126.

Chesshyre, E., Warren, F. C., Shore, A. C., Davies, J. C., Armstrong-James, D. and Warris, A., 2024. Long-Term Outcomes of Allergic Bronchopulmonary Aspergillosis and *Aspergillus* Colonization in Children and Adolescents with Cystic Fibrosis. *Journal of Fungi (Basel, Switzerland)*, 10 (9), 599.

Chotirat, S., Thongnoppakhun, W., Promsuwicha, O., Boonthimat, C. and Auewarakul, C. U., 2012. Molecular alterations of isocitrate dehydrogenase 1 and 2 (IDH1 and IDH2) metabolic genes and additional genetic mutations in newly diagnosed acute myeloid leukemia patients. *Journal of Hematology & Oncology*, 5, 5.

Curtis, A., Harrison, F. and Kavanagh, K., 2025. Proteomic characterization of *Aspergillus fumigatus* – host interactions using the ex-vivo pig lung (EVPL) model. *Virulence*, 16 (1), 2530675.

D'Arpa, P., Karna, S. L. R., Chen, T. and Leung, K. P., 2021. *Pseudomonas aeruginosa* transcriptome adaptations from colonization to biofilm infection of skin wounds. *Scientific Reports*, 11, 20632.

Dasari, P., Koleci, N., Shopova, I. A., Wartenberg, D., Beyersdorf, N., Dietrich, S., Sahagún-Ruiz, A., Figge, M. T., Skerka, C., Brakhage, A. A. and Zipfel, P. F., 2019. Enolase From *Aspergillus fumigatus* Is a Moonlighting Protein That Binds the Human Plasma Complement Proteins Factor H, FHL-1, C4BP, and Plasminogen. *Frontiers in Immunology* [online], 10. Available from: <https://www.frontiersin.org/journals/immunology/articles/10.3389/fimmu.2019.02573/full> [Accessed 18 Dec 2024].

DeSantis, T. Z., Hugenholtz, P., Larsen, N., Rojas, M., Brodie, E. L., Keller, K., Huber, T., Dalevi, D., Hu, P. and Andersen, G. L., 2006. Greengenes, a chimera-checked 16S rRNA gene database and workbench compatible with ARB. *Applied and Environmental Microbiology*, 72 (7), 5069–5072.

Dickerhof, N., Isles, V., Pattemore, P., Hampton, M. B. and Kettle, A. J., 2019. Exposure of *Pseudomonas aeruginosa* to bactericidal hypochlorous acid during neutrophil phagocytosis is compromised in cystic fibrosis. *The Journal of Biological Chemistry*, 294 (36), 13502–13514.

Dinarello, A., Betto, R. M., Diamante, L., Tesoriere, A., Ghirardo, R., Cioccarelli, C., Meneghetti, G., Peron, M., Laquatra, C., Tiso, N., Martello, G. and Argenton, F., 2023. STAT3 and HIF1 α cooperatively mediate the transcriptional and physiological responses to hypoxia. *Cell Death Discovery*, 9 (1), 1–12.

Dinov, I. D., Rubin, D., Lorenzen, W., Dugan, J., Ma, J., Murphy, S., Kirschner, B., Bug, W., Sherman, M., Floratos, A., Kennedy, D., Jagadish, H. V., Schmidt, J., Athey, B., Califano, A., Musen, M., Altman, R., Kikinis, R., Kohane, I., Delp, S., Parker, D. S. and Toga, A. W., 2008. iTools: A Framework for Classification, Categorization and Integration of Computational Biology Resources. *PLOS ONE*, 3 (5), e2265.

Dobrowolski, S. F., Alodaib, A., Karunanidhi, A., Basu, S., Holecko, M., Lichter-Konecki, U., Pappan, K. L. and Vockley, J., 2020. Clinical, biochemical, mitochondrial, and metabolomic aspects of methylmalonate semialdehyde dehydrogenase deficiency: Report of a fifth case. *Molecular Genetics and Metabolism*, 129 (4), 272–277.

Dunn, L. L., Kong, S. M. Y., Tumanov, S., Chen, W., Cantley, J., Ayer, A., Maghzal, G. J., Midwinter, R. G., Chan, K. H., Ng, M. K. C. and Stocker, R., 2021. Hmox1 (Heme Oxygenase-1) Protects Against Ischemia-Mediated Injury via Stabilization of HIF-1 α (Hypoxia-Inducible Factor-1 α). *Arteriosclerosis, Thrombosis, and Vascular Biology*, 41 (1), 317–330.

Edgar, R. C., Haas, B. J., Clemente, J. C., Quince, C. and Knight, R., 2011. UCHIME improves sensitivity and speed of chimera detection. *Bioinformatics (Oxford, England)*, 27 (16), 2194–2200.

Escobar, N., Valdes, I. D., Keizer, E. M., Ordóñez, S. R., Ohm, R. A., Wösten, H. A. B. and de Cock, H., 2018. Expression profile analysis reveals that *Aspergillus fumigatus* but not *Aspergillus niger* makes type II epithelial lung cells less immunological alert. *BMC Genomics*, 19 (1), 534.

Feehan, D. D., Jamil, K., Polyak, M. J., Ogbomo, H., Hasell, M., Li, S. S., Xiang, R. F., Parkins, M., Trapani, J. A., Harrison, J. J. and Mody, C. H., 2022. Natural killer cells kill extracellular *Pseudomonas aeruginosa* using contact-dependent release of granzymes B and H. *PLoS Pathogens*, 18 (2), e1010325.

Flynn, J. M., Niccum, D., Dunitz, J. M. and Hunter, R. C., 2016. Evidence and Role for Bacterial Mucin Degradation in Cystic Fibrosis Airway Disease. *PLOS Pathogens*, 12 (8), e1005846.

Gannon, A. D. and Darch, S. E., 2021. Same Game, Different Players: Emerging Pathogens of the CF Lung. *mBio*, 12 (1), 10.1128/mbio.01217-20.

Garbe, E. and Vylkova, S., 2019. Role of Amino Acid Metabolism in the Virulence of Human Pathogenic Fungi. *Current Clinical Microbiology Reports*, 6 (3), 108–119.

Ghosh, A. K. and Vaughan, D. E., 2012. PAI-1 in Tissue Fibrosis. *Journal of cellular physiology*, 227 (2), 493–507.

Grassi, L. and Crabbé, A., 2024. Recreating chronic respiratory infections in vitro using physiologically relevant models. *European Respiratory Review* [online], 33 (173). Available from: <https://publications.ersnet.org/content/errev/33/173/240062> [Accessed 6 Jun 2025].

Grilz, E., Mauracher, L., Posch, F., Königsbrügge, O., Zöchbauer-Müller, S., Marosi, C., Lang, I., Pabinger, I. and Ay, C., 2019. Citrullinated histone H3, a biomarker for neutrophil extracellular trap formation, predicts the risk of mortality in patients with cancer. *British Journal of Haematology*, 186 (2), 311–320.

Günther, K., Nischang, V., Cseresnyés, Z., Krüger, T., Sheta, D., Abboud, Z., Heinekamp, T., Werner, M., Kniemeyer, O., Beilhack, A., Figge, M. T., Brakhage, A. A., Werz, O. and Jordan, P. M., 2024. Aspergillus fumigatus-derived gliotoxin impacts innate immune cell activation through modulating lipid mediator production in macrophages. *Immunology*, 173 (4), 748–767.

Guruceaga, X., Ezpeleta, G., Mayayo, E., Sueiro-Olivares, M., Abad-Díaz-De-Cerio, A., Aguirre Urízar, J. M., Liu, H. G., Wiemann, P., Bok, J. W., Filler, S. G., Keller, N. P., Hernando, F. L., Ramirez-Garcia, A. and Rementeria, A., 2018. A possible role for fumagillin in cellular damage during host infection by Aspergillus fumigatus. *Virulence*, 9 (1), 1548–1561.

Hagiwara, D., Takahashi, H., Watanabe, A., Takahashi-Nakaguchi, A., Kawamoto, S., Kamei, K. and Gonoi, T., 2014. Whole-Genome Comparison of Aspergillus fumigatus Strains Serially Isolated from Patients with Aspergillosis. *Journal of Clinical Microbiology*, 52 (12), 4202–4209.

Harrington, N. E., Sweeney, E. and Harrison, F., 2020. Building a better biofilm - Formation of in vivo-like biofilm structures by Pseudomonas aeruginosa in a porcine model of cystic fibrosis lung infection. *Biofilm*, 2, 100024.

Harrison, F., Muruli, A., Higgins, S. and Diggle, S. P., 2014. Development of an Ex Vivo Porcine Lung Model for Studying Growth, Virulence, and Signaling of Pseudomonas aeruginosa. *Infection and Immunity*, 82 (8), 3312–3323.

Hartmann, T., Cairns, T. C., Olbermann, P., Morschhäuser, J., Bignell, E. M. and Krappmann, S., 2011. Oligopeptide transport and regulation of extracellular proteolysis are required for growth of Aspergillus fumigatus on complex substrates but not for virulence. *Molecular Microbiology*, 82 (4), 917–935.

Hastings, C. J., Syed, S. S. and Marques, C. N. H., 2023. Subversion of the Complement System by Pseudomonas aeruginosa. *Journal of Bacteriology*, 205 (8), e00018-23.

Hegewisch-Solloa, E., Seo, S., Mundy-Bosse, B. L., Mishra, A., Waldman, Erik. H., Maurrasse, S., Grunstein, E., Connors, T. J., Freud, A. G. and Mace, E. M., 2021. Differential integrin adhesome expression defines human natural killer cell residency and developmental stage. *Journal of immunology (Baltimore, Md. : 1950)*, 207 (3), 950–965.

Heldt, S., Eogl, S., Prattes, J., Flick, H., Rabensteiner, J., Prüller, F., Niedrist, T., Neumeister, P., Wölfler, A., Strohmaier, H., Krause, R. and Hoenigl, M., 2017. Levels of interleukin (IL)-6 and IL-8 are elevated in serum and bronchoalveolar lavage fluid of haematological patients with invasive pulmonary aspergillosis. *Mycoses*, 60 (12), 818–825.

Herrmann, C., Lingner, M., Herrmann, S., Brockhausen, I. and Tümmler, B., 2024. Mucin adhesion of serial cystic fibrosis airways Pseudomonas aeruginosa isolates. *Frontiers in Cellular and Infection Microbiology* [online], 14. Available from: <https://www.frontiersin.org/journals/cellular-and-infection-microbiology/articles/10.3389/fcimb.2024.1448104/full> [Accessed 30 Jun 2025].

Hong, G., Alby, K., Ng, S. C. W., Fleck, V., Kubrak, C., Rubenstein, R. C., Dorgan, D. J., Kawut, S. M. and Hadjiliadis, D., 2020. The presence of Aspergillus fumigatus is

associated with worse respiratory quality of life in cystic fibrosis. *Journal of Cystic Fibrosis: Official Journal of the European Cystic Fibrosis Society*, 19 (1), 125–130.

Huang, J., Filipe, A., Rahuel, C., Bonnin, P., Mesnard, L., Guérin, C., Wang, Y., Le Van Kim, C., Colin, Y. and Tharaux, P.-L., 2014. Lutheran/basal cell adhesion molecule accelerates progression of crescentic glomerulonephritis in mice. *Kidney International*, 85 (5), 1123–1136.

Huang, T., Zhang, M., Tong, X., Chen, J., Yan, G., Fang, S., Guo, Y., Yang, B., Xiao, S., Chen, C., Huang, L. and Ai, H., 2018. Microbial communities in swine lungs and their association with lung lesions. *Microbial Biotechnology*, 12 (2), 289–304.

Hughes, D. A., Archangelidi, O., Coates, M., Armstrong-James, D., Elborn, S. J., Carr, S. B. and Davies, J. C., 2022. Clinical characteristics of *Pseudomonas* and *Aspergillus* co-infected cystic fibrosis patients: A UK registry study. *Journal of Cystic Fibrosis*, 21 (1), 129–135.

Ibrahim-Granet, O., Dubourdeau, M., Latgé, J.-P., Ave, P., Huerre, M., Brakhage, A. A. and Brock, M., 2008. Methylcitrate synthase from *Aspergillus fumigatus* is essential for manifestation of invasive aspergillosis. *Cellular Microbiology*, 10 (1), 134–148.

Invernizzi, R., Lloyd, C. M. and Molyneaux, P. L., 2020. Respiratory microbiome and epithelial interactions shape immunity in the lungs. *Immunology*, 160 (2), 171–182.

Jia, L.-J., Krüger, T., Blango, M. G., von Eggeling, F., Kniemeyer, O. and Brakhage, A. A., 2020. Biotinylated Surfome Profiling Identifies Potential Biomarkers for Diagnosis and Therapy of *Aspergillus fumigatus* Infection. *mSphere*, 5 (4), 10.1128/msphere.00535-20.

Kang, Y.-H., Varghese, P. M., Aiyan, A. A., Pondman, K., Kishore, U. and Sim, R. B., 2024. Complement-Coagulation Cross-talk: Factor H-mediated regulation of the Complement Classical Pathway activation by fibrin clots. *Frontiers in Immunology* [online], 15. Available from: <https://www.frontiersin.org/journals/immunology/articles/10.3389/fimmu.2024.1368852/full> [Accessed 20 May 2025].

Kavanagh, D., Barratt, J., Schubart, A., Webb, N. J. A., Meier, M. and Fakhouri, F., 2025. Factor B as a therapeutic target for the treatment of complement-mediated diseases. *Frontiers in Immunology*, 16, 1537974.

Keown, K., Reid, A., Moore, J. E., Taggart, C. C. and Downey, D. G., 2020. Coinfection with *Pseudomonas aeruginosa* and *Aspergillus fumigatus* in cystic fibrosis. *European Respiratory Review*, 29 (158), 200011.

Kiani, A. A., Elyasi ,Hossein, Ghoreyshi ,Shadiyeh, Nouri ,Negar, Safarzadeh ,Ali and and Nafari, A., 2021. Study on hypoxia-inducible factor and its roles in immune system. *Immunological Medicine*, 44 (4), 223–236.

Kim, H.-J., Rhe, S.-Y. and Nam, J.-O., 2016. The effect on transforming growth factor-beta-induced protein (beta ig-h3) expression by LPS and MDP stimulation to mice bone marrow derived macrophages. *The Journal of Immunology*, 196 (1_Supplement), 50.4.

Kirschning, A., 2022. On the Evolutionary History of the Twenty Encoded Amino Acids. *Chemistry – A European Journal*, 28 (55), e202201419.

König, S., Pace, S., Pein, H., Heinekamp, T., Kramer, J., Romp, E., Straßburger, M., Troisi, F., Proschak, A., Dworschak, J., Scherlach, K., Rossi, A., Sautebin, L., Haeggström, J. Z., Hertweck, C., Brakhage, A. A., Gerstmeier, J., Proschak, E. and Werz, O., 2019. Gliotoxin from *Aspergillus fumigatus* Abrogates Leukotriene B4 Formation through Inhibition of Leukotriene A4 Hydrolase. *Cell Chemical Biology*, 26 (4), 524–534.e5.

Krappmann, S. and Braus, G. H., 2005. Nitrogen metabolism of *Aspergillus* and its role in pathogenicity. *Medical Mycology*, 43 (Supplement_1), S31–S40.

LaFayette, S. L., Houle, D., Beaudoin, T., Wojewodka, G., Radzioch, D., Hoffman, L. R., Burns, J. L., Dandekar, A. A., Smalley, N. E., Chandler, J. R., Zlosnik, J. E., Speert, D. P., Bernier, J., Matouk, E., Brochiero, E., Rousseau, S. and Nguyen, D., 2015. Cystic fibrosis–adapted *Pseudomonas aeruginosa* quorum sensing lasR mutants cause hyperinflammatory responses. *Science Advances*, 1 (6), e1500199.

Leal, S. M., Roy, S., Vareechon, C., Carrion, S. deJesus, Clark, H., Lopez-Berges, M. S., Di Pietro, A., Schrettl, M., Beckmann, N., Redl, B., Haas, H. and Pearlman, E., 2013. Targeting iron acquisition blocks infection with the fungal pathogens *Aspergillus fumigatus* and *Fusarium oxysporum*. *PLoS pathogens*, 9 (7), e1003436.

Li, R., Li, J. and Zhou, X., 2024. Lung microbiome: new insights into the pathogenesis of respiratory diseases. *Signal Transduction and Targeted Therapy*, 9, 19.

Libri, V., Schulte, D., van Stijn, A., Ragimbeau, J., Rogge, L. and Pellegrini, S., 2008. Jakmip1 Is Expressed upon T Cell Differentiation and Has an Inhibitory Function in Cytotoxic T Lymphocytes1. *The Journal of Immunology*, 181 (9), 5847–5856.

Lin, C. K. and Kazmierczak, B. I., 2017. Inflammation: A Double-Edged Sword in the Response to *Pseudomonas aeruginosa* Infection. *Journal of Innate Immunity*, 9 (3), 250–261.

Liu, J., Qi, Y., Chao, J., Sathuvalli, P., Y. Lee, L. and Li, S., 2021. CREG1 promotes lysosomal biogenesis and function. *Autophagy*, 17 (12), 4249–4265.

Lu, Y., Chen, J., Wang, S., Tian, Z., Fan, Y., Wang, M., Zhao, J., Tang, K. and Xie, J., 2021. Identification of Genetic Signature Associated With Aging in Pulmonary Fibrosis. *Frontiers in Medicine*, 8, 744239.

Lundgren, B. R., Shoytush, J. M., Scheel, R. A., Sain, S., Sarwar, Z. and Nomura, C. T., 2021. Utilization of L-glutamate as a preferred or sole nutrient in *Pseudomonas aeruginosa* PAO1 depends on genes encoding for the enhancer-binding protein AauR, the sigma factor RpoN and the transporter complex AatJQMP. *BMC Microbiology*, 21, 83.

Machata, S., Müller, Mario M., Lehmann, Roland, Sieber, Patricia, Panagiotou, Gianni, Carvalho, Agostinho, Cunha, Cristina, Lagrou, Katrien, Maertens, Johan, Slevogt, Hortense and Jacobsen, I. D., 2020. Proteome analysis of bronchoalveolar lavage fluids reveals host and fungal proteins highly expressed during invasive pulmonary aspergillosis in mice and humans. *Virulence*, 11 (1), 1337–1351.

Magoč, T. and Salzberg, S. L., 2011. FLASH: fast length adjustment of short reads to improve genome assemblies. *Bioinformatics*, 27 (21), 2957–2963.

Margalit, A., Carolan, J. C., Sheehan, D. and Kavanagh, K., 2020. The *Aspergillus fumigatus* Secretome Alters the Proteome of *Pseudomonas aeruginosa* to Stimulate Bacterial Growth: Implications for Co-infection. *Molecular & cellular proteomics: MCP*, 19 (8), 1346–1359.

Margalit, A., Sheehan, D., Carolan, J. C. and Kavanagh, K., 2022. Exposure to the *Pseudomonas aeruginosa* secretome alters the proteome and secondary metabolite production of *Aspergillus fumigatus*. *Microbiology*, 168 (3), 001164.

Martin, M., 2011. Cutadapt removes adapter sequences from high-throughput sequencing reads. *EMBnet.journal*, 17 (1), 10–12.

Matthaiou, E. I., Sass, G., Stevens, D. A. and Hsu, J. L., 2018. Iron: an essential nutrient for *Aspergillus fumigatus* and a fulcrum for pathogenesis. *Current opinion in infectious diseases*, 31 (6), 506–511.

Mayer-Hamblett, N., Ramsey, B. W., Kulasekara, H. D., Wolter, D. J., Houston, L. S., Pope, C. E., Kulasekara, B. R., Armbruster, C. R., Burns, J. L., Retsch-Bogart, G., Rosenfeld, M., Gibson, R. L., Miller, S. I., Khan, U. and Hoffman, L. R., 2014. *Pseudomonas aeruginosa* phenotypes associated with eradication failure in children with cystic fibrosis. *Clinical Infectious Diseases: An Official Publication of the Infectious Diseases Society of America*, 59 (5), 624–631.

McCormick, A., Heesemann, L., Wagener, J., Marcos, V., Hartl, D., Loeffler, J., Heesemann, J. and Ebel, F., 2010. NETs formed by human neutrophils inhibit growth of the pathogenic mold *Aspergillus fumigatus*. *Microbes and Infection*, 12 (12), 928–936.

Mereness, J. A. and Mariani, T. J., 2021. The critical role of collagen VI in lung development and chronic lung disease. *Matrix Biology Plus*, 10, 100058.

Meyer, M., Hollenbeck, J. C., Reunert, J., Seelhöfer, A., Rust, S., Fobker, M., Biskup, S., Och, U., Linden, M., Sass, J. O. and Marquardt, T., 2021. 3-Hydroxyisobutyrate dehydrogenase (HIBADH) deficiency-A novel disorder of valine metabolism. *Journal of Inherited Metabolic Disease*, 44 (6), 1323–1329.

Moore, M. M., 2013. The crucial role of iron uptake in *Aspergillus fumigatus* virulence. *Current Opinion in Microbiology*, 16 (6), 692–699.

Mukherjee, S., Stamatis, D., Bertsch, J., Ovchinnikova, G., Verezemyska, O., Isbandi, M., Thomas, A. D., Ali, R., Sharma, K., Kyripides, N. C. and Reddy, T. B. K., 2017. Genomes OnLine Database (GOLD) v.6: data updates and feature enhancements. *Nucleic Acids Research*, 45 (D1), D446–D456.

Navrátilová, A., Bečvář, V., Baloun, J., Damgaard, D., Nielsen, C. H., Veigl, D., Pavelka, K., Vencovský, J., Šenolt, L. and Andrés Cerezo, L., 2021. S100A11 (calgizzarin) is released via NETosis in rheumatoid arthritis (RA) and stimulates IL-6 and TNF secretion by neutrophils. *Scientific Reports*, 11 (1), 6063.

Nayir Buyuksahin, H., Yalçın, E., Emiralioglu, N., Hazirolan, G., Ademhan Tural, D., Ozsezen, B., Sunman, B., Guzelkas, I., Dogru, D., Ozcelik, U. and Kiper, N., 2022. The effect of *Pseudomonas aeruginosa* eradication regimens on chronic colonization and clinical outcomes in pediatric patients with cystic fibrosis. *Pediatrics International: Official Journal of the Japan Pediatric Society*, 64 (1), e15249.

Nazik, H., Sass, G., Déziel, E. and Stevens, D. A., 2020. Aspergillus Is Inhibited by *Pseudomonas aeruginosa* Volatiles. *Journal of Fungi*, 6 (3), 118.

Nguyen, M., Sharma, A., Wu, W., Gomi, R., Sung, B., Hospodsky, D., Angenent, L. T. and Worgall, S., 2016. The fermentation product 2,3-butanediol alters *P. aeruginosa* clearance, cytokine response and the lung microbiome. *The ISME Journal*, 10 (12), 2978–2983.

Nikitashina, L., Chen, X., Radosa, L., Li, K., Straßburger, M., Seelbinder, B., Böhnke, W., Vielreicher, S., Nietzsche, S., Heinekamp, T., Jacobsen, I. D., Panagiotou, G. and Brakhage, A. A., 2025. The murine lung microbiome is disbalanced by the human-pathogenic fungus *Aspergillus fumigatus* resulting in enrichment of anaerobic bacteria. *Cell Reports* [online], 44 (3). Available from: [https://www.cell.com/cell-reports/abstract/S2211-1247\(25\)00213-X](https://www.cell.com/cell-reports/abstract/S2211-1247(25)00213-X) [Accessed 4 Jun 2025].

O'Brien, S. and Fothergill, J. L., 2017. The role of multispecies social interactions in shaping *Pseudomonas aeruginosa* pathogenicity in the cystic fibrosis lung. *FEMS microbiology letters*, 364 (15), fnx128.

Perez-Riverol, Y., Bai, J., Bandla, C., García-Seisdedos, D., Hewapathirana, S., Kamatchinathan, S., Kundu, D. J., Prakash, A., Frericks-Zipper, A., Eisenacher, M., Walzer, M., Wang, S., Brazma, A. and Vizcaíno, J. A., 2021. The PRIDE database resources in 2022: a hub for mass spectrometry-based proteomics evidences. *Nucleic Acids Research*, 50 (D1), D543–D552.

Poletti, M., Arnauts, K., Ferrante, M. and Korcsmaros, T., 2020. Organoid-based Models to Study the Role of Host-microbiota Interactions in IBD. *Journal of Crohn's & Colitis*, 15 (7), 1222–1235.

Popovic, D., Kulas, J., Tucovic, D., Popov Aleksandrov, A., Glamocilja, J., Sokovic Bajic, S., Tolinacki, M., Golic, N. and Mirkov, I., 2023. Lung microbiota changes during pulmonary *Aspergillus fumigatus* infection in rats. *Microbes and Infection*, 25 (8), 105186.

Principi, L., Ferrini, E., Ciccimarra, R., Pagani, L., Chinello, C., Previtali, P., Smith, A., Villetti, G., Zoboli, M., Ravanetti, F., Stellari, F. F., Magni, F. and Piga, I., 2023. Proteomic Fingerprint of Lung Fibrosis Progression and Response to Therapy in Bleomycin-Induced Mouse Model. *International Journal of Molecular Sciences*, 24 (5), 4410.

Reece, E., Doyle, S., Greally, P., Renwick, J. and McClean, S., 2018. Aspergillus fumigatus Inhibits *Pseudomonas aeruginosa* in Co-culture: Implications of a Mutually Antagonistic Relationship on Virulence and Inflammation in the CF Airway. *Frontiers in Microbiology* [online], 9. Available from: <https://www.frontiersin.org/journals/microbiology/articles/10.3389/fmicb.2018.01205/full> [Accessed 4 Jun 2025].

Rogan, M. P., Taggart, C. C., Greene, C. M., Murphy, P. G., O'Neill, S. J. and McElvaney, N. G., 2004. Loss of microbicidal activity and increased formation of biofilm due to

decreased lactoferrin activity in patients with cystic fibrosis. *The Journal of Infectious Diseases*, 190 (7), 1245–1253.

Rogers, C. S., Abraham, W. M., Brogden, K. A., Engelhardt, J. F., Fisher, J. T., McCray, P. B., McLennan, G., Meyerholz, D. K., Namati, E., Ostedgaard, L. S., Prather, R. S., Sabater, J. R., Stoltz, D. A., Zabner, J. and Welsh, M. J., 2008. The porcine lung as a potential model for cystic fibrosis. *American Journal of Physiology - Lung Cellular and Molecular Physiology*, 295 (2), L240–L263.

Sabbagh, N. G. A. A.-A., Kao, H.-J., Yang, C.-F., Huang, C.-C., Lin, W.-D., Tsai, F.-J., Chen, T.-H., Tarn, W.-Y., Wu, J.-Y. and Chen, Y.-T., 2011. Alternative Splicing in Acad8 Resulting a Mitochondrial Defect and Progressive Hepatic Steatosis in Mice. *Pediatric Research*, 70 (1), 31–36.

Sass, G. and Stevens, D. A., 2023. Model of Pulmonary Co-Infection of Aspergillus and Pseudomonas in Immunocompetent Mice. *Microbiology Research*, 14 (4), 1843–1861.

Schaible, B., Taylor, C. T. and Schaffer, K., 2012. Hypoxia Increases Antibiotic Resistance in *Pseudomonas aeruginosa* through Altering the Composition of Multidrug Efflux Pumps. *Antimicrobial Agents and Chemotherapy*, 56 (4), 2114–2118.

Schöbel, F., Jacobsen, I. D. and Brock, M., 2010. Evaluation of Lysine Biosynthesis as an Antifungal Drug Target: Biochemical Characterization of *Aspergillus fumigatus* Homocitrate Synthase and Virulence Studies. *Eukaryotic Cell*, 9 (6), 878–893.

Schossleitner, K., Rauscher, S., Gröger, M., Friedl, H. P., Finsterwalder, R., Habertheuer, A., Sibilia, M., Brostjan, C., Födinger, D., Citi, S. and Petzelbauer, P., 2016. Evidence That Cingulin Regulates Endothelial Barrier Function In Vitro and In Vivo. *Arteriosclerosis, Thrombosis, and Vascular Biology*, 36 (4), 647–654.

Schrettl, M., Carberry, S., Kavanagh, K., Haas, H., Jones, G. W., O'Brien, J., Nolan, A., Stephens, J., Fenelon, O. and Doyle, S., 2010. Self-Protection against Gliotoxin—A Component of the Gliotoxin Biosynthetic Cluster, GliT, Completely Protects *Aspergillus fumigatus* Against Exogenous Gliotoxin. *PLOS Pathogens*, 6 (6), e1000952.

Song, J., Xia, T. and Jensen, R. A., 1999. PhhB, a *Pseudomonas aeruginosa* Homolog of Mammalian Pterin 4a-Carbinolamine Dehydratase/DCoH, Does Not Regulate Expression of Phenylalanine Hydroxylase at the Transcriptional Level. *Journal of Bacteriology*, 181 (9), 2789–2796.

Stanford, G. E., Dave, K. and Simmonds, N. J., 2021. Pulmonary Exacerbations in Adults With Cystic Fibrosis: A Grown-up Issue in a Changing Cystic Fibrosis Landscape. *Chest*, 159 (1), 93–102.

Steinhilber, D., Fischer, A. S., Metzner, J., Steinbrink, S. D., Roos, J., Ruthardt, M. and Maier, T. J., 2010. 5-Lipoxygenase: Underappreciated Role of a Pro-Inflammatory Enzyme in Tumorigenesis. *Frontiers in Pharmacology*, 1, 143.

Suarez-Cuartin, G., Smith, A., Abo-Leyah, H., Rodrigo-Troyano, A., Perea, L., Vidal, S., Plaza, V., Fardon, T. C., Sibila, O. and Chalmers, J. D., 2017. Anti-*Pseudomonas aeruginosa* IgG antibodies and chronic airway infection in bronchiectasis. *Respiratory Medicine*, 128, 1–6.

Sun, J., LaRock, D. L., Skowronski, E. A., Kimmey, J. M., Olson, J., Jiang, Z., O'Donoghue, A. J., Nizet, V. and LaRock, C. N., 2020. The *Pseudomonas aeruginosa* protease LasB directly activates IL-1 β . *EBioMedicine*, 60, 102984.

Sweeney, E., Harrington, N. E., Harley Henriques, A. G., Hassan, M. M., Crealock-Ashurst, B., Smyth, A. R., Hurley, M. N., Tormo-Mas, M. Á. and Harrison, F., 2021. An ex vivo cystic fibrosis model recapitulates key clinical aspects of chronic *Staphylococcus aureus* infection. *Microbiology (Reading, England)*, 167 (1).

The UniProt Consortium, 2025. UniProt: the Universal Protein Knowledgebase in 2025. *Nucleic Acids Research*, 53 (D1), D609–D617.

Tian, Y., Gawlak, G., Tian, X., Shah, A. S., Sarich, N., Citi, S. and Birukova, A. A., 2016. Role of Cingulin in Agonist-induced Vascular Endothelial Permeability. *The Journal of Biological Chemistry*, 291 (45), 23681–23692.

Toor, A., Culibrk, L., Singhera, G. K., Moon, K.-M., Prudova, A., Foster, L. J., Moore, M. M., Dorscheid, D. R. and Tebbutt, S. J., 2018. Transcriptomic and proteomic host response to *Aspergillus fumigatus* conidia in an air-liquid interface model of human bronchial epithelium. *PLoS ONE*, 13 (12), e0209652.

Urushiyama, H., Terasaki, Y., Nagasaka, S., Terasaki, M., Kunugi, S., Nagase, T., Fukuda, Y. and Shimizu, A., 2015. Role of $\alpha 1$ and $\alpha 2$ chains of type IV collagen in early fibrotic lesions of idiopathic interstitial pneumonias and migration of lung fibroblasts. *Laboratory Investigation; a Journal of Technical Methods and Pathology*, 95 (8), 872–885.

Visser, C., Rivieccio, F., Krüger, T., Schmidt, F., Cseresnyés, Z., Rohde, M., Figge, M. T., Kniemeyer, O., Blango, M. G. and Brakhage, A. A., 2024. Tracking the uptake of labelled host-derived extracellular vesicles by the human fungal pathogen *Aspergillus fumigatus*. *microLife*, 5, uqae022.

Wang, J. and Pan, W., 2020. The Biological Role of the Collagen Alpha-3 (VI) Chain and Its Cleaved C5 Domain Fragment Endotrophin in Cancer. *Oncotargets and therapy*, 13, 5779–5793.

Wang, Q. and Cole, J. R., 2024. Updated RDP taxonomy and RDP Classifier for more accurate taxonomic classification. *Microbiology Resource Announcements*, 13 (4), e0106323.

Wang, Q., Garrity, G. M., Tiedje, J. M. and Cole, J. R., 2007. Naive Bayesian classifier for rapid assignment of rRNA sequences into the new bacterial taxonomy. *Applied and Environmental Microbiology*, 73 (16), 5261–5267.

Wang, Y., Yang, X., Zhang, S., Ai, J., Wang, J., Chen, J., Zhao, L., Wang, W. and You, H., 2023. Comparative proteomics unveils the bacteriostatic mechanisms of Ga(III) on the regulation of metabolic pathways in *Pseudomonas aeruginosa*. *Journal of Proteomics*, 289, 105011.

Wartenberg, D., Lapp, K., Jacobsen, I. D., Dahse, H.-M., Kniemeyer, O., Heinekamp, T. and Brakhage, A. A., 2011. Secretome analysis of *Aspergillus fumigatus* reveals Asp-hemolysin as a major secreted protein. *International journal of medical microbiology: IJMM*, 301 (7), 602–611.

Williams, L., Layton, T., Yang, N., Feldmann, M. and Nanchahal, J., 2022. Collagen VI as a driver and disease biomarker in human fibrosis. *The FEBS Journal*, 289 (13), 3603–3629.

Wölbeling, F., Munder, A., Kerber-Momot, T., Neumann, D., Hennig, C., Hansen, G., Tümmler, B. and Baumann, U., 2011. Lung function and inflammation during murine *Pseudomonas aeruginosa* airway infection. *Immunobiology*, 216 (8), 901–908.

Yamanishi, Y., Mihara, H., Osaki, M., Muramatsu, H., Esaki, N., Sato, T., Hizukuri, Y., Goto, S. and Kanehisa, M., 2007. Prediction of missing enzyme genes in a bacterial metabolic network. *The FEBS Journal*, 274 (9), 2262–2273.

Yang, J., Zhao, H.-L., Ran, L.-Y., Li, C.-Y., Zhang, X.-Y., Su, H.-N., Shi, M., Zhou, B.-C., Chen, X.-L. and Zhang, Y.-Z., 2015. Mechanistic Insights into Elastin Degradation by Pseudolysin, the Major Virulence Factor of the Opportunistic Pathogen *Pseudomonas aeruginosa*. *Scientific Reports*, 5, 9936.

Yoo, D., Floyd, M., Winn, M., Moskowitz, S. M. and Rada, B., 2014. NET formation induced by *Pseudomonas aeruginosa* cystic fibrosis isolates measured as release of myeloperoxidase–DNA and neutrophil elastase–DNA complexes. *Immunology Letters*, 160 (2), 186–194.

Zaremba, K. A., Sugui, J. A., Chang, Y. C., Kwon-Chung, K. J. and Gallin, J. I., 2007. Human polymorphonuclear leukocytes inhibit *Aspergillus fumigatus* conidial growth by lactoferrin-mediated iron depletion. *Journal of Immunology (Baltimore, Md.: 1950)*, 178 (10), 6367–6373.

Zhang, S. and Yang, G., 2022. IL22RA1/JAK/STAT Signaling Acts As a Cancer Target Through Pan-Cancer Analysis. *Frontiers in Immunology* [online], 13. Available from: <https://www.frontiersin.org/journals/immunology/articles/10.3389/fimmu.2022.915246/full> [Accessed 13 Jun 2025].

Zhao, J., Cheng, W., He, X. and Liu, Y., 2018. The co-colonization prevalence of *Pseudomonas aeruginosa* and *Aspergillus fumigatus* in cystic fibrosis: A systematic review and meta-analysis. *Microbial Pathogenesis*, 125, 122–128.

Zhao, J., Schloss, P. D., Kalikin, L. M., Carmody, L. A., Foster, B. K., Petrosino, J. F., Cavalcoli, J. D., VanDevanter, D. R., Murray, S., Li, J. Z., Young, V. B. and LiPuma, J. J., 2012. Decade-long bacterial community dynamics in cystic fibrosis airways. *Proceedings of the National Academy of Sciences of the United States of America*, 109 (15), 5809–5814.

Zheng, Z., Zhang, X., Dang, C., Beanes, S., Chang, G. X., Chen, Y., Li, C.-S., Lee, K. S., Ting, K. and Soo, C., 2016. Fibromodulin Is Essential for Fetal-Type Scarless Cutaneous Wound Healing. *The American Journal of Pathology*, 186 (11), 2824– 2832.

Zhong, Y., Zhang, W., Zheng, C., Wu, H., Luo, J., Yuan, Z., Zhang, H., Wang, C., Feng, H., Wang, M., Zhang, Q., Ju, H. and Wang, G., 2025. Multi-omic analyses reveal PTPN6's impact on tumor immunity across various cancers. *Scientific Reports*, 15 (1), 11025.

Zhou, Y., Liu, Y.-X. and Li, X., 2024. USEARCH 12: Open-source software for sequencing analysis in bioinformatics and microbiome. *iMeta*, 3 (5), e236.

Chapter 7

General discussion

7.1 General discussion

Aspergillosis has been globally acknowledged as a serious health concern due to rising rates of immunosuppression, antifungal resistance, and its increased geographical distribution as a result of climate change. The vulnerable patient cohort of *A. fumigatus* infections is constantly increasing, with more people living with pre-existing lung damage, compounded by the wider prescription of immunosuppressive agents (Joshi, 2024; Martinson and Lapham, 2024). This coupled with the growing range of *A. fumigatus* as a result of climate change has resulted in increased occurrence of disease (George *et al.*, 2025). In addition, antifungal resistance against first-line therapeutics including triazoles represents a steadily growing challenge in the clinic. Despite this, the mechanisms governing the underlying resistance phenotypes are not fully elucidated (Kang *et al.*, 2025).

A. fumigatus infections are opportunistic and require specific conditions to develop and persist in the lung (Paulussen *et al.*, 2016). The human body is constantly exposed to *A. fumigatus* conidia from the environment. The average adult is estimated to inhale more than 100 conidia daily with only one required to initiate infection in a vulnerable individual (Ortiz *et al.*, 2022). Once the prerequisite conditions are present *A. fumigatus* can cause a range of devastating clinical manifestations which are highly dependent on the host's physiological and immunological status. This range of manifestations and the role of the host in shaping the form of disease present, complicates the understanding of host adaptation processes and fungal pathogenesis.

A. fumigatus virulence is complex and cannot be attributed to a single trait or factor. Many of these traits may have arisen from challenges observed in the soil niche such as nutrient limitation, adaptation to stress and competition with microorganisms and predatory amoeba (Askew, 2008; Earle *et al.*, 2023). These factors include mechanisms for nutrient acquisition and production of enzymes and mycotoxins and stress mitigation. The development and activity of many of these traits in the soil could imply off target effects and cross-reactivity are responsible for their impact on the human host, classifying *A. fumigatus* as a true "accidental pathogen" of humans. One example of this is gliotoxin, which was identified as a virulence factor in many models and experimental settings. Gliotoxin has long been classified as a virulence factor due to its immunosuppressive effects on macrophages and neutrophil recruitment (Schlam

et al., 2016; König *et al.*, 2019). Despite this, gliotoxin is also produced in the soil where it has amoebicidal activities against the natural fungal predator *Dictyostelium discoideum* (Hillmann *et al.*, 2015). Much of the basic machinery and signal transduction pathways of phagocytosis are evolutionarily conserved between amoeba and vertebrate macrophages, reflecting the ancient origins of this process (Gaudet *et al.*, 2016). This exemplifies the potential that gliotoxin toxicity has arisen in the soil niche and its role in human colonisation can be attributed to cross reactivity resulting in inhibition of human immune cells, although this is not conclusive.

Moreover, humans are considered to be a terminal host as *A. fumigatus* does not complete its lifecycle and does not display well developed mechanisms for dispersal once infection has been established (Hui *et al.*, 2024). This complicates our understanding of the disease as traits facilitating host-adaption and acquisition of antifungal resistance would become more prevalent in the clinic through transmission from patient to patient (Verweij *et al.*, 2020). The traits that enable survival of specific conidia in the presence of the host following inhalation from the environment also poses questions of fitness. Are specific conidia capable of adapting to persist in pressures exerted in the host environment? The alternative explanation is that the host simply serves as a selective bottleneck for strains already adapted to persist in the harsh environment imposed by the host (Ballard *et al.*, 2018). To understand the development of *A. fumigatus* in the host and examine these adaptation processes, systems must be developed to faithfully replicate the host environment or specific aspects of the host environment to assess how the fungus persists.

The work presented here utilised the *G. mellonella* larval model to emulate innate immune responses during chronic fungal infection and in host selection. The fungus was subjected to prolonged subculture on a bespoke agar containing the immune products and nutrients present within *G. mellonella* larvae. This approach was adopted to by-pass the short lifespan of the larvae following infection (Tsai *et al.*, 2016) and enable analysis of host selection from a single parent strain. Similar work was conducted *in vivo* using the pathogenic yeast *Cryptococcus neoformans* in *G. mellonella* larvae for 15 passages resulting in the generation of a strain that grew faster in haemolymph but displayed altered susceptibility to hydrogen peroxide and was less virulent (Ali *et al.*, 2020). *Aspergillus flavus*, demonstrated reduced genetic heterogeneity following cycling in *G. mellonella* (Scully and Bidochka, 2006). These

studies demonstrated fungal in host-adaptation and a potential shift towards persistence and chronicity. Our results demonstrated similar processes occurring in *A. fumigatus* giving rise to different phenotypes following 25 cycles on the galleria extract agar over 231 days. This indicates that the agar was imposing a selection pressure on *A. fumigatus* resulting in a shift towards persistence in the host. There was also variation in the phenotype among the passaged strains, indicating many adaptations can enable persistence in the host. These strains demonstrated similar growth rates and virulence *in vivo* but varied in gliotoxin production and antifungal susceptibility. The adapted strains demonstrated altered susceptibility to various stressors including increased persistence in the presence of host immune cells and altered susceptibility to oxidative stress and antifungals including itraconazole and amphotericin B. In a similar response to that observed in *C. neoformans* (Ali *et al.*, 2020) all adapted strains demonstrated reduced virulence in the host despite these adaptations indicating a shift towards chronicity could be occurring.

The most significant alteration was observed in the E lineage which was selected for proteomic analysis. The small number of alterations detected indicated an increased abundance of proteins associated with oxidative stress mitigation. Proteomic analysis also identified that changes were not likely to have occurred as a result of nutrient limitation. This would suggest host metabolism or utilisation of nutrients from the host can fuel fungal development and fungal adaptation to products of the innate immune response. The strains also demonstrated a rapid emergence of antifungal tolerance, despite being derived from a treatment naïve parental strain. It is postulated that this resistance can be attributed to decreased expression of mitochondria complex I intermediate associated protein and histone H2A.Z, which regulates catalase production. Mitochondria complex I is the main source of reactive oxygen species generation in response to antifungal treatment (Shekhova *et al.*, 2017). Production of reactive oxygen species by the innate immune response and fungal adaptations to persist in the presence of these stressors could influence antifungal susceptibility and response to the immune cells *in vivo*, offering an alternative explanation for the development of treatment tolerance in the clinic as this tolerance emerged in a similar time frame to clinically recommended treatment duration.

This study indicated that in the context of chronic infection the host microenvironment serves as a selective bottleneck of a heterogeneous environmental

inoculum resulting in effective colonisation of the host by the fittest subpopulation and only minor changes can convey this fitness and these can be acquired rapidly. Understanding these alterations in the proteome and the consequences they can have in the clinic is crucial to understanding host adaptation and the rate at which it occurs. The findings of this study also replicated what has been observed in the clinic where isolates from patients with aspergillomas were found to be significantly less genetically variable, indicating that aspergillomas may form following selection for strains fit prior to prolonged colonisation (Howard *et al.*, 2013).

Expanding on this work, a sublethal *A. fumigatus* infection was established *in vivo* in *G. mellonella* larvae to characterise the response of the fungus to innate immune antagonism experienced during initial host colonisation but also to assess the host proteomic response to infection. This study provides a deeper insight into products released by *A. fumigatus* during infection and the kinetics of virulence factor production. It also enabled simultaneous profiling of the proteomic response of the pathogen and the host during the early stages of chronic infection. During the early stages of infection there was initial utilisation of carbohydrates and then a shift towards protein metabolism, particularly amino acid metabolism at 72 hours post infection. This is also when detection of fungal effectors including gliotoxin and siderophore production was most prominent suggesting metabolism is tied to fungal virulence. Qualitative proteomic analysis which identified the markers of other mycotoxins including fumitremorgin and fumiquinazoline C. Many of these effectors are derived from aromatic amino acids, which can be synthesized through the Shikimate pathway (Sasse *et al.*, 2016). The detection of pentafunctional AROM polypeptide along with other proteins associated with aromatic amino acid biosynthesis suggest that this pathway may be involved in the virulence of *A. fumigatus* *in vivo*. This exemplifies that metabolism of the host protein heavily shapes the production of fungal toxins and fuels fungal development beyond 48 hours of infection.

Examination of the response of the infected larvae relative to uninfected controls demonstrated aspects of morbidity, melanisation and reduced mobility. The larval proteome displayed increased abundance of proteins associated with metabolism and detoxification. There was also more potent activation of the immune response primarily associated with antimicrobial peptide production, inflammation and pathogen binding. There was a decrease in proteins associated with nutrient

reservoirs indicating the fungus can corrupt these pathways to access host nutrients. There was evidence of tissue-specific proteins being released into cell-free haemolymph indicating tissue damage, including troponin T which is used as a biomarker in human diseases involving tissue degradation (Tanindi and Cemri, 2011). These results highlight the innate immune antagonism elicited within the host and the impact that it can have on fungal development and production of secondary metabolites.

The results obtained in the *G. mellonella* infection model identified that *A. fumigatus* can survive on nutrients present within the host and requires only minor proteomic alterations to persist in the presence of products of the innate immune response. The studies also provide insight into the production of various fungal factors such as mycotoxins and siderophores and how their production can be influenced by fungal metabolism from host resources. The results also support genome-wide analysis findings that indicate capacity to utilise aromatic amino acids as a key identifier of *A. fumigatus* virulence (Mirhakkak *et al.*, 2023). We have identified how this may be important in virulence as in *G. mellonella* larvae this metabolism coincides with the production of various amino acid derived virulence factors including siderophores and mycotoxins. The analysis of both sides of the host- pathogen interactions is crucial to provide insight into the consequences of the production of these molecules and the roles they have in facilitating fungal growth and survival within the host. These studies also identified that the host may exert selection pressure on the fungus and that products of the host immune response can contribute to antifungal tolerance in a treatment naïve isolate. This is likely to occur through cross- reactivity in the off-target effects of antifungals, inducing reactive oxygen species production in the fungus. Both effectors induce an evolutionary ancient mechanism of oxidative stress mitigation and thus chronic exposure to the products of the innate immune response could aid in the development of in-host tolerance to antifungal agents governed at the protein level, even in treatment naïve strains. This furthers our understanding of antifungal tolerance development within patients in the context chronic infection.

The host microenvironment in which *A. fumigatus* must develop is not sterile and as a result *A. fumigatus* must compete for resources and space with other microorganisms from the host microbiome and other invading pathogens. This is similar to its survival in the soil niche. The impact of microbial antagonism on *A.*

A. fumigatus development has often been overlooked and warrants further study. *K. pneumoniae* is a common co-pathogen with *A. fumigatus* in cystic fibrosis (CF) patients (Akyil *et al.*, 2025). The spatial arrangements and product exchanges during polymicrobial interactions are determining factors in the regulation of host microenvironment, impacting nutrient availability, distribution of microbial species and immune responses (Bitencourt *et al.*, 2024). To assess these interactions in a spatially independent manner, *A. fumigatus* was exposed to the secretome of *K. pneumoniae* in culture. This provides insight into the impact that this bacterial species can have on the fungus independent of physical interaction.

K. pneumoniae was grown for 96 hours to produce a culture filtrate which would contain secreted products but also products released during bacterial death which could interact with *A. fumigatus* in the lung microenvironment. Proteomic analysis of the culture filtrate identified 35 proteins which could alter fungal development. Three of these, a putative lipoprotein, outer membrane protein A and chaperone protein DnaK were physically bound to the fungal mycelia. These proteins were demonstrated to induce leakage in various other species and likely result in pore formation in the fungal membrane. The culture filtrate also contained enzymes associated with the bacterial cell wall and proteases which could potentially impact fungal activity. Proteins in the culture filtrate could also result in nutrient sequestering including non-siderophore iron uptake component EfeO and the high-affinity zinc uptake system protein ZnuA indicate metal starvation could be occurring. The culture filtrate significantly reduced fungal growth while promoting a shift towards secondary metabolism, particularly through the increased secretion of gliotoxin. Proteomic analysis of *A. fumigatus* exposed to the supernatant supports this as there was a significant increase in five out of thirteen proteins in the gliotoxin biosynthesis cluster. This would indicate that *A. fumigatus* is weakened through interactions with *K. pneumoniae* as it cannot grow as effectively but this growth inhibition results in the production of secondary metabolites that can be deleterious for the host and potentially fuel bacterial persistence through induced immunosuppression. The increase in gliotoxin production may be attributed to the physical binding of bacterial chaperones increasing *A. fumigatus* permeability and stimulating *de novo* gliotoxin biosynthesis (Reeves *et al.*, 2004). It has been previously demonstrated that zinc limitation results

in increased gliotoxin production and the growth-limiting effects of exogenous gliotoxin are relieved by the presence of zinc in media (Traynor *et al.*, 2021).

In addition to the significant increase in gliotoxin which can have severe consequences on the hosts ability to mount an effective immune response (Ye *et al.*, 2021) other factors influencing fungal interaction with the host were altered. Fibrinogen C-terminal domain-containing protein was the most significantly increased protein. This implies increased capacity to bind to the host extracellular matrix as fibrinogen deposits form at the surface of wounded epithelia in asthmatic individuals and when lung damage is present (Upadhyay *et al.*, 2012). These alterations in response to secreted microbial products in the absence of a host highlight the impact these interactions can have in shaping fungal virulence. These results also demonstrate that *A. fumigatus* is a weak competitor when exposed to products of bacterial pathogens as its development is severely hampered. In other studies of *K. pneumoniae* physical interaction was found to inhibit fungal germination (Nogueira *et al.*, 2019). Similar results were obtained when *A. fumigatus* was exposed to *P. aeruginosa* culture filtrate which also affected fungal growth and secondary metabolism, identifying a similar protein profile to that found in the current work (Margalit *et al.*, 2022). *P. aeruginosa* culture filtrate also contained the chaperone protein DnaK and proteins associated with uptake of nutrients, including ferric iron-binding periplasmic protein HitA. Despite these similarities, *K. pneumoniae* culture filtrate promoted gliotoxin biosynthesis, while *P. aeruginosa* inhibited it (Margalit *et al.*, 2022). These results highlight the importance of the microbial component of the host microenvironment and the value of replicating it where possible to understand fungal adaptation and colonisation in human patients.

To gain further insight into *A. fumigatus* host interactions with aspects of human airway colonisation the *ex-vivo* pig lung (EVPL) model was adapted for fungal development, as a model of lung physiology and architecture. The tissue also retains a host microbiome which is difficult to emulate in *in vitro* systems. A time course analysis was conducted to characterise the proteome of *A. fumigatus* during the first 96 hours of growth on alveolar explants of a pig lung grown in culture conditions. This analysis also facilitated simultaneous characterisation of the host response during infection.

A. fumigatus demonstrated reduced growth on the lung explants at 72 hours post infection compared to an agar control indicating increased challenge when growing on a realistic host tissue compared to standard culture medium. This can be attributed to the complex nutritional profile of the tissue but also immune antagonism occurring within the tissue. In a similar pattern of growth to what was observed in *G. mellonella* larvae, proteomic analysis of *A. fumigatus* indicated an increased abundance of proteins associated with growth and carbohydrate metabolism at 48 hours, whereas at 72 and

96 hours, proteins associated with amino acid metabolism were increased in abundance. This further supports the role of amino acid metabolism and biosynthesis in supporting fungal virulence. This is further supported by gene enrichment analysis at 96 hours post infection highlighted the increased abundance of proteins associated with ascorbate and aldarate metabolism, beta-alanine metabolism, fatty acid degradation, glycolysis/gluconeogenesis, tryptophan metabolism, and degradation of valine, leucine, and isoleucine. These have all been demonstrated to be enhanced following *A. fumigatus* exposure to human dendritic cells (Srivastava *et al.*, 2019).

There was also similarity to the *G. mellonella* experiments regarding secondary metabolite production being prominent in the later stages of colonisation on the EVPL tissue. The kinetics of mycotoxin production, including gliotoxin was confirmed through proteomic analysis. Other factors associated with virulence, including some factors not observed in larvae, were detected in the EVPL model. Pseurotin A production, as evidenced by detection of methyltransferase psoC and fungal enolase, and these were significantly increased in abundance at all time points. Fungal enolase has been identified as an inhibitor of the human complement cascade (Dasari *et al.*, 2019). Other factors influencing colonisation were detected including fungal allergens, proteins associated with adherence and markers of fungal stress mitigation. In a similar manner to that observed in *G. mellonella* *in vivo* infection fungal allergens were detected and these can induce an immune response in the host (Liu *et al.*, 2023). In addition, Cyanovirin-N domain-containing protein was also significantly increased in abundance at all timepoints. This protein may serve as a novel adhesin in *A. fumigatus* through strong interactions to mannose residues, potentially enhancing fungal attachment to the host (Koharudin *et al.*, 2008; Driessen *et al.*, 2012). Despite this range of effectors being produced there is also evidence of fungal stress responses indicating hostility in the tissue. There was evidence of hyphal

damage, exemplified by the detection of hexA associated with woronin body formation and the production of numerous detoxification enzymes. These markers indicate host antagonism is retained within the explants, and these factors can impede fungal development in a similar manner to that which is observed in the human lung.

The ability of *A. fumigatus* to induce and alter an immune response and persist despite the production of various antifungal responses is further supported when examining the proteome of the explant in response to infection. This includes detection of markers of leukocyte recruitment and activation in the initial 48 hours post-infection. There is also evidence of an initial allergic response possibly induced by the expression of allergens, as carbonic anhydrase 4, expressed in IL-5-activated eosinophils was increased in abundance. In murine studies, carbonic anhydrase 4 was enhanced following an allergic insult with *A. fumigatus* (Wen *et al.*, 2014). There was evidence of activation of the adaptive immune response with importin subunit alpha KPNA3 and KPNA4 increased in abundance and these are essential for TNF-alpha-stimulated NF-KB p50/p65 heterodimer translocation into the nucleus, resulting in a pro-inflammatory response (Fagerlund *et al.*, 2005).

Crucially immune response machinery known to be inhibited by *A. fumigatus* were inhibited in the explants including neutrophil degranulation and a decreased expression of pulmonary surfactant-associated protein A1 isoform X2. The levels of surfactant protein A are decreased in the lungs of patients with cystic fibrosis, acute respiratory distress syndrome and further chronic lung diseases (Heinrich, 2011). The specificity of the response to fungal pathogenesis is best exemplified by inhibition of the complement cascade. Components of the complement cascade were significantly decreased in abundance from 48 hours, and this was consistent at all subsequent timepoints. In addition, gene enrichment analysis also highlighted decreased complement and coagulation cascade activity at 96 hours post infection. This indicates potential immune evasion induced by the fungus could be occurring (Dasari *et al.*, 2019). These alterations occurred in the absence of other known complement evasion mechanisms and as such supports the role of enolase in this disruption and implies enolase is a potent inhibitor of this cascade or other factors yet to be identified are involved in the evasion observed in this study.

The EVPL model also indicated fungal utilisation of host nutrients for survival as observed in *G. mellonella*. Gene enrichment analysis across timepoints also highlighted a consistent decrease in proteins associated with the citrate cycle and amino acid degradation indicating the infected tissue is less metabolically active following infection. This is similar to that observed in murine models of invasive pulmonary Aspergillosis (Kale *et al.*, 2017). The EVPL tissue also demonstrated evidence of tissue damage as observed in the later stages of larval infection but goes beyond what is observed in the insect as there is evidence of fibrosis and tissue remodelling from 48 hours including collagen accumulation. This may be driven by transforming growth factor beta-1-induced transcript 1 protein increased as overexpression of TGF- β is known to induce collagen deposition in mice (Hillege *et al.*, 2020). From 72 hours many components of the extracellular matrix (ECM) increase in abundance in response to *A. fumigatus* infection. These markers are also induced during fibrosis and are associated with the establishment of invasive fungal diseases. The increased expression of ECM components could also facilitate the covering of fungal hyphae by these components (Loussert *et al.*, 2010). This can lead to the formation of aspergillomas where the hyphae are embedded together in this dense extracellular matrix, whereas in invasive aspergillosis hyphae are individually engulfed in the matrix (Müller *et al.*, 2011). The extracellular matrix coating protects the fungus against host immune effectors as well as antifungal drugs (Muszkieta *et al.*, 2013).

These results indicate dynamic and specific interactions occur between *A. fumigatus* and the EVPL explants and these responses share similarities to that observed in human patients and previously observed in *G. mellonella* larvae. *A. fumigatus* demonstrates a similar metabolic profile at similar stages of development and the kinetics of various virulence factor production in these models. However, the *ex-vivo* pig lung model goes further what was observed in *G. mellonella* larvae, providing insights into the attachment, metabolism, growth and virulence in response to a dynamic innate and adaptive immune response and complex tissue architecture. These results also demonstrate the importance of emulating the host as accurately as possible to gain insight into host-pathogen interactions.

To further utilise the newly adapted *ex-vivo* pig lung model we aimed to establish and assess the interactions of *A. fumigatus* during coinfection with *P. aeruginosa* in a realistic host tissue context and characterise all three species within this interaction simultaneously. Examination of infected explants demonstrated growth of both pathogens in isolation, however in coinfection there was weakened identifiers of each pathogen respectively particularly reduced fungal development. This indicated competition between pathogens within the co-infected tissue. This competition was supported through metataxonomic analysis of the explants which revealed that *A. fumigatus* infected explants resulted in dysbiosis of the tissue microbiome. This resulted in promotion of the Pseudomonadota phylum, but more specifically *P. aeruginosa* at the species level. Its abundance was significantly higher in co-infection relative to *P. aeruginosa* mono-infected explants. This confirms that *A. fumigatus* can facilitate *P. aeruginosa* dominance in the airways. Proteomic analysis of *A. fumigatus* in coinfection with *P. aeruginosa* relative to mono-infection suggests that *P. aeruginosa* dominance comes at the expense of *A. fumigatus* as there is a reduced abundance of proteins associated with virulence. In addition, enolase, previously demonstrated to inhibit the complement cascade (Dasari *et al.*, 2019) was decreased in abundance in *A. fumigatus* in coinfecting explants. These alterations can be attributed to a lack of nitrogen availability as proteins associated with numerous processes involving nitrogen utilisation and S-adenosylmethionine metabolism were decreased in abundance in coinfection. This indicates competition with *P. aeruginosa* for nitrogen as well as sulphur containing amino acids cysteine and methionine, both of which have been associated with fungal growth and virulence in the host (Amich *et al.*, 2016).

This explanation is further supported by analysis of the *P. aeruginosa* proteome which identified an increase in translation machinery and abundance of proteins involved with regulation of amino acids and their amide derivatives. This suggests increased cellular activity related to protein synthesis and nitrogen utilisation. All of these factors indicate reduced availability of crucial nutrients for *A. fumigatus* because of competition from *P. aeruginosa* and that *A. fumigatus* development is hampered by coinfection with *P. aeruginosa*. This is a similar to that observed when *A. fumigatus* was grown in the presence of the secreted products of *K. pneumoniae* and its growth was compromised. This also suggests that *A. fumigatus* enhances the development

of its competitors and can fuel their virulence resulting in enhanced damage to the host. This is exemplified through the decreased detection of elastase LasB which is associated with acute virulence and is the most abundant protease produced by *P. aeruginosa* (Sun *et al.*, 2020). LasB is a potent immune evasion molecule in acute infections through its ability to manipulate host responses (Suarez- Cuartin *et al.*, 2017). The gene *lasR* regulates LasB and loss of function mutants frequently arise in chronically infected CF patients and are associated with greater neutrophilic inflammation and immunopathology in both murine models and human patients (LaFayette *et al.*, 2015). The decreased abundance of elastase (LasB) in the coinfection group indicates this phenomenon could be occurring in the lung explants, driving inflammatory response at the expense of *A. fumigatus* clearance.

Characterisation of the tissue response to the various infection states highlight the impact each pathogen has on the host and the accumulative effect that occurs in coinfection. *A. fumigatus* mono-infection induces tissue fibrosis and inflammation as observed in the Chapter 5, but unlike the previous work there was activation of the alternative complement cascade pathway indicating that some differential responses may occur within the model. There was also a decrease in abundance of proteins associated with metabolic processes including valine, leucine and isoleucine degradation and 2-Oxocarboxylic acid, involved in the biosynthesis of the branched aliphatic proteinogenic amino acids (Kirschning, 2022). This further supports the previous *ex-vivo* pig lung results and the *G. mellonella* results which demonstrated amino acid metabolism from the host can fuel fungal virulence during the initial stages of host colonisation and immune antagonism. *A. fumigatus* relies heavily on the amino acids valine, isoleucine, and methionine during invasive aspergillosis (Ibrahim-Granet *et al.*, 2008), and these metabolic processes were decreased in the infected explants.

In response to *P. aeruginosa* mono-infection there was also evidence of fibrosis and alteration to the extracellular matrix in addition to stimulation of the immune response driven by natural killer cells. Proteins decreased in abundance were associated with different metabolic processes to that decreased in response to *A. fumigatus* indicating utilisation of host nutrients in a similar manner to *A. fumigatus* infection. Both species seem to reduce host valine degradation but *P. aeruginosa* also decreased

butanoate metabolism, associated with chronic persistence of *P. aeruginosa* in hypoxic biofilms (Abdelhamid and Yousef, 2024). Reduction in host butanoate metabolism could indicate leaching specific nutrients from the host to fuel its own chronicity. Additionally, glyoxylate and dicarboxylate metabolism was decreased in the host infected with *P. aeruginosa*. The glyoxylate cycle is upregulated in *P. aeruginosa* under conditions of oxidative and antibiotic stress (Matthaiou *et al.*, 2018).

The proteome of the coinfecting explants indicated a mixed phenotype when compared to both mono infections. This includes more potent immune responses including both the complement cascade and natural killer cell mediated toxicity observed in *A. fumigatus* and *P. aeruginosa* mono-infection respectively. There was also similarity in the decrease of metabolic processes with propanoate and valine leucine and isoleucine degradation, downregulated in both mono-infections and coinfection, indicating both pathogens require these resources. In addition, 2-Oxocarboxylic acid metabolism, only detected in *A. fumigatus* infection and glyoxylate and dicarboxylate metabolism, only detected in *P. aeruginosa* infection, were also decreased in coinfection indicating a combinational impact on the host tissue when both species are present.

The coinfecting EVPL induced a more potent adaptive immune activation and inflammatory response when compared to each mono-infection exemplified through elevated Interleukin-6 detection relative to both mono-infections. IL-6 has a crucial role in protective immunity against *A. fumigatus* infection in mice (Heldt *et al.*, 2017) and elevated IL-6 and lung oedema were characteristic signs of *P. aeruginosa* infection (Wölbeling *et al.*, 2011). Lactoferrin and ferritin light chain were both decreased in abundance in coinfecting EVPL relative to *P. aeruginosa* mono-infection potentially indicating the presence of *A. fumigatus* can disrupt host iron sequestering resulting in elevated iron availability fuelling bacterial development. This is similar to decreased expression of *G. mellonella* nutrient reservoir processes and can potentially be attributed to *A. fumigatus* in the EVPL model also. This work clearly demonstrates that single and dual infections by these two important pathogens have distinct pathologies within the EVPL tissue, inducing fibrosis and distinct immune responses.

These studies culminate to provide novel phenotypic and proteomic insight into the development of *A. fumigatus* in the presence of various stressors experienced within a host including immune antagonism, oxidative stress, nutrient limitation and competition with bacterial pathogens. When exposed to these stresses in isolation and in combination, *A. fumigatus* utilises effectors evolved and produced during survival in the soil to overcome these challenges and survive. The production of these effectors appears to be tightly linked with metabolite availability to *A. fumigatus* as their production in both model systems examined in this work was tied to protein and aromatic amino acid metabolism within the host. The main aim of the production of these effectors appears to be stress mitigation and nutrient salvage. Siderophores harvest iron from the host and even gliotoxin, long observed as an immunosuppressive toxin is capable of stripping metals such as zinc from the host, although fungal utilisation of this zinc is yet to be confirmed (Downes *et al.*, 2023).

The ability of *A. fumigatus* to persist following inhalation into the body requires a specific set of circumstances and mimicking these conditions experimentally often requires biasing the infection dose to facilitate establishment of infection. The ability of particular conidia to survive is partially driven by host selection pressure by which conidia with particular fitness traits in the environment are selected for within the host. As a result, the traits the fungus already possesses enable it to survive in the presence of host effectors. This is further supported by the fact that a small number of protein changes can significantly alter the phenotype and survival of a strain in such a hostile environment resulting in the capacity to cause chronic infection. This indicates that host-selection influences host adaptation processes by selecting for traits that exist in the soil that also provide fitness in the human airways and tolerance of antifungal agents, specifically those fit to tolerate oxidative stress.

The factors enabling fungal persistence requires the repurposing and utilisation of ancient and conserved mechanisms with cross-reactivity often to the detriment of the host, these include siderophores, mycotoxins and enzymes that can degrade host tissue and facilitate fungal invasion. It remains unclear if any effector identified as contributing to virulence in patients cannot be found in the soil as many are found to be produced in response to pressures exerted in this niche. The ability to repurpose these molecules implies that this accidental pathogen does display aspects of host adaptation and its ability to acquire and utilise host nutrients to survive supports this.

The ability of *A. fumigatus* to survive in the host environment can be attributed to selection for traits that enable the fungus to develop in its soil niche. These include its vast metabolic repertoire and versatility, its suite of fungal effectors and its rapid adaptability to stress. These factors make *A. fumigatus* a serious threat and the work presented here identifies only minor changes are required to facilitate its successful colonisation of the host from a wildtype strain. These findings suggest that strategies and effectors observed in the environment can give rise to pathogens without need for significant alterations within the host. Once a species can persist at suitable body temperature other environmental species may be equally as equipped to colonise humans through repurposing of enzymes, toxins and traits developed in the environment. This is of growing concern because of climate change as the number of fungal pathogens has already increased in recent years in a concerning trend that is likely to intensify. In some ways this work may confirm that *A. fumigatus* is an early emerging archetype of an environmental fungus whose environmental niche shaped its development and human disease is a consequence of how it has been shaped over evolutionary time. The inability of *A. fumigatus* to compete with bacterial pathogens as examined with *K. pneumoniae* and *P. aeruginosa* that inhabit a similar niche in the soil and in the lung further supports *A. fumigatus*' identity as an accidental pathogen. This can be attributed to the fact that these bacterial species possess more robust arsenals of effectors which consistently outcompete and exploit the fungus for their own gain even irrespective of physical interaction. Despite this, traits conferring the ability of *A. fumigatus* to grow and persist in the lung including mycotoxin production, host degrading enzymes and nutrient acquisition strategies may also be present in other environmental fungi shaped by competition with other organisms and screening for these traits in the environment can aid in identifying species that may emerge as future pathogens, given the development of thermotolerance.

The mechanisms governing *A. fumigatus* host adaptation and persistence though not uniquely produced in the host, give rise to a serious human health risk, resulting in the cost of many lives every year. In-depth analysis to understand these mechanisms is warranted in order to inform effective treatment of the disease. The nutritional requirements of *A. fumigatus* and its preferences towards aromatic amino acid metabolism offers a gap in its microbial armour and offers

exciting avenues for the development of targeted therapeutics potentially acting on the conserved shikimate pathway. Understanding the kinetics and production of specific effectors and what is required prior to their production offers opportunity to intercept or target them to weaken fungal disease but also prevent the detrimental impacts these factors have on the host. It is crucial to examine these factors in systems that replicate the complexity of the host microenvironment to gain true insight into how these factors facilitate fungal survival and disease development in order to find novel ways to overcome this threat.

7.2 Concluding remarks and future work

A. fumigatus is a serious cause of disease and death but many of the factors facilitating its virulence are attributable to the species development in the soil niche. These include oxidative stress mitigation, the biosynthesis and utilisation of aromatic amino acids, and the production of various effectors including mycotoxins and siderophores, some of which can be derived from these metabolites. Examination of these traits in alternative model systems mimicking aspects of the host in isolation has provided novel insight into the requirements for fungal survival and persistence within the host. This work has also examined how aspects of the host environment influence the production and kinetics of fungal effectors and the impact they have on the host. The work presented here provide insight into the dynamics of host-pathogen interaction and has identified immune evasion and mitigation strategies displayed by the fungus during the initial stages of this interaction. The work presented here also highlights that only minor alterations are required to facilitate fungal persistence in the human host and that these alterations can influence the efficacy of antifungal therapy. Despite the ability of *A. fumigatus* to persist in the presence of multiple stressors, it often competes poorly against other better equipped bacterial pathogens through both indirect interactions with secreted products and through direct competition within the host niche. Despite this inability to compete, the fungus still poses a threat to the host and its interactions with bacterial species can result in enhanced virulence and development of its microbial competitor at the expense of the host. Much remains to be understood about *A. fumigatus* interactions and adaptation within the host and this and future studies will equip clinicians and researchers with better targets for diagnostics and therapeutics in order to tackle this disease.

The work presented here primarily focused on proteomic analysis to elucidate mechanisms governing fungal survival in the host and utilised alternative model systems including *G. mellonella* and the *ex-vivo* pig lung model. Future work can expand this through examination of fungal development through transcriptomic analysis as a multi-omics approach can provide more robust and detailed insight into these factors. Further investigation into host-adaptation and passaging work in other model systems could be conducted to further elucidate the mechanisms governing in-host antifungal tolerance development as this poses a serious threat to human health and should be understood in better detail.

The *ex-vivo* pig lung model could be further developed for fungal biology and should be expanded to examine more polymicrobial interactions, antifungal efficacy in the context of tissue absorption and metabolism. The model could be further developed for use in examining other pulmonary fungal pathogens. The model would benefit from the development of further, more targeted endpoints to assess particular aspects of fungal virulence and development. The next iteration of the model could aim to utilise condition specific media such as artificial sputum media. This model would also be improved through the addition of perfusion to replenish nutrients in the system. The principles of the model could also be applied to other model systems including smaller mammals such as mice, where a whole lung model could be developed. The mice could be utilised from other experimental set ups that do not impact the lung or from breeding stock mice in line with the 3Rs principles to maximise the use of sacrificed mice. The development of a whole murine lung model could better emulate the structure and entry of a pathogen into the lung architecture and physiology. It would also by-pass the reliance on immune-suppressed mice currently found in fungal pathology literature enabling the immune response to be retained.

It is with hope that the work presented here will serve as a stepping stone for future breakthroughs, and that expansion of this work will aid in understanding the fundamentals of *A. fumigatus* pathogenesis and persistence. These expansions will identify strategies and targets for the next generation of antifungal agents and will aid in alleviating the growing threat of antifungal resistance and fungal disease.

Chapter 8

Bibliography

Abad, A., Victoria Fernández-Molina, J., Bikandi, J., Ramírez, A., Margareto, J., Sendino, J., Luis Hernando, F., Pontón, J., Garaizar, J. and Rementeria, A., 2010. What makes *Aspergillus fumigatus* a successful pathogen? Genes and molecules involved in invasive aspergillosis. *Revista Iberoamericana de Micología*, 27 (4), 155–182.

Abbas, R., Chakkour, M., Zein El Dine, H., Obaseki, E. F., Obeid, S. T., Jezzini, A., Ghssein, G. and Ezzeddine, Z., 2024. General Overview of *Klebsiella pneumoniae*: Epidemiology and the Role of Siderophores in Its Pathogenicity. *Biology*, 13 (2), 78.

Abdallah, Q. A., Choe, S.-I., Campoli, P., Baptista, S., Gravelat, F. N., Lee, M. J. and Sheppard, D. C., 2012. A Conserved C-Terminal Domain of the *Aspergillus fumigatus* Developmental Regulator MedA Is Required for Nuclear Localization, Adhesion and Virulence. *PLOS ONE*, 7 (11), e49959.

Abdelhamid, A. G. and Yousef, A. E., 2024. Untargeted metabolomics unveiled the role of butanoate metabolism in the development of *Pseudomonas aeruginosa* hypoxic biofilm. *Frontiers in Cellular and Infection Microbiology* [online], 14. Available from: <https://www.frontiersin.org/journals/cellular-and-infection-microbiology/articles/10.3389/fcimb.2024.1346813/full> [Accessed 21 May 2025].

Abdelwahed, K. S., Siddique, A. B., Mohyeldin, M. M., Qusa, M. H., Goda, A. A., Singh, S. S., Ayoub, N. M., King, J. A., Jois, S. D. and El Sayed, K. A., 2020. Pseurotin A as a novel suppressor of hormone dependent breast cancer progression and recurrence by inhibiting PCSK9 secretion and interaction with LDL receptor. *Pharmacological Research*, 158, 104847.

Abou-Kandil, A., Tröger-Görler, S., Pschibul, A., Krüger, T., Rosin, M., Schmidt, F., Akbarimoghaddam, P., Sarkar, A., Cseresnyés, Z., Shadkhan, Y., Heinekamp, T., Gräler, M. H., Barber, A. E., Walther, G., Figge, M. T., Brakhage, A. A., Oshrov, N. and Kniemeyer, O., 2025. The proteomic response of *Aspergillus fumigatus* to amphotericin B (AmB) reveals the involvement of the RTA-like protein RtaA in AmB resistance. *microLife*, 6, uqae024.

Achilonu, C. C., Davies, A., Kanu, O. O., Noel, C. B. and Oladele, R., 2024. Recent Advances and Future Perspectives in Mitigating Invasive Antifungal-Resistant Pathogen *Aspergillus fumigatus* in Africa. *Current Treatment Options in Infectious Diseases*, 16 (1), 14–33.

Ahadian, S., Civitarese, R., Bannerman, D., Mohammadi, M. H., Lu, R., Wang, E., Davenport-Huyer, L., Lai, B., Zhang, B., Zhao, Y., Mandla, S., Korolj, A. and Radisic, M., 2018. Organ-On-A-Chip Platforms: A Convergence of Advanced Materials, Cells, and Microscale Technologies. *Advanced Healthcare Materials*, 7 (2).

Akyıl, F. T., Gösterici, S., Abalı, H., Cenger, D. H., Sabancı, Ç., Sökücü, S. and Altın, S., 2025. Prevalence and clinical impact of bacterial co-infection in chronic pulmonary aspergillosis. *BMC Pulmonary Medicine*, 25 (1), 155.

Al-Amrani, S., Al-Jabri, Z., Al-Zaabi, A., Alshekaili, J. and Al-Khabori, M., 2021. Proteomics: Concepts and applications in human medicine. *World Journal of Biological Chemistry*, 12 (5), 57–69.

Albasanz-Puig, A., Gudiol, C., Parody, R., Tebe, C., Akova, M., Araos, R., Bote, A., Brunel, A.-S., Calik, S., Drgona, L., García, E., Hemmati, P., Herrera, F., Ibrahim, K. Y., Isler, B., Kanj, S., Kern, W., Maestro de la Calle, G., Manzur, A., Marin, J. I., Márquez-Gómez, I., Martín-Dávila, P., Mikulska, M., Montejo, J. M., Montero, M., Morales, H. M. P., Morales, I., Novo, A., Oltolini, C., Peghin, M., del Pozo, J. L., Puerta-Alcalde, P., Ruiz-Camps, I., Sipahi, O. R., Tilley, R., Yáñez, L., Gomes, M. Z. R. and Carratalà, J., 2019. Impact of antibiotic resistance on outcomes of neutropenic cancer patients with *Pseudomonas aeruginosa* bacteraemia (IRONIC study): study protocol of a retrospective multicentre international study. *BMJ Open*, 9 (5), e025744.

Alcántar-Curiel, M. D., Ledezma-Escalante, C. A., Jarillo-Quijada, M. D., Gayosso-Vázquez, C., Morfin-Otero, R., Rodríguez-Noriega, E., Cedillo-Ramírez, M. L., Santos-Preciado, J. I. and Girón, J. A., 2018. Association of Antibiotic Resistance, Cell Adherence, and Biofilm Production with the Endemicity of Nosocomial *Klebsiella pneumoniae*. *BioMed Research International*, 2018 (1), 7012958.

Aldrovandi, M., Banthiya, S., Meckelmann, S., Zhou, Y., Heydeck, D., O'Donnell, V. B. and Kuhn, H., 2018. Specific oxygenation of plasma membrane phospholipids by *Pseudomonas aeruginosa* lipoxygenase induces structural and functional alterations in mammalian cells. *Biochimica et Biophysica Acta (BBA) - Molecular and Cell Biology of Lipids*, 1863 (2), 152–164.

Ali, M. F., Tansie, S. M., Shahan, J. R., Seipelt-Thiemann, R. L. and McClelland, E. E., 2020. Serial Passage of *Cryptococcus neoformans* in *Galleria mellonella* Results in Increased Capsule and Intracellular Replication in Hemocytes, but Not Increased Resistance to Hydrogen Peroxide. *Pathogens*, 9 (9), 732.

Alkhazraji, S., Gebremariam, T., Alqarihi, A., Gu, Y., Mamouei, Z., Singh, S., Wiederhold, N. P., Shaw, K. J. and Ibrahim, A. S., 2020. Fosmanogepix (APX001) Is Effective in the Treatment of Immunocompromised Mice Infected with Invasive Pulmonary Scedosporiosis or Disseminated Fusariosis. *Antimicrobial Agents and Chemotherapy*, 64 (3), e01735-19.

Al-Maleki, A. R., Braima, K. and Rosli, N. A., 2023. Editorial: Integrated omics approaches in the understanding of host-pathogen interactions. *Frontiers in Cellular and Infection Microbiology*, 13, 1215104.

Almaliki, H. S., Angela, A., Goraya, N. J., Yin, G. and Bennett, J. W., 2021. Volatile Organic Compounds Produced by Human Pathogenic Fungi Are Toxic to *Drosophila melanogaster*. *Frontiers in Fungal Biology*, 1, 629510.

Alonso-Roman, R., Mosig, A. S., Figge, M. T., Papenfort, K., Eggeling, C., Schacher, F. H., Hube, B. and Gresnigt, M. S., 2024. Organ-on-chip models for infectious disease research. *Nature Microbiology*, 9 (4), 891–904.

Alser, M., Eudine, J. and Mutlu, O., 2025. Taming large-scale genomic analyses via sparsified genomics. *Nature Communications*, 16 (1), 876.

Alves, R., Barata-Antunes, C., Casal, M., Brown, A. J. P., Dijck, P. V. and Paiva, S., 2020. Adapting to survive: How *Candida* overcomes host-imposed constraints during human colonization. *PLOS Pathogens*, 16 (5), e1008478.

Amich, J., Dümig, M., O'Keefe, G., Binder, J., Doyle, S., Beilhack, A. and Krappmann, S., 2016. Exploration of Sulfur Assimilation of *Aspergillus fumigatus* Reveals Biosynthesis of Sulfur-Containing Amino Acids as a Virulence Determinant. *Infection and Immunity*, 84 (4), 917–929.

Amich, J. and Krappmann, S., 2012. Deciphering metabolic traits of the fungal pathogen *Aspergillus fumigatus*: redundancy vs. essentiality. *Frontiers in Microbiology*, 3, 414.

Amich, J., Schafferer, L., Haas, H. and Krappmann, S., 2013. Regulation of Sulphur Assimilation Is Essential for Virulence and Affects Iron Homeostasis of the Human-Pathogenic Mould *Aspergillus fumigatus*. *PLOS Pathogens*, 9 (8), e1003573.

Amin, S., Thywissen, A., Heinekamp, T., Saluz, H. P. and Brakhage, A. A., 2014. Melanin dependent survival of *Aspergillus fumigatus* conidia in lung epithelial cells. *International Journal of Medical Microbiology*, 304 (5), 626–636.

Anderson, K. G., Mayer-Barber, K., Sung, H., Beura, L., James, B. R., Taylor, J. J., Qunaj, L., Griffith, T. S., Vezys, V., Barber, D. L. and Masopust, D., 2014. Intravascular staining for discrimination of vascular and tissue leukocytes. *Nature Protocols*, 9 (1), 209–222.

Andes, D., Brüggemann, R. J., Flanagan, S., Lepak, A. J., Lewis, R. E., Ong, V., Rubino, C. M. and Sandison, T., 2025. The distinctive pharmacokinetic profile of rezafungin, a long-acting echinocandin developed in the era of modern pharmacometrics. *Journal of Antimicrobial Chemotherapy*, 80 (1), 18–28.

Aruanno, M., Glampedakis, E. and Lamoth, F., 2019. Echinocandins for the Treatment of Invasive Aspergillosis: from Laboratory to Bedside. *Antimicrobial Agents and Chemotherapy*, 63 (8), e00399-19.

Askew, D. S., 2008. *Aspergillus fumigatus*: virulence genes in a street-smart mold. *Current Opinion in Microbiology*, 11 (4), 331–337.

Bañas, N. and Wagner, A. E., 2019. *Drosophila melanogaster* as an alternative model organism in nutrigenomics. *Genes & Nutrition*, 14, 14.

Bahram, M. and Netherway, T., 2022. Fungi as mediators linking organisms and ecosystems.

FEMS Microbiology Reviews, 46 (2), fuab058.

Bailly, C. and Vergoten, G., 2020. Interaction of fumigaclavine C with High Mobility Group Box 1 protein (HMGB1) and its DNA complex: A computational approach. *Computational Biology and Chemistry*, 89, 107409.

Ballard, E., Melchers, W. J. G., Zoll, J., Brown, A. J. P., Verweij, P. E. and Warris, A., 2018. In-host microevolution of *Aspergillus fumigatus*: A phenotypic and genotypic analysis. *Fungal Genetics and Biology*, 113, 1–13.

Bao, Z., Chen, H., Zhou, M., Shi, G., Li, Q. and Wan, H., 2017. Invasive pulmonary aspergillosis in patients with chronic obstructive pulmonary disease: a case report and review of the literature. *Oncotarget*, 8 (23), 38069–38074.

Baran, S. W., Brown, P. C., Baudy, A. R., Fitzpatrick, S. C., Frantz, C., Fullerton, A., Gan, J., Hardwick, R. N., Hillgren, K. M., Kopec, A. K., Liras, J. L., Mendrick, D. L., Nagao, R., Proctor, W. R., Ramsden, D., Ribeiro, A. J. S., Stresser, D., Sung, K. E., Sura, R., Tetsuka, K., Tomlinson, L., Van Vleet, T., Wagoner, M. P., Wang, Q., Arslan, S. Y., Yoder, G. and Ekert, J. E., 2022. Perspectives on the evaluation and adoption of complex in vitro models in drug development: Workshop with the FDA and the pharmaceutical industry (IQ MPS Affiliate). *ALTEX*, 39 (2), 297–314.

Barber, M. F. and Fitzgerald, J. R., 2024. Mechanisms of host adaptation by bacterial pathogens. *FEMS Microbiology Reviews*, 48 (4), fuae019.

Barkal, L. J., Procknow, C. L., Álvarez-García, Y. R., Niu, M., Jiménez-Torres, J. A., Brockman-Schneider, R. A., Gern, J. E., Denlinger, L. C., Theberge, A. B., Keller, N. P., Berthier, E. and Beebe, D. J., 2017. Microbial volatile communication in human organotypic lung models. *Nature Communications*, 8 (1), 1770.

Basso, P., Ragno, M., Elsen, S., Reboud, E., Golovkine, G., Bouillot, S., Huber, P., Lory, S., Faudry, E. and Attrée, I., 2017. *Pseudomonas aeruginosa* Pore-Forming Exolysin and Type IV Pili Cooperate To Induce Host Cell Lysis. *mBio*, 8 (1), e02250-16.

Beck, J., Echtenacher, B. and Ebel, F., 2013. Woronin bodies, their impact on stress resistance and virulence of the pathogenic mould *Aspergillus fumigatus* and their anchoring at the septal pore of filamentous Ascomycota. *Molecular Microbiology*, 89 (5), 857–871.

Beck, J. M., Young, V. B. and Huffnagle, G. B., 2012. The microbiome of the lung. *Translational Research: The Journal of Laboratory and Clinical Medicine*, 160 (4), 258–266.

Benahmed, M. A., Elbayed, K., Daubeuf, F., Santelmo, N., Frossard, N. and Namer, I. J., 2014. NMR HRMAS spectroscopy of lung biopsy samples: Comparison study between human, pig, rat, and mouse metabolomics. *Magnetic Resonance in Medicine*, 71 (1), 35–43.

Ben-Ghazzi, N., Moreno-Velásquez, S., Seidel, C., Thomson, D., Denning, D. W., Read, N. D., Bowyer, P. and Gago, S., 2021. Characterisation of *Aspergillus fumigatus* Endocytic Trafficking within Airway Epithelial Cells Using High-Resolution Automated Quantitative Confocal Microscopy. *Journal of Fungi*, 7 (6), 454.

Bengoechea, J. A. and Sa Pessoa, J., 2018. *Klebsiella pneumoniae* infection biology: living to counteract host defences. *FEMS Microbiology Reviews*, 43 (2), 123–144.

Bercusson, A., Williams, T. J., Simmonds, N. J., Alton, E. W., Griesenbach, U., Shah, A., Warris, A. and Armstrong-James, D., 2025. Increased NFAT and NFκB signalling contribute to the hyperinflammatory phenotype in response to *Aspergillus fumigatus* in a mouse model of cystic fibrosis. *PLOS Pathogens*, 21 (2), e1012784.

Bergin, D., Reeves, E. P., Renwick, J., Wientjes, F. B. and Kavanagh, K., 2005. Superoxide Production in *Galleria mellonella* Hemocytes: Identification of Proteins Homologous to the NADPH Oxidase Complex of Human Neutrophils. *Infection and Immunity*, 73 (7), 4161–4170.

Bertorello, S., Cei, F., Fink, D., Niccolai, E. and Amedei, A., 2024. The Future Exploring of Gut Microbiome-Immunity Interactions: From In Vivo/Vitro Models to In Silico Innovations. *Microorganisms*, 12 (9), 1828.

Bertuzzi, M., Hayes, G. E., Icheoku, U. J., Van Rhijn, N., Denning, D. W., Osherov, N. and Bignell, E. M., 2018. Anti-*Aspergillus* Activities of the Respiratory Epithelium in

Health and Disease. *Journal of Fungi*, 4 (1), 8.

Bhatia, I. P. S., Singh, A., Hasvi, J., Rajan, A. and Venigalla, S. K., 2024. Coinfection of Klebsiella pneumoniae and Aspergillus in a patient with chronic obstructive pulmonary disease post cardiac arrest: a case report. *Journal of Medical Case Reports*, 18 (1), 427.

Bigot, J., Guillot, L., Guitard, J., Ruffin, M., Corvol, H., Balloy, V. and Hennequin, C., 2020. Bronchial Epithelial Cells on the Front Line to Fight Lung Infection-Causing Aspergillus fumigatus. *Frontiers in Immunology*, 11, 1041.

Bitencourt, T., Nogueira, F., Jenull, S., Phan-Canh, T., Tscherner, M., Kuchler, K. and Lion, T., 2024. Integrated multi-omics identifies pathways governing interspecies interaction between A. fumigatus and K. pneumoniae. *Communications Biology*, 7 (1), 1496.

Blomquist, K. C. and Nix, D. E., 2021. A Critical Evaluation of Newer β -Lactam Antibiotics for Treatment of Pseudomonas aeruginosa Infections. *The Annals of Pharmacotherapy*, 55 (8), 1010–1024.

Blum, G., Perkhofer, S., Haas, H., Schrett, M., Würzner, R., Dierich, M. P. and Lass-Flörl, C., 2008. Potential Basis for Amphotericin B Resistance in Aspergillus terreus. *Antimicrobial Agents and Chemotherapy*, 52 (4), 1553–1555.

Boers, E., Barrett, M., Su, J. G., Benjafield, A. V., Sinha, S., Kaye, L., Zar, H. J., Vuong, V., Tellez, D., Gondalia, R., Rice, M. B., Nunez, C. M., Wedzicha, J. A. and Malhotra, A., 2023. Global Burden of Chronic Obstructive Pulmonary Disease Through 2050. *JAMA Network Open*, 6 (12), e2346598.

Boita, M., Heffler, E., Pizzimenti, S., Raie, A., Saraci, E., Omedè, P., Bussolino, C., Bucca, C. and Rolla, G., 2015. Regulation of B-cell-activating factor expression on the basophil membrane of allergic patients. *International Archives of Allergy and Immunology*, 166 (3), 208–212.

Bongomin, F., Gago, S., Oladele, R. O. and Denning, D. W., 2017. Global and Multi-National Prevalence of Fungal Diseases—Estimate Precision. *Journal of Fungi*, 3 (4), 57.

Bosáková, V., Frič, J. and Zelante, T., 2023. Activation of TLRs by Opportunistic Fungi in Lung Organoids. *Methods in Molecular Biology (Clifton, N.J.)*, 2700, 271–284.

Botero Aguirre, J. P. and Restrepo Hamid, A. M., 2015. Amphotericin B deoxycholate versus liposomal amphotericin B: effects on kidney function. *The Cochrane Database of Systematic Reviews*, 2015 (11), CD010481.

Bouillot, S., Pont, S., Gallet, B., Moriscot, C., Deruelle, V., Attrée, I. and Huber, P., 2020. Inflammasome activation by Pseudomonas aeruginosa's ExLA pore-forming toxin is detrimental for the host. *Cellular Microbiology*, 22 (11), e13251.

van de Bovenkamp, F. S., Dijkstra, D. J., van Kooten, C., Gelderman, K. A. and Trouw, L. A., 2021. Circulating C1q levels in health and disease, more than just a biomarker. *Molecular Immunology*, 140, 206–216.

Braakhuis, H. M., He, R., Vandebril, R. J., Gremmer, E. R., Zwart, E., Vermeulen, J. P., Fokkens, P., Boere, J., Gosens, I. and Cassee, F. R., 2020. An Air-liquid Interface Bronchial Epithelial Model for Realistic, Repeated Inhalation Exposure to Airborne Particles for Toxicity Testing. *Journal of Visualized Experiments: JoVE*, (159).

Braus, G. H., Pries, R., Düvel, K. and Valerius, O., 2004. Molecular Biology of Fungal Amino Acid Biosynthesis Regulation. In: Kück, U., ed. *Genetics and Biotechnology* [online]. Berlin, Heidelberg: Springer Berlin Heidelberg, 239–269. Available from: http://link.springer.com/10.1007/978-3-662-07426-8_13 [Accessed 18 Jun 2025].

Brock, M. and Buckel, W., 2004. On the mechanism of action of the antifungal agent propionate. *European Journal of Biochemistry*, 271 (15), 3227–3241.

Brown, G. D., Ballou, E. R., Bates, S., Bignell, E. M., Borman, A. M., Brand, A. C., Brown, A. J. P., Coelho, C., Cook, P. C., Farrer, R. A., Govender, N. P., Gow, N. A. R., Hope, W., Hoving, J. C., Dangarembizi, R., Harrison, T. S., Johnson, E. M., Mukaremera, L., Ramsdale, M., Thornton, C. R., Usher, J., Warris, A. and Wilson, D., 2024. The pathobiology of human fungal infections. *Nature Reviews Microbiology*, 22 (11), 687–704.

Braem, S. G. E., Rooijakkers, S. H. M., van Kessel, K. P. M., de Cock, H., Wösten, H. A. B.,

van Strijp, J. A. G. and Haas, P.-J. A., 2015. Effective Neutrophil Phagocytosis of *Aspergillus fumigatus* Is Mediated by Classical Pathway Complement Activation. *Journal of Innate Immunity*, 7 (4), 364–374.

Browne, N., Heelan, M. and Kavanagh, K., 2013. An analysis of the structural and functional similarities of insect hemocytes and mammalian phagocytes. *Virulence*, 4 (7), 597–603.

Bryda, E. C., 2013. The Mighty Mouse: The Impact of Rodents on Advances in Biomedical Research. *Missouri Medicine*, 110 (3), 207–211.

Buil, J. B., Oliver, J. D., Law, D., Baltussen, T., Zoll, J., Hokken, M. W. J., Tehupeiry-Kooreman, M., Melchers, W. J. G., Birch, M. and Verweij, P. E., 2022. Resistance profiling of *Aspergillus fumigatus* to olorofim indicates absence of intrinsic resistance and unveils the molecular mechanisms of acquired olorofim resistance. *Emerging Microbes & Infections*, 11 (1), 703–714.

Bulati, M., Busà, R., Carcione, C., Iannolo, G., Di Mento, G., Cuscino, N., Di Gesù, R., Piccionello, A. P., Buscemi, S., Carreca, A. P., Barbera, F., Monaco, F., Cardinale, F., Conaldi, P. G. and Douradinha, B., 2021. *Klebsiella pneumoniae* Lipopolysaccharides Serotype O2afg Induce Poor Inflammatory Immune Responses Ex Vivo. *Microorganisms*, 9 (6), 1317.

Bultman, K. M., Kowalski, C. H. and Cramer, R. A., 2017. *Aspergillus fumigatus* virulence through the lens of transcription factors. *Medical Mycology*, 55 (1), 24–38.

Burke, R. M., Sabet, N., Ellis, J., Rangaraj, A., Lawrence, D. S., Jarvis, J. N., Falconer, J., Tugume, L., Bidwell, G., Berhanu, R. H., MacPherson, P. and Ford, N., 2025. Causes of hospitalisation among people living with HIV worldwide, 2014–23: a systematic review and meta-analysis. *The Lancet HIV*, 12 (5), e355–e366.

Burks, C., Darby, A., Londoño, L. G., Momany, M. and Brewer, M. T., 2021. Azole-resistant *Aspergillus fumigatus* in the environment: Identifying key reservoirs and hotspots of antifungal resistance. *PLOS Pathogens*, 17 (7), e1009711.

Cai, L., Gao, P., Wang, Z., Dai, C., Ning, Y., Ilkit, M., Xue, X., Xiao, J. and Chen, C., 2022. Lung and gut microbiomes in pulmonary aspergillosis: Exploring adjunctive therapies to combat the disease. *Frontiers in Immunology*, 13, 988708.

Calatayud, M., Dezutter, O., Hernandez-Sanabria, E., Hidalgo-Martinez, S., Meysman, F. J. R. and Van De Wiele, T., 2019. Development of a host-microbiome model of the small intestine. *The FASEB Journal*, 33 (3), 3985–3996.

Carolus, H., Pierson, S., Lagrou, K. and Van Dijck, P., 2020. Amphotericin B and Other Polyenes—Discovery, Clinical Use, Mode of Action and Drug Resistance. *Journal of Fungi*, 6 (4), 321.

Casadevall, A., 2012. Fungi and the Rise of Mammals. *PLoS Pathogens*, 8 (8), e1002808.

Cerrada, A., Haller, T., Cruz, A. and Pérez-Gil, J., 2015. Pneumocytes Assemble Lung Surfactant as Highly Packed/Dehydrated States with Optimal Surface Activity. *Biophysical Journal*, 109 (11), 2295–2306.

Chadha, J., Harjai, K. and Chhibber, S., 2022. Revisiting the virulence hallmarks of *Pseudomonas aeruginosa*: a chronicle through the perspective of quorum sensing. *Environmental Microbiology*, 24 (6), 2630–2656.

Challa, S., 2018. Pathogenesis and Pathology of Invasive Aspergillosis. *Current Fungal Infection Reports*, 12 (1), 23–32.

Chang, D., Sharma, L., Dela Cruz, C. S. and Zhang, D., 2021. Clinical Epidemiology, Risk Factors, and Control Strategies of *Klebsiella pneumoniae* Infection. *Frontiers in Microbiology* [online], 12. Available from: <https://www.frontiersin.org/journals/microbiology/articles/10.3389/fmicb.2021.750662/full> [Accessed 24 Jun 2025].

Chatterjee, P., Moss, C. T., Omar, S., Dhillon, E., Hernandez Borges, C. D., Tang, A. C., Stevens, D. A. and Hsu, J. L., 2024. Allergic Bronchopulmonary Aspergillosis (ABPA) in the Era of Cystic Fibrosis Transmembrane Conductance Regulator (CFTR) Modulators. *Journal of Fungi*, 10 (9), 65

Chen, C., Wang, J., Pan, D., Wang, X., Xu, Y., Yan, J., Wang, L., Yang, X., Yang, M. and Liu, G., 2023. Applications of multi-omics analysis in human diseases. *MedComm*, 4 (4), e315.

Choera, T., Zelante, T., Romani, L. and Keller, N. P., 2018. A Multifaceted Role of Tryptophan Metabolism and Indoleamine 2,3-Dioxygenase Activity in *Aspergillus fumigatus*–Host Interactions. *Frontiers in Immunology* [online], 8. Available from: <https://www.frontiersin.org/articles/10.3389/fimmu.2017.01996> [Accessed 29 Sep 2023]

Chow, E. W. L., Pang, L. M. and Wang, Y., 2023. Impact of the host microbiota on fungal infections: New possibilities for intervention? *Advanced Drug Delivery Reviews*, 198, 114896.

Chung, D., Barker, B. M., Carey, C. C., Merriman, B., Werner, E. R., Lechner, B. E., Dhingra, S., Cheng, C., Xu, W., Blosser, S. J., Morohashi, K., Mazurie, A., Mitchell, T. K., Haas, H., Mitchell, A. P. and Cramer, R. A., 2014. ChIP-seq and In Vivo Transcriptome Analyses of the *Aspergillus fumigatus* SREBP SrbA Reveals a New Regulator of the Fungal Hypoxia Response and Virulence. *PLOS Pathogens*, 10 (11), e1004487.

Cigana, C., Bianconi, I., Baldan, R., De Simone, M., Riva, C., Sipione, B., Rossi, G., Cirillo, D. M. and Bragonzi, A., 2018. *Staphylococcus aureus* Impacts *Pseudomonas aeruginosa* Chronic Respiratory Disease in Murine Models. *The Journal of Infectious Diseases*, 217 (6), 933–942.

Cigana, C., Castandet, J., Sprynski, N., Melessike, M., Beyria, L., Ranucci, S., Alcalá-Franco, B., Rossi, A., Bragonzi, A., Zalacain, M. and Everett, M., 2021. *Pseudomonas aeruginosa* Elastase Contributes to the Establishment of Chronic Lung Colonization and Modulates the Immune Response in a Murine Model. *Frontiers in Microbiology*, 11, 620819.

Cordell, H. J., 2009. Detecting gene–gene interactions that underlie human diseases. *Nature Reviews Genetics*, 10 (6), 392–404.

Cortés, J. C. G., Curto, M.-Á., Carvalho, V. S. D., Pérez, P. and Ribas, J. C., 2019. The fungal cell wall as a target for the development of new antifungal therapies. *Biotechnology Advances*, 37 (6), 107352.

Costantini, C., Pariano, M., Puccetti, M., Giovagnoli, S., Pampalone, G., Dindo, M., Cellini, B. and Romani, L., 2024. Harnessing inter-kingdom metabolic disparities at the human-fungal interface for novel therapeutic approaches. *Frontiers in Molecular Biosciences*, 11, 1386598.

Cramer, R. A., 2015. In vivo veritas: *Aspergillus fumigatus* proliferation and pathogenesis – conditionally speaking. *Virulence*, 7 (1), 7–10.

Croft, C. A., Culibrk, L., Moore, M. M. and Tebbutt, S. J., 2016. Interactions of *Aspergillus fumigatus* Conidia with Airway Epithelial Cells: A Critical Review. *Frontiers in Microbiology* [online], 7. Available from: <https://www.frontiersin.org/journals/microbiology/articles/10.3389/fmicb.2016.00472/full> [Accessed 13 Jun 2025].

Cui, N., Wang, H., Long, Y. and Liu, D., 2013. CD8⁺ T-cell counts: an early predictor of risk and mortality in critically ill immunocompromised patients with invasive pulmonary aspergillosis. *Critical Care (London, England)*, 17 (4), R157.

Dagenais, T. R. T. and Keller, N. P., 2009. Pathogenesis of *Aspergillus fumigatus* in Invasive Aspergillosis. *Clinical Microbiology Reviews*, 22 (3), 447–465.

Dai, X., Liu, X., Li, J., Chen, H., Yan, C., Li, Y., Liu, H., Deng, D. and Wang, X., 2024. Structural insights into the inhibition mechanism of fungal GWT1 by manogepix. *Nature Communications*, 15 (1), 9194.

Dai, X. and Shen, L., 2022. Advances and Trends in Omics Technology Development. *Frontiers in Medicine*, 9, 911861.

Dasari, P., Koleci, N., Shopova, I. A., Wartenberg, D., Beyersdorf, N., Dietrich, S., Sahagún-Ruiz, A., Figge, M. T., Skerka, C., Brakhage, A. A. and Zipfel, P. F., 2019. Enolase From *Aspergillus fumigatus* Is a Moonlighting Protein That Binds the Human Plasma Complement Proteins Factor H, FHL-1, C4BP, and Plasminogen. *Frontiers in*

10. Available from: <https://www.frontiersin.org/journals/immunology/articles/10.3389/fimmu.2019.02573/full> [Accessed 18 Dec 2024].

De Francesco, M. A., 2023. Drug-Resistant Aspergillus spp.: A Literature Review of Its Resistance Mechanisms and Its Prevalence in Europe. *Pathogens*, 12 (11), 1305.

Delliére, S. and Aimanianda, V., 2023. Humoral Immunity Against Aspergillus fumigatus. *Mycopathologia*, 188 (5), 603–621.

Denning, D. W., 2024. Global incidence and mortality of severe fungal disease. *The Lancet Infectious Diseases*, 24 (7), e428–e438.

Denning, D. W., Cadranel, J., Beigelman-Aubry, C., Ader, F., Chakrabarti, A., Blot, S., Ullmann, A. J., Dimopoulos, G. and Lange, C., 2016. Chronic pulmonary aspergillosis: rationale and clinical guidelines for diagnosis and management. *European Respiratory Journal*, 47 (1), 45–68.

Denning, D. W., Pleuvry, A. and Cole, D. C., 2011. Global burden of chronic pulmonary aspergillosis as a sequel to pulmonary tuberculosis. *Bulletin of the World Health Organization*, 89 (12), 864–872.

Desoubeaux, G. and Cray, C., 2018. Animal Models of Aspergillosis. *Comparative Medicine*, 68 (2), 109–123.

Detsika, M. G., Palamaris, K., Dimopoulou, I., Kotanidou, A. and Orfanos, S. E., 2024. The complement cascade in lung injury and disease. *Respiratory Research*, 25 (1), 20.

Dewi, I. M. W., van de Veerdonk, F. L. and Gresnigt, M. S., 2017. The Multifaceted Role of T-Helper Responses in Host Defense against Aspergillus fumigatus. *Journal of Fungi*, 3 (4), 55.

Dickwella Widanage, M. C., Gautam, I., Sarkar, D., Mentink-Vigier, F., Vermaas, J. V., Ding, S.-Y., Lipton, A. S., Fontaine, T., Latgé, J.-P., Wang, P. and Wang, T., 2024. Adaptative survival of Aspergillus fumigatus to echinocandins arises from cell wall remodeling beyond β -1,3-glucan synthesis inhibition. *Nature Communications*, 15 (1), 6382.

Diggle, S. P. and Whiteley, M., 2020. Microbe Profile: *Pseudomonas aeruginosa*: opportunistic pathogen and lab rat. *Microbiology*, 166 (1), 30–33.

Dong, F. and Perdew, G. H., 2020. The aryl hydrocarbon receptor as a mediator of host-microbiota interplay. *Gut Microbes*, 12 (1), 1859812.

Dong, Z. and Chen, Y., 2013. Transcriptomics: advances and approaches. *Science China. Life Sciences*, 56 (10), 960–967.

Donnelley, M. A., Zhu, E. S. and Thompson, G. R., 2016. Isavuconazole in the treatment of invasive aspergillosis and mucormycosis infections. *Infection and Drug Resistance*, 9, 79–86.

Downes, S. G., Owens, R. A., Walshe, K., Fitzpatrick, D. A., Dorey, A., Jones, G. W. and Doyle, S., 2023. Gliotoxin-mediated bacterial growth inhibition is caused by specific metal ion depletion. *Scientific Reports*, 13 (1), 16156.

Driessens, N. N., Boshoff, H. I. M., Maaskant, J. J., Gilissen, S. A. C., Vink, S., van der Sar, A. M., Vandebroucke-Grauls, C. M. J. E., Bewley, C. A., Appelmelk, B. J. and Geurtsen, J., 2012. Cyanovirin-N inhibits mannose-dependent *Mycobacterium*-C-type lectin interactions but does not protect against murine tuberculosis. *Journal of Immunology (Baltimore, Md.: 1950)*, 189 (7), 3585–3592.

Drinkwater, E., Robinson, E. J. H. and Hart, A. G., 2019. Keeping invertebrate research ethical in a landscape of shifting public opinion. *Methods in Ecology and Evolution*, 10 (8), 1265–1273.

Duarte-Mata, D. I. and Salinas-Carmona, M. C., 2023. Antimicrobial peptides' immune modulation role in intracellular bacterial infection. *Frontiers in Immunology*, 14, 1119574.

Duong, V.-A. and Lee, H., 2023. Bottom-Up Proteomics: Advancements in Sample Preparation. *International Journal of Molecular Sciences*, 24 (6), 5350.

Earle, K., Valero, C., Conn, D. P., Vere, G., Cook, P. C., Bromley, M. J., Bowyer, P. and Gago, S., 2023. Pathogenicity and virulence of *Aspergillus fumigatus*. *Virulence*, 14 (1), 2172264.

Dupree, E. J., Jayathirtha, M., Yorkey, H., Mihasan, M., Petre, B. A. and Darie, C. C., 2020. A Critical Review of Bottom-Up Proteomics: The Good, the Bad, and the Future of This Field. *Proteomes*, 8 (3), 14.

Emri, T., Antal, K., Varga, K., Gila, B. C. and Pócsi, I., 2024. The Oxidative Stress Response Highly Depends on Glucose and Iron Availability in *Aspergillus fumigatus*. *Journal of Fungi*, 10 (3), 221.

Ercan, H., Resch, U., Hsu, F., Mitulovic, G., Bilek, A., Gerner, C., Yang, J.-W., Geiger, M., Miller, I. and Zellner, M., 2023. A Practical and Analytical Comparative Study of Gel-Based Top-Down and Gel-Free Bottom-Up Proteomics Including Unbiased Proteoform Detection. *Cells*, 12 (5), 747.

Esquivel, B. D., Smith, A. R., Zavrel, M. and White, T. C., 2015. Azole Drug Import into the Pathogenic Fungus *Aspergillus fumigatus*. *Antimicrobial Agents and Chemotherapy*, 59 (6), 3390–3398.

Fabri, J. H. T. M., Rocha, M. C., Fernandes, C. M., Persinoti, G. F., Ries, L. N. A., Cunha, A. F. da, Goldman, G. H., Del Poeta, M. and Malavazi, I., 2021. The Heat Shock Transcription Factor HsfA Is Essential for Thermotolerance and Regulates Cell Wall Integrity in *Aspergillus fumigatus*. *Frontiers in Microbiology* [online], 12. Available from: <https://www.frontiersin.org/articles/10.3389/fmicb.2021.656548> [Accessed 19 Sep 2023].

Fagerlund, R., Kinnunen, L., Köhler, M., Julkunen, I. and Melén, K., 2005. NF-κB Is Transported into the Nucleus by Importin $\alpha 3$ and Importin $\alpha 4^*$. *Journal of Biological Chemistry*, 280 (16), 15942–15951.

Fallon, J. P., Reeves, E. P. and Kavanagh, K., 2010. Inhibition of neutrophil function following exposure to the *Aspergillus fumigatus* toxin fumagillin. *Journal of Medical Microbiology*, 59 (6), 625–633.

Fallon, J. P., Reeves, E. P. and Kavanagh, K., 2011. The *Aspergillus fumigatus* toxin fumagillin suppresses the immune response of *Galleria mellonella* larvae by inhibiting the action of haemocytes. *Microbiology (Reading, England)*, 157 (Pt 5), 1481–1488.

Fan, X., Shu, P., Wang, Y., Ji, N. and Zhang, D., 2023. Interactions between neutrophils and T-helper 17 cells. *Frontiers in Immunology*, 14, 1279837.

Feng, X., Krishnan, K., Richie, D. L., Aimanianda, V., Hartl, L., Grahl, N., Powers-Fletcher, M. V., Zhang, M., Fuller, K. K., Nierman, W. C., Lu, L. J., Latgé, J.-P., Woollett, L., Newman, S. L., Jr, R. A. C., Rhodes, J. C. and Askew, D. S., 2011. HacA-Independent Functions of the ER Stress Sensor IreA Synergize with the Canonical UPR to Influence Virulence Traits in *Aspergillus fumigatus*. *PLOS Pathogens*, 7 (10), e1002330.

Firacative, C., Khan, A., Duan, S., Ferreira-Paim, K., Leemon, D. and Meyer, W., 2020. Rearing and Maintenance of *Galleria mellonella* and Its Application to Study Fungal Virulence. *Journal of Fungi*, 6 (3), 130.

Fleming, A., 1929. On the Antibacterial Action of Cultures of a Penicillium, with Special Reference to their Use in the Isolation of *B. influenzae*. *British journal of experimental pathology*, 10 (3), 226.

Franco, N. H. and Olsson, I. a. S., 2014. Scientists and the 3Rs: attitudes to animal use in biomedical research and the effect of mandatory training in laboratory animal science. *Laboratory Animals*, 48 (1), 50–60.

Frank, D., Naseem, S., Russo, G. L., Li, C., Parashar, K., Konopka, J. B. and Carpino, N., 2018. Phagocytes from Mice Lacking the Sts Phosphatases Have an Enhanced Antifungal Response to *Candida albicans*. *mBio*, 9 (4), 10.1128/mbio.00782-18.

Gago, S., Denning, D. W. and Bowyer, P., 2019. Pathophysiological aspects of *Aspergillus* colonization in disease. *Medical Mycology*, 57 (Supplement_2), S219–S227.

Gallorini, M., Marinacci, B., Pellegrini, B., Cataldi, A., Dindo, M. L., Carradori, S. and Grande, R., 2024. Immunophenotyping of hemocytes from infected *Galleria mellonella* larvae as an innovative tool for immune profiling, infection studies and drug screening. *Scientific Reports*, 14 (1), 759.

Gannon, A. D. and Darch, S. E., 2021. Same Game, Different Players: Emerging Pathogens of the CF Lung. *mbio*, 12 (1), 10.1128/mbio.01217-20.

Garg, M., Bhatia, H., Chandra, T., Debi, U., Sehgal, I. S., Prabhakar, N., Sandhu, M. S. and Agarwal, R., 2022. Imaging Spectrum in Chronic Pulmonary Aspergillosis. *The American Journal of Tropical Medicine and Hygiene*, 108 (1), 15.

Gaudet, R. G., Bradfield, C. J. and MacMicking, J. D., 2016. Evolution of Cell-Autonomous Effector Mechanisms in Macrophages versus Non-Immune Cells. *Microbiology Spectrum*, 4 (6), 10.1128/microbiolspec.mchd-0050-2016.

Gayathri, L., Akbarsha, M. A. and Ruckmani, K., 2020. In vitro study on aspects of molecular mechanisms underlying invasive aspergillosis caused by gliotoxin and fumagillin, alone and in combination. *Scientific Reports*, 10 (1), 14473.

Geis-Asteggiante, L., Ostrand-Rosenberg, S., Fenselau, C. and Edwards, N. J., 2016. Evaluation of Spectral Counting for Relative Quantitation of Proteoforms in Top-Down Proteomics. *Analytical chemistry*, 88 (22), 10900–10907.

Georgacopoulos, O., Nunnally, N., Law, D., Birch, M., Berkow, E. L. and Lockhart, S. R., 2023. In Vitro Activity of the Novel Antifungal Olorofim against *Scedosporium* and *Lomentospora prolificans*. *Microbiology Spectrum*, 11 (1), e02789-22.

George, M. E., Gaitor, T. T., Cluck, D. B., Henao-Martínez, A. F., Sells, N. R. and Chastain, D. B., 2025. The impact of climate change on the epidemiology of fungal infections: implications for diagnosis, treatment, and public health strategies. *Therapeutic Advances in Infectious Disease*, 12, 20499361251313840.

Geunes-Boyer, S., Heitman, J., Wright, J. R. and Steinbach, W. J., 2010. Surfactant protein D binding to *Aspergillus fumigatus* hyphae is calcineurin-sensitive. *Medical Mycology*, 48 (4), 580–588.

Ghazaei, C., 2017. Molecular Insights into Pathogenesis and Infection with *Aspergillus fumigatus*. *The Malaysian Journal of Medical Sciences : MJMS*, 24 (1), 10–20.

Giamberardino, C. D., Schell, W. A., Tenor, J. L., Toffaletti, D. L., Palmucci, J. R., Marius, C., Boua, J.-V. K., Soltow, Q., Mansbach, R., Moseley, M. A., Thompson, J. W., Dubois, L. G., Hope, W., Perfect, J. R. and Shaw, K. J., 2022. Efficacy of APX2039 in a Rabbit Model of Cryptococcal Meningitis. *mbio*, 13 (6), e0234722.

Gilmour, B. C., Corthay, A. and Øynebråten, I., 2024. High production of IL-12 by human dendritic cells stimulated with combinations of pattern-recognition receptor agonists. *npj Vaccines*, 9 (1), 83.

Goletti, D., Meintjes, G., Andrade, B. B., Zumla, A. and Lee, S. S., 2025. Insights from the 2024 WHO Global Tuberculosis Report – More Comprehensive Action, Innovation, and Investments required for achieving WHO End TB goals. *International Journal of Infectious Diseases* [online], 150. Available from: [https://www.ijidonline.com/article/S1201-9712\(24\)00400-4/fulltext](https://www.ijidonline.com/article/S1201-9712(24)00400-4/fulltext) [Accessed 10 Jun 2025].

Gonçalves, S. M., Duarte-Oliveira, C., Campos, C. F., Aimanianda, V., ter Horst, R., Leite, L., Mercier, T., Pereira, P., Fernández-García, M., Antunes, D., Rodrigues, C. S., Barbosa-Matos, C., Gaifem, J., Mesquita, I., Marques, A., Osório, N. S., Torrado, E., Rodrigues, F., Costa, S., Joosten, L. A., Lagrou, K., Maertens, J., Lacerda, J. F., Campos, A., Brown, G. D., Brakhage, A. A., Barbas, C., Silvestre, R., van de Veerdonk, F. L., Chamilos, G., Netea, M. G., Latgé, J.-P., Cunha, C. and Carvalho, A., 2020. Phagosomal removal of fungal melanin reprograms macrophage metabolism to promote antifungal immunity. *Nature Communications*, 11 (1), 2282.

Gow, N. A. and Hube, B., 2012. Importance of the *Candida albicans* cell wall during commensalism and infection. *Current Opinion in Microbiology*, 15 (4), 406–412.

Grahl, N., Dinamarco, T. M., Willger, S. D., Goldman, G. H. and Cramer, R. A., 2012. *Aspergillus fumigatus* mitochondrial electron transport chain mediates oxidative stress homeostasis, hypoxia responses and fungal pathogenesis. *Molecular Microbiology*, 84

(2), 383–399.

Granato, E. T., Meiller-Legrand, T. A. and Foster, K. R., 2019. The Evolution and Ecology of Bacterial Warfare. *Current biology: CB*, 29 (11), R521–R537.

Grassl, N., Kulak, N. A., Pichler, G., Geyer, P. E., Jung, J., Schubert, S., Sinitcyn, P., Cox, J. and Mann, M., 2016. Ultra-deep and quantitative saliva proteome reveals dynamics of the oral microbiome. *Genome Medicine*, 8 (1), 44.

Gravelat, F. N., Beauvais, A., Liu, H., Lee, M. J., Snarr, B. D., Chen, D., Xu, W., Kravtsov, I., Hoareau, C. M. Q., Vanier, G., Urb, M., Campoli, P., Al Abdallah, Q., Lehoux, M., Chabot, J. C., Ouimet, M.-C., Baptista, S. D., Fritz, J. H., Nierman, W. C., Latgé, J. P., Mitchell, A. P., Filler, S. G., Fontaine, T. and Sheppard, D. C., 2013. Aspergillus galactosaminogalactan mediates adherence to host constituents and conceals hyphal β -glucan from the immune system. *PLoS pathogens*, 9 (8), e1003575.

Greco, T. M. and Cristea, I. M., 2017. Proteomics Tracing the Footsteps of Infectious Disease*. *Molecular & Cellular Proteomics*, 16 (4, Supplement 1), S5–S14.

Greenberger, P. A., 2013. When to suspect and work up allergic bronchopulmonary aspergillosis. *Annals of Allergy, Asthma & Immunology*, 111 (1), 1–4.

Gresnigt, M. S., Rekiki, A., Rasid, O., Savers, A., Jouvion, G., Dannaoui, E., Parlato, M., Fitting, C., Brock, M., Cavaillon, J.-M., van de Veerdonk, F. L. and Ibrahim-Granet, O., 2016. Reducing hypoxia and inflammation during invasive pulmonary aspergillosis by targeting the Interleukin-1 receptor. *Scientific Reports*, 6 (1), 26490.

Gründlinger, M., Gsaller, F., Schrettl, M., Lindner, H. and Haas, H., 2013. Aspergillus fumigatus SidJ Mediates Intracellular Siderophore Hydrolysis. *Applied and Environmental Microbiology*, 79 (23), 7534–7536.

Guegan, H., Prat, E., Robert-Gangneux, F. and Gangneux, J.-P., 2021. Azole Resistance in Aspergillus fumigatus: A Five-Year Follow Up Experience in a Tertiary Hospital With a Special Focus on Cystic Fibrosis. *Frontiers in Cellular and Infection Microbiology*, 10, 613774.

Günther, K., Nischang, V., Cseresnyés, Z., Krüger, T., Sheta, D., Abboud, Z., Heinekamp, T., Werner, M., Kniemeyer, O., Beilhack, A., Figge, M. T., Brakhage, A. A., Werz, O. and Jordan, P. M., 2024. Aspergillus fumigatus-derived gliotoxin impacts innate immune cell activation through modulating lipid mediator production in macrophages. *Immunology*, 173 (4), 748–767.

Guo, H., Wang, L., Deng, Y. and Ye, J., 2021. Novel perspectives of environmental proteomics. *Science of The Total Environment*, 788, 147588.

Gürsoy, G., Li, T., Liu, S., Ni, E., Brannon, C. M. and Gerstein, M. B., 2022. Functional genomics data: privacy risk assessment and technological mitigation. *Nature Reviews Genetics*, 23 (4), 245–258.

Guruceaga, X., Ezpeleta, G., Mayayo, E., Sueiro-Olivares, M., Abad-Díaz-De-Cerio, A., Aguirre Urizar, J. M., Liu, H. G., Wiemann, P., Bok, J. W., Filler, S. G., Keller, N. P., Hernando, F. L., Ramirez-Garcia, A. and Rementeria, A., 2018. A possible role for fumagillin in cellular damage during host infection by Aspergillus fumigatus. *Virulence*, 9 (1), 1548–1561.

Gutierrez Reyes, C. D., Alejo-Jacuinde, G., Perez Sanchez, B., Chavez Reyes, J., Onigbinde, S., Mogut, D., Hernández-Jasso, I., Calderón-Vallejo, D., Quintanar, J. L. and Mechref, Y., 2024. Multi Omics Applications in Biological Systems. *Current Issues in Molecular Biology*, 46 (6), 5777–5793.

Haas, D., Lesch, S., Buzina, W., Galler, H., Gutschi, A. M., Habib, J., Pfeifer, B., Luxner, J. and Reinthaler, F. F., 2016. Culturable fungi in potting soils and compost. *Medical Mycology*, 54 (8), 825–834.

Haas, H., 2012. Iron – A Key Nexus in the Virulence of Aspergillus fumigatus. *Frontiers in Microbiology* [online], 3. Available from: <https://www.frontiersin.org/journals/microbiology/articles/10.3389/fmicb.2012.00028/full> [Accessed 16 Jun 2025].

Habanjar, O., Diab-Assaf, M., Caldefie-Chezet, F. and Delort, L., 2021. 3D Cell Culture Systems: Tumor Application, Advantages, and Disadvantages. *International Journal of Molecular Sciences*, 22 (22), 12200.

Hall, S., McDermott, C., Anoopkumar-Dukie, S., McFarland, A. J., Forbes, A., Perkins, A. V., Davey, A. K., Chess-Williams, R., Kiefel, M. J., Arora, D. and Grant, G. D., 2016. Cellular Effects of Pyocyanin, a Secreted Virulence Factor of *Pseudomonas aeruginosa*. *Toxins*, 8 (8), 236.

Harrington, N. E., Allen, F., Garcia-Maset, R. and Harrison, F., 2022. *Pseudomonas aeruginosa* transcriptome analysis in a cystic fibrosis lung model reveals metabolic changes accompanying biofilm maturation and increased antibiotic tolerance over time.[online]. Available from: <https://www.biorxiv.org/content/10.1101/2022.06.30.498312v1> [Accessed 29 Jan 2025].

Harrington, N. E., Sweeney, E. and Harrison, F., 2020. Building a better biofilm - Formation of in vivo-like biofilm structures by *Pseudomonas aeruginosa* in a porcine model of cystic fibrosis lung infection. *Biofilm*, 2, 100024.

Harrison, F. and Diggle, S. P., 2016. An ex vivo lung model to study bronchioles infected with *Pseudomonas aeruginosa* biofilms. *Microbiology*, 162 (10), 1755–1760.

Harrison, F., Muruli, A., Higgins, S. and Diggle, S. P., 2014. Development of an Ex Vivo Porcine Lung Model for Studying Growth, Virulence, and Signaling of *Pseudomonas aeruginosa*. *Infection and Immunity*, 82 (8), 3312–3323.

Hartmann, T., Sasse, C., Schedler, A., Hasenberg, M., Gunzer, M. and Krappmann, S., 2011. Shaping the fungal adaptome – Stress responses of *Aspergillus fumigatus*. *International Journal of Medical Microbiology*, 301 (5), 408–416.

Hasin, Y., Seldin, M. and Lusis, A., 2017. Multi-omics approaches to disease. *Genome Biology*, 18 (1), 83.

Hastings, C. J., Syed, S. S. and Marques, C. N. H., 2023. Subversion of the Complement System by *Pseudomonas aeruginosa*. *Journal of Bacteriology*, 205 (8), e00018-23.

Hatinguais, R., Pradhan, A., Brown, G. D., Brown, A. J. P., Warris, A. and Shekhova, E., 2021. Mitochondrial Reactive Oxygen Species Regulate Immune Responses of Macrophages to *Aspergillus fumigatus*. *Frontiers in Immunology*, 12, 641495.

Hauser, A. R., 2009. The Type III Secretion System of *Pseudomonas aeruginosa*: Infection by Injection. *Nature reviews. Microbiology*, 7 (9), 654–665.

Hawksworth, D. L. and Lücking, R., 2017. Fungal Diversity Revisited: 2.2 to 3.8 Million Species. *Microbiology Spectrum*, 5 (4).

He, Q., Li, M., Cao, J., Zhang, M. and Feng, C., 2025. Clinical characteristics and risk factors analysis of allergic bronchopulmonary aspergillosis combined with bronchiectasis. *Frontiers in Medicine* [online], 12. Available from: <https://www.frontiersin.org/journals/medicine/articles/10.3389/fmed.2025.1557241/full> [Accessed 10 Jun 2025].

Heinekamp, T., Schmidt, H., Lapp, K., Pähtz, V., Shopova, I., Köster-Eiserfunke, N., Krüger, T., Kniemeyer, O. and Brakhage, A. A., 2015. Interference of *Aspergillus fumigatus* with the immune response. *Seminars in Immunopathology*, 37 (2), 141–152.

Heinekamp, T., Thywißen, A., Macheleidt, J., Keller, S., Valiante, V. and Brakhage, A. A., 2013. *Aspergillus fumigatus* melanins: interference with the host endocytosis pathway and impact on virulence. *Frontiers in Microbiology*, 3, 440.

Heinrich, S. M., 2011. Human SP-A- genes, structure, function- and lung diseases. Text.PhDThesis. [online]. Ludwig-Maximilians-Universität München. Available from: <https://edoc.ub.uni-muenchen.de/13834/> [Accessed 12 May 2025].

Heldt, S., Eigl, S., Prattes, J., Flick, H., Rabensteiner, J., Prüller, F., Niedrist, T., Neumeister, P., Wölfler, A., Strohmaier, H., Krause, R. and Hoenigl, M., 2017. Levels of interleukin (IL)-6 and IL-8 are elevated in serum and bronchoalveolar lavage fluid of haematological patients with invasive pulmonary aspergillosis. *Mycoses*, 60 (12), 818–825.

Herbst, S., Shah, A., Carby, M., Chusney, G., Kikkeri, N., Dorling, A., Bignell, E., Shaunak, S. and Armstrong-James, D., 2013. A new and clinically relevant murine model of solid-organ transplant aspergillosis. *Disease Models & Mechanisms*, 6 (3), 643–651.

Hewitt, R. J. and Lloyd, C. M., 2021. Regulation of immune responses by the airway epithelial cell landscape. *Nature Reviews Immunology*, 21 (6), 347–362.

Hillege, M. M. G., Galli Caro, R. A., Offringa, C., de Wit, G. M. J., Jaspers, R. T. and Hoogaars, W. M. H., 2020. TGF- β Regulates Collagen Type I Expression in Myoblasts and Myotubes via Transient Ctgf and Fgf-2 Expression. *Cells*, 9 (2), 375.

Hillmann, F., Novohradská, S., Mattern, D. J., Forberger, T., Heinekamp, T., Westermann, M., Winckler, T. and Brakhage, A. A., 2015. Virulence determinants of the human pathogenic fungus *Aspergillus fumigatus* protect against soil amoeba predation. *Environmental Microbiology*, 17 (8), 2858–28.

Hoang, T. N. M., Cseresnyés, Z., Hartung, S., Blickendorf, M., Saffer, C., Rennert, K., Mosig, A. S., von Lilienfeld-Toal, M. and Figge, M. T., 2022. Invasive aspergillosis-on-chip: A quantitative treatment study of human *Aspergillus fumigatus* infection. *Biomaterials*, 283, 121420.

Howard, S. J., Pasqualotto, A. C., Anderson, M. J., Leatherbarrow, H., Albarraq, A. M., Harrison, E., Gregson, L., Bowyer, P. and Denning, D. W., 2013. Major variations in *Aspergillus fumigatus* arising within aspergillomas in chronic pulmonary aspergillosis. *Mycoses*, 56 (4), 434–441.

Huang, T., Zhang, M., Tong, X., Chen, J., Yan, G., Fang, S., Guo, Y., Yang, B., Xiao, S., Chen, C., Huang, L. and Ai, H., 2018. Microbial communities in swine lungs and their association with lung lesions. *Microbial Biotechnology*, 12 (2), 289–304.

Huch, M. and Koo, B.-K., 2015. Modeling mouse and human development using organoid cultures. *Development (Cambridge, England)*, 142 (18), 3113–3125.

Hughes, D. A., Archangelidi, O., Coates, M., Armstrong-James, D., Elborn, S. J., Carr, S. B. and Davies, J. C., 2022. Clinical characteristics of *Pseudomonas* and *Aspergillus* co-infected cystic fibrosis patients: A UK registry study. *Journal of Cystic Fibrosis*, 21 (1), 129–135.

Hui, S. T., Gifford, H. and Rhodes, J., 2024. Emerging Antifungal Resistance in Fungal Pathogens. *Current Clinical Microbiology Reports*, 11 (2), 43–50.

Hunter, P., 2022. Replacing mammals in drug development. *EMBO Reports*, 24 (1), e56485.

Huszczynski, S. M., Lam, J. S. and Khursigara, C. M., 2020. The Role of *Pseudomonas aeruginosa* Lipopolysaccharide in Bacterial Pathogenesis and Physiology. *Pathogens*, 9 (1), 6.

Hüttel, W., 2021. Echinocandins: structural diversity, biosynthesis, and development of antimycotics. *Applied Microbiology and Biotechnology*, 105 (1), 55–66.

Ibrahim, S. R. M., Mohamed, H. M., Aljahdali, A. S., Murshid, S. S. A., Mohamed, S. G. A., Abdallah, H. M. and Mohamed, G. A., 2025. *Aspergillus fumigatus* from Pathogenic Fungus to Unexplored Natural Treasure: Changing the Concept. *Journal of Microbiology and Biotechnology*, 35, e2411082.

Ibrahim-Granet, O., Dubourdeau, M., Latgé, J.-P., Ave, P., Huerre, M., Brakhage, A. A. and Brock, M., 2008. Methylcitrate synthase from *Aspergillus fumigatus* is essential for manifestation of invasive aspergillosis. *Cellular Microbiology*, 10 (1), 134–148.

Invernizzi, R., Lloyd, C. M. and Molyneaux, P. L., 2020. Respiratory microbiome and epithelial interactions shape immunity in the lungs. *Immunology*, 160 (2), 171–182.

Ivashkiv, L. B., 2018. IFN γ : signalling, epigenetics and roles in immunity, metabolism, disease and cancer immunotherapy. *Nature reviews. Immunology*, 18 (9), 545–558.

Jackson, J. C., Higgins, L. A. and Lin, X., 2009. Conidiation Color Mutants of *Aspergillus fumigatus* Are Highly Pathogenic to the Heterologous Insect Host *Galleria mellonella*. *PLOS ONE*, 4 (1), e4224.

Jean Beltran, P. M., Federspiel, J. D., Sheng, X. and Cristea, I. M., 2017. Proteomics and integrative omic approaches for understanding host-pathogen interactions and infectious diseases. *Molecular Systems Biology*, 13 (3), 922.

Jensen, K. B. and Little, M. H., 2023. Organoids are not organs: Sources of variation and misinformation in organoid biology. *Stem Cell Reports*, 18 (6), 1255–1270.

Jessen, H., Hoyer, N., Prior, T. S., Frederiksen, P., Karsdal, M. A., Leeming, D. J., Bendstrup, E., Sand, J. M. B. and Shaker, S. B., 2021. Turnover of type I and III collagen predicts progression of idiopathic pulmonary fibrosis. *Respiratory Research*, 22 (1), 205.

Jia, L.-J., Rafiq, M., Radosa, L., Hortschansky, P., Cunha, C., Cseresnyés, Z., Krüger, T., Schmidt, F., Heinekamp, T., Straßburger, M., Löffler, B., Doenst, T., Lacerda, J. F.,

Campos, A., Figge, M. T., Carvalho, A., Kniemeyer, O. and Brakhage, A. A., 2023. *Aspergillus fumigatus* hijacks human p11 to redirect fungal-containing phagosomes to non-degradative pathway. *Cell Host & Microbe*, 31 (3), 373-388.e10.

Jiménez-Ortigosa, C., Moore, C., Denning, D. W. and Perlin, D. S., 2017. Emergence of Echinocandin Resistance Due to a Point Mutation in the *fks1* Gene of *Aspergillus fumigatus* in a Patient with Chronic Pulmonary Aspergillosis. *Antimicrobial Agents and Chemotherapy*, 61 (12), 10.1128/aac.01277-17.

Jo, E.-K., 2019. Interplay between host and pathogen: immune defense and beyond. *Experimental & Molecular Medicine*, 51 (12), 1-3.

Jørgensen, K. M., Astvad, K. M. T. and Arendrup, M. C., 2020. In Vitro Activity of Manogepix (APX001A) and Comparators against Contemporary Molds: MEC Comparison and Preliminary Experience with Colorimetric MIC Determination. *Antimicrobial Agents and Chemotherapy*, 64 (8), 10.1128/aac.00730-20.

Joshi, P. R., 2024. Pulmonary Diseases in Older Patients: Understanding and Addressing the Challenges. *Geriatrics*, 9 (2), 34.

Junqueira, J. C. and Mylonakis, E., 2019. Current Status and Trends in Alternative Models to Study Fungal Pathogens. *Journal of Fungi*, 5 (1), 12.

Kale, S. D., Ayubi, T., Chung, D., Tubau-Juni, N., Leber, A., Dang, H. X., Karyala, S., Hontecillas, R., Lawrence, C. B., Cramer, R. A. and Bassaganya-Riera, J., 2017. Modulation of Immune Signaling and Metabolism Highlights Host and Fungal Transcriptional Responses in Mouse Models of Invasive Pulmonary Aspergillosis. *Scientific Reports*, 7 (1), 17096.

Kamai, Y., Lossinsky, A. S., Liu, H., Sheppard, D. C. and Filler, S. G., 2009. Polarized Response of Endothelial Cells to Invasion by *Aspergillus fumigatus*. *Cellular Microbiology*, 11 (1), 170-182.

Kanaujia, R., Singh, S. and Rudramurthy, S. M., 2023. Aspergillosis: an Update on Clinical Spectrum, Diagnostic Schemes, and Management. *Current Fungal Infection Reports*, 17 (2), 144-155.

Kang, Y., Ma, W., Li, Q., Wang, P. and Jia, W., 2025. Epidemiology, antifungal susceptibility and biological characteristics of clinical *Aspergillus fumigatus* in a tertiary hospital. *Scientific Reports*, 15 (1), 16906.

Kanj, A., Abdallah, N. and Soubani, A. O., 2018. The spectrum of pulmonary aspergillosis. *Respiratory Medicine*, 141, 121-131.

Kaplan, B. L. F., Hoberman, A. M., Slikker, W., Smith, M. A., Corsini, E., Knudsen, T. B., Marty, M. S., Sobrian, S. K., Fitzpatrick, S. C., Ratner, M. H. and Mendrick, D. L., 2024. Protecting Human and Animal Health: The Road from Animal Models to New Approach Methods. *Pharmacological Reviews*, 76 (2), 251-266.

Katsoulis, O., Pitts, O. R. and Singanayagam, A., 2024. The airway mycobiome and interactions with immunity in health and chronic lung disease. *Oxford Open Immunology*, 5 (1), iqae009.

Katt, M. E., Placone, A. L., Wong, A. D., Xu, Z. S. and Searson, P. C., 2016. In Vitro Tumor Models: Advantages, Disadvantages, Variables, and Selecting the Right Platform. *Frontiers in Bioengineering and Biotechnology*, 4, 12.

Kaur, N. and Dey, P., 2023. Bacterial exopolysaccharides as emerging bioactive macromolecules: from fundamentals to applications. *Research in Microbiology*, 174 (4), 104024.

Keown, K., Reid, A., Moore, J. E., Taggart, C. C. and Downey, D. G., 2020. Coinfection with *Pseudomonas aeruginosa* and *Aspergillus fumigatus* in cystic fibrosis. *European Respiratory Review*, 29 (158), 200011.

Khan, M. M., Ernst, O., Manes, N. P., Oyler, B. L., Fraser, I. D. C., Goodlett, D. R. and Nita-Lazar, A., 2019. Multi-Omics Strategies Uncover Host-Pathogen Interactions. *ACS infectious diseases*, 5 (4), 493-505.

Khedr, M. A., Massarotti, A. and Mohamed, M. E., 2018. Rational Discovery of (+) (S) Abscisic Acid as a Potential Antifungal Agent: a Repurposing Approach. *Scientific Reports*, 8 (1), 8565.

Kiani, A. K., Pheby, D., Henehan, G., Brown, R., Sieving, P., Sykora, P., Marks, R., Falsini, B., Capodicasa, N., Miertus, S., Lorusso, L., Dondossola, D., Tartaglia, G. M., Ergoren, M. C., Dundar, M., Michelini, S., Malacarne, D., Bonetti, G., Dautaj, A., Donato, K., Medori, M. C., Beccari, T., Samaja, M., Connelly, S. T., Martin, D., Morresi, A., Bacu, A., Herbst, K. L., Kapustin, M., Stupbia, L., Lumer, L., Farronato, G., Bertelli, M., and INTERNATIONAL BIOETHICS STUDY GROUP, 2022. Ethical considerations regarding animal experimentation. *Journal of Preventive Medicine and Hygiene*, 63 (2 Suppl 3), E255–E26

Kim, B.-G., Choi, Y. S., Shin, S. H., Lee, K., Um, S.-W., Kim, H., Jeon, Y. J., Lee, J., Cho, J. H., Kim, H. K., Kim, J., Shim, Y. M. and Jeong, B.-H., 2022. Mortality and lung function decline in patients who develop chronic pulmonary aspergillosis after lung cancer surgery. *BMC Pulmonary Medicine*, 22 (1), 436.

Kim, J., Koo, B.-K. and Knoblich, J. A., 2020. Human organoids: model systems for human biology and medicine. *Nature Reviews. Molecular Cell Biology*, 21 (10), 571–584.

Kim, T. H., Kim, H., Oh, J., Kim, S., Miligkos, M., Yon, D. K. and Papadopoulos, N. G., 2025. Global burden of asthma among children and adolescents with projections to 2050: a comprehensive review and forecasted modeling study. *Clinical and Experimental Pediatrics*, 68 (5), 329–343.

Kim, W., Gwon, Y., Park, S., Kim, H. and Kim, J., 2023. Therapeutic strategies of three-dimensional stem cell spheroids and organoids for tissue repair and regeneration. *Bioactive Materials*, 19, 50–74.

King, J., Dambuza, I. M., Reid, D. M., Yuecel, R., Brown, G. D. and Warris, A., 2023. Detailed characterisation of invasive aspergillosis in a murine model of X-linked chronic granulomatous disease shows new insights in infections caused by *Aspergillus fumigatus* versus *Aspergillus nidulans*. *Frontiers in Cellular and Infection Microbiology*, 13, 1241770.

Kingsley, R. A. and Bäumler, A. J., 2000. Host adaptation and the emergence of infectious disease: the *Salmonella* paradigm. *Molecular Microbiology*, 36 (5), 1006–1014.

Kirschning, A., 2022. On the Evolutionary History of the Twenty Encoded Amino Acids. *Chemistry – A European Journal*, 28 (55), e202201419.

Klein, S. G., Steckbauer, A., Alsolami, S. M., Arossa, S., Parry, A. J., Li, M. and Duarte, C. M., 2022. Toward Best Practices for Controlling Mammalian Cell Culture Environments. *Frontiers in Cell and Developmental Biology* [online], 10. Available from: <https://www.frontiersin.org/journals/cell-and-developmental-biology/articles/10.3389/fcell.2022.788808/full> [Accessed 9 Apr 2025].

Koharudin, L. M. I., Visconti, A. R., Jee, J.-G., Ottonello, S. and Gronenborn, A. M., 2008. The Evolutionarily Conserved Family of Cyanovirin-N Homologs: Structures and Carbohydrate Specificity. *Structure*, 16 (4), 570–584.

Köhler, J. R., Casadevall, A. and Perfect, J., 2015. The Spectrum of Fungi That Infects Humans. *Cold Spring Harbor Perspectives in Medicine*, 5 (1), a019273.

Kolostyak, Z., Bojcsuk, D., Baksa, V., Szigeti, Z. M., Bene, K., Czimmerer, Z., Boto, P., Fadel, L., Poliska, S., Halasz, L., Tzerpos, P., Berger, W. K., Villabona-Rueda, A., Varga, Z., Kovacs, T., Patsalos, A., Pap, A., Vamosi, G., Bai, P., Dezso, B., Spite, M., D'Alessio, F. R., Szatmari, I. and Nagy, L., 2024. EGR2 is an epigenomic regulator of phagocytosis and antifungal immunity in alveolar macrophages. *JCI insight*, 9 (17), e164009.

Kong, F.-D., Huang, X.-L., Ma, Q.-Y., Xie, Q.-Y., Wang, P., Chen, P.-W., Zhou, L.-M., Yuan, J.-Z., Dai, H.-F., Luo, D.-Q. and Zhao, Y.-X., 2018. Helvolic Acid Derivatives with Antibacterial Activities against *Streptococcus agalactiae* from the Marine-Derived Fungus *Aspergillus fumigatus* HNMF0047. *Journal of Natural Products*, 81 (8), 1869–1876.

König, S., Pace, S., Pein, H., Heinekamp, T., Kramer, J., Romp, E., Straßburger, M., Troisi, F., Proschak, A., Dworschak, J., Scherlach, K., Rossi, A., Sautebin, L., Haeggström, J. Z., Hertweck, C., Brakhage, A. A., Gerstmeier, J., Proschak, E. and Werz, O., 2019. Gliotoxin from *Aspergillus fumigatus* Abrogates Leukotriene B4 Formation through Inhibition of Leukotriene A4 Hydrolase. *Cell Chemical Biology*, 26 (4),

Kousha, M., Tadi, R. and Soubani, A. O., 2011. Pulmonary aspergillosis: a clinical review. *European Respiratory Review*, 20 (121), 156–174.

Kramer, J., Özkaya, Ö. and Kümmeli, R., 2020. Bacterial siderophores in community and host interactions. *Nature reviews. Microbiology*, 18 (3), 152–163.

Krappmann, S. and Braus, G. H., 2005. Nitrogen metabolism of *Aspergillus* and its role in pathogenicity. *Medical Mycology*, 43 (Supplement_1), S31–S40.

Kuek, L. E. and Lee, R. J., 2020. First contact: the role of respiratory cilia in host-pathogen interactions in the airways. *American Journal of Physiology - Lung Cellular and Molecular Physiology*, 319 (4), L603–L619.

Kumamoto, C. A., Gresnigt, M. S. and Hube, B., 2020. The gut, the bad and the harmless: *Candida albicans* as a commensal and opportunistic pathogen in the intestine. *Current opinion in microbiology*, 56, 7–15.

Kumari, A., Tripathi, Ankita H., Gautam, Poonam, Gahtori, Rekha, Pande, Amit, Singh, Yogendra, Madan, Taruna and Upadhyay, S. K., 2021. Adhesins in the virulence of opportunistic fungal pathogens of human. *Mycology*, 12 (4), 296–324.

Kuplińska, A. and Rząd, K., 2021. Molecular targets for antifungals in amino acid and protein biosynthetic pathways. *Amino Acids*, 53 (7), 961–991.

Kurucz, V., Krüger, T., Antal, K., Dietl, A.-M., Haas, H., Pócsi, I., Kniemeyer, O. and Emri, T., 2018. Additional oxidative stress reroutes the global response of *Aspergillus fumigatus* to iron depletion. *BMC Genomics*, 19 (1), 357.

LaFayette, S. L., Houle, D., Beaudoin, T., Wojewodka, G., Radzioch, D., Hoffman, L. R., Burns, J. L., Dandekar, A. A., Smalley, N. E., Chandler, J. R., Zlosnik, J. E., Speert, D. P., Bernier, J., Matouk, E., Brochiero, E., Rousseau, S. and Nguyen, D., 2015. Cystic fibrosis–adapted *Pseudomonas aeruginosa* quorum sensing lasR mutants cause hyperinflammatory responses. *Science Advances*, 1 (6), e1500199.

Lal, K., Grover, A., Ragshaniya, A., Aslam, Mohd., Singh, P. and Kumari, K., 2025. Current advancements and future perspectives of 1,2,3-triazoles to target lanosterol 14 α -demethylase (CYP51), a cytochrome P450 enzyme: A computational approach. *International Journal of Biological Macromolecules*, 315, 144240.

Lan, P., Yan, R., Lu, Y., Zhao, D., Shi, Q., Jiang, Y., Yu, Y. and Zhou, J., 2021. Genetic diversity of siderophores and hypermucoviscosity phenotype in *Klebsiella pneumoniae*. *Microbial Pathogenesis*, 158, 105014.

Lange, S. and Inal, J. M., 2024. Animal Models of Human Disease 2.0. *International Journal of Molecular Sciences*, 25 (24), 13743.

Last, A., Maurer, M., S Mosig, A., S Gresnigt, M. and Hube, B., 2021. In vitro infection models to study fungal-host interactions. *FEMS microbiology reviews*, 45 (5), fuab005.

Leão, R. S., Pereira, R. H. V., Folescu, T. W., Albano, R. M., Santos, E. A., Junior, L. G. C. and Marques, E. A., 2011. KPC-2 Carbapenemase-producing *Klebsiella pneumoniae* isolates from patients with Cystic Fibrosis. *Journal of Cystic Fibrosis*, 10 (2), 140–142.

Lee, Y., Robbins, N. and Cowen, L. E., 2023. Molecular mechanisms governing antifungal drug resistance. *npj Antimicrobials and Resistance*, 1 (1), 5.

León, B., 2023. Understanding the development of Th2 cell-driven allergic airway disease in early life. *Frontiers in Allergy*, 3, 1080153.

Levdansky, E., Kashi, O., Sharon, H., Shadkchan, Y. and Osherov, N., 2010. The *Aspergillus fumigatus* cspA Gene Encoding a Repeat-Rich Cell Wall Protein Is Important for Normal Conidial Cell Wall Architecture and Interaction with Host Cells. *Eukaryotic Cell*, 9 (9), 1403–1415.

Li, S.-M., 2011. Genome mining and biosynthesis of fumitremorgin-type alkaloids in ascomycetes. *The Journal of Antibiotics*, 64 (1), 45–49.

Liang, J., Tian, J., Zhang, H., Li, H. and Chen, L., 2025. Proteomics: An In-Depth Review on Recent Technical Advances and Their Applications in Biomedicine. *Medicinal Research Reviews*, 45 (4), 1021–1044.

Ligthart, K., Belzer, C., de Vos, W. M. and Tytgat, H. L. P., 2020. Bridging Bacteria and the

Gut: Functional Aspects of Type IV Pili. *Trends in Microbiology*, 28 (5), 340–348.

Lin, H.-C., Chooi, Y.-H., Dhingra, S., Xu, W., Calvo, A. M. and Tang, Y., 2013. The fumagillin biosynthetic gene cluster in *Aspergillus fumigatus* encodes a cryptic terpene cyclase involved in the formation of β -trans-bergamotene. *Journal of the American Chemical Society*, 135 (12), 4616–4619

Lin, Z., Wang, J.-L., Cheng, Y., Wang, J.-X. and Zou, Z., 2020. Pattern recognition receptors from lepidopteran insects and their biological functions. *Developmental and Comparative Immunology*, 108, 103688.

Lionakis, M. S., Drummond, R. A. and Hohl, T. M., 2023. Immune responses to human fungal pathogens and therapeutic prospects. *Nature Reviews Immunology*, 23 (7), 433–452.

Liu, H., Liang, Z., Cao, N., Yi, X., Tan, X., Liu, Z., Wang, F., Yang, Y., Li, C., Xiang, Z., He, Y., Su, J., Wang, Z., Chen, R. and Zhou, H., 2021. Airway bacterial and fungal microbiome in chronic obstructive pulmonary disease. *Medicine in Microecology*, 7, 100035.

Liu, T., Wang, Y., Zhang, Z., Jia, L., Zhang, J., Zheng, S., Chen, Z., Shen, H., Piao, C. and Du, J., 2023. Abnormal adenosine metabolism of neutrophils inhibits airway inflammation and remodeling in asthma model induced by *Aspergillus fumigatus*. *BMC Pulmonary Medicine*, 23, 258.

Llanos, A., Achard, P., Bousquet, J., Lozano, C., Zalacain, M., Sable, C., Revillet, H., Murris, M., Mittaine, M., Lemonnier, M. and Everett, M., 2023. Higher levels of *Pseudomonas aeruginosa* LasB elastase expression are associated with early-stage infection in cystic fibrosis patients. *Scientific Reports*, 13 (1), 14208.

Lofgren, L. A., Ross, B. S., Cramer, R. A. and Stajich, J. E., 2022. The pan-genome of *Aspergillus fumigatus* provides a high-resolution view of its population structure revealing high levels of lineage-specific diversity driven by recombination. *PLOS Biology*, 20 (11), e3001890.

Lothér, J., Breitschopf, T., Krappmann, S., Morton, C. O., Bouzani, M., Kurzai, O., Gunzer, M., Hasenberg, M., Einsele, H. and Loeffler, J., 2014. Human dendritic cell subsets display distinct interactions with the pathogenic mould *Aspergillus fumigatus*. *International journal of medical microbiology: IJMM*, 304 (8), 1160–1168.

Loussert, C., Schmitt, C., Prevost, M.-C., Balloy, V., Fadel, E., Philippe, B., Kauffmann-Lacroix, C., Latgé, J. P. and Beauvais, A., 2010. In vivo biofilm composition of *Aspergillus fumigatus*. *Cellular Microbiology*, 12 (3), 405–410.

Lowe, R., Shirley, N., Bleackley, M., Dolan, S. and Shafee, T., 2017. Transcriptomics technologies. *PLOS Computational Biology*, 13 (5), e1005457.

Luni, C., Serena, E. and Elvassore, N., 2014. Human-on-chip for therapy development and fundamental science. *Current Opinion in Biotechnology*, 25, 45–50.

Lv, Q., Elders, B. B. L. J., Warris, A., Caudri, D., Ciet, P. and Tiddens, H. A. W. M., 2021. *Aspergillus*-related lung disease in people with cystic fibrosis: can imaging help us to diagnose disease? *European Respiratory Review* [online], 30 (162). Available from: <https://publications.ersnet.org/content/errev/30/162/210103> [Accessed 8 Jul 2025].

MacCallum, D. M., 2013. Mouse model of invasive fungal infection. *Methods in Molecular Biology (Clifton, N.J.)*, 1031, 145–153.

Maerker, C., Rohde, M., Brakhage, A. A. and Brock, M., 2005. Methylcitrate synthase from *Aspergillus fumigatus*. Propionyl-CoA affects polyketide synthesis, growth and morphology of conidia. *The FEBS journal*, 272 (14), 3615–363

Magwalivha, M., Rikhotso, M. C., Kachienga, L. O., Musoliwa, R., Banda, N. T., Mashilo, M. S., Tshiteme, T., Mphaphuli, A. M., Mahamud, H. A., Patel, S., Ngandu, J.-P. K., Patel, S., Potgieter, N. and Traoré, A. N., 2025. Bacterial co-occurrence with pulmonary TB, a respiratory tract infection (RTI): A cross-sectional study in a resource-limited setting. *Journal of Clinical Tuberculosis and Other Mycobacterial Diseases*, 40, 100534.

Manfiolli, A. O., Mattos, E. C., de Assis, L. J., Silva, L. P., Ulaş, M., Brown, N. A., Silva-Rocha, R., Bayram, Ö. and Goldman, G. H., 2019. *Aspergillus fumigatus* High Osmolarity Glycerol Mitogen Activated Protein Kinases SakA and MpKc Physically Interact During Osmotic and Cell Wall Stresses. *Frontiers in Microbiology*, 10, 918

Margalit, A., Carolan, J. C., Sheehan, D. and Kavanagh, K., 2020. The *Aspergillus fumigatus* Secretome Alters the Proteome of *Pseudomonas aeruginosa* to Stimulate Bacterial Growth: Implications for Co-infection. *Molecular & cellular proteomics: MCP*, 19 (8), 1346–1359

Margalit, A. and Kavanagh, K., 2015. The innate immune response to *Aspergillus fumigatus* at the alveolar surface. *FEMS Microbiology Reviews*, 39 (5), 670–687.

Margalit, A., Sheehan, D., Carolan, J. C. and Kavanagh, K., 2022. Exposure to the *Pseudomonas aeruginosa* secretome alters the proteome and secondary metabolite production of *Aspergillus fumigatus*. *Microbiology (Reading, England)*, 168 (3), 001164.

Martinson, M. L. and Lapham, J., 2024. Prevalence of Immunosuppression Among US Adults. *JAMA*, 331 (10), 880–882.

Matthaiou, E. I., Sass, G., Stevens, D. A. and Hsu, J. L., 2018. Iron: an essential nutrient for *Aspergillus fumigatus* and a fulcrum for pathogenesis. *Current opinion in infectious diseases*, 31 (6), 506–511.

McColl, E. R., Asthana, R., Paine, M. F. and Piquette-Miller, M., 2019. The Age of Omics-Driven Precision Medicine. *Clinical Pharmacology & Therapeutics*, 106 (3), 477–481.

McCormick, A., Heesemann, L., Wagener, J., Marcos, V., Hartl, D., Loeffler, J., Heesemann, J. and Ebel, F., 2010. NETs formed by human neutrophils inhibit growth of the pathogenic mold *Aspergillus fumigatus*. *Microbes and Infection*, 12 (12), 928–936.

McDonagh, A., Fedorova, N. D., Crabtree, J., Yu, Y., Kim, S., Chen, D., Loss, O., Cairns, T., Goldman, G., Armstrong-James, D., Haynes, K., Haas, H., Schrett, M., May, G., Nierman, W. C. and Bignell, E., 2008. Sub-telomere directed gene expression during initiation of invasive aspergillosis. *PLoS pathogens*, 4 (9), e1000154.

Megger, D. A., Bracht, T., Meyer, H. E. and Sitek, B., 2013. Label-free quantification in clinical proteomics. *Biochimica et Biophysica Acta (BBA) - Proteins and Proteomics*, 1834 (8), 1581–1590.

Ménard, G., Rouillon, A., Cattoir, V. and Donnio, P.-Y., 2021. *Galleria mellonella* as a Suitable Model of Bacterial Infection: Past, Present and Future. *Frontiers in Cellular and Infection Microbiology*, 11, 782733.

Mendes, M. L. and Dittmar, G., 2022. Targeted proteomics on its way to discovery. *Proteomics*, 22 (15–16), e2100330.

Meneau, I., Coste, A. T. and Sanglard, D., 2016. Identification of *Aspergillus fumigatus* multidrug transporter genes and their potential involvement in antifungal resistance. *Medical Mycology*, 54 (6), 616–627.

Meurens, F., Summerfield, A., Nauwynck, H., Saif, L. and Gerdts, V., 2012. The pig: a model for human infectious diseases. *Trends in Microbiology*, 20 (1), 50–57.

Miller, A. J. and Spence, J. R., 2017. In Vitro Models to Study Human Lung Development, Disease and Homeostasis. *Physiology*, 32 (3), 246–260.

Mills, C. D., 2015. Anatomy of a Discovery: M1 and M2 Macrophages. *Frontiers in Immunology* [online], 6. Available from: <https://www.frontiersin.org/journals/immunology/articles/10.3389/fimmu.2015.00212/full> [Accessed 12 Jun 2025].

Mirhakkak, M. H., Chen, X., Ni, Y., Heinekamp, T., Sae-Ong, T., Xu, L.-L., Kurzai, O., Barber, A. E., Brakhage, A. A., Boutin, S., Schäuble, S. and Panagiotou, G., 2023. Genome-scale metabolic modeling of *Aspergillus fumigatus* strains reveals growth dependencies on the lung microbiome. *Nature Communications*, 14 (1), 4369.

Misslinger, M., Hortschansky, P., Brakhage, A. A. and Haas, H., 2021. Fungal iron homeostasis with a focus on *Aspergillus fumigatus*. *Biochimica et Biophysica Acta (BBA) - Molecular Cell Research*, 1868 (1), 118885.

Modlinska, K. and Pisula, W., 2020. The Norway rat, from an obnoxious pest to a laboratory pet. *eLife*, 9, e50651.

Mohd Asri, N. A., Ahmad, S., Mohamud, R., Mohd Hanafi, N., Mohd Zaidi, N. F., Irekeola, A. A., Shueb, R. H., Yee, L. C., Mohd Noor, N., Mustafa, F. H., Yean, C. Y. and

Yusof, N. Y., 2021. Global Prevalence of Nosocomial Multidrug-Resistant *Klebsiella pneumoniae*: A Systematic Review and Meta-Analysis. *Antibiotics*, 10 (12), 1508.

Moldoveanu, B., Gearhart, A. M., Jalil, B. A., Saad, M. and Guardiola, J. J., 2021. Pulmonary Aspergillosis: Spectrum of Disease. *The American Journal of the Medical Sciences*, 361 (4), 411–419.

Moore, M. M., 2013. The crucial role of iron uptake in *Aspergillus fumigatus* virulence. *Current Opinion in Microbiology*, 16 (6), 692–699.

Mosig, A. S., 2016. Organ-on-chip models: new opportunities for biomedical research. *Future Science OA*, 3 (2), FSO130.

Mroczyńska, M. and Brzillowska-Dąbrowska, A., 2020. Review on Current Status of Echinocandins Use. *Antibiotics (Basel, Switzerland)*, 9 (5), 227.

Mudaliar, S. B. and Bharath Prasad, A. S., 2024. A biomedical perspective of pyocyanin from *Pseudomonas aeruginosa*: its applications and challenges. *World Journal of Microbiology and Biotechnology*, 40 (3), 90.

Mukherjee, P., Roy, S., Ghosh, D. and Nandi, S. K., 2022. Role of animal models in biomedical research: a review. *Laboratory Animal Research*, 38 (1), 18.

Müller, F.-M. C., Seidler, M. and Beauvais, A., 2011. *Aspergillus fumigatus* biofilms in the clinical setting. *Medical Mycology*, 49 (Supplement_1), S96–S100.

Muraille, E., Leo, O. and Moser, M., 2014. Th1/Th2 Paradigm Extended: Macrophage Polarization as an Unappreciated Pathogen-Driven Escape Mechanism? *Frontiers in Immunology*, 5, 603.

Muszkieta, L., Beauvais, A., Pähltz, V., Gibbons, J., Anton Leberre, V., Beau, R., Shibuya, K., Rokas, A., Francois, J. M., Kniemeyyer, O., Brakhage, A. A. and Latge, J. P., 2013. Investigation of *Aspergillus fumigatus* biofilm formation by various “omics” approaches. *Frontiers in Microbiology* [online], 4. Available from: <https://www.frontiersin.org/journals/microbiology/articles/10.3389/fmicb.2013.00013/full> [Accessed 8 Jan 2025].

Myszka, K. and Czaczyk, K., 2009. Characterization of Adhesive Exopolysaccharide (EPS) Produced by *Pseudomonas aeruginosa* Under Starvation Conditions. *Current Microbiology*, 58 (6), 541–546.

Naranjo-Ortiz, M. A. and Gabaldón, T., 2019. Fungal evolution: major ecological adaptations and evolutionary transitions. *Biological Reviews of the Cambridge Philosophical Society*, 94 (4), 1443–1476.

Nazik, H., Sass, G., Déziel, E. and Stevens, D. A., 2020. *Aspergillus* Is Inhibited by *Pseudomonas aeruginosa* Volatiles. *Journal of Fungi*, 6 (3), 118.

Neilson, K. A., Ali, N. A., Muralidharan, S., Mirzaei, M., Mariani, M., Assadourian, G., Lee, A., van Sluyter, S. C. and Haynes, P. A., 2011. Less label, more free: approaches in label-free quantitative mass spectrometry. *Proteomics*, 11 (4), 535–553.

Netea, M. G., Joosten, L. A. B., van der Meer, J. W. M., Kullberg, B.-J. and van de Veerdonk, F. L., 2015. Immune defence against *Candida* fungal infections. *Nature Reviews. Immunology*, 15 (10), 630–642.

Nickerson, R., Thornton, C. S., Johnston, B., Lee, A. H. Y. and Cheng, Z., 2024. *Pseudomonas aeruginosa* in chronic lung disease: untangling the dysregulated host immune response. *Frontiers in Immunology*, 15, 1405376.

Nnadi, N. E. and Carter, D. A., 2021. Climate change and the emergence of fungal pathogens. *PLOS Pathogens*, 17 (4), e1009503.

Nogueira, M. F., Pereira, L., Jenull, S., Kuchler, K. and Lion, T., 2019. *Klebsiella pneumoniae* prevents spore germination and hyphal development of *Aspergillus* species. *Scientific Reports*, 9 (1), 218.

Novohradská, S., Ferling, I. and Hillmann, F., 2017. Exploring Virulence Determinants of Filamentous Fungal Pathogens through Interactions with Soil Amoebae. *Frontiers in Cellular and Infection Microbiology* [online], 7. Available from: <https://www.frontiersin.org/journals/cellular-and-infection-microbiology/articles/10.3389/fcimb.2017.00497/full> [Accessed 10 Jun 2025].

Nunzi, E., Pariano, M., Costantini, C., Garaci, E., Puccetti, P. and Romani, L., 2025. Host–

microbe serotonin metabolism. *Trends in Endocrinology & Metabolism*, 36 (1), 83–95

Nywening, A. V., Rybak, J. M., Rogers, P. D. and Fortwendel, J. R., 2020. Mechanisms of triazole resistance in *Aspergillus fumigatus*. *Environmental Microbiology*, 22 (12), 4934–4952.

Obar, J. J., Hohl, T. M. and Cramer, R. A., 2016. New Advances in Invasive Aspergillosis Immunobiology Leading the Way Towards Personalized Therapeutic Approaches. *Cytokine*, 84, 63–73.

Oliveira, M., Oliveira, D., Lisboa, C., Boechat, J. L. and Delgado, L., 2023. Clinical Manifestations of Human Exposure to Fungi. *Journal of Fungi*, 9 (3), 381.

Oliver, J. D., Sibley, G. E. M., Beckmann, N., Dobb, K. S., Slater, M. J., McEntee, L., du Pré, S., Livermore, J., Bromley, M. J., Wiederhold, N. P., Hope, W. W., Kennedy, A. J., Law, D. and Birch, M., 2016. F901318 represents a novel class of antifungal drug that inhibits dihydroorotate dehydrogenase. *Proceedings of the National Academy of Sciences*, 113 (45), 12809–12814.

Ortiz, S. C., Pennington, K., Thomson, D. D. and Bertuzzi, M., 2022. Novel Insights into *Aspergillus fumigatus* Pathogenesis and Host Response from State-of-the-Art Imaging of Host–Pathogen Interactions during Infection. *Journal of Fungi*, 8 (3), 264.

Paczosa, M. K. and Mecsas, J., 2016. *Klebsiella pneumoniae*: Going on the Offense with a Strong Defense. *Microbiology and Molecular Biology Reviews*, 80 (3), 629–661.

Palabiyik, A. A. and Palabiyik, E., 2025. Proteomics in biomarker discovery: uncovering disease-specific interactome and post-translational modification networks. *Journal of Proteins and Proteomics* [online]. Available from: <https://doi.org/10.1007/s42485-025-00190-y> [Accessed 26 Jun 2025]

Panse, P., Smith, M., Cummings, K., Jensen, E., Gotway, M. and Jokerst, C., 2016. The many faces of pulmonary aspergillosis: Imaging findings with pathologic correlation. *Radiology of Infectious Diseases*, 3 (4), 192–200.

Paplińska-Goryca, M., Nejman-Gryz, P., Chazan, R. and Grubek-Jaworska, H., 2013. The expression of the eotaxins IL-6 and CXCL8 in human epithelial cells from various levels of the respiratory tract. *Cellular & Molecular Biology Letters*, 18 (4), 612–630.

Pardo-Saganta, A., Law, B. M., Gonzalez-Celeiro, M., Vinarsky, V. and Rajagopal, J., 2013. Ciliated cells of pseudostratified airway epithelium do not become mucous cells after ovalbumin challenge. *American Journal of Respiratory Cell and Molecular Biology*, 48 (3), 364–373.

Patel, R., Hossain, M. A., German, N. and Al-Ahmad, A. J., 2018. Gliotoxin penetrates and impairs the integrity of the human blood-brain barrier in vitro. *Mycotoxin Research*, 34 (4), 257–268.

Pathak, V., Hurtado Rendon, I. S. and Ciubotaru, R. L., 2011. Invasive pulmonary aspergillosis in an immunocompetent patient. *Respiratory Medicine CME*, 4 (3), 105–106.

Patradoon-Ho, P. and Fitzgerald, D. A., 2007. Lung abscess in children. *Paediatric Respiratory Reviews*, 8 (1), 77–84.

Paul, S., Diekema, D. and Moye-Rowley, W. S., 2017. Contributions of both ATP-Binding Cassette Transporter and Cyp51A Proteins Are Essential for Azole Resistance in *Aspergillus fumigatus*. *Antimicrobial Agents and Chemotherapy*, 61 (5), e02748-16.

Paulussen, C., Hallsworth, J. E., Álvarez-Pérez, S., Nierman, W. C., Hamill, P. G., Blain, D., Rediers, H. and Lievens, B., 2016. Ecology of aspergillosis: insights into the pathogenic potency of *Aspergillus fumigatus* and some other *Aspergillus* species. *Microbial Biotechnology*, 10 (2), 296–322.

Pawlowska, T. E., 2024. Symbioses between fungi and bacteria: from mechanisms to impacts on biodiversity. *Current Opinion in Microbiology*, 80, 102496.

Peignier, A. and Parker, D., 2020. *Pseudomonas aeruginosa* Can Degrade Interferon λ , Thereby Repressing the Antiviral Response of Bronchial Epithelial Cells. *Journal of Interferon & Cytokine Research*, 40 (8), 429–431.

Peleg, A. Y., Hogan, D. A. and Mylonakis, E., 2010. Medically important bacterial-fungal interactions. *Nature Reviews. Microbiology*, 8 (5), 340–349.

Perakakis, N., Yazdani, A., Kaniadakis, G. E. and Mantzoros, C., 2018. Omics, big data and machine learning as tools to propel understanding of biological mechanisms and to discover novel diagnostics and therapeutics. *Metabolism: clinical and experimental*, 87, A1–A9.

Perez-Cuesta, U., Guruceaga, X., Cendon-Sanchez, S., Pelegri-Martinez, E., Hernando, F. L., Ramirez-Garcia, A., Abad-Diaz-de-Cerio, A. and Rementeria, A., 2021. Nitrogen, Iron, and Zinc Acquisition: Key Nutrients to *Aspergillus fumigatus* Virulence. *Journal of Fungi*, 7 (7), 518.

Petrocheilou, A., Moudaki, A. and Kaditis, A. G., 2022. Inflammation and Infection in Cystic Fibrosis: Update for the Clinician. *Children*, 9 (12), 1898.

Pfliegler, W. P., Pócsi, I., Győri, Z. and Pusztahelyi, T., 2020. The Aspergilli and Their Mycotoxins: Metabolic Interactions With Plants and the Soil Biota. *Frontiers in Microbiology* [online], 10. Available from: <https://www.frontiersin.org/journals/microbiology/articles/10.3389/fmich.2019.02921/full> [Accessed 16 Jun 2025].

Poirier, V. and Av-Gay, Y., 2015. Intracellular Growth of Bacterial Pathogens: The Role of Secreted Effector Proteins in the Control of Phagocytosed Microorganisms. *Microbiology Spectrum*, 3 (6), 10.1128/microbiolspec.vmbf-0003-2014.

Poletti, M., Arnauts, K., Ferrante, M. and Korcsmaros, T., 2020. Organoid-based Models to Study the Role of Host-microbiota Interactions in IBD. *Journal of Crohn's & Colitis*, 15 (7), 1222–1235.

Postel, M. D., Culver, J. O., Ricker, C. and Craig, D. W., 2022. Transcriptome analysis provides critical answers to the “variants of uncertain significance” conundrum. *Human Mutation*, 43 (11), 1590–1608.

Price, C. T. D., Hanford, H. E., Al-Quadan, T., Santic, M., Shin, C. J., Da'as, M. S. J. and Abu Kwaik, Y., 2024. Amoebae as training grounds for microbial pathogens. *mBio*, 15 (8), e00827-24.

Prüfer, S., Weber, M., Stein, P., Bosmann, M., Stassen, M., Kreft, A., Schild, H. and Radsak, M. P., 2014. Oxidative burst and neutrophil elastase contribute to clearance of *Aspergillus fumigatus* pneumonia in mice. *Immunobiology*, 219 (2), 87–96.

Puerner, C., Vellanki, S., Strauch, J. L. and Cramer, R. A., 2023. Recent Advances in Understanding the Human Fungal Pathogen Hypoxia Response in Disease Progression. *Annual review of microbiology*, 77, 403–425.

Qi, P., Liu, X., Li, C., Xu, Q., Hu, L., Duan, H., Zhao, G. and Lin, J., 2024. Programulin Protects against *Aspergillus fumigatus* Keratitis by Attenuating the Inflammatory Response through Enhancing Autophagy. *ACS infectious diseases*, 10 (8), 2826–2835.

Qin, S., Xiao, W., Zhou, C., Pu, Q., Deng, X., Lan, L., Liang, H., Song, X. and Wu, M., 2022. *Pseudomonas aeruginosa*: pathogenesis, virulence factors, antibiotic resistance, interaction with host, technology advances and emerging therapeutics. *Signal Transduction and Targeted Therapy*, 7, 199.

Qu, S., Xu, R., Yi, G., Li, Z., Zhang, H., Qi, S. and Huang, G., 2024. Patient-derived organoids in human cancer: a platform for fundamental research and precision medicine. *Molecular Biomedicine*, 5, 6.

Raffa, N. and Keller, N. P., 2019. A call to arms: Mustering secondary metabolites for success and survival of an opportunistic pathogen. *PLOS Pathogens*, 15 (4), e1007606.

Rafiq, M., Rivieccio, F., Zimmermann, A.-K., Visser, C., Bruch, A., Krüger, T., González Rojas, K., Kniemeyer, O., Blango, M. G. and Brakhage, A. A., 2022. PLB-985 Neutrophil-Like Cells as a Model To Study *Aspergillus fumigatus* Pathogenesis. *mSphere*, 7 (1), e0094021.

Ramirez-Ortiz, Z. G. and Means, T. K., 2012. The role of dendritic cells in the innate recognition of pathogenic fungi (*A. fumigatus*, *C. neoformans* and *C. albicans*). *Virulence*, 3 (7), 635–646.

Reece, E., Doyle, S., Greally, P., Renwick, J. and McClean, S., 2018. *Aspergillus fumigatus* Inhibits *Pseudomonas aeruginosa* in Co-culture: Implications of a Mutually Antagonistic Relationship on Virulence and Inflammation in the CF Airway. *Frontiers in Microbiology* [online], 9. Available from: <https://www.frontiersin.org/journals/microbiology/articles/10.3389/fmich.2019.02921/full> [Accessed 16 Jun 2025].

<https://www.frontiersin.org/journals/microbiology/articles/10.3389/fmicb.2018.01205/full> [Accessed 4 Jun 2025].

Reeves, E. P., Murphy, T., Daly, P. and Kavanagh, K., 2004. Amphotericin B enhances the synthesis and release of the immunosuppressive agent gliotoxin from the pulmonary pathogen *Aspergillus fumigatus*. *Journal of Medical Microbiology*, 53 (Pt 8), 719–725.

Reichert-Lima, F., Lyra, L., Pontes, L., Moretti, M. L., Pham, C. D., Lockhart, S. R. and Schreiber, A. Z., 2018. Surveillance for azoles resistance in *Aspergillus* spp. highlights a high number of amphotericin B-resistant isolates. *Mycoses*, 61 (6), 360–365.

Reynolds, D. and Kollef, M., 2021. The Epidemiology and Pathogenesis and Treatment of *Pseudomonas aeruginosa* Infections: An Update. *Drugs*, 81 (18), 2117–2131.

Rezzoagli, C., Granato, E. T. and Kümmeli, R., 2020. Harnessing bacterial interactions to manage infections: a review on the opportunistic pathogen <i>Pseudomonas aeruginosa</i> as a case example. *Journal of medical microbiology*, 69 (2), 147–161.

Rhijn, N. van, Uzzell, C. and Shelton, J., 2025. Climate change-driven geographical shifts in *Aspergillus* species habitat and the implications for plant and human health. [online]. Available from: <https://www.researchsquare.com/article/rs-6545782/v1> [Accessed 10 Jun 2025].

Ries, L. N. A., Alves de Castro, P., Pereira Silva, L., Valero, C., dos Reis, T. F., Saborano, R., Duarte, I. F., Persinoti, G. F., Steenwyk, J. L., Rokas, A., Almeida, F., Costa, J. H., Fill, T., Sze Wah Wong, S., Aimanianda, V., Rodrigues, F. J. S., Gonçales, R. A., Duarte-Oliveira, C., Carvalho, A. and Goldman, G. H., 2021. *Aspergillus fumigatus* Acetate Utilization Impacts Virulence Traits and Pathogenicity. *mBio*, 12 (4), 10.1128/mbio.01682-21.

Ries, L. N. A., Beattie, S., Cramer, R. A. and Goldman, G. H., 2018. Overview of carbon and nitrogen catabolite metabolism in the virulence of human pathogenic fungi. *Molecular Microbiology*, 107 (3), 277–297.

Ries, L. N. A., Steenwyk, J. L., de Castro, P. A., de Lima, P. B. A., Almeida, F., de Assis, L. J., Manfiolli, A. O., Takahashi-Nakaguchi, A., Kusuya, Y., Hagiwara, D., Takahashi, H., Wang, X., Obar, J. J., Rokas, A. and Goldman, G. H., 2019. Nutritional Heterogeneity Among *Aspergillus fumigatus* Strains Has Consequences for Virulence in a Strain- and Host-Dependent Manner. *Frontiers in Microbiology*, 10, 854.

Riwu, K. H. P., Effendi, M. H., Rantam, F. A., Khairullah, A. R. and Widodo, A., 2022. A review: Virulence factors of *Klebsiella pneumonia* as emerging infection on the food chain. *Veterinary World*, 15 (9), 2172–2179.

Robinson, S. L. and Panaccione, D. G., 2015. Diversification of Ergot Alkaloids in Natural and Modified Fungi. *Toxins*, 7 (1), 201–218.

Rokas, A., Mead, M. E., Steenwyk, J. L., Oberlies, N. H. and Goldman, G. H., 2020. Evolving moldy murderers: *Aspergillus* section Fumigati as a model for studying the repeated evolution of fungal pathogenicity. *PLOS Pathogens*, 16 (2), e1008315.

Ross, B. S., Lofgren, L. A., Ashare, A., Stajich, J. E. and Cramer, R. A., 2021. *Aspergillus fumigatus* In-Host HOG Pathway Mutation for Cystic Fibrosis Lung Microenvironment Persistence. *mBio*, 12 (4), 10.1128/mbio.02153-21.

Santella, B., Boccella, M., Folliero, V., Iervolino, D., Pagliano, P., Fortino, L., Serio, B., Vozzella, E. A., Schiavo, L., Galdiero, M., Capunzo, M., Boccia, G. and Franci, G., 2024. Antimicrobial Susceptibility Profiles of *Klebsiella pneumoniae* Strains Collected from Clinical Samples in a Hospital in Southern Italy. *The Canadian Journal of Infectious Diseases & Medical Microbiology = Journal Canadien des Maladies Infectieuses et de la Microbiologie Médicale*, 2024, 5548434.

Santos, A. L. S., Silva, B. A., da Cunha, M. M. L., Branquinha, M. H. and Mello, T. P., 2023. Fibronectin-binding molecules of *Scedosporium apiospermum*: focus on adhesive events. *Brazilian Journal of Microbiology*, 54 (4), 2577–2585.

Sarkar, S. and Heise, M. T., 2019. Mouse Models as Resources for Studying Infectious Diseases. *Clinical Therapeutics*, 41 (10), 1912–1922.

Sass, G., Miller Conrad, L. C., Nguyen, T.-T. H. and Stevens, D. A., 2020. The *Pseudomonas aeruginosa* product pyochelin interferes with *Trypanosoma cruzi* infection and multiplication in vitro. *Transactions of The Royal Society of Tropical Medicine and Hygiene*, 114 (7), 492–498.

Sass, G. and Stevens, D. A., 2023. Model of Pulmonary Co-Infection of *Aspergillus* and *Pseudomonas* in Immunocompetent Mice. *Microbiology Research*, 14 (4), 1843–1861.

Sasse, A., Hamer, S. N., Amich, J., Binder, J. and Krappmann, S., 2016. Mutant characterization and *in vivo* conditional repression identify aromatic amino acid biosynthesis to be essential for *Aspergillus fumigatus* virulence. *Virulence*, 7 (1), 56–62.

Sathe, N., Beech, P., Croft, L., Suphioglu, C., Kapat, A. and Athan, E., 2023. *Pseudomonas aeruginosa*: Infections and novel approaches to treatment “Knowing the enemy” the threat of *Pseudomonas aeruginosa* and exploring novel approaches to treatment. *Infectious Medicine*, 2 (3), 178–194.

Scharf, D. H., Brakhage, A. A. and Mukherjee, P. K., 2016. Gliotoxin – bane or boon? *Environmental Microbiology*, 18 (4), 1096–1109.

Schiefermeier-Mach, N., Polleux, J., Heinrich, L., Lechner, L., Vorona, O. and Perkhofer, S., 2025. Biological boundary conditions regulate the internalization of *Aspergillus fumigatus* conidia by alveolar cells. *Frontiers in Cellular and Infection Microbiology* [online], 15. Available from: <https://www.frontiersin.org/journals/cellular-and-infection-microbiology/articles/10.3389/fcimb.2025.1515779/full> [Accessed 10 Jun 2025].

Schlamp, D., Canton, J., Carreño, M., Kopinski, H., Freeman, S. A., Grinstein, S. and Fairn, G. D., 2016. Gliotoxin Suppresses Macrophage Immune Function by Subverting Phosphatidylinositol 3,4,5-Trisphosphate Homeostasis. *mBio*, 7 (2), e02242-15.

Schrettl, M. and Haas, H., 2011. Iron homeostasis—Achilles’ heel of *Aspergillus fumigatus*? *Current Opinion in Microbiology*, 14 (4), 400–405.

Scott, J., Sueiro-Olivares, M., Thornton, B. P., Owens, R. A., Muhamadali, H., Fortune-Grant, R., Thomson, D., Thomas, R., Hollywood, K., Doyle, S., Goodacre, R., Tabernero, L., Bignell, E. and Amich, J., 2020. Targeting Methionine Synthase in a Fungal Pathogen Causes a Metabolic Imbalance That Impacts Cell Energetics, Growth, and Virulence. *mBio*, 11 (5), 10.1128/mbio.01985-20.

Scully, L. R. and Bidochka, M. J., 2006. The host acts as a genetic bottleneck during serial infections: an insect-fungal model system. *Current Genetics*, 50 (5), 335–345.

Seidel, C., Moreno-Velásquez, S. D., Ben-Ghazzi, N., Gago, S., Read, N. D. and Bowyer, P., 2020. Phagolysosomal Survival Enables Non-lytic Hyphal Escape and Ramification Through Lung Epithelium During *Aspergillus fumigatus* Infection. *Frontiers in Microbiology* [online], 11. Available from: <https://www.frontiersin.org/journals/microbiology/articles/10.3389/fmicb.2020.01955/full> [Accessed 16 Jun 2025].

Seifert, M., Nairz, M., Schroll, A., Schrettl, M., Haas, H. and Weiss, G., 2008. Effects of the *Aspergillus fumigatus* siderophore systems on the regulation of macrophage immune effector pathways and iron homeostasis. *Immunobiology*, 213 (9), 767–778.

Serafini, M. S., Lopez-Perez, L., Fico, G., Licitra, L., De Cecco, L. and Resteghini, C., 2020. Transcriptomics and Epigenomics in head and neck cancer: available repositories and molecular signatures. *Cancers of the Head & Neck*, 5 (1), 2.

Seyedmousavi, S., Chang, Y. C., Law, D., Birch, M., Rex, J. H. and Kwon-Chung, K. J., 2019. Efficacy of Olorofim (F901318) against *Aspergillus fumigatus*, *A. nidulans*, and *A. tanneri* in Murine Models of Profound Neutropenia and Chronic Granulomatous Disease. *Antimicrobial Agents and Chemotherapy*, 63 (6), e00129-19.

Shankar, J., Thakur, R., Clemons, K. V. and Stevens, D. A., 2024. Interplay of Cytokines and Chemokines in Aspergillosis. *Journal of Fungi*, 10 (4), 251.

Shaw, K. J. and Ibrahim, A. S., 2020. Fosmanogepix: A Review of the First-in-Class Broad Spectrum Agent for the Treatment of Invasive Fungal Infections. *Journal of Fungi*, 6 (4), 239.

Shekhova, E., Kniemeyer, O. and Brakhage, A. A., 2017. Induction of Mitochondrial Reactive Oxygen Species Production by Itraconazole, Terbinafine, and Amphotericin B as a Mode of Action against *Aspergillus fumigatus*. *Antimicrobial Agents and Chemotherapy*, 61 (11), e00978-17.

Shende, R., Wong, S. S. W., Meitei, H. T., Lal, G., Madan, T., Aimanianda, V., Pal, J. K. and Sahu, A., 2022. Protective role of host complement system in *Aspergillus fumigatus* infection. *Frontiers in Immunology*, 13, 978152.

Sheshachalam, A., Srivastava, N., Mitchell, T., Lacy, P. and Eitzen, G., 2014. Granule Protein Processing and Regulated Secretion in Neutrophils. *Frontiers in Immunology*, 5, 448.

Siegel, R. L., Giaquinto, A. N. and Jemal, A., 2024. Cancer statistics, 2024. *CA: a cancer journal for clinicians*, 74 (1), 12–49.

Silva-Gomes, R., Caldeira, I., Fernandes, R., Cunha, C. and Carvalho, A., 2024. Metabolic regulation of the host–fungus interaction: from biological principles to therapeutic opportunities. *Journal of Leukocyte Biology*, 116 (3), 469–486.

Singh, R. P., Kapoor, A., Sinha, A., Ma, Y. and Shankar, M., 2025. Virulence factors of *Klebsiella pneumoniae*: Insights into canonical and emerging mechanisms driving pathogenicity and drug resistance. *The Microbe*, 7, 100289.

Singh, S., Kanaujia, R., Rudramurthy, S. M., Singh, S., Kanaujia, R. and Rudramurthy, S. M., 2021. Immunopathogenesis of Aspergillosis. In: *The Genus Aspergillus - Pathogenicity, Mycotoxin Production and Industrial Applications* [online]. IntechOpen. Available from: <https://www.intechopen.com/chapters/78761> [Accessed 8 Jul 2025].

Singh, V., Rai, R., Mathew, B. J., Chourasia, R., Singh, A. K., Kumar, A. and Chaurasiya, S. K., 2023. Phospholipase C: underrated players in microbial infections. *Frontiers in Cellular and Infection Microbiology*, 13, 1089374.

Sinha, A. and Mann, M., 2020. A beginner's guide to mass spectrometry–based proteomics. *The Biochemist*, 42 (5), 64–69.

Slater, J. L., Gregson, L., Denning, D. W. and Warn, P. A., 2011. Pathogenicity of *Aspergillus fumigatus* mutants assessed in *Galleria mellonella* matches that in mice. *Medical Mycology*, 49 Suppl 1, S107-113.

Smith, D. and Casadevall, A., 2021. Fungal immunity and pathogenesis in mammals versus the invertebrate model organism *Galleria mellonella*. *Pathogens and Disease*, 79 (3), ftab013.

Souza, C. M. de, Bezerra, B. T., Mellon, D. A. and de Oliveira, H. C., 2025. The evolution of antifungal therapy: Traditional agents, current challenges and future perspectives. *Current Research in Microbial Sciences*, 8, 100341.

Srivastava, M., Bencurova, E., Gupta, S. K., Weiss, E., Löffler, J. and Dandekar, T., 2019. *Aspergillus fumigatus* Challenged by Human Dendritic Cells: Metabolic and Regulatory Pathway Responses Testify a Tight Battle. *Frontiers in Cellular and Infection Microbiology*, 9, 168.

Stączek, S., Zdybicka-Barabas, A., Wojda, I., Wiater, A., Mak, P., Suder, P., Skrzypiec, K. and Cytryńska, M., 2021. Fungal α -1,3-Glucan as a New Pathogen-Associated Molecular Pattern in the Insect Model Host *Galleria mellonella*. *Molecules*, 26 (16), 5097.

Stewart Merrill, T. E., Rapti, Z. and Cáceres, C. E., 2021. Host Controls of Within-Host Disease Dynamics: Insight from an Invertebrate System. *The American Naturalist*, 198 (3), 317–332.

Suarez-Cuartin, G., Smith, A., Abo-Leyah, H., Rodrigo-Troyano, A., Perea, L., Vidal, S., Plaza, V., Fardon, T. C., Sibila, O. and Chalmers, J. D., 2017. Anti-Pseudomonas aeruginosa IgG antibodies and chronic airway infection in bronchiectasis. *Respiratory Medicine*, 128, 1–6.

Subramanian, I., Verma, S., Kumar, S., Jere, A. and Anamika, K., 2020. Multi-omics Data Integration, Interpretation, and Its Application. *Bioinformatics and Biology Insights*, 14, 1177932219899051.

Sukumaran, A., Coish, J. M., Yeung, J., Muselius, B., Gadjeva, M., MacNeil, A. J. and Geddes-McAlister, J., 2019. Decoding communication patterns of the innate immune system by quantitative proteomics. *Journal of Leukocyte Biology*, 106 (6), 1221–1232.

Sukumaran, A., Woroszchuk, E., Ross, T. and Geddes-McAlister, J., 2021. Proteomics of host-bacterial interactions: new insights from dual perspectives. *Canadian Journal of Microbiology*, 67 (3), 213–225.

Sułkowska-Ziaja, K., Trepa, M., Olechowska-Jarząb, A., Nowak, P., Ziaja, M., Kała, K. and Muszyńska, B., 2023. Natural Compounds of Fungal Origin with Antimicrobial Activity—Potential Cosmetics Applications. *Pharmaceuticals*, 16 (9), 1200.

Sun, J., LaRock, D. L., Skowronski, E. A., Kimmey, J. M., Olson, J., Jiang, Z., O'Donoghue, A. J., Nizet, V. and LaRock, C. N., 2020. The *Pseudomonas aeruginosa* protease LasB directly activates IL-1 β . *EBioMedicine*, 60, 102984.

Swarengen, J. R., 2018. Choosing the right animal model for infectious disease research. *Animal Models and Experimental Medicine*, 1 (2), 100–108.

Sweeney, E., Harrington, N. E., Harley Henriques, A. G., Hassan, M. M., Crealock-Ashurst, B., Smyth, A. R., Hurley, M. N., Tormo-Mas, M. Á. and Harrison, F., 2021. An ex vivo cystic fibrosis model recapitulates key clinical aspects of chronic *Staphylococcus aureus* infection. *Microbiology (Reading, England)*, 167 (1).

Szymański, M., Chmielewska, Sandra, Czyżewska, Urszula, Malinowska, Marta and Tylicki, A., 2022. Echinocandins – structure, mechanism of action and use in antifungal therapy. *Journal of Enzyme Inhibition and Medicinal Chemistry*, 37 (1), 876–894.

Takazono, T. and Sheppard, D. C., 2017. Aspergillus in chronic lung disease: Modeling what goes on in the airways. *Medical Mycology*, 55 (1), 39–47.

Takemori, A., Butcher, D. S., Harman, V. M., Brownridge, P., Shima, K., Higo, D., Ishizaki, J., Hasegawa, H., Suzuki, J., Yamashita, M., Loo, J. A., Loo, R. R. O., Beynon, R. J., Anderson, L. C. and Takemori, N., 2020. PEPPi-MS: Polyacrylamide-Gel-Based Prefractionation for Analysis of Intact Proteoforms and Protein Complexes by Mass Spectrometry. *Journal of Proteome Research*, 19 (9), 3779–3791.

Takemori, A., Kaulich, P. T., Cassidy, L., Takemori, N. and Tholey, A., 2022. Size-Based Proteome Fractionation through Polyacrylamide Gel Electrophoresis Combined with LC–FAIMS–MS for In-Depth Top-Down Proteomics. *Analytical Chemistry*, 94 (37), 12815–12821.

Takemori, A., Kaulich, P. T., Konno, R., Kawashima, Y., Hamazaki, Y., Hoshino, A., Tholey, A. and Takemori, N., 2024. GeLC-FAIMS-MS workflow for in-depth middle-down proteomics. *PROTEOMICS*, 24 (3–4), 2200431.

Talento, A. F., Fitzgerald, M., Redington, B., O'Sullivan, N., Fenelon, L. and Rogers, T. R., 2019. Prevention of healthcare-associated invasive aspergillosis during hospital construction/renovation works. *Journal of Hospital Infection*, 103 (1), 1–12.

Tan, R. M., Kuang, Z., Hao, Y. and Lau, G. W., 2013. Type IV Pilus of *Pseudomonasaeruginosa* Confers Resistance to Antimicrobial Activities of the Pulmonary Surfactant Protein-A. *Journal of Innate Immunity*, 6 (2), 227–239.

Tanindi, A. and Cemri, M., 2011. Troponin elevation in conditions other than acute coronary syndromes. *Vascular Health and Risk Management*, 7, 597–603.

Tanner, C. D. and Rosowski, E. E., 2024. Macrophages inhibit extracellular hyphal growth of *A. fumigatus* through Rac2 GTPase signaling. *Infection and Immunity*, 92 (2), e0038023.

Tarizzo, M., Lemonnier, L., Leblanc, S., Bigot, J., Thouvenin, G., Guillot, L. and Corvol, H., 2025. Allergic bronchopulmonary aspergillosis in cystic fibrosis: Case-control study from the French registry. *Medical Mycology*, 63 (4), myaf030.

Tashiro, M., Takazono, T. and Izumikawa, K., 2024. Chronic pulmonary aspergillosis: comprehensive insights into epidemiology, treatment, and unresolved challenges. *Therapeutic Advances in Infectious Disease*, 11, 20499361241253750.

Tian, Q., Wang, J., Shao, S., Zhou, H., Kang, J., Yu, X., Huang, M., Qiu, G. and Shen, L., 2024. Combining metabolomics and transcriptomics to analyze key response metabolites and molecular mechanisms of *Aspergillus fumigatus* under cadmium stress. *Environmental Pollution*, 356, 124344.

Toor, A., Culibrk, L., Singhera, G. K., Moon, K.-M., Prudova, A., Foster, L. J., Moore, M. M., Dorscheid, D. R. and Tebbutt, S. J., 2018. Transcriptomic and proteomic host response to *Aspergillus fumigatus* conidia in an air-liquid interface model of human bronchial epithelium. *PLOS ONE*, 13 (12), e0209652.

Torres, M., de Cock, H. and Celis Ramírez, A. M., 2020. In Vitro or In Vivo Models, the Next Frontier for Unraveling Interactions between *Malassezia* spp. and Hosts. How Much Do We Know? *Journal of Fungi*, 6 (3), 155.

Torres-Sangiao, E., Giddey, A. D., Leal Rodriguez, C., Tang, Z., Liu, X. and Soares, N. C., 2022. Proteomic Approaches to Unravel Mechanisms of Antibiotic Resistance and Immune Evasion of Bacterial Pathogens. *Frontiers in Medicine* [online], 9. Available from: <https://www.frontiersin.org/journals/medicine/articles/10.3389/fmed.2022.850374/full> [Accessed 27 Jun 2025].

Toya, S., Struyf, S., Huerta, L., Morris, P., Gavioli, E., Minnella, E. M., Cesta, M. C., Allegretti, M. and Proost, P., 2024. A narrative review of chemokine receptors CXCR1 and CXCR2 and their role in acute respiratory distress syndrome. *European Respiratory Review*, 33 (173), 230172.

Traynor, A. M., Owens, R. A., Coughlin, C. M., Holton, M. C., Jones, G. W., Calera, J. A. and Doyle, S., 2021. At the metal-metabolite interface in *Aspergillus fumigatus*: towards untangling the intersecting roles of zinc and gliotoxin. *Microbiology (Reading, England)*, 167 (11), 001106.

Trevijano-Contador, N. and Zaragoza, O., 2018. Immune Response of *Galleria mellonella* against Human Fungal Pathogens. *Journal of Fungi (Basel, Switzerland)*, 5 (1), 3.

Tsai, C. J.-Y., Loh, J. M. S. and Proft, T., 2016. *Galleria mellonella* infection models for the study of bacterial diseases and for antimicrobial drug testing. *Virulence*, 7 (3), 214–229.

Tunnicliffe, G., Schomberg, L., Walsh, S., Tinwell, B., Harrison, T. and Chua, F., 2013. Airway and parenchymal manifestations of pulmonary aspergillosis. *Respiratory Medicine*, 107 (8), 1113–1123.

Turco, M. Y., Gardner, L., Hughes, J., Cindrova-Davies, T., Gomez, M. J., Farrell, L., Hollinshead, M., Marsh, S. G. E., Brosens, J. J., Critchley, H. O., Simons, B. D., Hemberger, M., Koo, B.-K., Moffett, A. and Burton, G. J., 2017. Long-term, hormone-responsive organoid cultures of human endometrium in a chemically- defined medium. *Nature cell biology*, 19 (5), 568–577.

Ulfig, A. and Leichert, L. I., 2021. The effects of neutrophil-generated hypochlorous acid and other hypohalous acids on host and pathogens. *Cellular and Molecular Life Sciences*, 78 (2), 385–414.

Upadhyay, S. K., Gautam, P., Pandit, H., Singh, Y., Basir, S. F. and Madan, T., 2012. Identification of fibrinogen-binding proteins of *Aspergillus fumigatus* using proteomic approach. *Mycopathologia*, 173 (2–3), 73–82.

Upadhyay, S. K., Mahajan, L., Ramjee, S., Singh, Y., Basir, S. F. and Madan, T., 2009. Identification and characterization of a laminin-binding protein of *Aspergillus fumigatus*: extracellular thaumatin domain protein (AfCalAp). *Journal of Medical Microbiology*, 58 (Pt 6), 714–722.

Vandendriessche, S., Cambier, S., Proost, P. and Marques, P. E., 2021. Complement Receptors and Their Role in Leukocyte Recruitment and Phagocytosis. *Frontiers in Cell and Developmental Biology* [online], 9. Available from: <https://www.frontiersin.org/journals/cell-and-developmental-biology/articles/10.3389/fcell.2021.624025/full> [Accessed 9 Jul 2025].

Verweij, P. E., Lucas, J. A., Arendrup, M. C., Bowyer, P., Brinkmann, A. J. F., Denning, D. W., Dyer, P. S., Fisher, M. C., Geenen, P. L., Gisi, U., Hermann, D., Hoogendijk, A.,

Kiers, E., Lagrou, K., Melchers, W. J. G., Rhodes, J., Rietveld, A. G., Schoustra, S. E., Stenzel, K., Zwaan, B. J. and Fraaije, B. A., 2020. The one health problem of azole resistance in *Aspergillus fumigatus*: current insights and future research agenda. *Fungal Biology Reviews*, 34 (4), 202–214.

Vickers, I., Reeves, E. P., Kavanagh, K. A. and Doyle, S., 2007. Isolation, activity and immunological characterisation of a secreted aspartic protease, CtsD, from *Aspergillus fumigatus*. *Protein Expression and Purification*, 53 (1), 216–224.

Atoki, A.V., Aja, P. M., Shinkafi, T. S., Ondari, E. N., Adeniyi, A. I., Fasogbon, I. V., Dangana, R. S., Shehu, U. U. and Akin-Adewumi, A., 2025. Exploring the versatility of *Drosophila melanogaster* as a model organism in biomedical research: a comprehensive review. *Fly*, 19 (1), 2420453.

Wang, H., Agrawal, A., Wang, Y., Crawford, D. W., Siler, Z. D., Peterson, M. L., Woofter, R. T., Labib, M., Shin, H. Y., Baumann, A. P. and Phillips, K. S., 2021. An ex vivo model of medical device-mediated bacterial skin translocation. *Scientific Reports*, 11 (1), 5746.

Wang, L., Hu, D., Xu, J., Hu, J. and Wang, Y., 2024. Complex in vitro model: A transformative model in drug development and precision medicine. *Clinical and Translational Science*, 17 (2), e13695.

Wang, X., Mohammad, I. S., Fan, L., Zhao, Z., Nurunnabi, M., Sallam, M. A., Wu, J., Chen, Z., Yin, L. and He, W., 2021. Delivery strategies of amphotericin B for invasive fungal infections. *Acta Pharmaceutica Sinica B*, 11 (8), 2585–2604.

Wang, Y., Chang, Y., Ortañez, J., Peña, J. F., Carter-House, D., Reynolds, N. K., Smith, M. E., Benny, G., Mondo, S. J., Salamov, A., Lipzen, A., Pangilinan, J., Guo, J., LaButti, K., Andreopolous, W., Tritt, A., Keymanesh, K., Yan, M., Barry, K., Grigoriev, I. V., Spatafora, J. W. and Stajich, J. E., 2023. Divergent Evolution of Early Terrestrial Fungi Reveals the Evolution of Mucormycosis Pathogenicity Factors. *Genome Biology and Evolution*, 15 (4), evad046.

Wang, Z., Liu, P.-K. and Li, L., 2024. A Tutorial Review of Labeling Methods in Mass Spectrometry-Based Quantitative Proteomics. *ACS Measurement Science Au*, 4 (4), 315–337.

Wen, T., Mingler, M. K., Wahl, B., Khorki, M. E., Pabst, O., Zimmermann, N. and Rothenberg, M. E., 2014. Carbonic Anhydrase IV Is Expressed on IL-5-Activated Murine Eosinophils. *The Journal of Immunology*, 192 (12), 5481–5489.

WHO., 2022. *WHO Fungal Priority Pathogens List to Guide Research, Development and Public Health Action*. 1st ed. Geneva: World Health Organization.

Wiederhold, N. P., Najvar, L. K., Jaramillo, R., Olivo, M., Wickes, B. L., Catano, G. and Patterson, T. F., 2019. Extended-Interval Dosing of Rezafungin against Azole-Resistant *Aspergillus fumigatus*. *Antimicrobial Agents and Chemotherapy*, 63 (10), 10.1128/aac.01165-19.

Wiederhold, N. P., Shubitz, L. F., Najvar, L. K., Jaramillo, R., Olivo, M., Catano, G., Trinh, H. T., Yates, C. M., Schotzinger, R. J., Garvey, E. P. and Patterson, T. F., 2018. The Novel Fungal Cyp51 Inhibitor VT-1598 Is Efficacious in Experimental Models of Central Nervous System Coccidioidomycosis Caused by *Coccidioides posadasii* and *Coccidioides immitis*. *Antimicrobial Agents and Chemotherapy*, 62 (4), 10.1128/aac.02258-17.

Willger, S. D., Grahl, N. and Cramer, R. A., 2009. *Aspergillus fumigatus* metabolism: Clues to mechanisms of in vivo fungal growth and virulence. *Medical mycology : official publication of the International Society for Human and Animal Mycology*, 47 (Suppl 1), S72–S79.

Williams, C. C., Gregory, J. B. and Usher, J., 2024. Understanding the clinical and environmental drivers of antifungal resistance in the One Health context. *Microbiology*, 170 (10), 001512.

Wippel, H. H., Chavez, J. D., Tang, X. and Bruce, J. E., 2022. Quantitative interactome analysis with chemical crosslinking and mass spectrometry. *Current opinion in chemical biology*, 66, 102076.

Wishart, D. S., Cheng, L. L., Copié, V., Edison, A. S., Eghbalnia, H. R., Hoch, J. C., Gouveia, G. J., Pathmasiri, W., Powers, R., Schock, T. B., Sumner, L. W. and Uchimiya, M., 2022. NMR and Metabolomics—A Roadmap for the Future. *Metabolites*, 12 (8), 678

Wölbeling, F., Munder, A., Kerber-Momot, T., Neumann, D., Hennig, C., Hansen, G., Tümmeler, B. and Baumann, U., 2011. Lung function and inflammation during murine *Pseudomonas aeruginosa* airway infection. *Immunobiology*, 216 (8), 901–908.

Wong, S. S. W., Daniel, I., Gangneux, J.-P., Jayapal, J. M., Guegan, H., Delliére, S., Lalitha, P., Shende, R., Madan, T., Bayry, J., Guijarro, J. I., Kuppamuthu, D. and Aimananda, V., 2020. Differential Interactions of Serum and Bronchoalveolar Lavage Fluid Complement Proteins with Conidia of Airborne Fungal Pathogen *Aspergillus fumigatus*. *Infection and Immunity*, 88 (9), e00212-20.

Wong, S. S. W., Delliére, S., Schiefermeier-Mach, N., Lechner, L., Perkhofer, S., Bomme, P., Fontaine, T., Schlosser, A. G., Sorensen, G. L., Madan, T., Kishore, U. and Aimananda, V., 2022. Surfactant protein D inhibits growth, alters cell surface polysaccharide exposure and immune activation potential of *Aspergillus fumigatus*. *The Cell Surface*, 8, 100072.

Wood, S. J., Kuzel, T. M. and Shafikhani, S. H., 2023. *Pseudomonas aeruginosa*: Infections, Animal Modeling, and Therapeutics. *Cells*, 12 (1), 199.

Yaakoub, H., Mina, S., Calenda, A., Bouchara, J.-P. and Papon, N., 2022. Oxidative stress response pathways in fungi. *Cellular and Molecular Life Sciences: CMLS*, 79 (6), 333.

Ye, W., Liu, T., Zhang, W. and Zhang, W., 2021. The Toxic Mechanism of Gliotoxins and Biosynthetic Strategies for Toxicity Prevention. *International Journal of Molecular Sciences*, 22 (24), 13510.

Yokoi, F., Deguchi, S. and Takayama, K., 2023. Organ-on-a-chip models for elucidating the cellular biology of infectious diseases. *Biochimica et Biophysica Acta (BBA) - Molecular Cell Research*, 1870 (6), 119504.

Yoon, J., Kimura, S., Maruyama, J. and Kitamoto, K., 2009. Construction of quintuple protease gene disruptant for heterologous protein production in *Aspergillus oryzae*. *Applied Microbiology and Biotechnology*, 82 (4), 691–701.

Yu, C., Wang, X. and Huang, L., 2022. Developing a Targeted Quantitative Strategy for Sulfoxide-Containing MS-Cleavable Cross-Linked Peptides to Probe Conformational Dynamics of Protein Complexes. *Analytical Chemistry*, 94 (10), 4390–4398.

Zelante, T., Choera, T., Beauvais, A., Fallarino, F., Paolicelli, G., Pieraccini, G., Pieroni, M., Galosi, C., Beato, C., De Luca, A., Boscaro, F., Romoli, R., Liu, X., Warris, A., Verweij, P. E., Ballard, E., Borghi, M., Pariano, M., Costantino, G., Calvitti, M., Vacca, C., Oikonomou, V., Gargaro, M., Wong, A. Y. W., Boon, L., den Hartog, M., Spáčil, Z., Puccetti, P., Latgè, J.-P., Keller, N. P. and Romani, L., 2021. *Aspergillus fumigatus* tryptophan metabolic route differently affects host immunity. *Cell Reports*, 34 (4), 108673.

Zhai, P., Shi, L., Zhong, G., Jiang, J., Zhou, J., Chen, X., Dong, G., Zhang, L., Li, R. and Song, J., 2021. The OxrA Protein of *Aspergillus fumigatus* Is Required for the Oxidative Stress Response and Fungal Pathogenesis. *Applied and Environmental Microbiology*, 87 (22), e0112021.

Zhang, B., Zhou, Y.-T., Jiang, S.-X., Zhang, Y.-H., Huang, K., Liu, Z.-Q. and Zheng, Y.-G., 2020. Amphotericin B biosynthesis in *Streptomyces nodosus*: quantitative analysis of metabolism via LC–MS/MS based metabolomics for rational design. *Microbial Cell Factories*, 19, 18.

Zhang, J., Verweij, P. E., Rijs, A. J. M. M., Debets, A. J. M. and Snelders, E., 2022. Flower Bulb Waste Material is a Natural Niche for the Sexual Cycle in *Aspergillus fumigatus*. *Frontiers in Cellular and Infection Microbiology* [online], 11. Available from: <https://www.frontiersin.org/journals/cellular-and-infection-microbiology/articles/10.3389/fcimb.2021.785157/full> [Accessed 10 Jun 2025].

Zhao, J., Cheng, W., He, X. and Liu, Y., 2018. The co-colonization prevalence of *Pseudomonas aeruginosa* and *Aspergillus fumigatus* in cystic fibrosis: A systematic review and meta-analysis. *Microbial Pathogenesis*, 125, 122–128.

Zhao, Z., Song, J., Yang, C., Yang, L., Chen, J., Li, X., Wang, Y. and Feng, J., 2021. Prevalence of Fungal and Bacterial Co-Infection in Pulmonary Fungal Infections: A Metagenomic Next Generation Sequencing-Based Study. *Frontiers in Cellular and Infection Microbiology*, 11, 749905.

Chapter 9

Appendix

Chapter 2 Supplementary



<https://www.mdpi.com/article/10.3390/cells12071065/s1>

Chapter 3 Supplementary



https://www.microbiologyresearch.org/content/journal/jmm/10.1099/jmm.0.001844#supplementary_data

Chapter 4 Supplementary



<https://www.mdpi.com/article/10.3390/jof9020222/s1>

Chapter 5 Supplementary



https://figshare.com/articles/journal_contribution/Proteomic_characterisation_of_i_Aspergillus_fumigatus_i_host_interactions_using_the_i_ex-vivo_i_pig_lung_EVPL_model_b_b_Suppfigures_and_tables_evpl_paper_pdf/28418183?file=52368533

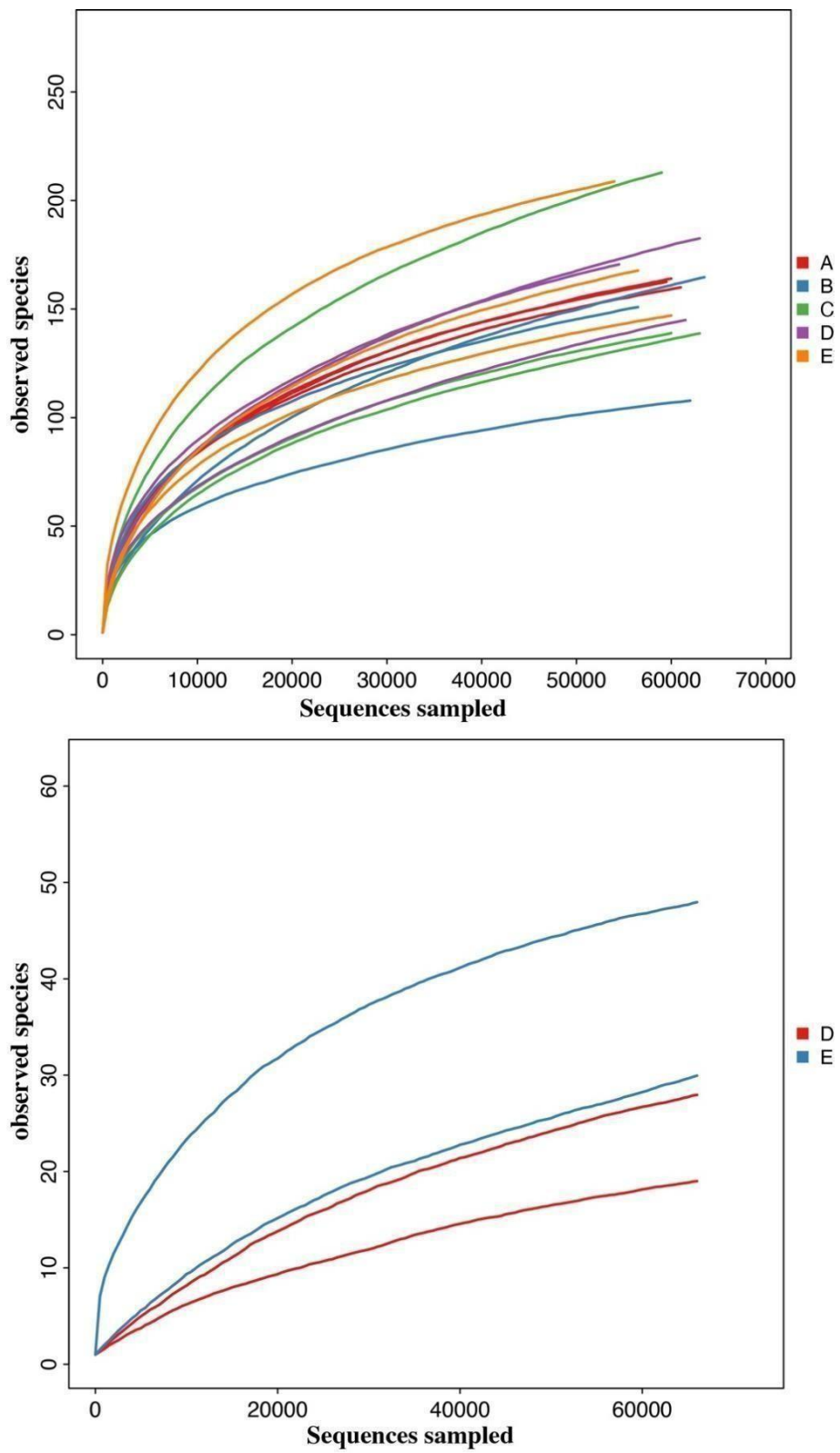


Figure S6.1: Species rarefaction plots for all 16S and ITS2 samples. A: unwashed tissue, B: washed tissue, C: *P. aeruginosa* mono-infection, D: *A. fumigatus* mono-infection, E: coinfection.

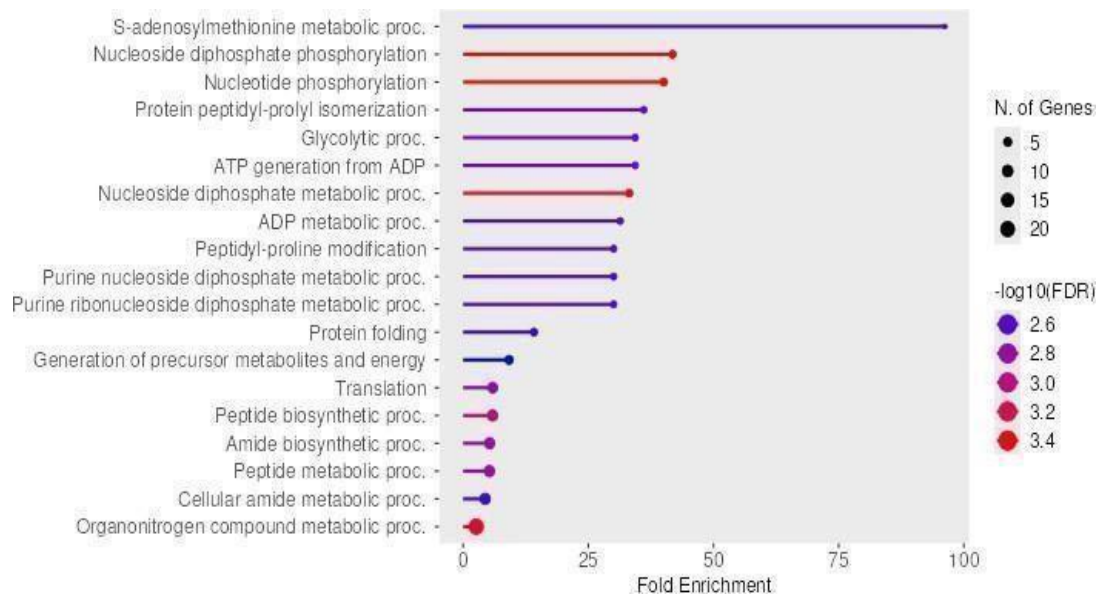


Figure S6.2: Gene enrichment analysis highlighting biological processes decreased in expression in *A. fumigatus* when in coinfection with *P. aeruginosa* relative to growth in mono-infection

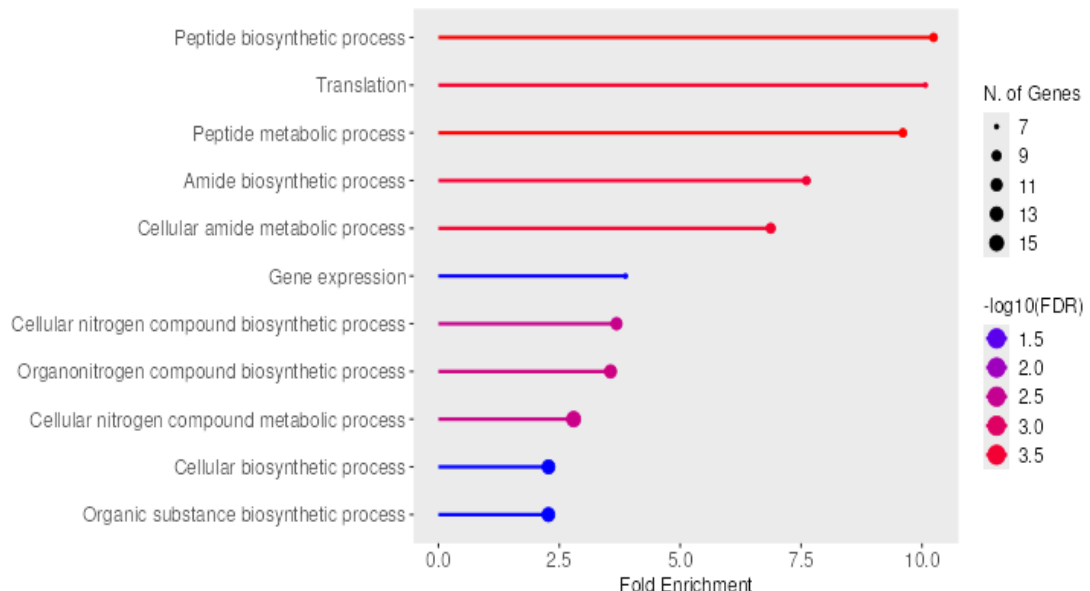


Figure S6.3: Gene enrichment analysis highlighting biological processes increased in expression in *P. aeruginosa* when in coinfection with *A. fumigatus* relative to growth in mono-infection

Table S6.1: 16S sequencing results at the Phylum, Genus and Species levels A: unwashed tissue, B: washed tissue, C: *P. aeruginosa* mono-infection, D: *A. fumigatus* mono-infection, E: coinfection.

Phylum					
Taxon	A	B	C	D	E
Thermomicrobiota	0.00%	0.00%	0.00%	0.00%	0.00%
Planctomycetota	0.00%	0.00%	0.00%	0.00%	0.00%
Thermotogota	0.00%	0.00%	0.00%	0.00%	0.00%
Nitrospirota	0.00%	0.00%	0.00%	0.00%	0.00%
Spirochaetota	0.00%	0.00%	0.00%	0.00%	0.00%
Gemmatimonadota	0.00%	0.00%	0.00%	0.00%	0.00%
CandidatusSaccharibacteria	0.00%	0.00%	0.00%	0.00%	0.00%
Mycoplasmatota	0.00%	0.00%	0.00%	0.00%	0.00%
Other	0.00%	0.00%	0.00%	0.00%	0.00%
Synergistota	0.00%	0.00%	0.01%	0.00%	0.00%
Campylobacterota	0.01%	0.00%	0.00%	0.01%	0.02%
Acidobacteriota	0.02%	0.01%	0.01%	0.00%	0.01%
Deinococcota	0.04%	0.02%	0.00%	0.00%	0.00%
Fusobacteriota	0.35%	0.02%	0.01%	0.61%	0.04%
Actinomycetota	1.73%	0.09%	0.10%	0.18%	0.32%
Bacteroidota	4.48%	11.68%	8.06%	7.14%	5.12%
Bacillota	9.75%	8.14%	24.83%	4.83%	7.97%
Pseudomonadota	83.61%	80.04%	66.96%	87.22%	86.51%
Genus					
Taxon	A	B	C	D	E
Acinetobacter	0.05%	0.04%	0.03%	2.84%	0.02%
Peptoniphilus	0.30%	0.07%	0.00%	0.00%	2.84%
Sporanaerobacter	0.00%	3.63%	0.02%	0.03%	0.01%
Porphyromonas	0.02%	4.38%	0.22%	0.19%	0.04%
Streptococcus	1.02%	1.80%	0.09%	0.05%	2.22%
Aeromonas	0.00%	0.03%	0.03%	5.71%	0.00%
Clostridiumsensustricto	3.54%	0.76%	0.01%	0.98%	0.56%
Prevotella	0.15%	4.45%	0.61%	2.07%	0.06%
Phocaeicola	1.72%	0.06%	5.68%	1.23%	0.13%
Bacteroides	1.46%	1.24%	0.25%	2.88%	3.76%
Comamonas	0.00%	6.78%	0.06%	3.19%	0.01%
Peptostreptococcus	2.60%	1.20%	4.03%	2.80%	0.00%
Supraeoptans	0.63%	0.07%	19.29%	0.43%	0.04%
Other	8.07%	3.13%	3.32%	3.05%	5.15%
Actinobacillus	0.16%	53.13%	0.62%	0.33%	0.32%
Pseudomonas	0.02%	0.17%	31.81%	0.22%	49.69%
Escherichia	80.25%	19.06%	33.92%	73.99%	35.15%

Taxon	species				
	A	B	C	D	E
Acinetobacter_baumannii	0.01%	0.01%	0.02%	2.83%	0.00%
Bacteroides_heparinolyticus	1.21%	0.01%	0.05%	2.22%	0.01%
Sporanaerobacter_acetigenes	0.00%	3.63%	0.02%	0.03%	0.01%
Bacteroides_fragilis	0.00%	0.19%	0.08%	0.01%	3.70%
Porphyromonas_macacae	0.01%	4.38%	0.01%	0.00%	0.00%
Peptostreptococcus_porci	2.60%	1.20%	4.03%	2.80%	0.00%
Supraeoptans_intestinalis	0.63%	0.07%	19.29%	0.43%	0.04%
Pseudomonas_aeruginosa	0.02%	0.17%	31.81%	0.22%	49.69%
Other	95.51%	90.34%	44.68%	91.47%	46.55%

Table S6.2. ITS2 sequencing results at phylum, genus and species level A: unwashed tissue, B: washed tissue, C: *P. aeruginosa* mono-infection, D: *A. fumigatus* mono-infection, E: coinfection.

Phylum		
Taxon	D	E
Other	7.56E-06	7.56E-06
Mortierellomycota	2.27E-05	5.29E-05
Basidiomycota	6.05E-05	0.000665
Ascomycota	0.999909	0.999274
Genus		
Taxon	D	E
Other	0.000726	0.007849
Aspergillus	0.999274	0.992151
Species		
Taxon	D	E